

6-2017

## INVESTIGATION INTO THE SUSPECTED LATE HOLOCENE DECLINE IN OBSIDIAN USE AT SITES ON EDWARDS AIR FORCE BASE

Richard Gerard Bark  
*California State University - San Bernardino*

Follow this and additional works at: <https://scholarworks.lib.csusb.edu/etd>

 Part of the [Archaeological Anthropology Commons](#)

---

### Recommended Citation

Bark, Richard Gerard, "INVESTIGATION INTO THE SUSPECTED LATE HOLOCENE DECLINE IN OBSIDIAN USE AT SITES ON EDWARDS AIR FORCE BASE" (2017). *Electronic Theses, Projects, and Dissertations*. 468.  
<https://scholarworks.lib.csusb.edu/etd/468>

This Thesis is brought to you for free and open access by the Office of Graduate Studies at CSUSB ScholarWorks. It has been accepted for inclusion in Electronic Theses, Projects, and Dissertations by an authorized administrator of CSUSB ScholarWorks. For more information, please contact [scholarworks@csusb.edu](mailto:scholarworks@csusb.edu).

INVESTIGATION INTO THE SUSPECTED LATE HOLOCENE DECLINE IN  
OBSIDIAN USE AT SITES ON EDWARDS AIR FORCE BASE

---

A Thesis  
Presented to the  
Faculty of  
California State University,  
San Bernardino

---

In Partial Fulfillment  
of the Requirements for the Degree  
Master of Arts  
in  
Applied Archaeology

---

by  
Richard Gerard Bark  
June 2017

INVESTIGATION INTO THE SUSPECTED LATE HOLOCENE DECLINE IN  
OBSIDIAN USE AT SITES ON EDWARDS AIR FORCE BASE

---

A Thesis  
Presented to the  
Faculty of  
California State University,  
San Bernardino

---

by  
Richard Gerard Bark

June 2017

Approved by:

Dr. Amy Gusick, Committee Chair, Anthropology

Dr. Micah J. Hale, Committee Member

Dr. Peter Robertshaw, Committee Member

© 2017 Richard Gerard Bark



## ABSTRACT

Archaeological investigations at Edwards Air Force Base (AFB) have been ongoing for more than 40 years. Yet the findings from the vast majority of those efforts are available only as grey literature that is known only to a relative few. The primary purpose of this thesis was to investigate a late Holocene decline in obsidian frequency reported by researchers working in the Bissell Basin and Rosamond Dry Lake region of Edwards AFB near the turn of the 21<sup>st</sup> century. A secondary purpose of this thesis was to shine a light on an area of the western Mojave Desert that is not widely known despite more than four decades of research.

In order to explore the reported decline in obsidian frequency, I created an obsidian database using data gleaned from nearly 50 cultural resources management reports and supplemented those data with sourcing and hydration information for 39 additional obsidian artifacts. Those data were organized into tables, charts, and histograms to look for patterns that would support or refute the claim that obsidian use decreased significantly after the Gypsum time period (4000 to 1500 Before Present [B.P.]). Two patterns emerged from my analysis.

The first was one where the overall abundance of obsidian at Edwards AFB did not decrease during the late Holocene, thus contradicting the conclusions made in the previous research. The second was one where the obsidian abundance shifted among the various regions of the installation. Yet these shifts are nowhere near as significant as the previously reported decline.

Therefore, while the total amount of obsidian that entered the archaeological record at Edwards remained relatively stable from 1500 to 100 B.P., the amount of obsidian decreased in certain regions and increased in others.

Although not within the scope of my original intent, my research also identified two areas for future research. The first involves an apparent pattern where the number of archaeological sites from which obsidian was recovered gradually decreases during the middle-Holocene even as the overall quantity of obsidian remains essentially unchanged. The second relates to the lack of a well-established hydration rate formula for obsidian recovered from archaeological sites on Edwards AFB.

Ultimately, I concluded that the previous findings that obsidian declined during the late Holocene were affected by sampling bias and faulty data organization. Most archaeologists understand that poorly implemented sampling can lead to poorly derived findings and conclusions. What may not be as well understood is that a perfectly appropriate sample where the data are not organized well can also lead to flawed results and conclusions. It is hoped that this thesis will inform archaeologists not only about how the manner in which they organize their data can affect their interpretation of past human behavior, but also about additional research opportunities at Edwards AFB.

## ACKNOWLEDGEMENTS

However much of a cliché this statement is, writing a thesis is not an easy task, nor one that can be accomplished by one person. In the case of this thesis, doing so was made all the more difficult by several significant life changing events. As I prepared to write, circumstances necessitated a 200 mile move from Rosamond to San Diego, CA in order to begin a new job. Therefore, this thesis could not have been completed without the support and assistance of the following individuals:

Apasara – More than any other, you are the person who endured the most during the past 18 months. Words cannot capture the magnitude of my love for you, or the extent of my gratitude for your continuous support. I am sorry for ruining Portishead.

Richard and Betty Bark – My parents, who generously offered up a room for me to work in and whose timely road trip to Texas provided me with the solitude I needed to write.

Electra – The funny little creature who sat with me night after night as I toiled away at my laptop.

Jessica Porter-Rodriguez – My carpool pal and fellow researcher at Edwards AFB. I'm not sure I could have gone through this without somebody familiar by my side.

Dr. Micah Hale – The person who planted the idea for this thesis in my head and provided enough guidance to keep me focused.

Dr. Amy Gusick, Dr. Peter Robertshaw, and Dr. Guy Hepp – Although the Applied Archaeology program is new, it is clear from the support you provided and the demands you placed on the graduate students that each of you are committed to the success of both the students and the program. Thank you all for the time you took out of your schedules to listen and provide feedback.

Dr. Heather Thakar, Dr. Ismael Diaz, and Leon “Pele” Groenwegen – Without input from each of you I would still be struggling with statistics. I am particularly indebted to Dr. Thakar, whose early suggestion on how to organize the obsidian data set me down the right path.

Dr. Eric Melchiorre – For providing access to and instructions on how to use the Niton XRF in order to source the unsourced obsidian artifacts.

Jimmy Daniels – Thank you for taking time out of your schedule to interpret the output from the XRF analysis.

Alex Sinclair – The Photoshop wizard extraordinaire responsible for cleaning up the photos used in Figures 9, 10, and 11.

Rick Norwood – Without the robust cultural resources management program that you built at Edwards it is unlikely that this thesis would have even been possible. I am also indebted to the scores of archaeologists who conducted site excavations at Edwards AFB for more than 40 years. While Rick laid the foundation, your efforts provided the raw materials used to build this thesis.

Roscoe Loetzerich – Thank you for continuing Rick’s legacy and allowing me access to the Edwards AFB data.

Nathan Anderson and Escee Lopez – The fieldwork you conducted for the artifact migration study helped me better articulate the ongoing post-depositional processes at Edwards AFB.

Dr. Steve Bouscaren and Dr. Robert Bettinger – I would not be the archaeologist I am today had I not attended each of your field schools.

The funding for the supplemental obsidian analysis for this thesis was provided by an ASA Southern California Archaeology Endowment.

## DEDICATION

This thesis is dedicated to:

Apasara – No matter which tube you find yourself in, I will be there with you.

and

My furry little study buddy and the most magical of all the cats, Electra.

## TABLE OF CONTENTS

|  |      |
|--|------|
| ABSTRACT .....   | iii  |
| ACKNOWLEDGEMENTS.....  | v    |
| LIST OF TABLES .....   | viii |
| LIST OF FIGURES .....  | ix   |
| CHAPTER ONE: INTRODUCTION TO EDWARDS AIR FORCE BASE          |      |
| Introduction .....   | 1    |
| Geologic and Environmental Contexts for Edwards AFB.....     | 2    |
| Preservation Issues.....                                     | 6    |
| Cultural Context for Edwards AFB .....                       | 9    |
| Research Setting at Edwards AFB.....                         | 12   |
| Management Regions Studies .....                             | 16   |
| Conclusion .....   | 18   |
| CHAPTER TWO: THEORETICAL ORIENTATION AND RESEARCH QUESTIONS  |      |
| Introduction .....   | 20   |
| Hunter-Gatherers and Lithic Technology .....                 | 21   |
| Obsidian Analyses .....                                      | 23   |
| Human Behavioral Ecology.....                                | 27   |
| Obsidian Use, Edwards AFB, and Human Behavioral Ecology..... | 32   |
| Research Questions .....                                     | 35   |
| CHAPTER THREE: RESEARCH OBJECTIVE AND METHODS                |      |
| Introduction .....   | 38   |
| Research Methods.....  | 38   |

|   |     |
|---|-----|
| Supplemental Obsidian Data .....  | 39  |
| Obsidian Database Fields .....  | 45  |
| Acknowledgement of Biases and Assumptions.....                                  | 53  |
| Analytical Approach .....   | 54  |
| CHAPTER FOUR: OBSIDIAN ANALYSIS RESULTS   |     |
| Introduction .....  | 57  |
| Supplemental Obsidian Data .....  | 58  |
| General Patterns for Obsidian at Edwards AFB .....                              | 63  |
| Obsidian Date Histograms .....  | 69  |
| Number of Sites vs. Number of Dates.....  | 83  |
| Introduction of the Bow and Arrow .....   | 85  |
| Conclusion .....  | 88  |
| CHAPTER FIVE: DISCUSSION  |     |
| Introduction .....  | 89  |
| Obsidian Decline at Edwards AFB .....   | 89  |
| Influence of the Bow and Arrow .....  | 91  |
| Sampling Bias and Data Organization .....                                       | 92  |
| An Alternative Method for Data Normalization .....                              | 98  |
| Hydration Rate at Edwards AFB .....   | 101 |
| Recommendations for Further Research .....                                      | 102 |
| CHAPTER SIX: CONCLUSION.....  | 105 |
| APPENDIX A: BIBLIOGRAPHY OF REPORTS CONTAINING OBSIDIAN<br>HYDRATION DATA ..... | 108 |
| APPENDIX B: OBSIDIAN DATABASE .....   | 113 |



|   |     |
|---|-----|
| APPENDIX C: SUPPLEMENTAL OBSIDIAN LOCATION MAPS.....                      | 153 |
| APPENDIX D: SUPPLEMENTAL OBSIDIAN SOURCING AND<br>HYDRATION REPORTS ..... | 161 |
| REFERENCES CITED .....  | 177 |

## LIST OF TABLES

|  |    |
|--|----|
| Table 1. Cultural Sequence for Edwards Air Force Base .....  | 11 |
| Table 2. Edwards AFB Site Types.....   | 13 |
| Table 3. Artifacts Selected for Sourcing and Hydration Studies .....   | 40 |
| Table 4. Results of Sourcing and Hydration Analysis .....  | 58 |
| Table 5. Quantity of Obsidian by Site Type .....   | 65 |
| Table 6. Alternative Obsidian Sources .....  | 65 |
| Table 7. Quantity of Artifact Classes .....  | 66 |
| Table 8. Chi-Square Test of Obsidian Frequency by Management<br>Region for Three 1400 Year Time Intervals..... | 86 |
| Table 9. Chi-Square Test of Obsidian Frequency by Management<br>Region for Two 1400 Year Time Intervals .....  | 87 |

## LIST OF FIGURES

|  |    |
|--|----|
| Figure 1. The Edwards AFB vicinity.....  | 3  |
| Figure 2. The Major Land Features of Edwards AFB. ....   | 4  |
| Figure 3. Photograph of a Typical Prehistoric Site on Edwards AFB.....                               | 7  |
| Figure 4. Management Regions of Edwards AFB.....   | 14 |
| Figure 5. Aggregate Obsidian Hydration Profile for<br>Edwards AFB as of 2000. ....                   | 17 |
| Figure 6. Rosamond Lake Obsidian Hydration Profile. ....   | 17 |
| Figure 7. Artifacts Selected for Source and Hydration Analysis. ....                                 | 42 |
| Figure 8. X-ray Fluorescence Analysis in Progress. ....  | 44 |
| Figure 9. Artifacts 10818 and 10819, Flakes Collected from an<br>Obsidian Chipping Station. ....     | 60 |
| Figure 10. Artifacts 400-46, a Dart Point Fragment and 10727,<br>a Lake Mojave Dart Point. ....      | 62 |
| Figure 11. Artifacts 616-01 and 10742, Rose Spring Arrow Points.....                                 | 63 |
| Figure 12. Distribution of All Obsidian by Site Type.....  | 64 |
| Figure 13. Distribution of Coso Obsidian by Artifact Class. ....                                     | 67 |
| Figure 14. Distribution of Formal and Expedient Tools Manufactured<br>from Coso Obsidian. ....       | 68 |
| Figure 15. Distribution of Coso Obsidian Debitage.....   | 69 |
| Figure 16. Coso Obsidian Hydration Date Frequency for All of<br>Edwards AFB in 1000 Year Bins. ....  | 70 |
| Figure 17. Coso Obsidian Hydration Date Frequency for<br>Management Region 1 in 1000 Year Bins. .... | 71 |
| Figure 18. Coso Obsidian Hydration Date Frequency for<br>Management Region 2 in 1000 Year Bins. .... | 71 |

|  |    |
|--|----|
| Figure 19. Coso Obsidian Hydration Date Frequency for<br>Management Region 3 in 1000 Year Bins. ....             | 72 |
| Figure 20. Coso Obsidian Hydration Date Frequency for<br>Management Region 4 in 1000 Year Bins. ....             | 72 |
| Figure 21. Coso Obsidian Hydration Date Frequency for<br>Management Region 5 in 1000 Year Bins. ....             | 73 |
| Figure 22. Coso Obsidian Hydration Date Frequency for<br>All Of Edwards AFB in 500 Year Bins.....                | 77 |
| Figure 23. Coso Obsidian Hydration Date Frequency for<br>Management Region 1 in 500 Year Bins. ....              | 77 |
| Figure 24. Coso Obsidian Hydration Date Frequency for<br>Management Region 2 in 500 Year Bins. ....              | 78 |
| Figure 25. Coso Obsidian Hydration Date Frequency for<br>Management Region 3 in 500 Year Bins. ....              | 78 |
| Figure 26. Coso Obsidian Hydration Date Frequency for<br>Management Region 4 in 500 Year Bins. ....              | 79 |
| Figure 27. Coso Obsidian Hydration Date Frequency for<br>Management Region 5 in 500 Year Bins. ....              | 79 |
| Figure 28. Comparison of the Number Of Hydration Dates<br>to the Number of Sites Producing Those Dates.....      | 84 |
| Figure 29. Frequencies of Coso Obsidian Hydration Rims<br>By Project, Region, And Time Period. ....              | 94 |
| Figure 30. Distribution of Coso Obsidian Hydration Dates for<br>All of Edwards AFB by Cultural Time Period. .... | 96 |
| Figure 31. Histogram of Coso Obsidian Micron Readings for<br>All of Edwards AFB.....                             | 97 |
| Figure 32. Distribution of Coso Obsidian Hydration Dates for<br>All of Edwards AFB in 500 Year Intervals. ....   | 98 |

# CHAPTER ONE

## INTRODUCTION TO EDWARDS AIR FORCE BASE

### Introduction

The prehistory of Edwards Air Force Base (AFB) is informed primarily from the stone tool assemblages that have been recovered. This is largely dictated by preservation issues typical of a desert environment. While sources of toolstone quality chert and rhyolite are found in both Edwards AFB and the surrounding area, the nearest obsidian source is the Coso obsidian fields, located some 75 miles (120 km) to the north. The obsidian hydration data accumulated from more than four decades worth of archaeological investigations at Edwards Air Force Base (AFB) is the subject of this thesis research. Specifically, I examine an apparent late Holocene decline in the prehistoric use of obsidian in the Western Mojave. Previous research conducted in the late 1990s and early 2000s noted a dearth in Coso obsidian micron readings starting at around 1500 Before Present (B.P.) in both the Bissell Basin (Giambastiani and Basgall 2000) and Rosamond Dry Lake regions of Edwards AFB (Basgall and Overly 2004). To explore this phenomenon, I conducted a comprehensive literature review and compiled obsidian source and hydration data from 48 reports and supplemented these data with new source and hydration analysis of 39 specimens selected from the collections curated at Edwards AFB. Analyses of these data produced trends in the frequency of Coso obsidian that run counter to those observed by previous researchers. That is, analyses conducted using a more comprehensive and

representative database indicate that Coso obsidian frequency did not decline in the late Holocene, but remained at economically significant levels. I conclude that earlier reports of the declining frequency of Coso obsidian resulted from sampling bias. The implication of this finding is that, contrary to widely accepted ideas related to cultural patterns associated with lithic procurement, prehistoric people residing in this portion of the Western Mojave Desert continued to acquire and use obsidian at a relatively constant rate throughout the late Holocene.

### Geologic and Environmental Contexts for Edwards AFB

Edwards AFB encompasses approximately 310,000 acres near the center of the southern California's Antelope Valley, which is within the western Mojave Desert (Figure 1). The Antelope Valley also forms the extreme southwestern portion of the Great Basin. Roughly triangular in shape, the Antelope Valley is defined by the Tehachapi Mountains to the northwest, the San Gabriel Mountains to the southwest, and by a poorly defined eastern boundary that is generally considered to stretch northward from Big Rock Creek, near the small community of Llano, in foothills of the San Gabriel Mountains, where it passes through Kramer Junction before terminating in the Rand Mountains near Randsburg, California (Earle et al. 1997). The most notable geologic features of Edwards AFB are three Pleistocene dry lakebeds; in decreasing order of size these are Rogers, Rosamond, and Buckhorn lakes (Figure 2) which represent the lowest portions of the Antelope Valley (2,270 feet above sea level). These lakes are

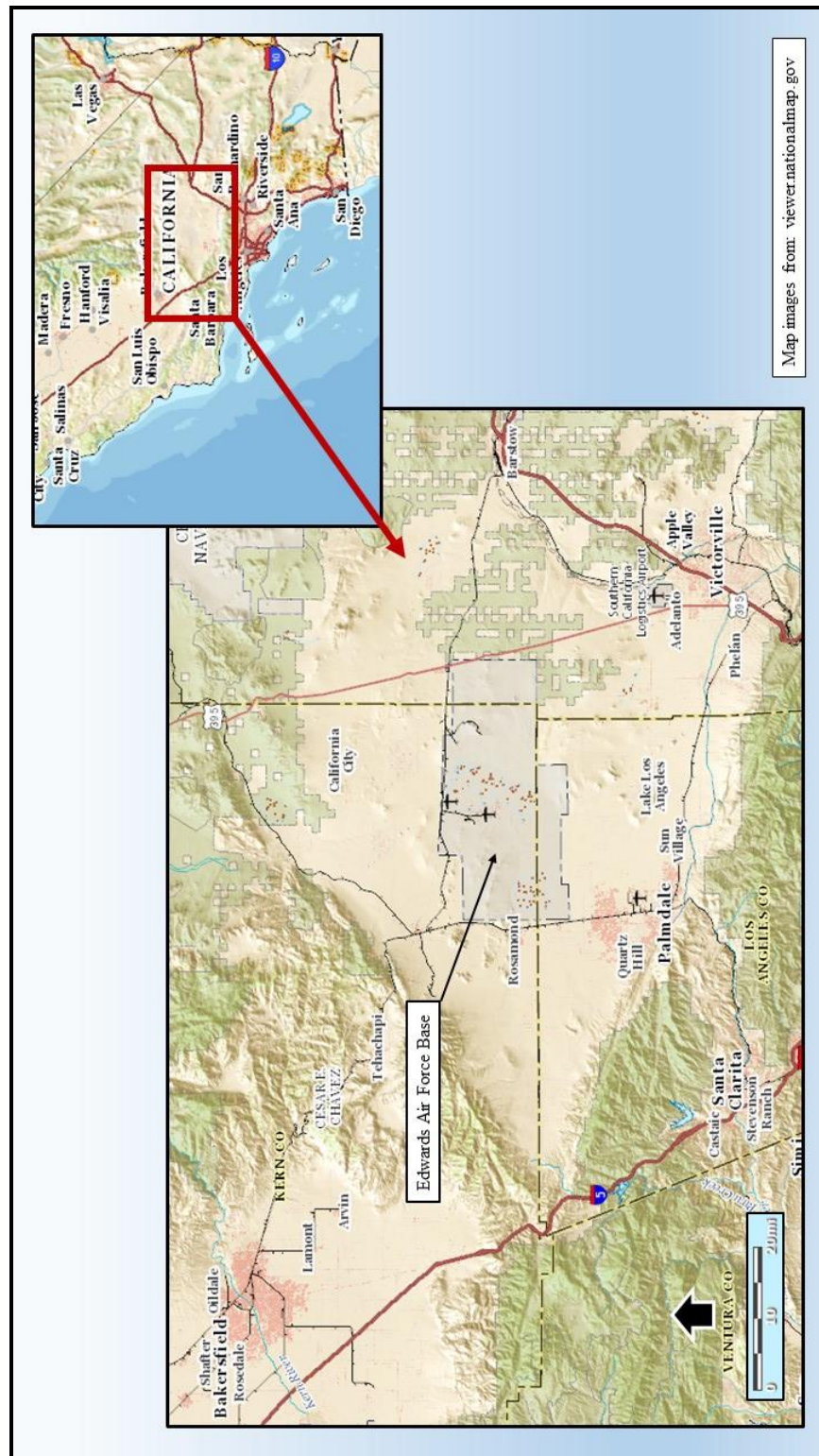
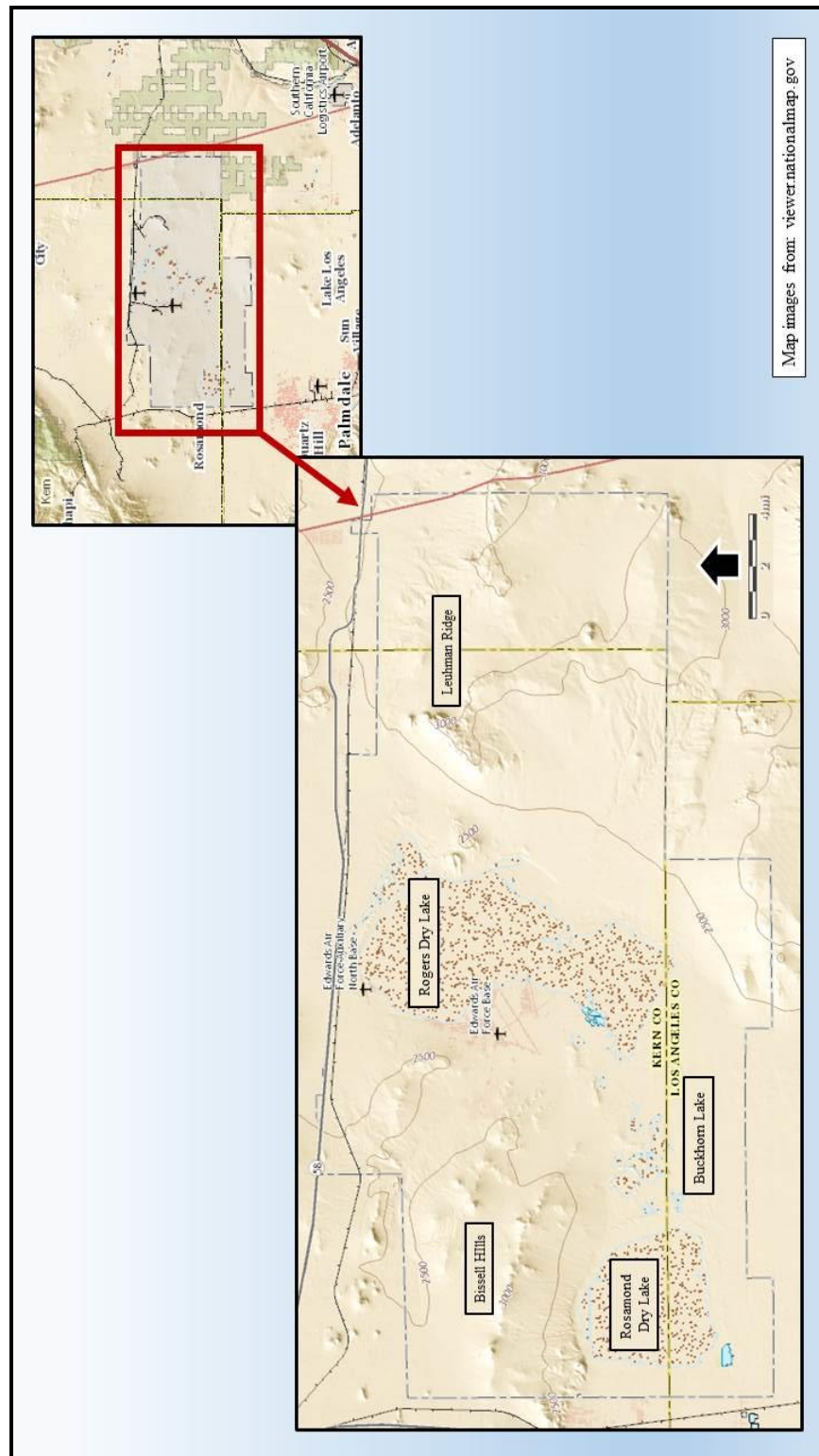


Figure 1. The Edwards AFB Vicinity.



Map images from: [viewer.nationalmap.gov](http://viewer.nationalmap.gov)

Figure 2. The Major Land Features of Edwards AFB.



themselves the remnants of the even earlier Pleistocene Lake Thompson which began desiccating sometime around 17,000 B.P. (Orme and Yuretich 2004).

Lake Thompson's lengthy desiccation resulted in the creation of a vast patchwork of seasonally flooded claypans separated by aeolian dunes that are scattered throughout the low lying interstitial areas between and adjacent to the larger dry lakes. While it was not part of Lake Thompson, the Bissell Basin, located in the northwest portion of the base, also contains a mosaic of seasonally flooded claypans and aeolian dunes. The dry lakes are bracketed by the Rosamond and Bissell Hills in the west and by Leuhman Ridge in the east, which represents the highest elevation on the base (3,400 feet above sea level). East of Leuhman Ridge, the landform consists of broad alluvial plains sporadically cut by seasonal drainages with very few areas of claypan that retain water.

The soils found within Edwards AFB are poorly developed and consist primarily of "a complex suite of lacustrine, aeolian, and fluvial deposits" of Quaternary alluvium, however pre-Quaternary igneous and metamorphic rock formations comprise the Rosamond and Bissell Hills as well as Leuhman Ridge (Orme and Yuretich 2004:2). Found anywhere from 50 to 150 centimeters (cm) below the ground surface is a caliche layer dating to the mid to late Pleistocene, beneath which no cultural deposits are found (Earle et al. 1997). In addition, a combination of sparse vegetation and strong westerly winds has a significant effect on the landscape. The wind is an especially prominent natural phenomenon at Edwards; newcomers to the installation are advised that the

windy season begins on the first of January and lasts until the thirty-first of December.

The vegetation community present on Edwards is Mojave Desert scrub (Vasek and Barbour 1977) consisting of four communities: saltbush (halophytic and xerophytic) scrub, creosote bush scrub, Joshua tree woodland, and mesquite bosque (Sawyer 1994) and ethnographic accounts indicate upwards of 90 plants from all four communities were used by the prehistoric people inhabiting the region. These vegetation communities support a wide range of both large (bobcats, badgers, and coyotes) and small mammals (rats, rabbits, and squirrels), birds (dove, raven, quail, and a variety of raptors), reptiles (desert tortoise, snakes, and lizards), and insects (ants, tarantulas, and grasshoppers), while the dry lakes support three varieties of fairy shrimp (Earle et al. 1997). Due to Edwards' position in the Pacific Flyway, the seasonally flooded lakebeds and claypans "become productive wetlands temporarily supporting a variety of hydrophytes, invertebrates, waterfowl, and shore birds" (Earle et al. 1997:49) which undoubtedly drew prehistoric people to those locations.

### Preservation Issues

A factor of the broader landscape, archaeological sites on Edwards AFB are commonly found in areas of open exposure with little in the way of vegetation (Figure 3). While this provides excellent surface visibility for archaeologists surveying for new sites, when combined with the aforementioned high energy



Figure 3. Photograph of a Typical Prehistoric Site on Edwards AFB.

environmental conditions the result is a highly dynamic landscape that complicates archaeological excavations in that there is very little in the way of vertical deposition or truly stratified deposits. Rather, in those sites with evidence of long term habitation it typically manifests as horizontal deposition. Indeed, some locations at Edwards AFB exhibit vertical stratification in archaeological deposits; however, these locations are primarily found in stabilized dunes or accreted alluvial deposits (Byrd 1996).

A recently completed year-long monitoring study of some 30 sites spread throughout three of the five Management Regions provides insight into the preservation issues affecting sites on Edwards AFB. In this study, archaeologists established a sub-datum near artifact deposits at three prehistoric sites from which they established a 1 meter (m) square grid that was used to document the movement of artifacts throughout the year. Over the course of three visits, the archaeologists documented fluctuations in the number of artifacts within the grid; in some cases previously undocumented artifacts appeared within the grid, and in other cases previously documented artifacts were found outside the grid. In some instances, individual artifacts moved more than 20 centimeters (cm) between visits (Anderson 2016). While animal tracks were noted in the mapping grid on a few occasions, the constant aeolian activity characteristic of the Western Mojave is the most probable cause for the observed changes in the disposition of the surface artifacts.

In another portion of this study, the archaeologists documented the immediate aftermath of a modern fire hearth created as part of an Air Force training mission. A follow up visit to the modern hearth was conducted several months later at which time the archaeologists noted that aeolian activity had removed all the charcoal remnants observed during the initial visit (Nathan Anderson, personal communication 2016). The implication of the findings made during this study with regard to the theory and science of obsidian hydration dating are discussed further in Chapter Two. The basic conclusion is that these post depositional processes can have a substantial effect on the specimens available to archaeologists for sampling during fieldwork and as well as for determinations of association. The dynamics of spatial association and dissociation at Edwards AFB undoubtedly affect results from standard archaeological field methods where relatively small analytical units (shovel test pits or 1x1 m test units) are typically employed. Rather, more systematic surface collection or in-field sampling are likely to be more efficacious in understanding the broader archaeological deposits.

#### Cultural Context for Edwards AFB

In his discussion of California's desert region, Warren (1984) presents a synthesis of the competing cultural chronologies developed by different researchers. In their overview of the culture history for Edwards AFB, Earle and companions (1997) note that researchers have struggled to develop a widely accepted prehistoric cultural chronology for the western Mojave region primarily

because there is a scarcity of chronometric data upon which to build. Resulting from this, the culture history for Edwards borrows from other regions with minor modifications based on what little data are available. Researchers differentiate the sequences using various horizons, technologies, or stages. The chronology used for this research effort is adapted from that presented by Warren (1984), as presented in Basgall and Overly (2004), Earle et al. (1997), Giambastiani et al. (2014), and Sutton (2017); it relies primarily on time-sensitive projectile points and shell bead sequences. This chronology consists of the Lake Mojave, Pinto, Gypsum, Saratoga Springs, and Shoshonean Periods. Furthermore, based on evidence from Edwards AFB (Rondeau 2016), a late Pleistocene Fluted Point Period is proposed prior to the Lake Mojave Period (Table 1).

Ethnographic studies of the western Mojave region resulted in the delineation of a cultural geography placing Edwards AFB in what can be best described as the frontier of the Numic and Takic linguistic groups (Bettinger and Baumhoff 1982; Earle et al. 1997; Kroeber 1925). Whether this was the result of environmental factors or economically driven, the ethnographic and protohistoric settlement patterns of this region remain a subject of continued research. Currently, the region is characterized as a cultural crossroads for the Kawaiisu (Numic) to the north and the Kitanemuk and Vanyume Serrano (Takic) to the south, where it is likely that people from both linguistic groups exploited seasonally available resources (Earle et al. 1997; Sutton 2017). Although there are locations within Edwards containing evidence of repeated habitation, the

Table 1. Cultural Sequence for Edwards Air Force Base

| Cultural Period  | Approximate Time Period | Adaptive Strategy   | Cultural Markers  |
|------------------|-------------------------|---|---|
| Late Pleistocene | >11,500 B.P.            | Generalized foraging; exploitation of megafauna and smaller fauna; lakeshore habitation   | Fluted points, crescents, graters, scrapers, choppers   |
| Lake Mojave      | 11,500 to 7,500 B.P.    | Generalized foraging; shifting focus to plants and smaller fauna; occupation of wider range of landscapes and habitats  | Lake Mojave, Silverlake, and Great Basin<br>Stemmed points; crescents   |
| Pinto            | 7,500 to 4,000 B.P.     | More specialized foraging with emphasis on plant, grass seeds, and small fauna resources; potential population decline or shift to higher elevations              | Pinto and leaf-shaped points; <i>Olivella</i> beads   |
| Gypsum           | 4,000 to 1,500 B.P.     | Beginning of vegetal resource intensification; gradual population growth; settlement focused near springs and streams; incipient increase in social complexity    | Elko, Gypsum, and Humboldt points; <i>Olivella</i> beads; quartz crystals, paint, rock art  |
| Saratoga Springs | 1,500 to 700 B.P.       | Increased regional population growth inferred from increased number of sites; continued emphasis on vegetal resources, possible resurgence in artiodactyl hunting | Rose Spring and Eastgate points; <i>Olivella</i> beads; stone knives and drills, stone pipes, bone awls, milling implements                 |
| Shoshonean       | 700 to 100 B.P.         | Slight increase in seasonal sedentism and subsistence intensification, population decrease inferred from decreased number of sites                                | Desert Side-notched and Cottonwood points; ceramics; <i>Olivella</i> and steatite beads; slate pendants, incised stones, milling implements |

Note: B.P.=Before present (A.D. 1950)

characterization of the region as a seasonally exploited crossroads is supported by the fact that to date researchers have not identified any village sites within the

installation's boundaries that exhibit the hallmarks of long term prehistoric settlements, such as deep midden deposits, house pit remains, or "evidence of men, women, and children, evidence of ritual activities, an associated cemetery, and evidence of occupation during all four seasons" (Sutton 2017:1).

#### Research Setting at Edwards AFB

The history of archaeological investigations at sites on Edwards AFB dates back more than 40 years to at least the early 1970s. The earliest of those investigations were conducted by members of the (now defunct) Antelope Valley Archaeological Society (Norwood 1994). However, the first professional archaeological research began a few years later in 1976 (Basgall and Overly 2004). While the products of the Antelope Valley Archaeological Society's efforts are largely unavailable, the collections associated with the vast majority of the subsequent investigations are currently housed in the Edwards AFB curatorial facility.

In the early 1980s a series of archaeologists were employed on a short-term basis by the Air Force who were charged with the responsibility of managing Edwards' cultural resources. By 1986 the position was made permanent which afforded the base archaeologist the opportunity to develop a long-term management plan that included a standardized site classification system, a systematic sample survey of the installation, and a number of project specific site excavations (Basgall and Overly 2004; Norwood 1994). The site types and their cultural constituents relevant to this research project are shown in Table 2.



Table 2. Edwards AFB Site Types

| Site Type      | Site Constituents   |
|----------------|---|
| Base Camp      | Extensive deposits of habitation debris, including midden deposits  |
| Hearth         | Fire-affected rock features with fewer than 10 associated artifacts |
| Isolate        | A location with no more than two artifacts                          |
| Lithic Deposit | Artifact deposits comprised exclusively of flaked stone artifacts   |
| Quarry         | An area of tool stone procurement                                   |
| Rock Shelter   | Artifacts found in caves, rock shelters, or overhangs               |
| Temporary Camp | Sparse deposits of habitation debris with no associated midden      |

To assist with the administration of the resources found within an area as expansive as Edwards AFB, the base archaeologist divided the installation into five management regions (MR). The region delineations are in rough alignment with identifiably different geographic locations, however some consideration was given to Air Force mission activities (Figure 4). The five regions are: 1) Bissell Basin, 2) Rosamond Lake, 3) Central Base (i.e. Rogers Lake), 4) Air Force Research Lab (i.e. Leuhman Ridge), and 5) Precision Impact Range Area (PIRA).

The efforts of the cultural resources management (CRM) program have, to date, resulted in the survey of more than 50% of the base (excluding the surfaces of Rogers and Rosamond lakes) and the recordation of more than 2,500 prehistoric sites. In the installation's site classification system, researchers have found fewer than 15 sites containing the cultural constituents of a base camp; the majority of sites fall into one of two categories: temporary camps or lithic

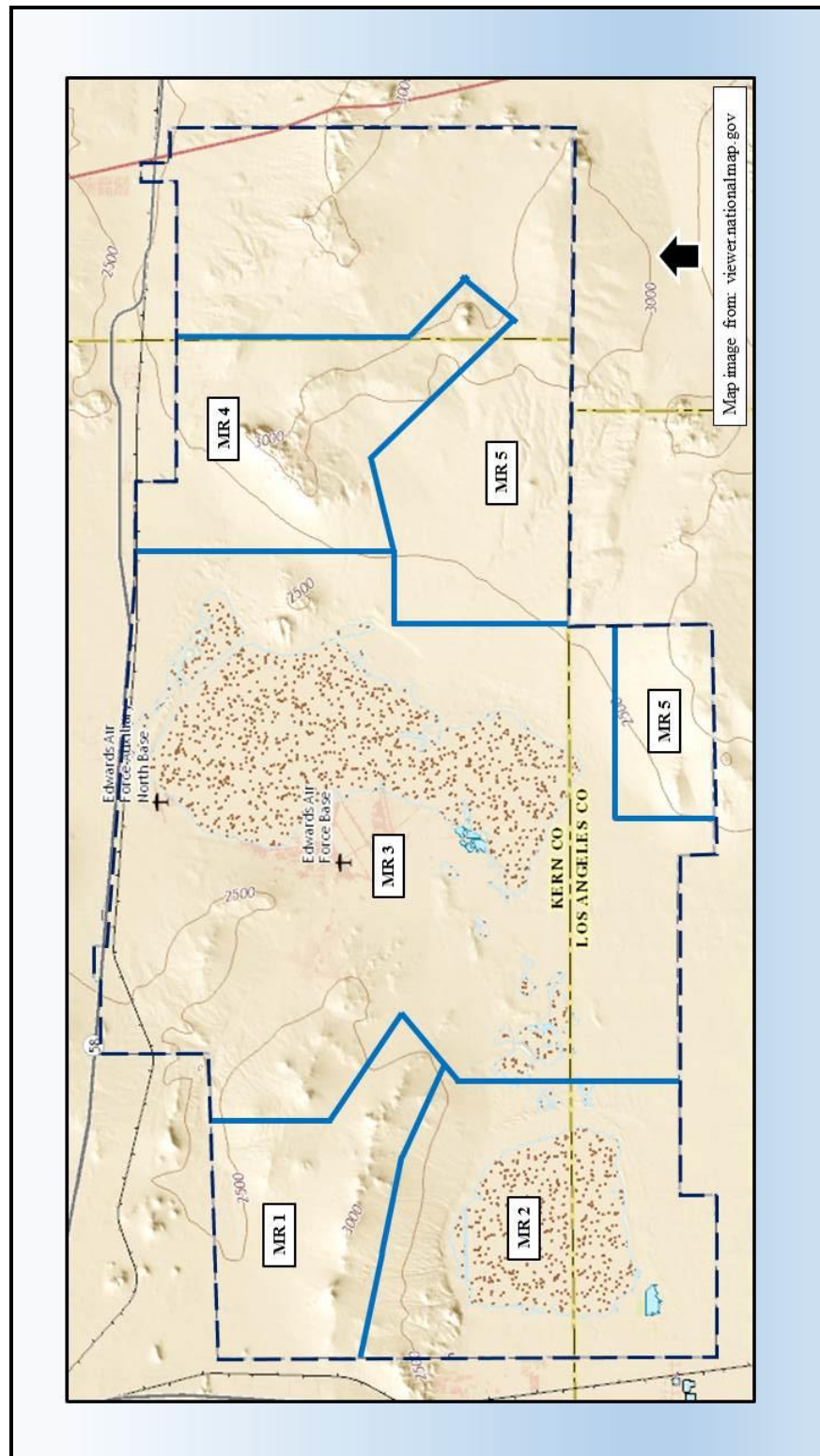


Figure 4. Management Regions of Edwards AFB.

deposits, with the remainder consisting of specialized sites such as quarries, milling stations, or hearth features.

In the mid-1990s the CRM program published an overview of the prehistoric resources (Earle et al. 1997) that summarized the results of all the earlier archaeological investigations. This overview also contained a research design intended to be the framework under which future archaeological investigations on Edwards AFB operated. The research design included research issues such as chronology, subsistence, technology, and settlement patterns among others.

Even with the umbrella research design in place, with few exceptions, the majority of the site investigations at Edwards AFB have been compliance-driven efforts intended to satisfy regulatory requirements, which meant they focused on making recommendations for National Register of Historic Places eligibility at the expense of providing substantive contributions to the understanding of Edwards' prehistory. The regulatory nature of these investigations (and the accompanying reports) has also resulted in a segmented view of the base's prehistory in that sites were frequently excavated in advance of expected impacts from federal undertakings rather than as part of a directed research effort. Even when there was no impending undertaking, many of the investigations selected sites for excavation based on the likelihood of future impacts and often consisted of a "grab-bag" of historic period and prehistoric period sites in the same study. With

that said, on the whole the reports have produced a substantial body of archaeological data that are ripe for additional research.

### Management Regions Studies

Two exceptions to the typical approach to archaeological research at Edwards AFB occurred around the year 2000 and consisted of the archaeological investigations of sites in the two western management regions. The first, conducted in 1999, involved the evaluation of 22 prehistoric loci comprising two large temporary camps in the Bissell Basin (Management Region 1) (Giambastiani and Basgall 2000). The second, conducted in 2003, involved the evaluation of 41 prehistoric sites in the vicinity of Rosamond Dry Lake (Management Region 2) (Basgall and Overly 2004). In these studies, the researchers used obsidian frequency as a proxy to analyze regional occupational intensity as well as the inhabitants' access to obsidian (Basgall and Overly 2004; Giambastiani and Basgall 2000). The researchers' conclusions on the occupational trends for the study areas were based on interpretation of obsidian hydration profiles (Figure 5 and 6) and argued that the obsidian data indicated a decline in activity beginning in the Pinto period and continuing through the Shoshonean period. As seen in each of these figures, the bulk of the hydration rim thicknesses fall between 4.0 and 10.4 microns. According to the hydration date formula proposed by the authors, this places the majority of those artifacts in the Pinto and Gypsum time periods (8000 to 1500 B.P.). For the Rosamond

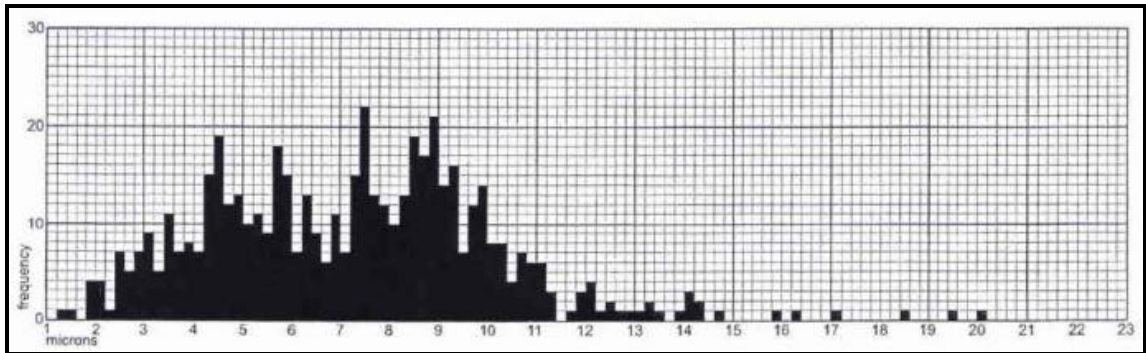


Figure 5. Aggregate Obsidian Hydration Profile for Edwards AFB as of 2000.  
 (Source: Giambastiani, M. A., and M. E. Basgall  
 2000 *An Archaeological Evaluation of Sites CA-KER-4733/H and CA-KER-2016  
 in the Bissell Basin, Edwards Air Force Base, California*).

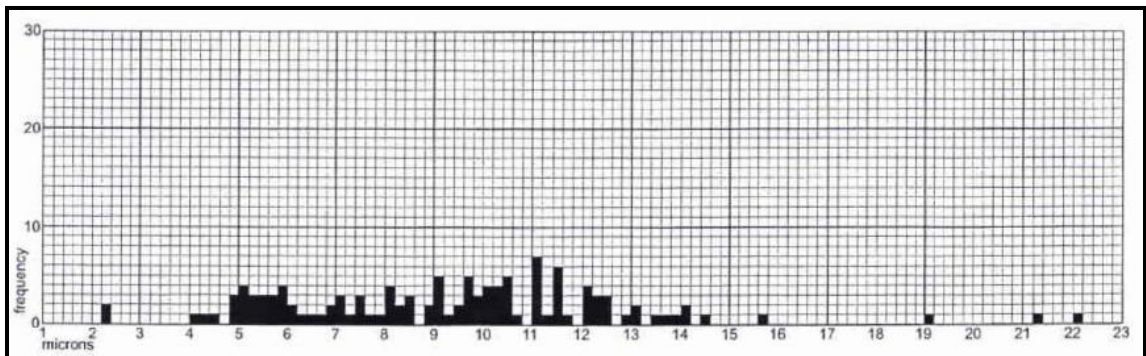


Figure 6. Rosamond Lake Obsidian Hydration Profile.  
 (Source: Basgall, M. E., and S. A. Overly,  
 2004 *Prehistoric Archaeology of the Rosamond Lake Basin: Phase II Cultural  
 Resource Evaluations at 41 Sites in Management Region 2, Edwards Air  
 Force Base, California*).

Lake hydration profile, there is a near absence of smaller hydration rim readings corresponding to the Saratoga Springs and Shoshonean time periods (1500 to 100 B.P.) (Basgall and Overly 2004).

As noteworthy as these hydration profiles appear, discussion of the projects' chronometric data did not explore the matter in any great detail. For the Rosamond Dry Lake study in particular, the authors did not arrive at a substantive conclusion other than an assumption the decline is related to unfavorable local environmental conditions in the area of Rosamond Dry Lake during the late Holocene. This lack of further exploration is reflective of the underlying regulatory nature of the studies in which the overall goal was to establish whether or not the sites subject to investigation had the potential to answer broad research questions as opposed to actually answering very specific questions about prehistoric human behavior.

### Conclusion

The central focus of this thesis is an examination of the apparent decline in obsidian hydration readings noted by previous researchers with the intent to determine whether or not it is the result of sampling bias. Most of the archaeological studies at Edwards that have identified similar declines in obsidian hydration readings have been driven by either Section 106 or 110 (of the National Historic Preservation Act) compliance projects that are focused primarily on supporting the Edwards AFB mission demands or other environmental compliance imperatives. Therefore, this thesis represents a unique opportunity to conduct an investigation of Edwards AFB archaeological data purely for research purposes. Because the fundamental concern is to establish the veracity of the trends in late prehistoric use of obsidian, it was

appropriate to conduct additional source and hydration analyses from existing collections from Edwards AFB to bolster the pool of data used to address questions of sampling bias, whether or not the trend is a localized phenomenon, and, if the trend is confirmed, to explain how these results might relate to prehistoric human behavior.

## CHAPTER TWO

### THEORETICAL ORIENTATION AND RESEARCH QUESTIONS

#### Introduction

There has been interest in the study of “primitive” hunter-gatherers long before anthropology and archaeology were formal academic disciplines. In this chapter I sketch a very brief summary of historical interest in hunter-gatherers, address the role that lithic technology plays in these studies, the contributions that obsidian dating and sourcing techniques have made to the larger realm of stone tool research, and summarize the various critiques of obsidian dating. Following this, I transition to a discussion of a theoretical framework for studying hunter-gatherers that is grounded in human behavioral ecology (HBE), beginning with its origins in Julian Steward’s (1955) seminal concept of cultural ecology in which humankind’s adaptation to the environment is used to explain culture change, and then touching on the further development of this contextual-functional paradigm during the New Archaeology. The chapter concludes with a hypothesis to be tested and further avenues of research, rooted in HBE, which may explain the phenomenon that prompted this research effort.



## Hunter-Gatherers and Lithic Technology

In the 19th century, studies of hunter-gatherers often focused on fitting these so-called exotic or primitive people into various “social evolutionary schemes” (Jordan and Cummings 2014:2). These schema were strongly influenced by ideas of social Darwinism which viewed hunter-gatherers as occupying the basal level of Tylor and Morgan’s Three-Age model of cultural evolution (i.e. Savagery → Barbarism → Civilization) (Willey and Sabloff 1993) and were intended to demonstrate the “stages in the progression of humanity toward higher levels of cultural, moral, and intellectual achievement” (Jordan and Cummings 2014:2). An implicit belief of this model was the notion that “mankind advanced through gradual emancipation from nature” (Bettinger 1991:17), which meant that the study of hunter-gatherers was, by extension, study of the earliest stages of human existence. In the early 20th century, scholars began moving beyond this often racist paradigm of cultural evolution which resulted in a flourishing interest in hunter-gatherers. However, due to the influence of American anthropologist Franz Boas, most of these studies looked at various hunter-gatherers as unique entities that could only be understood within their own context and “should always be studied on an individual case-by-case basis” (Jordan and Cummings 2014:3). By the 1930s, hunter-gatherer anthropology and archaeology began shifting away from the limitations of historic particularism and took steps toward the development of more scientific and nomothetic, or generalizing, approaches. This paradigm shift was fully realized in the 1960s and

1970s and became known as the New Archaeology which brought with it an overt goal to “be more scientific and more anthropological” (Johnson 2011:21). A wide array of individuals, each with their own ideas and approaches comprised the New Archaeology; however, a number of key themes pervaded their work. These include an emphasis on cultural evolution, systems thinking, and scientific method (including acknowledgement of researcher bias), the belief that culture was adaptive to the external environment, the idea of culture process to answer questions of ‘why’ rather than ‘when,’ and a concern with understanding variability through the examination of more than just “the biggest and best sites, or the most beautiful artifacts” (Johnson 2011:23-27).

Notwithstanding this concern with variability in archaeological research, within the realm of hunter-gatherer studies, a long-standing focus on lithic technology is undeniable. While it has been argued that stone tools do not represent humankind’s first material expression of culture (Slocum 2013:312), the fact remains that, due to preservation bias, stone tools are often the only form of material culture available for archaeologists to work with. As such, the study of lithic technology has figured prominently in a variety of archaeological problems ranging from ideas on site formation (Binford 1980), establishing chronologies (Bettinger et al. 1991; Flenniken and Wilke 1989), culture spread (Bettinger and Baumhoff 1982), mobility patterns (Bamforth 1991; Kelly 1988; Smith 2010), sedentism and technological change (Parry and Kelly 1986), technological

adaptation and change (Bleed 1986; Blitz 1988; Hildebrandt and King 2012), and prehistoric trade patterns (Eerkens et al. 2007; Scharlotta 2014) among others.

### Obsidian Analyses

One aspect of the New Archaeology of the 1950s and 1960s was an effort to incorporate other scientific disciplines and techniques in pursuit of solving archaeological problems (Johnson 2011). One important scientific tool with archaeological applications developed during the 1960s was the method of dating obsidian by measuring hydration rim thickness (Friedman and Smith 1960). As described in Volume 25 of *American Antiquity*, the dating technique is relatively simple and involves cutting one or more thin segments from an obsidian artifact, grinding the segment to a uniform thickness (approximately 0.1mm), and then using a high power microscope to measure how far, using microns for unit of measure, water had penetrated into the flaked surface of the obsidian artifact (Friedman and Smith 1960; Aitken 1990). Among archaeologists, the results of this technique for measuring how far water has penetrated into the surface of obsidian are commonly referred to as “rims,” “rinds,” and/or “microns.”

While Friedman and Smith’s (1960) initial article identified temperature as the key factor affecting obsidian’s absorption of water, subsequent studies have found that the effective hydration temperature (EHT), i.e. a mathematically derived temperature that accounts for the diurnal and annual fluctuations in temperature at an archaeological site (Rogers 2007) as well as the elemental

composition of the obsidian and the relative humidity from where it was recovered, also influence the hydration rate (Friedman et al. 1994; Friedman et al. 1997; Friedman and Long 1976; Friedman and Trembour 1983). Therefore, reliably converting the hydration rim thickness taken from an artifact to an absolute age requires knowledge of the specimen's chemical composition and the temperature at the site from which it was recovered, including the temperature regimes from past climatic conditions; whereas calculating a relative date requires only knowledge of the obsidian source and the associated hydration formula. An added benefit of the fact that each obsidian flow displays a unique elemental composition is that "these differences may be used to characterize or 'fingerprint'" obsidian sources (Jack and Carmichael 1969). The development of the obsidian dating technique combined with the implications of obsidian sourcing has allowed archaeologists to use obsidian artifacts to further explore a variety of research problems that include the introduction of new technologies (Yohe 1998), mobility (Eerkens et al. 2007), prehistoric trade (Gilreath and Hildebrandt 2011; Hughes and Milliken 2007), and the re-use of projectile points (Rogers and Yohe 2014).

Limitations and Criticisms of Hydration Dating. Despite the initial enthusiasm with the prospect of obsidian hydration dating "as an easy, inexpensive, yet powerful chronometric tool" (Ridings 1996:136), over the years that enthusiasm has fluctuated as researchers have identified shortcomings with the technique as a reliable method for absolute dating. In fact, in an article

published in the same volume of *American Antiquity* as the description of the method, researchers urged caution against the uncritical use of the dating method (Evans and Meggers 1960). Specifically, these researchers identified two problems or limitations with the method; the first technical and the second archaeological. The technical limitations relate to the geochemical properties of obsidian, as discussed earlier, and how they may affect the rate at which it hydrates. The archaeological problems concern “the inability to evaluate the possibility of re-use or accidental association of earlier objects, or the intrusion of later ones into an earlier site” resulting from inferences about the site based on the hydration date produced from a single artifact (Evans and Meggers 1960:537). The authors advise that hydration rates should be established using specimens acquired from sites where there are solid chronological data using other methods such as radiocarbon or dendrochronology (Evans and Meggers 1960).

Thirty years after Friedman and Smith’s (1960) influential article, Basgall (1990) grappled with the problem of researchers using site specific or local region specific hydration rate formulae to calculate dates for Coso obsidian. To demonstrate the problem, Basgall compared dates calculated using the various formulae that had been proposed at the time. The results of this exercise were a range of dates derived from the same micron reading that varied anywhere from 10,600 to more than 88,000 years (Basgall 1990). In the spirit of Evans and Meggers (1960), Basgall developed a hydration formula for the southern third of

California that was grounded in ten solid radiocarbon-hydration pairings from a site in the Owen's Valley (Basgall 1990). That formula is:

$$\text{Years B.P.} = 31.62 \text{microns}^{2.32}$$

However, Basgall revisited this problem again 14 years later, as will be discussed in Chapter Three.

As the dating technique matured, other researchers continued to explore the problems associated with it. Ridings (1996) scrutinized the effect a region's variable surface temperature can have on the EHT used to calculate hydration dates. Specifically, she cautions that the reliability of dates derived using depth-specific EHT "are not likely to be representative of artifact hydration histories in locations where the amplitude of the annual surface temperature is large" (Ridings 1996:145-146). A few years later, Anovitz and associates (1999:735) argued "the standard [obsidian hydration dating] equations are inappropriate and that traditional optical measurements are inherently flawed." This argument was based on analytic comparisons of hydration dates derived from artifacts recovered from a number of different Mesoamerican sites with firmly established chronologies. The findings led the authors to argue that there is "a fundamental problem with the [obsidian hydration dating] method which ... lies in the use of an inappropriate model of the hydration process, and the inherent inaccuracy of the optical measurements" (Anovitz et al. 1999:736). Despite these criticisms,

traditional optical measurement remains the most frequently used method for measuring hydration rinds. The traditional optical measurement method was employed for this thesis in order to ensure the new data were comparable to the data generated by previous researchers. Meanwhile, researchers continue efforts to improve and refine obsidian hydration rate formulae (Hull 2001; King 2004; Rogers 2008, 2017; Rogers and Yohe 2011; Stevens 2002, 2005).

### Human Behavioral Ecology

For studies of prehistoric people living in an environment as marginal as the Western Mojave Desert, it is appropriate to examine the patterns of their behavior through a theoretical framework grounded in the interactions of humans and their environment. Early 20th century attempts by scholars to explore the role the environment played with regard to culture and cultural variation fall into three general categories. Initial efforts to tackle this issue, exemplified by geographer Huntington who argued “certain climatic conditions are especially favorable to human progress, and that the greatest progress usually takes place in regions where those conditions are most closely approached” (1922:xii), were eventually viewed as overly deterministic and steeped in the outdated concept of progressive cultural evolution. In contrast to Huntington, Kroeber (1939) viewed the environment as a constraining or limiting but not determining factor for cultural behavior and variability; a view commonly referred to as “environmental possibilism.” Finally, Steward (1955:5) presented a less deterministic or possibilistic “method for recognizing the ways in which culture change is induced

by adaptation to environment.” Steward called this adaptation cultural ecology, and argued that it was a creative process between environment and culture.

Although cultural ecology is considered by some to be the precursor to HBE (Kelly 2007; Winterhalder and Smith 1992), Steward was not the only scholar in the 1950s to consider the relationship between environment and culture (Meggers 1955). Johnson (2011:173) describes cultural ecology as “the belief that societies will be more or less adapted to their material environment, and therefore that the characteristics of those societies can be explained in terms of such adaptation.” As groundbreaking as cultural ecology was in the 1950s for supplanting environmental possibilism with a rudimentary concept of environmental adaptation it was not nomothetic because it “[sought] to explain the origin of particular cultural features and patterns which characterize different areas *rather than to derive general principles applicable to any cultural-environmental situation*” (Steward 1955:36; emphasis added). For the New Archaeologists of the 1960s, cultural ecology lacked the generalizing scientific laws that were a fundamental part of the ethos. Essentially, cultural ecology fell out of favor because Steward “never came up with an explanation or mechanism for adaptive optimization” (Winterhalder and Smith 1992:21).

Despite the perceived shortcomings and accompanying criticisms, like people building atop the collapsed ruins of a previous culture, other scholars built on the theoretical foundation established by cultural ecology, leading to a host of ecology based research. Human behavioral ecology is a broad theoretical



umbrella under which can be found a variety of more narrowly focused theories and models for explaining human behavior. The types of models used include, but are not limited to, those for predicting prey choice or diet breadth, technological changes associated with improvements in handling efficiency, and predictions of changes in territoriality and interpersonal violence (Broughton and O'Connell 1999). Proponents of this theoretical approach tout it as providing a solid framework for being able to answer questions such as why there were prehistoric people living in a region (like the Great Basin) who shared culture, language, and technology, but who displayed vastly different logistic mobility and subsistence strategies (i.e. full-time foragers versus full-time collectors) (Bettinger 1991).

The publication of *Theory of Culture Change* (Steward 1955) spawned a wide range of ecology based research under a bewildering array of names used to describe the approach – evolutionary ecology, behavioral ecology, and human behavioral ecology being the most common. Regardless of the name used, they all share a common theoretical underpinning: a neo-Darwinian “application of natural selection theory to the study of adaption and biological design in an ecological setting” (Winterhalder and Smith 1992:5). Implicit in this is the underlying notion of biological fitness as contributing to human adaptive behavior. One reason for the success of the various ecological theoretical approaches is that they employ the type of hypothetico-deductive-nomological models that the New Archaeology found so appealing. Proponents of the

ecological approach argue its strengths include that it is 1) comprehensive in that it can be used to create predictions of nearly any type of biological fitness related behavior; 2) integrative in that it can be used to predict connections between variation in different facets of behavior; and 3) produces models that are testable and which can be proven empirically false (Broughton and O'Connell 1999). Typically, the application of ecological theory begins with a question related to human behavior as it applies to biological fitness and the development of optimality models against which the behavior is tested. These models,

... require hypotheses about a possible fitness-related goal for the behavior of interest, the alternate strategies to achieve that goal (including constraints that limit the field of possible strategies), the costs and benefits associated with each strategy, and the currencies in which those costs and benefits are to be measured. Combined in model form, these hypotheses predict an optimal pattern of behavior. Comparison between predicted and observed behaviors constitutes a test. Any mismatch implies that one or more hypotheses involving the available strategies, constraints, costs and benefits of different strategies, or currencies, is false [Broughton and O'Connell 1999:153-154].

Arguably the most recognized and well developed model employed by HBE is optimal foraging theory. Originally adapted from biology, optimal foraging

theory actually falls within a subset of models that attend “to the rational decision making of individuals under a set of specified conditions that include limited resources and unlimited needs” (Bettinger 1991:84-85). Among these are models for predicting diet choice, foraging location, duration, and group size, and settlement location. The anthropological application of optimal foraging theory “asserts that in certain arenas, human decisions are made to maximize the net *rate of energy gain*” (Bettinger 1991:84; emphasis in original). Based on these definitions and the heavy use of “simple” mathematical models, it is fair to say that optimal foraging theory appears overly mechanistic. However, unlike Leslie White’s concept of culture as the mechanism by which humans “harness and control energy so that it may be put to work in man’s service” (1949:367) proponents of HBE argue the difference is that optimal foraging theory is grounded in seeking explanations for variability in human behavior. Furthermore,

It also is important to emphasize that this approach does *not* imply that selection will produce the “best imaginable” designs or behaviors ... On the contrary, the optimization logic predicts only that selection will tend to favor the best strategy among *a defined set of alternatives possible in the context of interest*. It makes no claim about optimization in any absolute sense [Broughton and O’Connell 1999:154; emphasis in original].

## Obsidian Use, Edwards AFB, and Human Behavioral Ecology

Having presented a synopsis of HBE, I now turn my attention to back how that theoretical framework may elucidate the pattern of obsidian use that inspired this thesis. Research has indicated that when access to high quality tool stone is constrained, hunter-gatherer societies respond by showing a preference for using high-quality material to manufacture formal tools (Andrefsky 1994), such as projectile points, knives, or another tool with a sharp edge that is kept in a kit until needed. However, obsidian hydration data from work conducted in the Bissell Basin and Rosamond Dry Lake identified a potential late Holocene decline in the frequency of obsidian in that portion of the Western Mojave that roughly coincides with the Saratoga Springs period (1500 to 700 B.P.) (Basgall and Overly 2004; Giambastiani and Basgall 2000). A similar shift in toolstone quality has been noted by other researchers working in western North America, with the phenomenon being attributed variously to restricted access for the purpose of trade (Gilreath and Hildebrandt 2011), change in lithic procurement strategies associated with sedentism (Parry and Kelly 1986), or the introduction of the bow and arrow (Basgall and Giambastiani 2000; Hale et al. 2009; Hale et al. 2010; Railey 2010).

Given that the closest source of obsidian for the prehistoric people who inhabited the Edwards AFB region is the Coso obsidian field, located approximately 70 miles (120 km) to the north, this apparent decline represents an interesting research topic because of insights into aboriginal adaptive strategies

that can be gained based on limited access to the high quality lithic resource. Therefore, the immediate goal of this thesis is to determine if the decline in obsidian hydration readings dating to the Saratoga Springs time period (indicating a decline in obsidian acquisition and use) at Edwards AFB is the result of sampling bias. If analysis shows the observed decrease in hydration readings is not due to sampling bias, then the task becomes one of explaining the phenomenon. To that end, this study will consider the possibility that the widespread adoption of the bow and arrow sometime around A.D. 500 (Blitz 1988) resulted in changes in socioeconomic strategies and/or lithic procurement strategies that influenced the use of Coso obsidian by prehistoric people inhabiting the Western Mojave. Within the larger heuristic sphere of HBE I have identified two models with the potential to explain why the prehistoric people inhabiting the Edwards AFB region during the late Holocene may have used less obsidian after the bow and arrow was adopted. Specifically, the models for time allocation (Hames 1992) and technological investment (Bettinger 2009) are employed to explain for the trans-Holocene trend in Coso obsidian use noted in two studies published in the early 2000s.

At the heart of HBE is a question that asks, “What role do ecological, social, biological, and cultural variables play in decisions? How do hunter-gatherers ... decide whether calories, protein, or something else, is the criterion with which to rank foods?” (Kelly 2007:340-341). Or, what raw material should be used for manufacturing tools? Both of the time allocation and technological

investment models attempt to predict human decision making related to resource procurement, which ultimately leads to biological success.

Hames' (1992:203) time allocation model is "founded on the basic economic assumption that time and resources are limited and have alternative uses." Under this model individual success depends on engaging in activities that maximize resource acquisition (before reaching the point of diminishing returns) while minimizing opportunity cost (i.e. the benefit lost from continued pursuit of a particular behavior). Applying this model to the decline in obsidian use at Edwards involves comparing of the cost/benefit ratio for procuring Coso obsidian to manufacture arrow points to the cost/benefit ratio of manufacturing arrow points from locally procured raw materials (i.e. chert, rhyolite, etc.).

Bettinger's (2009) technological investment model is intended to explain the conditions under which hunter-gatherer technology might improve or when one particular technology might be chosen over another. In this model, the relationship of resource procurement rate to manufacturing time for various technologies are compared in order to make inferences regarding when an individual should use less productive technologies based on lower manufacturing times. For the two competing technologies to be viable in relation to each other there are two conditions that must be met:

- (1) The costlier technology must result in a higher production rate, and

- (2) The lower producing technology must have a return rate to manufacturing time that is at least equal to the technology with a higher return [Bettinger 2009:61-62].

In situations when one technology is shown to have an equal or higher rate of return as well as a lower manufacturing time, then it is superior to the competing technology. In applying this model to the problem of the late Holocene decrease in obsidian use at Edwards, time spent acquiring raw material for an arrow point is included in the manufacturing time.

### Research Questions

Returning to the heart of this thesis, the goal is to determine whether or not the trend in obsidian frequency observed by past researchers is the result of sampling bias. To address this, I developed two simple, yet potentially informative research questions:

1. Does the frequency of obsidian hydration dates across Edwards AFB drop from the Gypsum to the Shoshonean time periods?
2. Are there regional differences in the frequency of obsidian hydration dates from the Gypsum to the Shoshonean time periods?

An answer of “yes” to the first question, then, would support the findings of previous researchers who had assumed a positive correlation between obsidian frequency and habitation intensity, and who had concluded that obsidian quantities declined at Edwards AFB after the Gypsum period (i.e. after 1500 B.P.). Whereas, an answer of “no” to the first question suggests that those

findings were the result of sampling bias, and that there was no diachronic change in habitation intensity at Edwards AFB during the late Holocene.

The second research question seeks to focus in on the trends in obsidian hydration date frequency at a level that is more refined than the entirety of Edwards AFB. A “yes” answer to the second question might ameliorate the finding of sampling bias in the previous researchers’ conclusions if the regional patterns are similar to those presented for the regions where their studies were focused. On the other hand, a “no” answer to the second question would reinforce the finding that those findings were the product of sampling bias, and lend further support to the notion that habitation intensity did not change during the late Holocene.

In the event that analysis of the data produces a “yes” answer to either question, then several additional avenues of research, and associated data needs, open up that might provide an explanation for a reduction in the number of obsidian hydration dates associated with the prehistoric people residing in the Western Mojave Desert during the late Holocene. These research questions include:

- Are the regional changes in the frequency of obsidian hydration dates reflective of diachronic change in habitation areas, resource exploitation, and/or mobility patterns?
- Research suggests the bow and arrow had a significant effect on late prehistoric people residing in the Great Basin and elsewhere (Basgall and



Giambastiani 2000; Bettinger 2013, 2015; Hale et al. 2009; Hale et al. 2010; Railey 2010); therefore, what role (if any) does this technological advancement play in the prevalence of obsidian hydration dates, at both the installation and regional level, during the late Holocene? Furthermore, if the bow and arrow does play a role, how does this manifest itself in the archaeological record?

Exploring these topics further requires solid chronometric (i.e. radiocarbon) samples, robust faunal and paleoethnobotanical samples, as well as habitation features such as well-developed midden deposits and/or structural remains that date to the time periods in question. To be sure, the taphonomic and other post-depositional processes at Edwards AFB present significant impediments to acquiring the types and quantities of data requirements necessary to fully explore these additional research domains. Regardless of the answers obtained, the research proposed here has the potential to provide important insights into the trans-Holocene use of obsidian in the western Mojave Desert by the prehistoric hunter-gatherers who lived in the vicinity of the area now encompassed by Edwards AFB.

## CHAPTER THREE

### RESEARCH OBJECTIVE AND METHODS

#### Introduction

The goal of this research project is to determine whether a) obsidian use among hunter-gatherers in the Western Mojave truly declined during the late Holocene or b) the phenomenon is the product of sampling bias. As discussed previously, the inspiration for this research stems from observations made from data acquired by researchers working in the vicinity of Rosamond Lake in 2003. At that time, those researchers based their analysis and discussion of the broad temporal trends of obsidian use on an obsidian data inventory that was current as of 2000 (Basgall and Overly 2003). That inventory consisted of 819 obsidian artifacts with 605 of those sourced to the Coso obsidian fields. Therefore, a primary imperative for this research was to develop an obsidian data inventory that incorporated the obsidian hydration accumulated in the intervening 16 years.

#### Research Methods

As with any scientific research endeavor, the initial step taken in pursuit of making this determination consisted of a comprehensive literature review of the published excavation reports on file at the Edwards AFB curation facility. The intent of this review was to identify all the sites where obsidian has been observed and/or recovered. A selection of reports containing obsidian source and hydration data was collected from a larger body of reports on file at the curation

facility. This subset of reports was used as the primary data source for developing an obsidian database employed to analyze the trends in obsidian use. A table of the reports that provided obsidian data is found in Appendix A and the database created from those obsidian data is found in Appendix B. The data fields included in the database are discussed below.

#### Supplemental Obsidian Data

After the obsidian database was populated with existing data, the next step consisted of an examination of the Edwards AFB artifact collections to identify obsidian specimens that had not yet been submitted for sourcing and hydration analysis. An Archaeological Survey Association (ASA) Southern California Archaeology Endowment grant provided funding for the analysis of up to 40 artifacts, so an effort was made to acquire the requisite number of specimens. In the course of conducting the literature review I discovered one project where researchers had collected obsidian artifacts from several sites, but did not submit those artifacts for sourcing or hydration analysis. The details for those sites were noted and follow up research was performed to locate artifacts from that project suitable for obsidian analyses. All told, this particular project provided 19 specimens from six sites and in all cases obsidian data had not been previously obtained from these sites. Additionally, I selected 13 artifacts from the curated collections that had been recovered from nine sites. Rounding out the specimens submitted for analysis were eight artifacts from six sites, and one isolated artifact that were collected during a survey project I directed in the spring

of 2016. The provenience and nature of each artifact selected to bolster the existing Edwards AFB obsidian data are provided in Table 3 and a map depicting the locations where the artifacts were recovered shown in Figure 7. More detailed maps of the artifact locations are found in Appendix C.

Table 3. Artifacts Selected for Sourcing and Hydration Studies

| Trinomial     | Cat No.  | Artifact | Unit (depth) | Site Type      | MR |
|---------------|----------|----------|--------------|----------------|----|
| CA-KER-1161   | 5396     | Flake    | Surface      | Temp camp      | 2  |
| CA-KER-1161   | 5397     | RTF      | Unknown      | Temp camp      | 2  |
| CA-KER-1161   | 5400     | UTF      | Unknown      | Temp camp      | 2  |
| CA-KER-11884  | 4820     | Flake    | Surface      | Temp camp      | 2  |
| CA-KER-11884  | 4819     | Flake    | Surface      | Temp camp      | 2  |
| CA-KER-533    | 246-5    | Flake    | Surface      | Temp camp      | 3  |
| CA-KER-2007   | 559-1    | Flake    | Surface      | Temp camp      | 3  |
| CA-KER-2007   | 559-12   | Flake    | ST A (0-10)  | Temp camp      | 3  |
| CA-KER-2154   | 6836     | UTF      | Unknown      | Hearth         | 3  |
| CA-KER-3273/H | 4823     | Flake    | Surface      | Temp camp      | 2  |
| CA-KER-486    | 10738    | BFF      | Surface      | Lithic Deposit | 2  |
| CA-KER-4929   | 2402-98  | Flake    | Surface      | Temp camp      | 1  |
| CA-KER-4929   | 2402-119 | Flake    | Surface      | Temp camp      | 1  |
| CA-KER-4929   | 2402-5   | Flake    | Surface      | Temp camp      | 1  |
| CA-KER-4929   | 2402-49  | Flake    | Surface      | Temp camp      | 1  |
| CA-KER-4929   | 2402-183 | Flake    | Surface      | Temp camp      | 1  |
| CA-KER-503    | 236-55   | Flake    | SS 1 (0-5)   | Lithic Deposit | 2  |
| CA-KER-503    | 236-66   | Flake    | SS 1 (0-5)   | Lithic Deposit | 2  |
| CA-KER-503    | 236-40   | Flake    | TU 2 (40-50) | Lithic Deposit | 2  |
| CA-KER-5661   | 10742    | RSP      | Surface      | Temp camp      | 2  |
| CA-KER-698/H  | 10691    | Flake    | STP 12 (0)   | Temp camp      | 3  |
| CA-KER-7578   | 4188-172 | Flake    | Surface      | Temp camp      | 1  |
| CA-KER-7578   | 4188-95  | Flake    | Surface      | Temp camp      | 1  |
| CA-KER-7578   | 4188-182 | Flake    | ST 6 (0-10)  | Temp camp      | 1  |
| CA-LAN-1189/H | 400-22   | Dart     | 121 (0-5)    | Temp camp      | 5  |
| CA-LAN-1189/H | 400-46   | PTF      | Surface      | Temp camp      | 5  |
| CA-LAN-1307   | 616-1    | RSP      | Surface      | Temp camp      | 3  |
| CA-LAN-1465/H | 4024     | Flake    | Surface      | Isolate        | 2  |
| CA-LAN-2397   | 2021-27b | Flake    | ST 2 (0)     | Temp camp      | 3  |

| Trinomial   | Cat No.  | Artifact | Unit (depth) | Site Type      | MR |
|-------------|----------|----------|--------------|----------------|----|
| CA-LAN-2397 | 2021-2   | Flake    | Surface      | Temp camp      | 3  |
| CA-LAN-2397 | 2021-13  | Flake    | Surface      | Temp camp      | 3  |
| CA-LAN-2397 | 2021-22  | Flake    | Surface      | Temp camp      | 3  |
| CA-LAN-2397 | 2021-27a | Flake    | ST 2 (0)     | Temp camp      | 3  |
| CA-LAN-716  | 10818    | Flake    | Surface      | Temp camp      | 2  |
| CA-LAN-716  | 10819    | Flake    | Surface      | Temp camp      | 2  |
| Isolate     | 10716    | Flake    | Surface      | Isolate        | 2  |
| TBD         | 10721    | BFF      | Surface      | Lithic Deposit | 1  |
| TBD         | 10727    | LMO      | Surface      | Lithic Deposit | 2  |
| TBD         | 10729    | Flake    | STP 13 (0)   | Temp camp      | 2  |
| TBD         | 10735    | BFF      | Surface      | Temp camp      | 2  |

Notes: BFF = Biface fragment; LMO = Lake Mojve point; MR = Management region; PTF = Point fragment; RSP = Rose spring point; RTF = Retouched flake; SS = Shovel scrape; ST = Shovel test; STP = Shovel test pit; TBD = To be determined; Temp = Temporary; TU = Test unit; UTF = Utilized flake

These 40 obsidian specimens were first sent to Dr. Richard Hughes' Geochemical Research Laboratory where they underwent non-destructive energy dispersive X-ray fluorescence (XRF) analysis to determine the quantitative elemental composition estimates necessary to identify the source flows for each artifact. Following the completion of source analysis, the specimens were shipped to Origer's Obsidian Laboratory where thin sections were prepared and hydration band measurements taken. The laboratory reports for both the sourcing and hydration analyses are found in Appendix D.

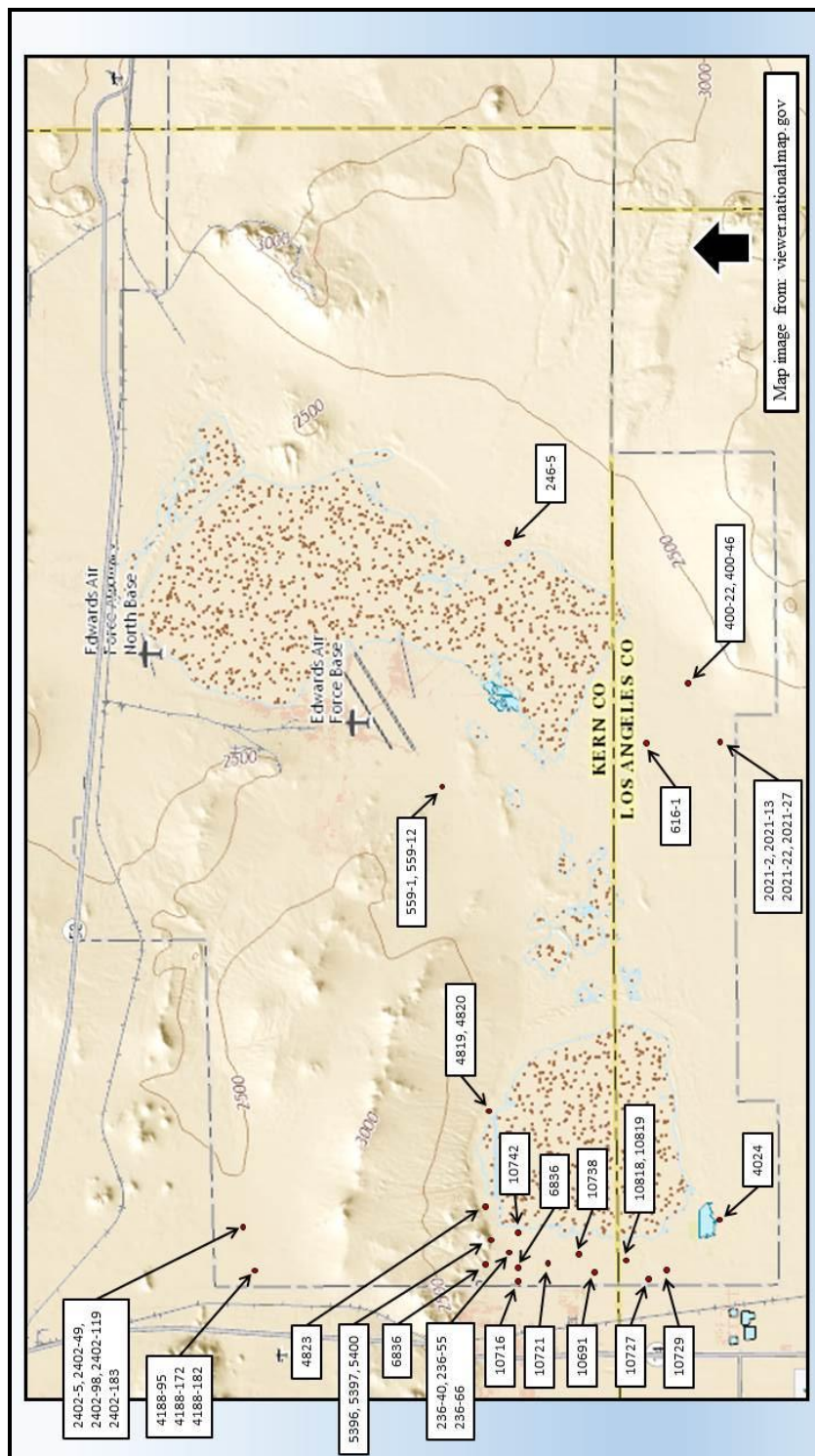


Figure 7. Artifacts Selected for Source and Hydration Analysis.

Supplemental source data. While entering data from the existing obsidian reports it became clear that several hundred specimens had been cut for hydration without having been sourced. Because they were unsourced, these hydration readings would be excluded from my analysis, therefore I pursued a way to source as many of these artifacts as possible in order to maximize the total sample. The details for these artifacts (project and site number, catalog number, and artifact description) were noted and follow up research was conducted to locate as many of those artifacts that were suitable for source identification. In this case two factors reduced the overall quantity of cut but not sourced artifacts pulled from the Edwards AFB collection. Specimens where a hydration rim could not be measured by the laboratory were excluded, as were specimens that were either completely destroyed or returned as small chips as part of the hydration analysis. All told, 120 artifacts were removed from the collection for sourcing.

Over the course of a month, with the assistance of Geological Sciences professor Dr. Erik Melchiorre, I conducted XRF analysis of those 120 artifacts at the California State University San Bernardino (CSUSB) College of Natural Sciences, Geological Sciences department laboratory. The XRF analysis was accomplished using a Niton<sup>TM</sup> FXL FM-XRF, which is a portable, bench-top-style elemental analyzer (Figure 8). During this process, one of the artifacts was excluded for analysis because it was determined too small. Therefore, a total of 119 artifacts that had been cut for hydration, but not sourced, were analyzed.

The readings from these analyses were output into an Excel workbook containing the quantities (in parts per million) for 39 elements for each artifact. To interpret the data I consulted with Jimmy Daniels, an archaeologist employed by

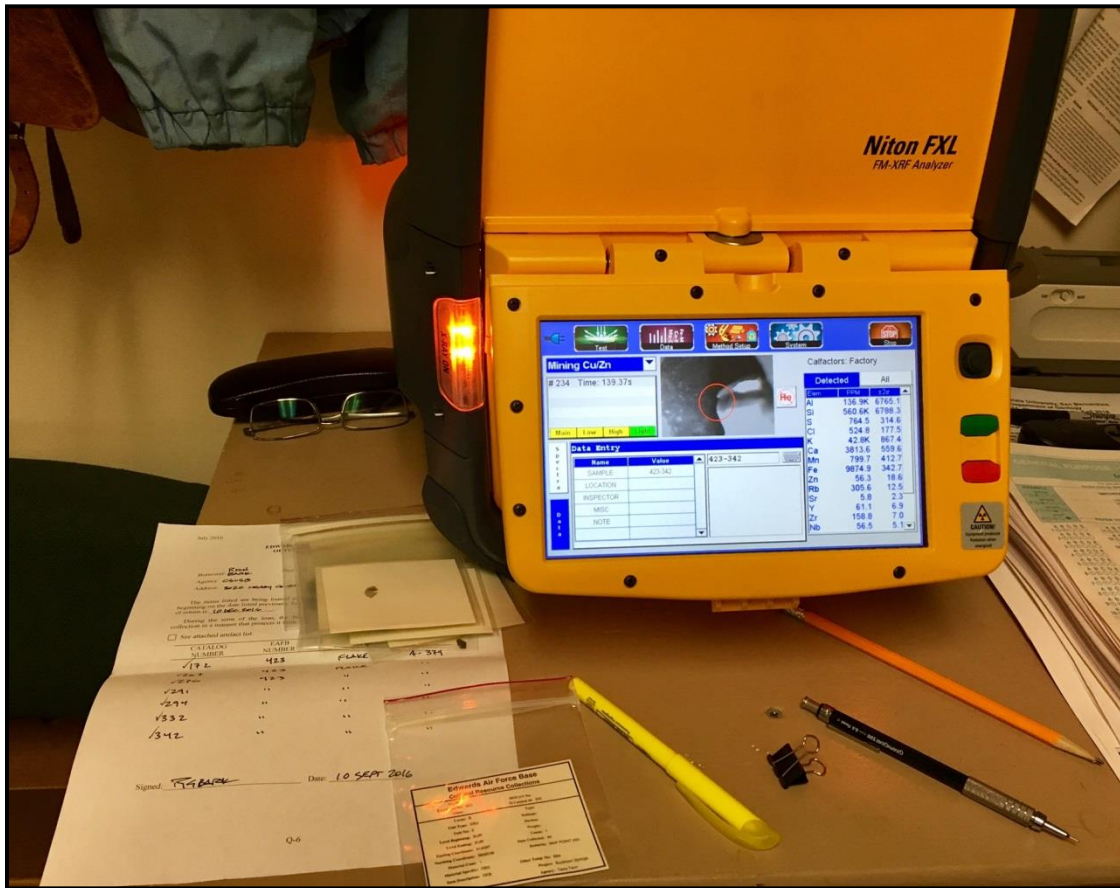


Figure 8. X-ray Fluorescence Analysis in Progress.

ASM Affiliates, who regularly conducts obsidian source analysis in the course of his professional work. Mr. Daniels plotted the elemental readings produced from my analysis against an obsidian source data library and determined the probability of each specimen “belonging to a source reference group based on a



canonical discriminant analysis” (Jimmy Daniels, personal communications 2017). Canonical discriminant analysis is a type of multivariate analysis that derives “linear combinations of interval variables that summarize between-class variation in much the same way that principal components summarize total variation” (SAS Institute Inc. 1999). The results of this source analysis were then incorporated into the main obsidian database. Of the 119 specimens analyzed, only four were not confidently assigned a sub-source. However, each of these four specimens was attributed to the Coso volcanic fields with the uncertainty lying in the sub-source. In the end, that uncertainty had no bearing on my findings because my analysis was limited to looking only at the broader obsidian sources. The obsidian source analysis table and associated plots are also included in Appendix D.

#### Obsidian Database Fields

The database created from the existing obsidian source and hydration reports included both administrative and analytical fields. A brief explanation of each field follows.

- **Project number** – The Edwards AFB CRM program assigns a unique identifier to every effort that produces archaeological data. This is an administrative field not included in the final table.
- **EAFB number** – The Edwards AFB CRM program assigns a unique identifier to minimize confusion associated with trinomials from three counties. This is an administrative field not included in the final table.

- **Trinomial** – The official identifier assigned by the California Historic Resources Information System.
- **Catalog number** – The number assigned to the obsidian specimen as indicated in the project report or obsidian study report if no catalog was present. The format used for catalog numbers found in older reports often varied from project to project, hence the lack of standardized numbering in this field.
- **Artifact** – A description of the obsidian specimen as described in the project report catalog or obsidian study report if no catalog was present. The artifact descriptions from some of the older reports did not conform to the Edwards AFB artifact classification system; in those instances an updated description was entered into this field.
- **Unit** – The type of unit, the unit number (if known) and the depth from which the obsidian specimen was recovered. Artifacts collected from the surface are indicated as such.
- **Raw Micron** – The mean hydration rim measurement, in microns, that appears in the hydration report. Further discussion on this appears below.
- **Raw Years BP** – The date derived from the above micron reading using the hydration rate formula from Basgall and Overly (2004).
- **Adjusted Microns** – An adjusted hydration rim thickness reading based on a proposed correction factor for obsidian recovered from Edwards AFB (Basgall and Overly 2004). This is discussed in further detail, below.

- **Adjusted Years BP** – The date derived from the adjusted micron reading using the hydration rate formula from Basgall and Overly (2004). This is also discussed further, below.
- **Time Period** – The culture chronology time period corresponding to the adjusted years B.P.
- **Source** – The obsidian source that provided the raw material comprising the artifact as determined by the artifact-to-source analysis. This is discussed in further detail, below.
- **Sub-source** – Many obsidian sources are known to have chemically distinct flows, that information is documented here.
- **Management Region** – As described in Chapter One, the general geographic region from where the obsidian specimen was recovered.
- **Management Area** – The subdivided area within each of the five management regions from where the obsidian specimen was recovered.
- **Comments** – This field was used to capture a variety of different comments that were made about the artifacts in the source reports. These comments included, but were not limited to, whether the hydration rim was diffuse, the artifact was weathered, or if more than one rim thickness was measured. This is an administrative field not included in the final table.

Micron Reading Discussion. In the more than 40 years that formal archaeological investigation has occurred on Edwards AFB, it came as no surprise that researchers employed the services of a variety of different

laboratories to conduct obsidian hydration analyses. While the techniques for conducting hydration readings are nominally the same for each lab, in the course of compiling the hydration database for this thesis, reviewing the hydration reports revealed that the manner in which the data are presented varied between labs as well as over time. For instance, some labs merely provided the mean rim thickness reading, while others provided a range of micron readings and a corresponding mean. Additionally, while most labs provided hydration rims measured to two significant digits, other labs measured to three. Therefore, when preparing the hydration database for this research, the micron readings were rounded to two significant digits using the “Banker’s Rule” in which digits “followed by a 5 that [are] either standing alone or followed by zeros [are] rounded to the nearest even number” (VanPool and Leonard 2011:22). For example, hydration rim measurements of 4.23 and 4.25 were rounded to 4.2 microns, while measurements of 4.35 and 4.36 were rounded to 4.4 microns. The rationale for this rule is that “about half the time the number will be rounded up, and half the time it will be rounded down” (VanPool and Leonard 2011:22).

Another factor that had to be accounted for when compiling the data from the obsidian hydration reports was the presentation of rims with variable widths. Only a few specimens from the entire suite of hydration reports were noted as having variable widths. For those six artifacts, a mean rim thickness was derived using the minimum and maximum readings provided in the hydration report.

A final factor that had to be considered when compiling data from the obsidian hydration reports was accounting for artifacts where two hydration rim readings were reported. After careful consideration of the problem, a decision was made to enter each micron reading as a separate line of data with an entry in the comments column indicating whether the micron measurement corresponded to “band 1” or “band 2” as noted in the original report. For the purpose of using this database for analysis, both bands were included in analyses that looked at patterns in dates. However, only “band 1” was used for analyses that looked at artifact frequencies, etc.

Obsidian Source Discussion. Similar to the above discussion, over the years, researchers working at Edwards AFB have also employed a variety of different obsidian sourcing laboratories. The implications of this situation for this study are twofold. First, each lab presented their source data slightly differently and frequently used different marker elements to identify particular obsidian sources. Second, as time passed and more analyses were conducted the various labs refined their source data library of elemental markers used to identify specific sources or sub-sources. Whereas older source reports merely attributed obsidian artifacts to the Coso fields in general, later reports began to differentiate between the various flows. Furthermore, older reports might identify a source as “unknown” because that specific flow was not in the lab’s library, while those same sources are identified in later reports due to the lab’s accumulation of more comparative source data. The end result being that while analyses related to

primary obsidian sources are possible, analyses conducted on the sub-source level are unreliable.

Adjusted Microns and Calculated Date Discussion. As noted in Chapter Two, there are a number of competing theories related to the formula used to convert hydration rim readings to calendrical years. While this thesis is based on observations made in Basgall and Overly's 2004 excavation report, it is necessary to provide some additional context regarding the hydration date formula used in that report and in this thesis. Although Basgall (1990) proposed a formula for Southern California based on pairings with robust radiocarbon dates, he has revisited this problem twice while conducting research at Edwards AFB.

In 2000, Basgall co-authored a report for the excavation of two large temporary camps in the Bissell Basin (Management Region 1) (Giambastiani and Basgall 2000). At that time the researchers collected 47 obsidian artifacts, sourced to the Coso volcanic fields, from which thin slices were taken for hydration readings. To interpret those readings, the researchers developed a hydration formula based on regression analysis of diagnostic projectile points against the presumed age range for those artifacts (Giambastiani and Basgall 2000). This analysis produced a hydration formula of:

$$\text{years B.P.} = 15.18 \text{ microns}^{2.80}$$

“with a correlation coefficient (R value) of 0.988” which the researchers inferred reinforced the year-to-micron relationship of the sample (Giambastiani and Basgall 2000:43).

Several years later, when analyzing the obsidian data recovered from sites near Rosamond Dry Lake (Management Region 2), Basgall and Overly (2004) were forced to revisit the problem of the obsidian hydration rate formula for Coso obsidian. This reevaluation stemmed from a recognition that the formula developed for Bissell Basin (above) produced exceptionally old dates when applied to the hydration profile for the Rosamond Dry Lake data. The researchers expressed their concern using the following example, “micron values of 11.0 or more are common in [this] sample, and these are assigned ages in excess of 12,500 years” (Basgall and Overly 2004:57). To reconcile this problem, the researchers returned to the earlier rate formulation proposed by Basgall (1990) for Southern California which they adjusted using an EHT derived from long term climate data from the nearby city of Lancaster, CA. Based on the slightly higher EHT for the region, the researchers assumed Coso obsidian found at Edwards AFB should hydrate at a slightly faster rate.

Scrutiny of the dates derived using Basgall's (1990) formula adjusted for the local EHT, however, proved problematic for the researchers because the “results were inconsistent with the [Edwards] hydration distributions” which lead them to believe that obsidian found at Edwards AFB actually hydrates at a slower rate than it does in the Owen's Valley (Basgall and Overly 2004:57). Further

reflection on the problem prompted Basgall and Overly to propose a correction factor that should be used when calculating hydration dates for obsidian recovered from the Edwards AFB region. Specifically, they recommend micron readings should be multiplied by 1.05 before employing Basgall's (1990) rate for the Owen's Valley. For example, a reading of 12.0 microns multiplied by 1.05 produces an adjusted reading of 12.6 microns, which converts to a date of approximately 11,290 B.P.

For the purpose of this research, then, the question is which hydration rate formula to use to convert the micron readings into dates for the purpose of exploring the trends in obsidian use in the Western Mojave? Ultimately, and in keeping with the research that inspired this thesis, I decided the best course of action was to employ the correction factor proposed by Basgall and Overly (2004) before using Basgall's (1990) hydration rate formula for Owens Valley:

$$\text{Years B.P.} = 31.62\text{microns}^{2.32}$$

This formula was applied to both the reported (i.e. "raw microns") and adjusted micron readings produced from applying the correction factor. Analyses to explore the problem of late Holocene obsidian decline were conducted using the adjusted dates; however dates derived from the raw micron readings are included for comparative purposes.



Despite the presentation of hydration dates in Appendix B in absolute form, the potential for variability in those dates should be considered due to the, as of yet, unresolved limitations with hydration dating noted in Chapter Two. While determining the various contributing factors and, more importantly, establishing a solid hydration date formula for Coso obsidian found at Edwards AFB is an avenue of research clearly deserving of further attention, it is well beyond the scope of this thesis.

#### Acknowledgement of Biases and Assumptions

In keeping with the New Archaeology, it is important to acknowledge biases that may affect any research effort and this thesis is no different. In this particular case there are two forms of bias that are inherent to any study that focuses on data derived from obsidian analyses. Specifically, due to the mechanics of sourcing and hydration rim measurements, small artifacts must be excluded. This is necessarily so because a certain minimum mass of material is required to take an accurate geochemical reading of a piece of obsidian. Similarly, the process of cutting a specimen to measure a hydration rind also required a minimum sized artifact. Therefore, small chips of obsidian, such as those produced by pressure flaking, cannot be sourced or hydrated which creates an undeniable bias. The types of bias more directly related to the context of this thesis are the site preservation issues discussed in Chapter One and the uncertainty of the hydration date formula. Since there are unanswered questions about the hydration rate for obsidian at Edwards AFB, the dates derived using

the formula proposed by Basgall and Overly (2004) should be considered relative dates until such time as research is conducted to calculate an EHT and associated hydration formula.

During the analysis conducted using the obsidian database, the following assumptions were made: 1) errors resulting from methodological differences between analysts is negligible, given the overall sample size; 2) there is internal consistency in the classification of artifacts and the projectile point types all conform to the local classification system; and 3) the obsidian source identifications expressed in the original reports are all correct. Additionally, with the exception of describing the total number of obsidian pieces found on Edwards AFB and the associated site types, only artifacts from Coso are included in the analysis. Artifacts ascribed to geochemical sources other than Coso were excluded.

### Analytical Approach

At the outset of my thesis research I was heavily influenced by the approaches employed in the earlier studies and sought to build on them by simply adding the source and hydration data accumulated since 2000 to the preexisting data and then creating similar histograms. However, as I began exploring the matter further, it became clear that in order to make meaningful comparisons the data should be organized in a manner that factored out the effects of the different lengths of time comprising each cultural time period had when quantifying the hydration dates. Additionally, at the recommendation of

CSUSB Psychology professor, Dr. Ismael Diaz, a descriptive framework was used to analyze the obsidian data. Therefore, in order to analyze the obsidian hydration data the following steps were taken:

- The micron readings were converted into dates using the correction factor and hydration date formula proposed by Basgall and Overly (2004).
- Artifacts from sources other than Coso were excluded from the pool of hydration dates because a reliable date could not be calculated.
- Hydration dates younger than 100 B.P. were excluded under the assumption they fall after European contact and may not reflect aboriginal behavior.
- Hydration dates older than 14,100 B.P. were also excluded under the assumption they fall prior to the commonly accepted human colonization of North America.

Once these steps were complete, the hydration dates were placed in bins of different intervals that were then used to create a variety of histograms that might reveal patterns in the data. To that end, intervals of 1000, 500, 250, and 100 years were used to bin the data; this process was completed for the data at the installation-wide level as well as for each of the management regions. In the case of the 100 year interval bins, only dates from the Gypsum to the Shoshonean time periods (i.e. 4000 – 100 B.P.) were organized in this manner due to increasing frequency of intervals with zero dates. Ultimately, the 250 and 100 year bins did not prove useful for identifying patterns in the trans-Holocene

abundance of obsidian, thus they are not included in my analysis. Finally, chi-square analysis was conducted on a subset of the data in order to explore the role that the introduction of the bow and arrow may have had on the obsidian frequencies at Edwards AFB. The results of these various analyses of the obsidian data are presented in the next chapter.

## CHAPTER FOUR

### OBSIDIAN ANALYSIS RESULTS

#### Introduction

Near the turn of the century two archaeological investigations were completed on Edwards AFB in which the researchers made observations about both management region specific and base wide trends in the obsidian profile that were interpreted as showing a decline in obsidian frequency during the late Holocene (Basgall and Overly 2004; Giambastiani and Basgall 2000). Given that habitation of the Edwards AFB region is known to have persisted throughout the Holocene, the decline in frequency of a high quality toolstone like obsidian is noteworthy for the potential insights the phenomenon may give researchers regarding behavioral changes of the aboriginal inhabitants of the Western Mojave. The first step in exploring this phenomenon is to determine whether the decline is real or is the product of sampling bias. In this chapter I present the results of the obsidian source and hydration studies intended to supplement the existing body of obsidian data, present some general trends in the obsidian artifacts recovered from Edwards AFB, and conclude with analyses of those data as they pertain to the research questions intended to address the larger question of sampling bias in past researchers' observation of a late Holocene decline in obsidian frequency at Edwards AFB.

### Supplemental Obsidian Data

To bolster the total sample size used to explore the trans-Holocene trend in obsidian use at Edwards AFB, I collected 40 specimens that were submitted for source and hydration analysis. The artifacts selected for this purpose were acquired from both the existing collection and from a survey I led during the spring of 2016. A total of three biface fragments, three flake-based tools, five projectile points, and 29 pieces of debitage were submitted. Of the specimens submitted for source analysis, 35 artifacts were manufactured from Coso, two from Casa Diablo, and two from Saline obsidian. The final artifact was determined to be manufactured from a stone other than obsidian (probably chert). The results of the source analysis and hydration rim readings for the 39 obsidian artifacts analyzed for this thesis are presented in Table 4.

Table 4. Results of Sourcing and Hydration Analysis

| <b>Trinomial</b> | <b>Cat No.</b> | <b>Artifact</b> | <b>Source</b> | <b>Hydration Rim</b> |
|------------------|----------------|-----------------|---------------|----------------------|
| CA-KER-1161      | 5396           | Flake           | Coso          | 10.3                 |
| CA-KER-1161      | 5397           | RTF             | Coso          | 9.7/14.4             |
| CA-KER-1161      | 5400           | UTF             | Coso          | 10.8                 |
| CA-KER-11884     | 4820           | Flake           | Coso          | 8.8                  |
| CA-KER-11884     | 4819           | Flake           | Coso          | 6.8                  |
| CA-KER-533       | 246-5          | Flake           | Coso          | 7.0                  |
| CA-KER-2007      | 559-1          | Flake           | Coso          | 9.0                  |
| CA-KER-2007      | 559-12         | Flake           | Coso          | 4.6                  |
| CA-KER-2154      | 6836           | UTF             | Coso          | 8.3                  |
| CA-KER-3273/H    | 4823           | Flake           | Coso          | 4.8                  |
| CA-KER-486       | 10738          | BFF             | Coso          | 6.3                  |
| CA-KER-4929      | 2402-98        | Flake           | Coso          | 8.9/10.0             |
| CA-KER-4929      | 2402-119       | Flake           | Coso          | 11.8                 |
| CA-KER-4929      | 2402-5         | Flake           | Coso          | 5.0                  |

| Trinomial     | Cat No.  | Artifact | Source       | Hydration Rim |
|---------------|----------|----------|--------------|---------------|
| CA-KER-4929   | 2402-49  | Flake    | Coso         | 6.5           |
| CA-KER-4929   | 2402-183 | Flake    | Not obsidian | n/a           |
| CA-KER-503    | 236-55   | Flake    | Coso         | DH            |
| CA-KER-503    | 236-66   | Flake    | Coso         | 12.0          |
| CA-KER-503    | 236-40   | Flake    | Casa Diablo  | 11.2          |
| CA-KER-5661   | 10742    | RSP      | Coso         | 5.0           |
| CA-KER-698/H  | 10691    | Flake    | Coso         | NVB           |
| CA-KER-7578   | 4188-172 | Flake    | Coso         | 6.8           |
| CA-KER-7578   | 4188-95  | Flake    | Coso         | 8.1           |
| CA-KER-7578   | 4188-182 | Flake    | Coso         | 7.7           |
| CA-LAN-1189/H | 400-22   | Dart     | Casa Diablo  | 7.2           |
| CA-LAN-1189/H | 400-46   | PTF      | Coso         | 6.0           |
| CA-LAN-1307   | 616-1    | RSP      | Coso         | 3.6           |
| CA-LAN-1465/H | 4024     | Flake    | Coso         | 9.6           |
| CA-LAN-2397   | 2021-27b | Flake    | Coso         | 4.6           |
| CA-LAN-2397   | 2021-2   | Flake    | Coso         | 7.5           |
| CA-LAN-2397   | 2021-13  | Flake    | Coso         | 9.2           |
| CA-LAN-2397   | 2021-22  | Flake    | Coso         | 9.6           |
| CA-LAN-2397   | 2021-27a | Flake    | Coso         | 9.8           |
| CA-LAN-716    | 10818    | Flake    | Saline       | 4.8           |
| CA-LAN-716    | 10819    | Flake    | Saline       | 6.3           |
| Isolate       | 10716    | Flake    | Coso         | DH            |
| TBD           | 10721    | BFF      | Coso         | 14.9          |
| TBD           | 10727    | LMO      | Coso         | 11.9          |
| TBD           | 10729    | Flake    | Coso         | VW            |
| TBD           | 10735    | BFF      | Coso         | 8.1           |

Notes: BFF = Biface fragment; DH = Diffuse hydration; LMO = Lake Mojave point; NVB = No visible band; PTF = Point fragment; RSP = Rose spring point; RTF = Retouched flake; SLP = Silverlake point; TBD = To be determined; UTF = Utilized flake; VW = Variable width

Two pieces of debitage (Figure 9) were collected from a small chipping station containing more than 20 early and middle stage reduction flakes and one

broken bifacial core clustered in an area no greater than 1m x 1m. One of the flakes observed, but not collected, had 100% cortex on its dorsal surface,



Figure 9. Artifacts 10818 (top) and 10819 (bottom), Flakes Collected from an Obsidian Chipping Station.



suggesting that a complete or nearly complete cobble was transported to the site prior to lithic reduction. The artifacts were selected from this feature specifically to compare hydration rim thicknesses of two artifacts ostensibly produced during the same event. As shown in Table 4, the mean hydration reading for one flake (cat. no. 10819) is 1.5 microns thicker than the other (cat. no. 10818). The implications associated with these different hydration rim thicknesses are discussed further in Chapter Five.

The projectile points selected to supplement the obsidian data consisted of one large, non-diagnostic dart tip, one complete Lake Mojave dart point (Figure 10), and two complete Rose Spring arrow points (Figure 11). There is general concordance between these point forms and the hydration rim thicknesses. Measured at 6.0 microns, the hydration rim for the dart tip (cat. no. 400-46) corresponds to the Gypsum time period, while a measurement of 11.9 microns places the Lake Mojave point (cat. no. 10727) toward the beginning of the Lake Mojave time period. With a hydration rim measured at 3.6 microns, one of the Rose Spring points (cat. no. 616-01) falls on the cusp of the Saratoga Springs/Shoshonean time periods. The hydration rim for other Rose Spring point (cat. no. 10742) was measured at 5.0 microns, which places it near the beginning of the Saratoga Springs period. Based on its curved profile and characteristic flake patterning, this particular point appears to have been manufactured from a large percussion flake that may have been scavenged.

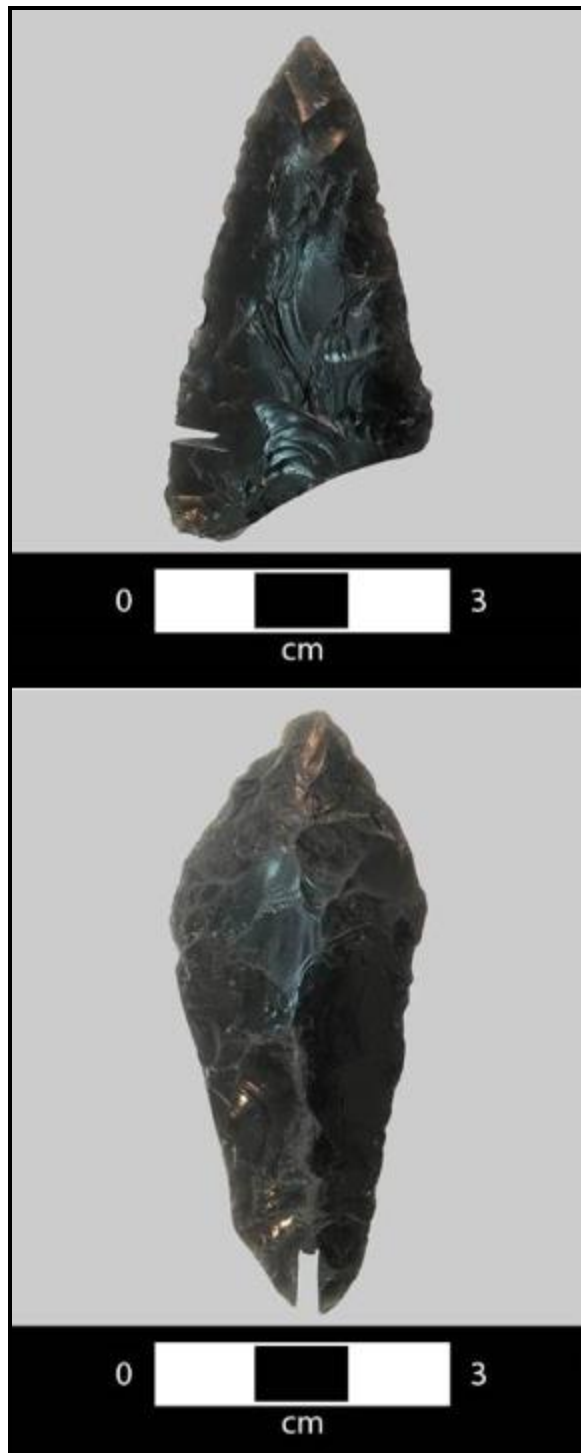


Figure 10. Artifacts 400-46 (top), Dart Point Fragment and 10727 (bottom), Lake Mojave Dart Point.



Figure 11. Artifacts 616-01 (top) and 10742 (bottom), Rose Spring Arrow Points. Note the un-modified ventral flake surface near the base of the bottom point.

#### General Patterns for Obsidian at Edwards AFB

Examination of the database developed for this thesis gives the impression that obsidian artifacts are a relatively infrequent occurrence in the landscape of Edwards AFB. Of the 2,500 or so prehistoric sites that have been recorded to date, only 256 (10.2%) of those sites contributed obsidian artifacts

that were submitted for analysis. Additionally, 25 of the obsidian artifacts included in the supplemental analyses were recovered as isolated finds. The distribution of localities from which the obsidian included in this study was recovered is shown in Figure 12 and quantified in Table 5. It is almost certain that more obsidian artifacts await discovery or have been observed and recorded,

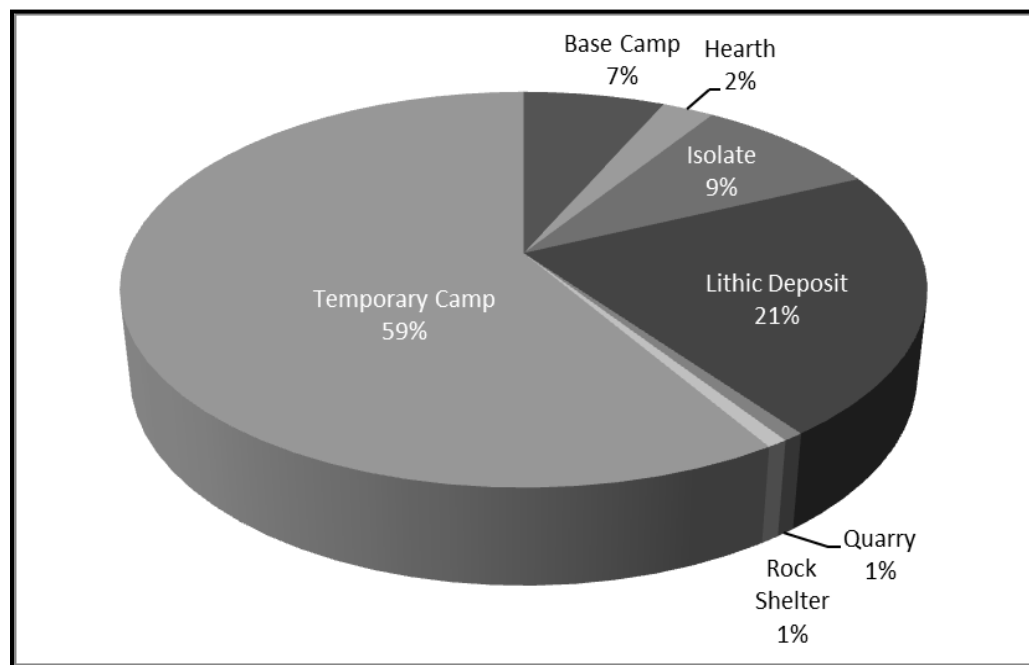


Figure 12. Distribution of All Obsidian by Site Type.

but not collected for analysis. However, by the very nature of their status as not having been analyzed, they were not captured by the methods employed for this study.

Table 5. Quantity of Obsidian by Site Type

| Site Type      | Quantity of obsidian | Percentage  |
|----------------|----------------------|-------------|
| Base Camp      | 19                   | 7%          |
| Hearth         | 7                    | 2%          |
| Isolate        | 25                   | 9%          |
| Lithic Deposit | 61                   | 22%         |
| Quarry         | 2                    | 1%          |
| Rock Shelter   | 2                    | 1%          |
| Temporary Camp | 165                  | 59%         |
| <b>Total</b>   | <b>281</b>           | <b>100%</b> |

The entire obsidian database compiled for this thesis contains 1,231 artifacts. That total includes the addition of 40 pieces newly submitted for source and hydration analysis. Additionally, the source information was added for 119 previously unsourced specimens that had been cut for hydration. Of the artifacts comprising the database, 89% (n=1,096) originate from the Coso obsidian fields. For the remaining 135 artifacts, a source has not been identified for the vast

Table 6. Alternative Obsidian Sources

| Source            | No. Artifacts | Percentage  |
|-------------------|---------------|-------------|
| Bristol Mountain  | 2             | 0.2%        |
| Casa Diablo       | 7             | 0.6%        |
| Fish Spring       | 1             | 0.1%        |
| Mono              | 1             | 0.1%        |
| Obsidian Butte    | 1             | 0.1%        |
| Queen             | 1             | 0.1%        |
| Saline            | 2             | 0.2%        |
| Shoshone Mountain | 1             | 0.1%        |
| <b>Total</b>      | <b>16</b>     | <b>1.3%</b> |

majority (n=118), with the final remainder originating from the alternative geochemical sources shown in Table 6. Given the preponderance of Coso obsidian found at Edwards AFB, it is presumable that most, if not all, of the unsourced specimens also originate from Coso. To be sure, exploring the dominance of Coso obsidian in the archaeological record of Edwards AFB compared to obsidian from other sources is intriguing and warrants further investigation. Unfortunately, the overall low frequency of specimens from alternate sources makes such an endeavor an exceptional challenge.

Examining the distribution of artifact classes represented, 865 (79%) specimens are debitage, 226 (21%) are tools of some variety, one is a core (<1%), and the nature of four (<1%) specimens is not known despite a search of the collection housed at the Edwards AFB curation facility in an attempt to locate and classify them. The distribution of artifact classes is presented in Figure 13, while the quantity of each artifact class is provided in Table 7.

Table 7. Quantity of Artifact Classes

| <b>Artifact</b> | <b>Quantity</b> | <b>Percentage</b> |
|-----------------|-----------------|-------------------|
| Arrow           | 54              | 5%                |
| Biface          | 66              | 6%                |
| Core            | 1               | 0%                |
| Dart            | 41              | 4%                |
| Debitage        | 865             | 79%               |
| Point           | 28              | 3%                |
| Tool            | 37              | 3%                |
| Unknown         | 4               | 0%                |
| <b>Total</b>    | <b>1096</b>     | <b>100%</b>       |

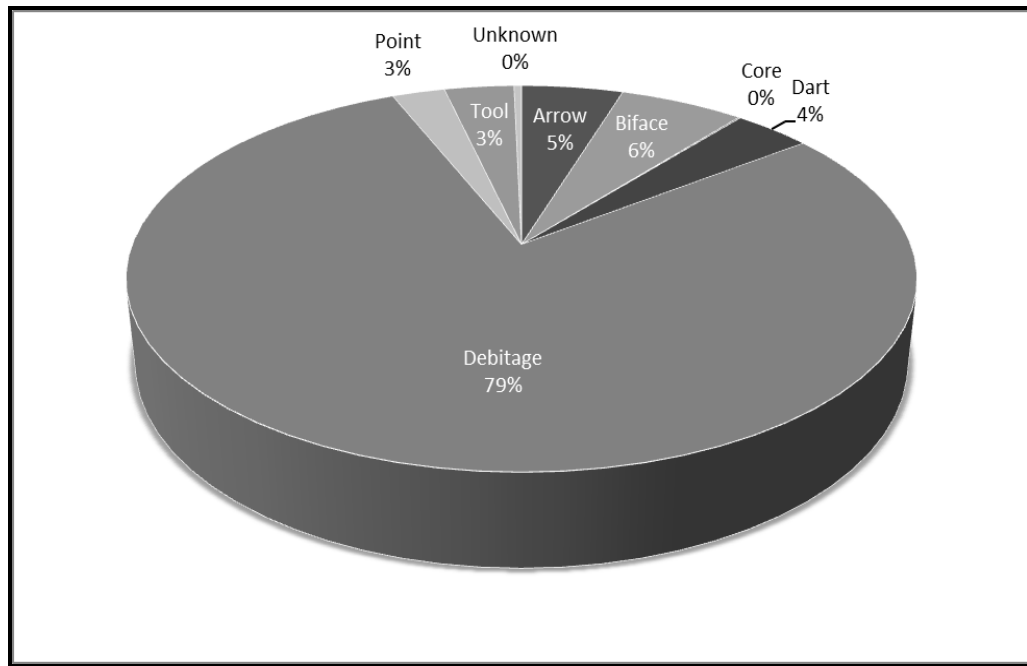


Figure 13. Distribution of Coso Obsidian by Artifact Class.

It is noteworthy that of the artifacts that can be generally classified as tools (i.e. not debitage, core, or unknown), fully 84% (n=189) are formal tools (arrow and dart points, bifaces, etc.) while the remaining 16% (n=37) consist of expedient tools such as utilized flakes, retouched flakes, and the like (Figure 14). In this case, artifacts classified simply as “tools” were also considered expedient tools under the assumption that they would have been assigned to a more formal category by the analysts who originally examined them if the relevant diagnostic attributes were present. In contrast, fully 90% (n=783) of the debitage are classified simply as flakes with the remaining artifacts falling into the shatter

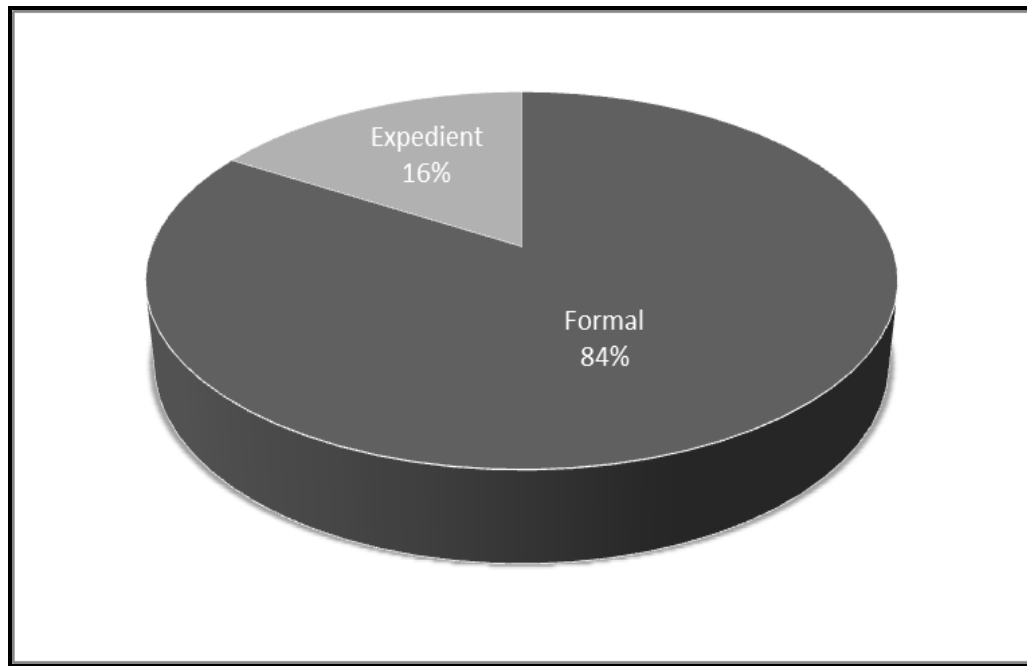


Figure 14. Distribution of Formal and Expedient Tools Manufactured from Coso Obsidian.

(n=22; 3%) or biface thinning (n=60; 7%) categories (Figure 15). A more in-depth analysis of the debitage assemblage is complicated by the fact that over the years some researchers invested more effort in describing and cataloging the debitage collected during their site investigations. Consequently, deriving meaningful inferences about aboriginal lithic reduction strategies would require re-analysis of the entire obsidian debitage assemblage. Although such an effort is beyond the scope of this thesis, it would likely contribute to our understanding of the prehistoric lifeways of the aboriginal inhabitants of Edwards AFB.



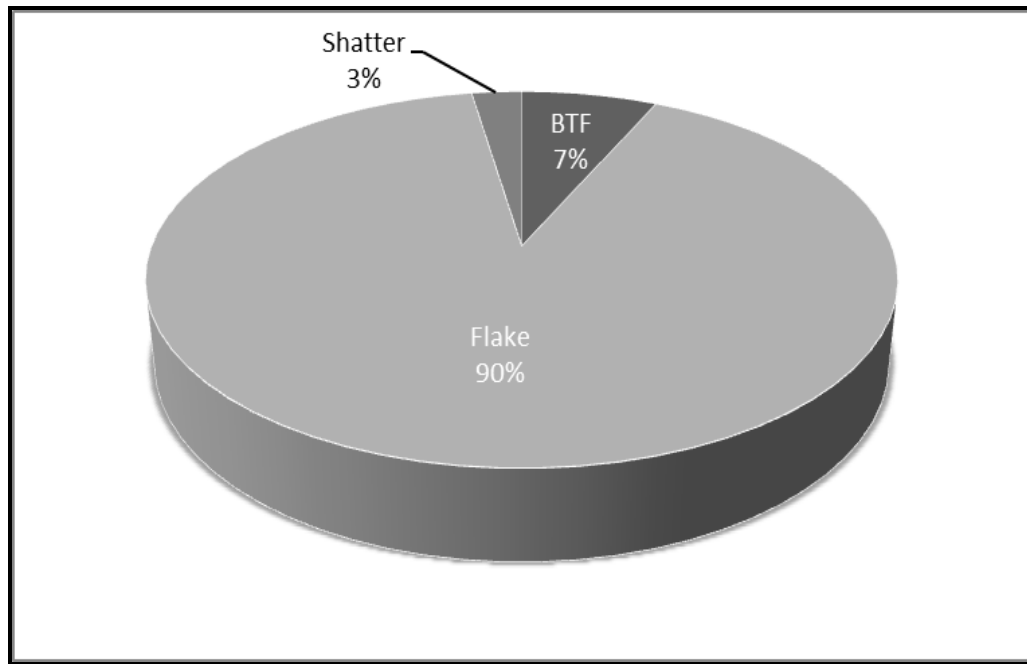


Figure 15. Distribution of Coso Obsidian Debitage.

### Obsidian Date Histograms

As described in Chapter Three, the obsidian data compiled for this thesis was organized in bins of different lengths of time for the purpose of creating histograms that were then used to look for patterns in the obsidian dates and are presented below. Histograms for the Edwards AFB aggregate obsidian dates as well as the management regions produced from the 1000 year bins are presented first. They are followed by the same arrangement of histograms produced from the 500 year bins. The histograms created from the 250 and 100 year intervals are provided in Appendix E.

1000 Year Bins. Figures 16 through 21 present histograms of the obsidian hydration date frequencies for all of Edwards AFB and for each of the

management regions at a 1000 year bin interval. Intervals of this size are useful for illustrating the trend in obsidian hydration date frequency for the entire Holocene, but do not provide fine enough resolution to capture changes that occur within or between cultural time periods.

An immediately obvious pattern emerges when hydration date profile for all of Edwards AFB is examined (Figure 16). Obsidian date frequencies are low during the early Holocene and begin to increase slowly during the Lake Mojave period (11,500 to 7500 B.P.) and into the Pinto period (7500 to 4000 B.P.). The frequency of hydration dates increased by more than 50% near the mid-point of the Pinto period (6100 to 5100 B.P.; 72 dates → 120 dates). From that point on

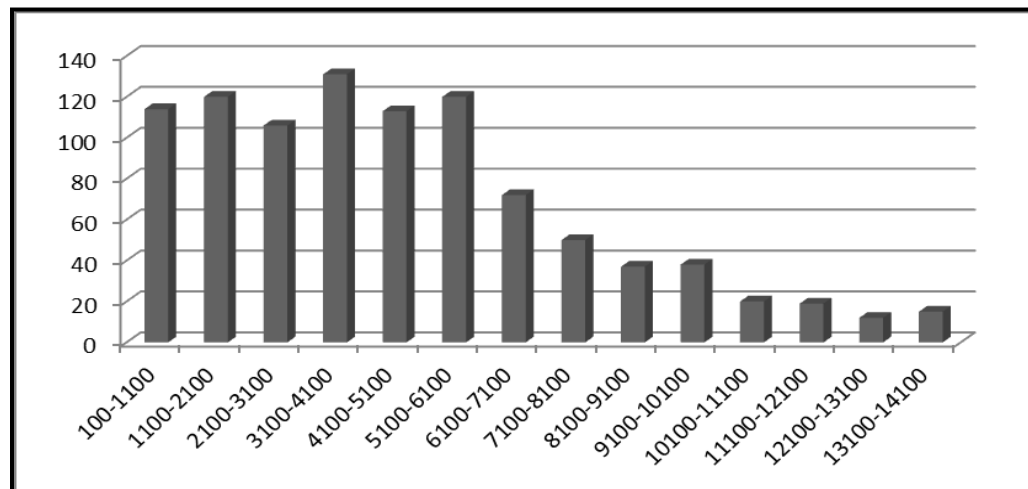


Figure 16. Coso Obsidian Hydration Date Frequency for all of Edwards AFB in 1000 Year Bins.

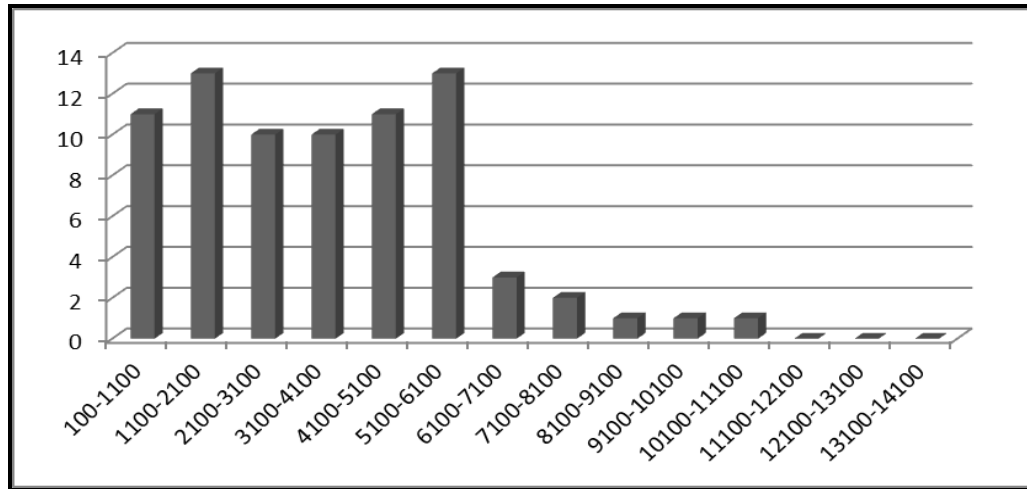


Figure 17. Coso Obsidian Hydration Date Frequency for Management Region 1 in 1000 Year Bins.

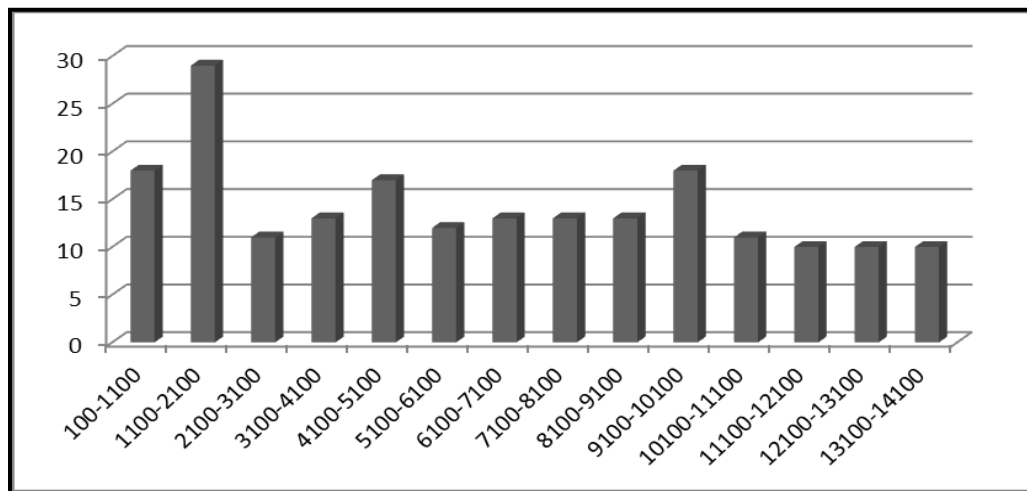


Figure 18. Coso Obsidian Hydration Date Frequency for Management Region 2 in 1000 Year Bins.

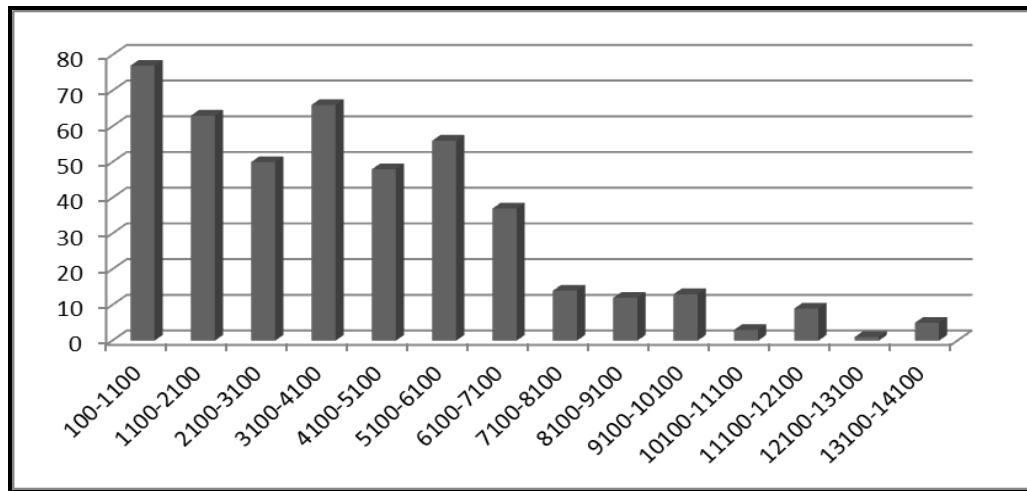


Figure 19. Coso Obsidian Hydration Date Frequency for Management Region 3 in 1000 Year Bins.

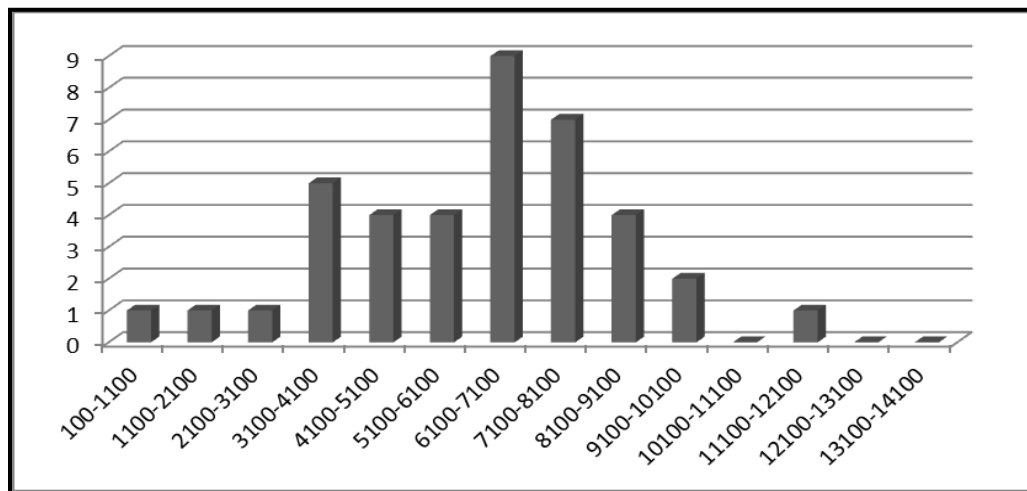


Figure 20. Coso Obsidian Hydration Date Frequency for Management Region 4 in 1000 Year Bins.

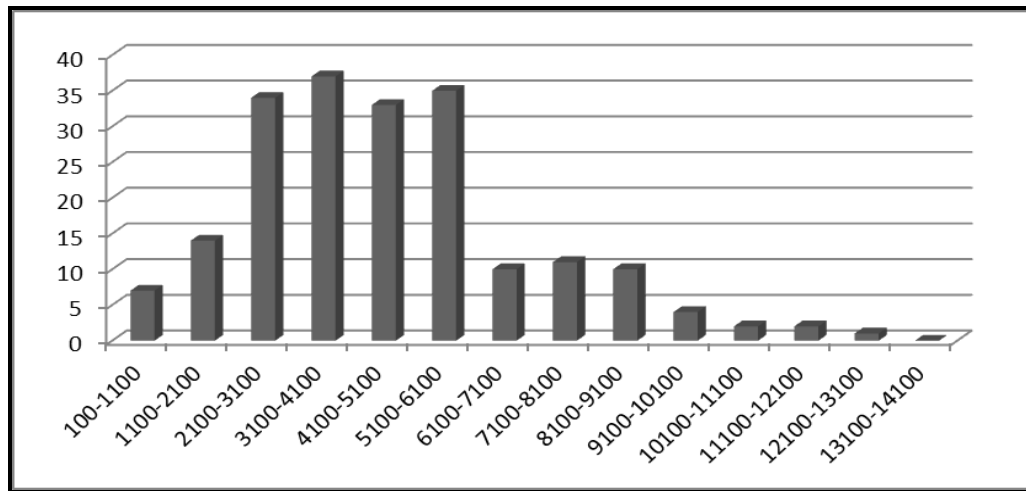


Figure 21. Coso Obsidian Hydration Date Frequency for Management Region 5 in 1000 Year Bins.

there are minor fluctuations in the number of hydration dates in each bin; however there is an average 117 hydration dates per period. There is a slight increase in the number of hydration dates sometime around the transition from the Pinto to Gypsum period (4100 to 3100 B.P.) which is followed by a nearly equal drop in frequency in the middle of the Gypsum period (3100 to 2100 B.P.), however neither is as large a change as occurred during the Pinto period.

Examining the histograms for the five management regions tells another tale. Notably, there is no consistent pattern in the obsidian hydration date frequencies across the management regions. In fact, no two regions share a similar pattern.

The obsidian hydration date frequencies for Management Region 1 (Figure 17) shows no or very low quantities from the Late Pleistocene to the Pinto period. There is a threefold jump in the frequency of dates near the middle

of the Pinto period, after which they average 11 dates per interval through to the end of the Shoshonean period. Despite the dramatic upsurge in hydration dates noted for the middle Pinto, the overall quantity (n=76; 8% of total) of hydration dates for Management Region 1 is low compared to the quantities for nearly all of remaining regions. A discussion of the current findings compared to those of Giambastiani and Basgall (2000) appears in Chapter Five.

The hydration profile for Management Region 2 (Figure 18) presents a very different picture. For most of prehistory in this region of the base the frequency of obsidian hydration dates fluctuates around an average of 13 dates per interval. Very minor increases are observed in the Lake Mojave and Pinto periods. However, a significant proliferation in dates occurs sometime around the transition from the Gypsum to Saratoga Springs period (11 dates → 29 dates). This is followed by a moderate decline in hydration dates for the interval covering the transition from the Saratoga Springs to the Shoshonean period (29 dates → 18 dates). The overall total of obsidian hydration dates derived from Management Region 2 is fairly robust (n=198; 20% of total). The implications associated with this pattern compared to the observations made by Basgall and Overly (2004) are discussed further in Chapter Five.

Turning to Management Region 3, still another pattern in the obsidian hydration date frequencies emerges (Figure 19). The frequency of obsidian hydration dates is low during the early Holocene, averaging eight dates per time interval through to the beginning of the Pinto period. During the 7100 to 6100

B.P. interval the frequency more than doubles (14 → 37 dates); this is followed by an undulating series of increases that culminates in 77 hydration dates from the 1100 to 100 B.P. time interval. While this is the single highest total for any time interval in all the management regions, the intervals that are within the span of time from 6100 to 100 B.P. are consistently higher than the same intervals in the other management regions as well. Consequently, the total number of hydration dates for Management Region 3 (n=454; 47% of total) is more than double that of the management region with the next highest total (Management Region 5; n=200). Given the overall contribution that Management Region 3 makes to the aggregate hydration dates for all of Edwards AFB, it is unsurprising that there is similarity between the two patterns. If obsidian hydration date frequency is truly a proxy for habitation intensity, then clearly prehistoric hunter-gatherers concentrated their attention in the areas near Rogers Dry Lake.

The pattern of obsidian hydration date frequency for Management Region 4 is unusual, but not surprising given the nature of the region (Figure 20). Primarily encompassing Leuhman Ridge, this management region contains few locations where the prehistoric inhabitants would have access to reliable water sources. As a result, Management Region 4 contains the lowest quantity of obsidian hydration dates (n=39; 4% of total). The pattern for this paltry sum is unique in that the dates are concentrated in the Lake Mojave through Gypsum period (i.e. 10,100 to 3100 B.P.), with the greatest number (n=9) found near the middle of the Pinto period (7100 to 6100 B.P.)

Finally, the pattern of obsidian hydration dates for Management Region 5 (Figure 21) demonstrates a distinctly elevated frequency from the middle of the Pinto Period through to the middle of the Gypsum period (i.e. 6100 to 2100 B.P.) There is an average of 35 hydration dates in each interval for this span of time, whereas the average is 10 dates per interval for those that immediately precede and succeed this time span. Despite the unusual pattern, Management Region 5 contains the second highest total of hydration dates (n=200; 21% of total). This pattern can be interpreted as period of high activity in this region from the mid to beginning of the late Holocene.

500 Year Bins. Figures 22 through 27 present histograms of the obsidian hydration date frequencies for all of Edwards AFB and for each of the management regions at a 500 year bin interval. Intervals of this size are also useful for illustrating the trend in obsidian hydration date frequency for the entire Holocene. Unlike the 1000 year bins, however, the 500 year interval is small enough to provide the fine resolution needed to capture changes that occur within and between cultural time periods. This interval also provides the opportunity to compare the number of hydration dates before and after the arrival of bow and arrow technology to this portion of the Western Mojave Desert.



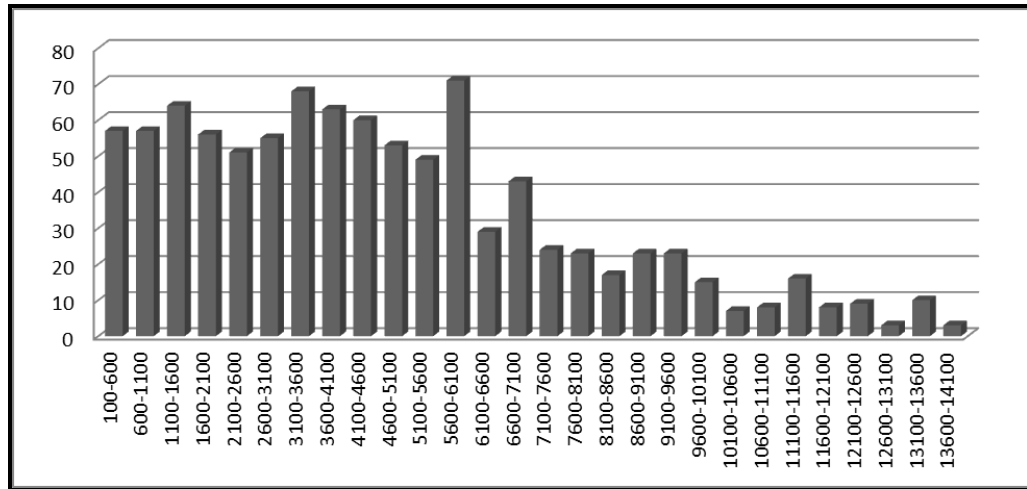


Figure 22. Coso Obsidian Hydration Date Frequency for all of Edwards AFB in 500 Year Bins.

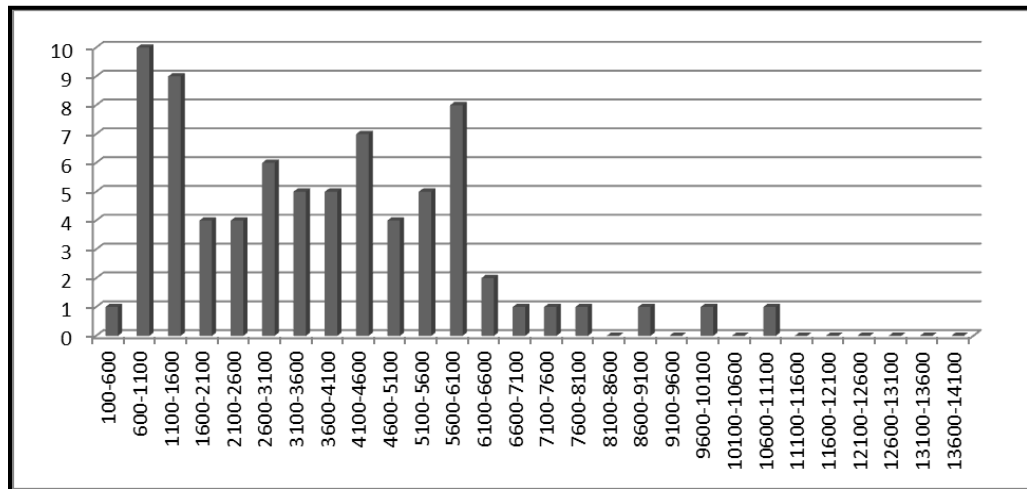


Figure 23. Coso Obsidian Hydration Date Frequency For Management Region 1 In 500 Year Bins.

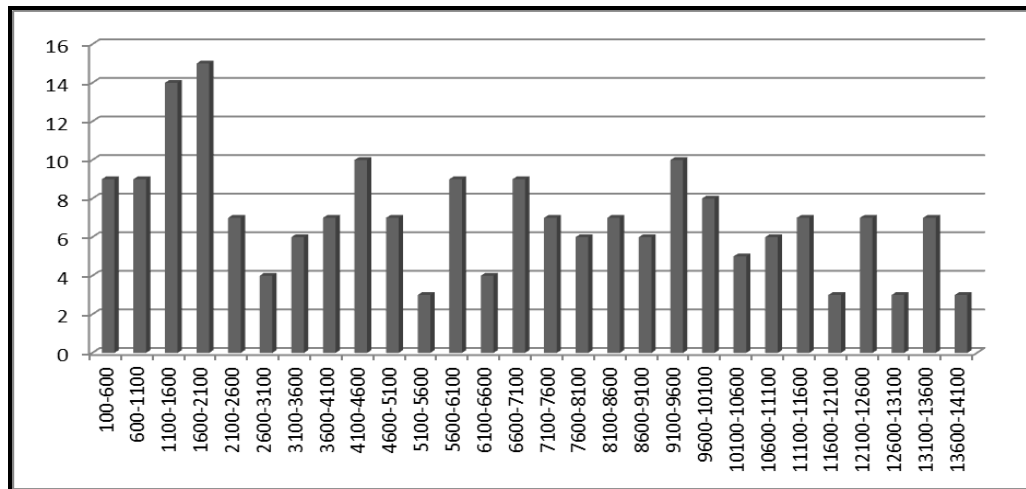


Figure 24. Coso Obsidian Hydration Date Frequency for Management Region 2 in 500 Year Bins.

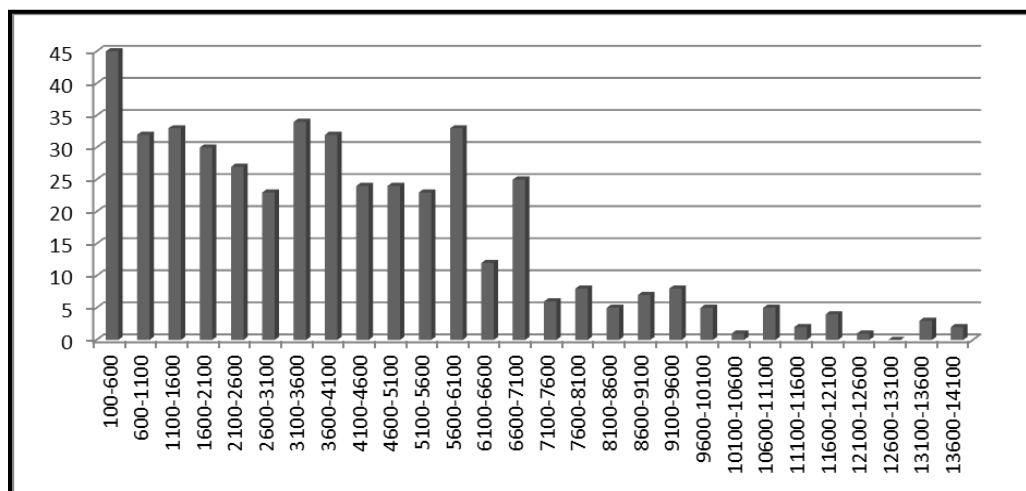


Figure 25. Coso Obsidian Hydration Date Frequency for Management Region 3 in 500 Year Bins.

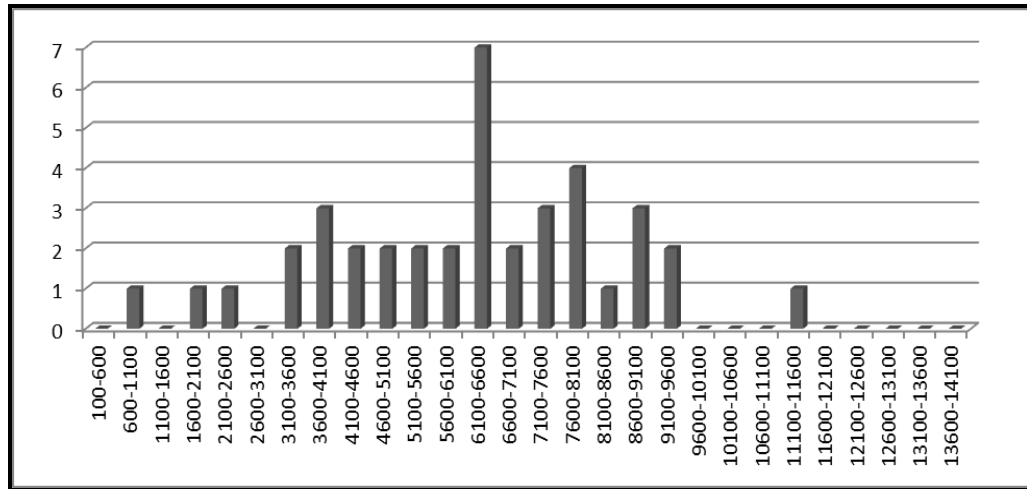


Figure 26. Coso Obsidian Hydration Date Frequency for Management Region 4 in 500 Year Bins.

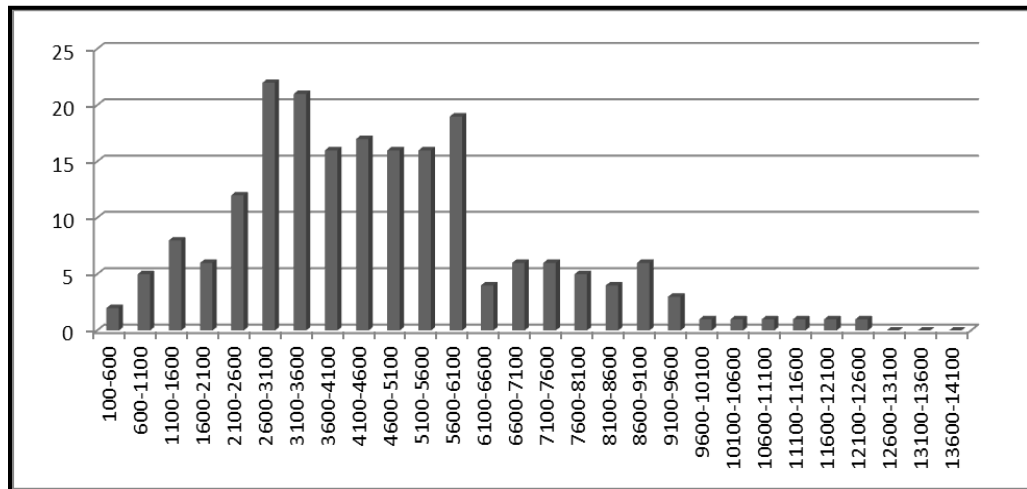


Figure 27. Coso Obsidian Hydration Date Frequency for Management Region 5 in 500 Year Bins.

At both the individual management region level and the combined Edwards AFB level, the patterns in hydration date frequency visible in the figures for the 500 year intervals are largely similar to the figures for the 1000 year intervals. With minimal recapping those similarities, some noteworthy differences do occur and they are discussed here.

Beginning with the combined profile for all of Edwards AFB (Figure 22), the previously noted increase in the number of hydration dates that occurs during the Pinto period becomes more pronounced, and can be narrowed down to the span of time between 6100 and 5600 B.P., placing this event in the middle of that cultural period. A sharp decline occurs in the immediately succeeding interval (71 → 49 dates), which is followed by a steady increase until the 3600 to 3100 B.P. interval, at which point the number of dates dips slightly until leveling off in the last two intervals (1100 to 100 B.P.). Notably, there is a slight increase (56 → 64 dates) in the interval (1600 to 1100 B.P.) spanning the time when the bow and arrow is believed to have been adopted by the inhabitants of these environs. Admittedly, this rise is not great, however its presence suggests the bow and arrow did not have a negative effect on the prehistoric use of obsidian. All told, the general tendency of a consistent frequency of hydration dates in the late Holocene does not change when examined under the slightly higher resolution provided by the 500 year interval.

For Management Region 1, the 500 year interval hydration date profile (Figure 23) follows a similar pattern as the one observed in the 1000 year interval

(Figure 17). The notable exception occurs in the very last interval at which point the number of hydration dates drops precipitously ( $10 \rightarrow 1$  dates). Such a steep drop may indicate a shift in habitation in this region of Edwards AFB very late in prehistory. With regard to the effect the bow and arrow had on obsidian use in this region of Edwards AFB, there is a considerable jump ( $4 \rightarrow 9$  dates) in the frequency of hydration dates from the before to after intervals (i.e. between 2100 to 1600 B.P. and 1600 to 1000 B.P.). That said, these quantities may not be large enough to be provide meaningful insight into the matter.

The 500 year interval hydration date profile for Management Region 2 (Figure 24) does not reveal any new patterns when compared to the 1000 year interval profile (Figure 18). Both profiles display the same undulating pattern of hydration date frequency throughout the early and middle Holocene, with a spike ( $7 \rightarrow 15$  dates) near the end of prehistory. That spike occurs just prior to the introduction of the bow and arrow with a barely perceptible decline ( $15 \rightarrow 14$  dates) occurring in the immediately succeeding interval. The hydration date frequency for Management Region 2 stabilizes at 9 dates during the final two intervals.

A comparison of the 500 year profile to the 1000 year profile for Management Region 3 reveals one new insight into the frequency of hydration dates. As noted in the discussion of the 1000 year profile, the greatest number of hydration dates ( $n=77$ ) for any of the management regions is found in the final interval for Management Region 3 (Figure 19). Examining the 500 year profile

(Figure 25) shows that the bulk of the hydration dates (n=45) occur in the final interval (600 to 100 B.P.). Focusing in on the transition from the Gypsum to Saratoga Springs cultural periods (i.e. about when the bow and arrow entered the area), a very small increase in hydration dates is noted (27 → 30 dates) which again suggests that the new technology did not result in a declining use of obsidian. Aside from this, the 500 year profile narrows down the timing for the fluctuations in the number of hydration dates through the middle Holocene, but does not reveal any other changes to the overall pattern seen in the 1000 year profile.

The 500 year profile for Management Region 4 (Figure 26) provides no substantive insight into the frequency of obsidian hydration dates for this portion of Edwards AFB. The most noteworthy observation to be made is that the elevation of hydration dates previously noted during the Pinto period can be narrowed down to having occurred in the span of time between 6600 and 6100 B.P. Additionally, at the point in time when bow and arrow technology reaches the Western Mojave Desert, the frequency of obsidian dates for this management region are practically non-existent. Stated again, the lack of access to reliable water sources in this portion of Edwards AFB likely explains the overall low number of dates recovered from this management region.

Examining the 500 year profile (Figure 27) for Management Region 5 serves to narrow down the timing on some of the trends observed in the 1000 year profile (Figure 21). Specifically, the distinct rise in hydration dates noted in

middle Holocene occurred sometime between 6100 and 5600 B.P. and consisted of nearly a fivefold increase (4 → 19 dates). Additionally, the late Holocene decline in hydration dates (c. 3100 – 2100 B.P.) visible in the 1000 year profile, while distinct, is not nearly as sharp when viewed from the perspective of 500 year profile. As seen in the profiles for other management regions, there is a very slight boost in the number of hydration dates around the time at which bow and arrow technology arrived at Edwards AFB. However, the quantities involved are small and not significantly different enough (i.e. 6 → 8 dates) to be able to make a definitive statement about the effect the new technology had on the pattern of obsidian use by the prehistoric inhabitants of this management region.

#### Number of Sites vs. Number of Dates

Another pattern in the Coso obsidian hydration data for Edwards AFB emerges when the number of hydration dates is compared to the number of sites that produced those dates (Figure 28). During the early Holocene there is a close relationship between the frequency of hydration dates and the frequency of sites that produced those dates, with 20 or fewer dates and sites recorded from 14,100 to 11,100 B.P. Following that point in time a slight gap appears between the the frequency of dates and sites. The gap continues to widen as time progresses with the number of sites increasing slowly compared to the number of hydration dates they produced. During the middle Holocene, corresponding to the middle of the Pinto cultural period (i.e. 6100 to 5100 B.P.), there is a significant (100%)

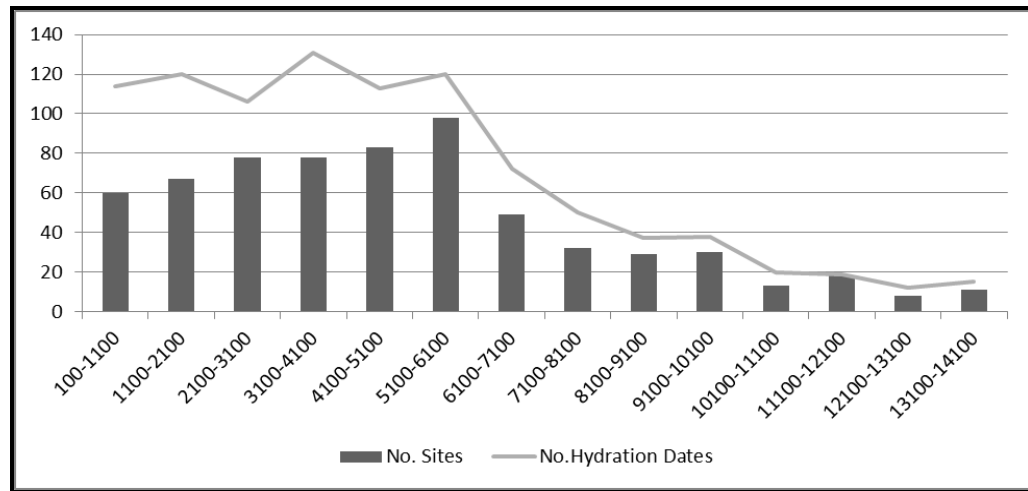


Figure 28. Comparison of the Number of Hydration Dates to the Number of Sites Producing Those Dates.

increase in the number of sites (49 → 98) that is accompanied by a slightly smaller (67%) increase in the number of dates (72 → 120). From this point until the end of prehistory the number of hydration dates fluctuates around an average of 117 dates per 1000 years. However the number of sites producing those dates shows a gradual decline; first dropping to 113 sites in the period immediately following (5100 to 4100 B.P.) before falling to a mere 60 sites at the end of prehistory (100 to 1100 B.P.).

Taking obsidian frequency in the landscape as a proxy for habitation density (Giambastiani and Basgall 2000), then the pattern exhibited in Figure 28 indicates a shift in the way in which prehistoric hunter-gatherers inhabited this portion of the Western Mojave Desert. Specifically, after 5100 B.P. it appears people began concentrating in fewer locations even while producing similar quantities of obsidian. Additional data are required to fully explore the



implications of this pattern, however it may also provide new insights into population density, mobility patterns, and/or a shift in the formality of tool manufacture that produced more wastage.

#### Introduction of the Bow and Arrow

A number of archaeologists have suggested that bow and arrow technology sparked a wide range of change among prehistoric hunter-gatherers in the Great Basin and elsewhere in the western United States (Basgall and Giambastiani 2000; Bettinger 2013, 2015; Hale et al. 2009; Hale et al. 2010; Railey 2010). A Chi-square analysis comparing the frequency of obsidian dates of three 1,400 year bins that span from 100 BP to 4300 B.P. was completed to test whether this new technology had an effect on the use of obsidian by the aboriginal inhabitants of the Edwards AFB region (Table 8). There are no significant changes in the aggregate number of dates per bin (Bin 1 = 165, Bin 2 = 155, Bin 3 = 179), which suggests that the bow and arrow did not have an effect on the overall amount of obsidian being used prehistorically at Edwards AFB.

However, the results of the Chi-square analysis do suggest that the distribution of obsidian between the management regions is significantly different across the bin intervals. Specifically, there are minor changes in hydration dates for Management Regions 1 and 2, and major changes in hydration dates for Management Regions 3 and 5. The data for Management Region 4 are

insufficiently large to make meaningful inferences and will not be addressed further. Regions 1 and 2 both show slight increases in the amount of obsidian

Table 8. Chi-Square Test of Obsidian Frequency by Management Region for Three 1400 Year Time Intervals

| MR/Bin  | Observed   | Expected   | (Obs-Exp) | (Obs-Exp) <sup>2</sup> | (Obs-Exp) <sup>2</sup> /Exp        |
|---|------------|------------|-----------|------------------------|------------------------------------|
| MR 1/Bin 1  | 20         | 15.9       | 4.1       | 17.04                  | 1.07                               |
| MR 1/Bin 2  | 12         | 14.9       | -2.9      | 8.47                   | 0.57                               |
| MR 1/Bin 3  | 16         | 17.2       | -1.2      | 1.48                   | 0.09                               |
| MR 2/Bin 1  | 27         | 24.5       | 2.5       | 6.41                   | 0.26                               |
| MR 2/Bin 2  | 28         | 23.0       | 5.0       | 25.14                  | 1.09                               |
| MR 2/Bin 3  | 19         | 26.5       | -7.5      | 56.93                  | 2.14                               |
| MR 3/Bin 1  | 103        | 88.9       | 14.1      | 197.46                 | 2.22                               |
| MR 3/Bin 2  | 77         | 83.6       | -6.6      | 43.00                  | 0.51                               |
| MR 3/Bin 3  | 89         | 96.5       | -7.5      | 56.17                  | 0.58                               |
| MR 4/Bin 1  | 1          | 3.3        | -2.3      | 5.32                   | 1.61                               |
| MR 4/Bin 2  | 2          | 3.1        | -1.1      | 1.22                   | 0.39                               |
| MR 4/Bin 3  | 7          | 3.6        | 3.4       | 11.65                  | 3.25                               |
| MR 5/Bin 1  | 14         | 32.4       | -18.4     | 338.74                 | 10.45                              |
| MR 5/Bin 2  | 36         | 30.4       | 5.6       | 30.90                  | 1.02                               |
| MR 5/Bin 3  | 48         | 35.2       | 12.8      | 165.01                 | 4.69                               |
| Total   | <b>499</b> | <b>499</b> | <b>0</b>  | <b>964.95</b>          | <b><math>\chi^2 = 29.96</math></b> |
| Notes: Bin 1 = 100-1500 BP; Bin 2 = 1500-2900 BP;<br>Bin 3 = 2900-4300 BP; MR = management region |            |            |           |                        | df=8<br>$p=.003$                   |

found after 1500 B.P. In contrast, Region 3 shows a sizeable increase in the amount of obsidian found after 1500 B.P. whereas in Region 5 there is an even greater decrease in the amount of obsidian found during that same timespan.

To explore this even further, a second Chi-square analysis of just bins 2 and 3 was performed (Table 9). The goal of the second analysis was to look for a difference in the frequency of obsidian dates throughout Edwards AFB before

and after 2900 B.P. The results of that test indicate that there is not a significant difference in the frequency of obsidian throughout Edwards AFB in the 1,400 years before or after 2900 B.P. This finding, then, confirms that a change did occur in the distribution of Coso obsidian within and between the management regions following the introduction of the bow and arrow at 1500 B.P. Again, the overall amount of obsidian being used by the prehistoric people living in the Western Mojave did not change; however the patterns of use within the various

Table 9. Chi-Square Test of Obsidian Frequency by Management Region for Two 1400 Year Time Intervals

| MR/Bin   | Observed   | Expected   | (Obs-Exp)  | (Obs-Exp) <sup>2</sup> | (Obs-Exp) <sup>2</sup> /Exp       |
|--|------------|------------|------------|------------------------|-----------------------------------|
| MR 1/Bin 2   | 12         | 13.0       | -1.0       | 0.99                   | 0.08                              |
| MR 1/Bin 3   | 16         | 15.0       | 1.0        | 0.99                   | 0.07                              |
| MR 2/Bin 2   | 28         | 21.8       | 6.2        | 38.30                  | 1.76                              |
| MR 2/Bin 3   | 19         | 25.2       | -6.2       | 38.30                  | 1.52                              |
| MR 3/Bin 2   | 77         | 77.0       | 0.0        | 0.00                   | 0.00                              |
| MR 3/Bin 3   | 89         | 89.0       | 0.0        | 0.00                   | 0.00                              |
| MR 4/Bin 2   | 2          | 4.2        | -2.2       | 4.74                   | 1.13                              |
| MR 4/Bin 3   | 7          | 4.8        | 2.2        | 4.74                   | 0.98                              |
| MR 5/Bin 2   | 36         | 39.0       | -3.0       | 8.89                   | 0.23                              |
| MR 5/Bin 3   | 48         | 45.0       | 3.0        | 8.89                   | 0.20                              |
| Total  | <b>334</b> | <b>334</b> | <b>0.0</b> | <b>105.84</b>          | <b><math>\chi^2 = 5.96</math></b> |
| Notes: Bin 2 = 1500-2900 BP; Bin 3 = 2900-4300 BP;<br>MR = management region |            |            |            |                        | df=4<br>$p=.2022$                 |

regions of Edwards AFB did change. Specifically, the quantity of obsidian found in Region 3 increased after 1500 B.P. while the quantity found in Region 5 decreased at the same time. The phenomenon identified in these analyses may

have resulted from changes to the settlement patterns and/or food exploitation following the arrival of bow and arrow technology. However, additional investigations are needed to develop a better understanding of the cause of behind these changes in obsidian use in this portion of the Western Mojave Desert.

### Conclusion

Throughout this chapter, I have employed a variety of means to examine the obsidian data from Edwards AFB. From these investigations it is clear that even though it is not toolstone commonly found at sites on the base, obsidian from Edwards AFB can provide insight into prehistoric human behavior when examined through an appropriate lens. The histograms produced from the obsidian hydration data clearly illustrate that using arbitrary slices of time to create periods of equal length to view those data results in more interpretable patterns compared to looking at those same data using unequal periods of time. However, there are limits to the utility of this method. As noted in Chapter Three, the data were also divided into 250 and 100 year intervals; however the resulting patterns were too pixelated to provide additional insight. In this instance the most meaningful patterns about the prehistoric use of Coso obsidian at Edwards AFB were teased out from the data when it was viewed in 500 and 1000 year slices of time. Finally, the examinations of the data show distinct changes in the distribution of obsidian across the landscape and through time. Both the patterns and the organization of data will be discussed further in Chapter Five.

## CHAPTER FIVE

### DISCUSSION

#### Introduction

In this chapter I consider the meaning of the results presented in the preceding chapter. I begin by returning to the questions set out in Chapter 2; explore whether the conclusions arrived at by previous researchers were affected by sampling bias, and provide commentary on how data organization can influence research findings. I then segue to a brief proposal for an alternative method for data normalization. This is followed by an examination of the implications associated with the difference in hydration rim thicknesses for two artifacts that were part of the supplemental analysis. This chapter concludes with a summary of a critical research avenue identified in this thesis.

#### Obsidian Decline at Edwards AFB

This thesis is inspired by observations on the pattern of obsidian deposition at Edwards AFB made in two studies published in the early 2000s (Basgall and Overly 2004; Giambastiani and Basgall 2000). In these studies the researchers concluded that habitation intensity declined during the late Holocene based on two factors. The first factor was the low quantities of artifacts with small hydration rim readings they recovered in their fieldwork. The second factor was their interpretation of a histogram of hydration rim thicknesses for all of Edwards AFB that was current as of 2000. In response to their conclusion, my research

seeks to answer the following question: Does the amount of obsidian in the archaeological record at Edwards AFB truly decline during the late Holocene?

Although this appears to be a straight forward question that should have an equally straight forward answer, as with most aspects of archaeological research, the actual answer to this question is equivocal.

At the installation-wide level there is no late Holocene decline in obsidian frequency. In fact, the trans-Holocene pattern of obsidian abundance for the whole of Edwards AFB shows quite a different pattern. Obsidian quantities are generally low during the late Pleistocene and early Holocene (14,100 to 10,100 B.P.), gradually increase through the remainder of the early Holocene and into the middle Holocene (10,100 to 6100 B.P.), then increase significantly and remain at a stable level for the duration of the late Holocene (6100 to 100 B.P.).

On the other hand, when the obsidian frequencies for the five management regions are examined, different patterns emerge. Although each is slightly different, the pattern of obsidian frequency for Management Regions 1, 2, and 3 all show an increase in abundance during the late Holocene. However, slight declines occur in Regions 1 and 2 during the Shoshonean period (i.e. 700 to 100 B.P.) while a significant increase occurs in Management Region 3 at that same time. In contrast, Management Region 5 shows a distinct decline during the late Holocene. The pattern for Management Region 4 also declines sharply during the late Holocene; however the overall low quantity of obsidian recovered from this region should be considered a red flag when drawing conclusions. The

end result, however, is that during the late Holocene some portions of Edwards AFB experienced an increase in the amount of obsidian being used by prehistoric hunter-gatherers, while other portions a decrease occurred. Further investigation into this causes behind the patterning of obsidian across Edwards AFB are well worth pursuing.

These findings also prompt a different question: are obsidian hydration dates a reliable proxy for habitation intensity? This theoretical approach is understandable for those portions of the Great Basin, such as in the Owens Valley, where obsidian is ubiquitous, contribute greatly to the artifact assemblage, and the hydration rate is well understood. However, it is a problematic approach for an area like Edwards AFB where obsidian is not commonly found; when it is found its contribution to the artifact assemblage is frequently measured in single digits, and the rate at which obsidian hydrates is poorly understood. Individually, any one of these factors should instill caution in archaeologists when equating the abundance of obsidian hydration dates to habitation levels. In a case like Edwards where all three factors are present, the use of obsidian as a proxy for habitation intensity should be considered highly problematic.

#### Influence of the Bow and Arrow

Another aspect of my research was to examine the impact a new weapon technology may have had on obsidian use in the western Mojave Desert. Researchers working in the Great Basin or elsewhere in the western United

States have observed declines in obsidian during the late Holocene (Gilreath and Hildebrandt 2011; Parry and Kelly 1987). Some researchers have advanced the idea that the introduction of the bow and arrow was the cause (Hale et al. 2009; Hale et al. 2010; Railey 2010). My analysis of the obsidian data for Edwards AFB did identify a change in the pattern of obsidian discard that coincides with the arrival of the bow and arrow (c. 1500 B.P.). That change was limited to Management Region 3, where obsidian quantities increased, and Management Region 5, where obsidian quantities decreased. For the whole of Edwards AFB, however, there is no discernable change in the quantity of obsidian after 1500 B.P. Additional data are required to confirm whether the changes in obsidian frequency in the two management regions are specifically tied to changes to residential mobility, settlement patterns, or economic strategies associated with bow and arrow technology, or if some other factor is involved.

#### Sampling Bias and Data Organization

My research also sought to determine whether sampling bias played a role in the previous researchers' conclusions that obsidian use at Edwards AFB declined during the late Holocene. Again, the answer to this question is ambiguous. The stark difference between my findings and those from the reports published in the early 2000s strongly suggests that those earlier efforts were affected by sampling bias. Differences in the obsidian distribution between my findings and those of the earlier studies were visible whether comparing the aggregate obsidian data, or those for Management Regions 1 or 2 (i.e. the areas



studied by the earlier researchers). It very well could be that the addition obsidian sourcing and hydration data from the past 16 years contributed to findings that contradicted this decline. However, extended rumination on the subject of sampling bias leads me to believe that data organization played an equal or greater role in the erroneous conclusions arrived at by past researchers.

Returning to the two studies that inspired my thesis, the researchers considered both the obsidian assemblages collected during their fieldwork and the aggregate obsidian assemblage for all of Edwards AFB as proxies for analyzing regional occupation intensity as well as the inhabitant's access to obsidian (Giambastiani and Basgall 2000, Basgall and Overly 2004). In each instance the researchers based their analyses and conclusions on histograms created from the micron thicknesses measured for the specimens collected during their fieldwork (Figure 5), or for all of the obsidian collected on Edwards (Figure 6). Later researchers who also explored this apparent trend in obsidian frequency at Edwards AFB went a step further and created histograms from the hydration rim frequencies grouped by the time periods for the cultural sequence for the installation (Figure 29) (Hale, et al. 2009:39). As can be seen in these figures, both approaches create convincing graphical evidence of a decline in obsidian use at Edwards AFB.

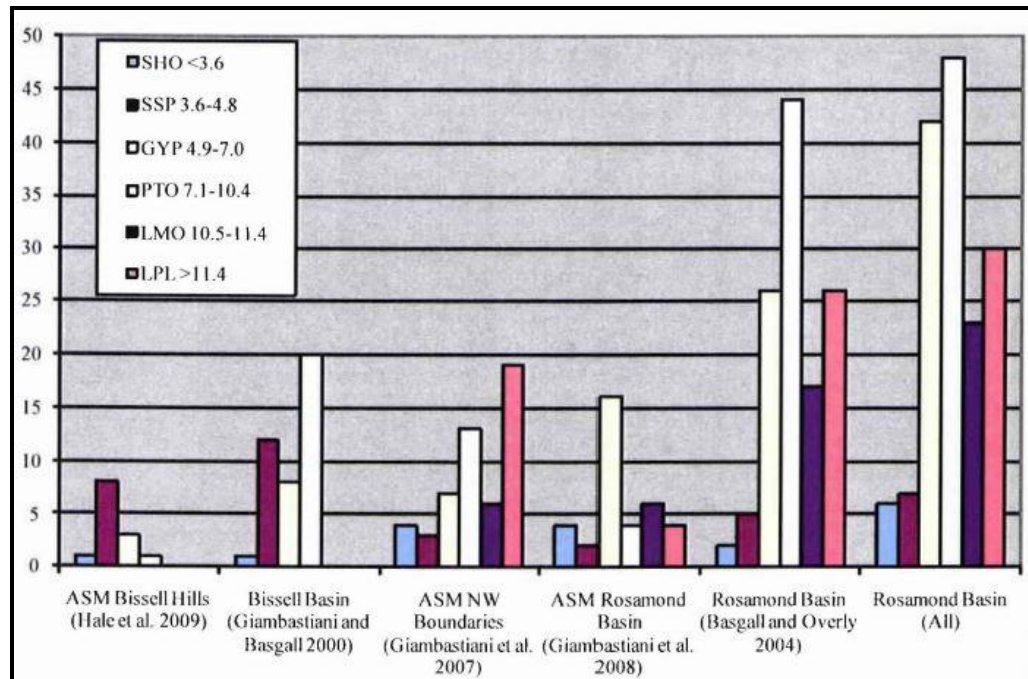


Figure 29. Frequencies of Coso Obsidian Hydration Rims by Project, Region, and Time Period.

(Source: Hale, M., M. Giambastiani, D. Iversen, and M. Richards, 2009 *Phase II Cultural Resource Evaluation at 51 Archaeological Sites in Management Regions 1A, 1B, 2B, 2C, and 3E, Bissell Hills and Paiute Ponds, Edwards Air Force Base, Kern and Los Angeles Counties, California*)

When I began this research project, my efforts were heavily influenced by the way that these previous researchers organized their obsidian data. My initial explorations of the data consisted of replicating those types of data presentation using a much larger suite of source and hydration data. However, the further I delved into my research, the clearer it became there was a flaw with this form of data organization. Specifically, both approaches do not take into consideration the fact that each cultural time period constitutes a different span of time. In fact, creating histograms based on hydration date frequency for each time period

compresses the dates in such a manner that results in elevated quantities in a seemingly uniform distribution. For example, compare the following three figures prepared using the data compiled for this thesis. The first is a histogram of the Coso obsidian hydration dates for all of Edwards AFB grouped by the cultural sequence for Edwards AFB (Figure 30). The second is a histogram of the micron readings for all Coso obsidian artifacts recovered from Edwards AFB (Figure 31). The third is a histogram where the data are arranged in 500 year intervals (Figure 32).

Examining Figure 30, there are significantly more hydration dates for both the Pinto and Gypsum time periods compared to those that come before or after. If obsidian date frequency can truly be considered a proxy for habitation intensity, then taking this figure at face value gives the viewer the impression of a significant jump in habitation activity during the Pinto and Gypsum periods that is followed by an even greater decline in habitation during the Saratoga Springs and Shoshonean time periods. What this type of histogram fails to take into account, however, is the dissimilar time spans each of these cultural periods represents. The Pinto period spans 3,500 years and the Gypsum period spans 2,500 years compared to the Saratoga Springs period (800 years) and the Shoshonean period (600 years). Recognizing the different lengths of time associated with each cultural period, it is understandable that more obsidian entered the archaeological record during those longer spans of time. By

extension, less obsidian would have entered the record during the shorter spans of time.

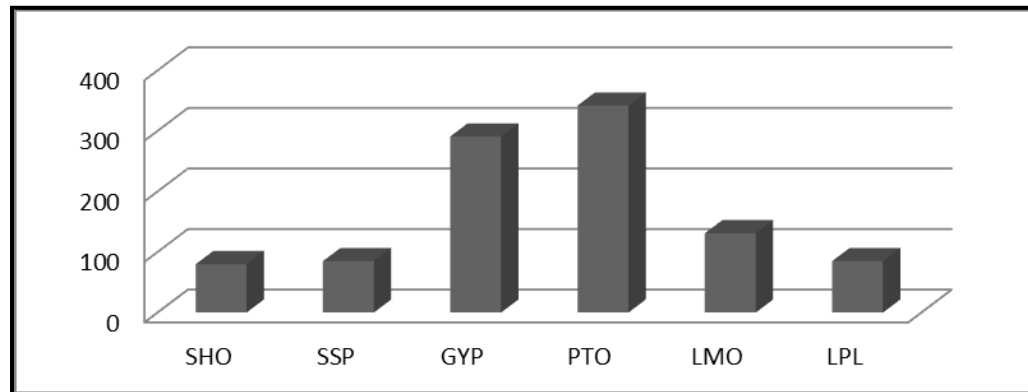


Figure 30. Distribution of Coso Obsidian Hydration Dates for all of Edwards AFB by Cultural Time Period.

A commonly employed method for displaying obsidian hydration data is to simply construct a histogram based on the micron readings for each specimen in the sample. Once constructed, archaeologists use the micron readings intervals assigned to the various cultural time periods to analyze and interpret the distribution of those micron readings; the inset box of Figure 29 is an example of this type of micron interval for the cultural periods at Edwards AFB. Figure 31 is just such a histogram created from the data compiled for this study; the red vertical bars indicate the micron reading serving as the dividing point for each cultural time periods. To be sure, the micron readings from this data set create a classic 'battleship' shape with multimodal distribution and the bulk of the readings falling within the lines bounding the Pinto time period. As is the case with Figure

30, however, this method of displaying the data does not take into consideration the different length of time each cultural period represents. Consequently, inferences about prehistoric human behavior relying on this type of diagram are based on unequal distributions of the data and do not account for the reasonable expectation that more obsidian would have entered the archaeological record during a longer span of time.

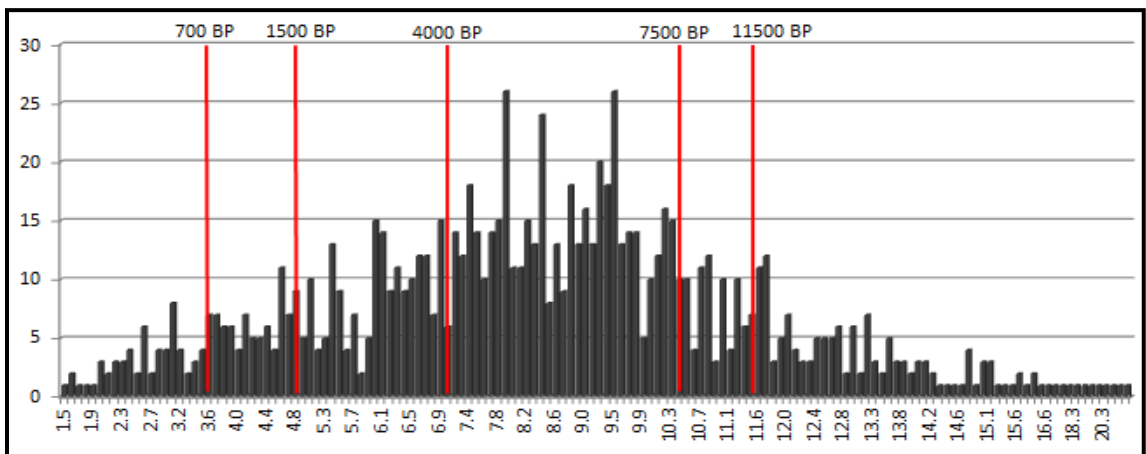


Figure 31. Histogram of Coso Obsidian Micron Readings for all of Edwards AFB.

In contrast to those two methods of data organization, the distribution of obsidian hydration dates depicted in Figure 32 shows a radically different pattern. As in Figure 30, the quantities of obsidian hydration dates in the earliest periods (Late Pleistocene and Lake Mojave) are low. However, there are two jumps in obsidian frequency during the Pinto period. The first is a moderate increase in the 7,100 to 6,600 B.P. interval while the second is an even larger increase in the 6,100 to 5,600 B.P. interval. From 5,600 to 100 B.P. there are some fluctuations

in the quantity of obsidian dates for each 500 year interval, but during that span of time each interval has an average of 58 dates. Importantly, this illustrates a pattern of obsidian dates that is relatively stable across the date intervals corresponding to the Gypsum and Saratoga Springs time periods compared to

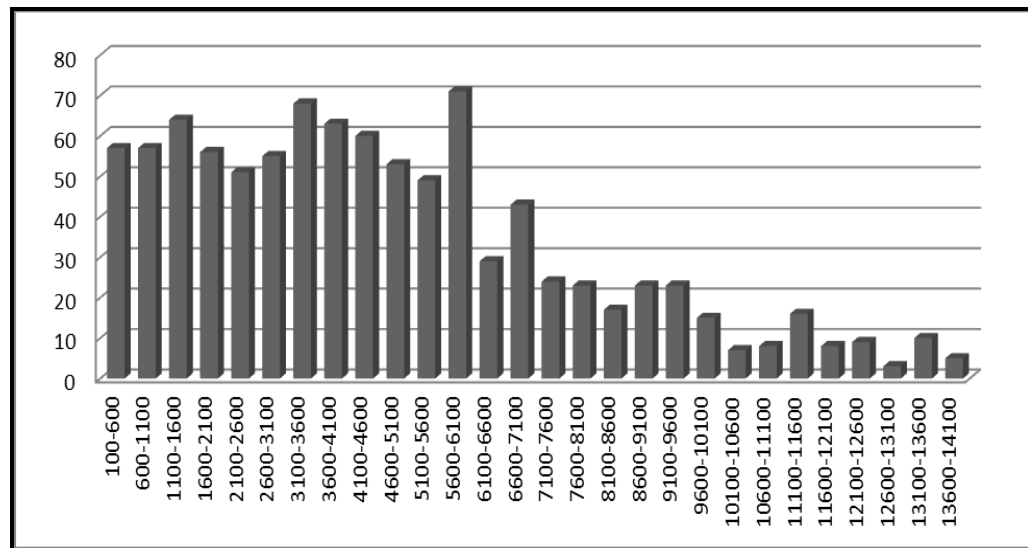


Figure 32. Distribution of Coso Obsidian Hydration Dates for all of Edwards AFB in 500 Year Intervals.

the dramatic decline suggested in Figure 30. An added benefit of using arbitrary, but equally long, time slices is that it affords archaeologists the opportunity to identify patterns that serve as launching points for further research that would ordinarily be obscured by simply grouping data by cultural time period.

#### An Alternative Method for Data Normalization

As noted previously, the researchers who inspired my project explored the issue of habitation intensity by simply interpreting the hydration profiles

generated by their field efforts and the aggregate for all of Edwards AFB (that was current as of 2000) without factoring for the disproportionate lengths of time for each cultural period. That is, they did not normalize the data when conducting their analysis. The problem with this lack of normalization is that it does not factor for the high likelihood that more obsidian will enter the archaeological record given a longer span of time. My approach to normalizing the data consisted of “slicing” it into equal segments and then examining the outcome. However, further pondering on the problem of the led me to arrive at another, perhaps simpler, approach.

This approach begins with a basic assumption that the rate of obsidian deposition remains constant for each cultural time period. From this starting point, it is possible to determine a multiplier needed to equalize the time spans being compared, i.e. increase the ‘smaller’ time period so that it is equal to the ‘larger’ time period. Once that multiplier is identified, it can then be applied to the quantity of obsidian for the smaller time period in order to arrive at the quantity of obsidian that would have been deposited if the smaller time period had lasted as long as the larger time period. As an example using the data from this thesis, a comparison of the obsidian frequency for the Saratoga Springs and Gypsum time periods would look like this:

- The Gypsum period lasted for 2,500 years (4000 to 1500 BP) and produced 291 hydration dates.

- The Saratoga Springs period lasted for 800 years (1500 to 700 BP) and produced 85 hydration dates.
- There is difference of 206 hydration dates between these two cultural periods (i.e. there are 206 more Gypsum period dates).
- A multiplier of 3.125 is needed to increase the duration of the Saratoga Springs period so that it is equal to the Gypsum period ( $3.125 \times 800 = 2500$ ).
- Applying the multiplier to the quantity of hydration dates for the Saratoga Springs period produces a total of 266 dates ( $3.125 \times 85 = 265.6$  rounded up).
- Therefore, assuming that obsidian was deposited into the archaeological record at a constant rate for this elongated Saratoga Springs period, then we would expect analysis of those artifacts to produce 266 hydration dates.

Clearly, 266 is still a smaller quantity of hydration dates than the 289 for the Gypsum period. However, the difference is only 25 dates, which is significantly less than a difference of 206 arrived at when comparing totals from the unequal lengths of time.

The above is a proof-of-concept for an alternate method for normalizing data to make in comparable between disproportionate time spans. A caveat must be given that this method was not exhaustively tested using all of the obsidian hydration dates for Edwards AFB or for the various management regions.



However, this initial exercise suggests this method may be useful for providing a different view of the data in order lend confidence to interpretations of the data from the “time slice” method of data normalization.

#### Hydration Rate at Edwards AFB

Two of the obsidian artifacts (cat. no. 10818 and 10819) included in the supplemental sourcing and hydration analysis for my thesis were selected specifically because they were part of an obsidian chipping station. Specifically, a discrete lithic feature of this nature can be considered a temporally bounded activity because it is located well away from the original lithic source which reduces the possibility of multiple deposition episodes. Additionally, the flakes comprising the feature can be assumed to have been produced in a short time span; perhaps even in a single sitting. Therefore, my intention in selecting two artifacts from such a temporally bounded feature was to empirically assess the rate that obsidian hydrates at Edwards AFB.

Considering the context from which they were recovered it comes as no surprise that both specimens have the same geochemical signature. Unfortunately, that signature places them as originating from the Saline Range source, which means that dates cannot be derived using Basgall’s (1990) Coso hydration formula. Therefore, my assessment of the obsidian hydration rate at Edwards AFB is based simply on a comparison of the hydration rims. In the case of these artifacts, the hydration rim for one flake (cat. no. 10819) was measured as 1.5 microns thicker than the other flake (cat. no. 10818). As can be seen in

the hydration report found in Appendix D, the largest measurement taken for artifact number 10818 is still 1.2 microns smaller than the smallest measurement taken for artifact 10819. Had these artifacts been from the Coso volcanic fields, then the age difference between the two artifacts would be 1,185 years with one flake dating to the Gypsum period and the other to the Saratoga Springs period. This large of a difference between the micron readings for two artifacts recovered from this context is clearly problematic. Again the context in which these artifacts were found must be considered. It is assumed these two flakes were created during the same temporally discrete event that created the chipping station – if not on the same day, certainly within a time span that cannot be picked up by obsidian hydration dating. Therefore, scavenging is not a probable explanation for the difference in rim thicknesses. A more likely explanation for the divergence in the hydration rim readings is that one of the artifacts spent more time on the surface than the other. Given the depositional forces noted in Chapter 1, this supposition is not unreasonable. However, this finding raises a question regarding the reliability of hydration rim readings measured on artifacts recovered from Edwards AFB.

### Recommendations for Further Research

A recurrent concern I had with my research efforts was the effect that various factors have on obsidian hydration and the impact that had on the dates derived for my analysis. Ultimately, I rationalized using the adjustment to Basgall's (1990) Coso hydration formula proposed by Basgall and Overly (2004)

because doing so allows for the comparison of my findings to theirs using the same metric, thus strengthening the results of my analysis. Using another hydration formula, would have produced a different suite of dates and removed the ability to compare between our studies. Revisiting the criticism of the obsidian hydration dating method, the concordance between the point forms and the hydration rim thicknesses returned from the supplemental analysis conducted for this thesis suggests that the matter is not as dire as the critics suggest.

However, the fact remains that a hydration formula grounded in solid research that accounts for variables such as EHT, humidity, intrinsic water, and depositional forces, does not currently exist for the Edwards AFB region. Consequently, researchers who want to incorporate obsidian hydration dates in their investigations are forced to make do with applying formulae developed for other regions of the Great Basin. Therefore, future archaeological investigations in and around Edwards AFB would benefit greatly from a comprehensive research effort that established an obsidian hydration formula specifically for this region of the western Mojave Desert.

As evidenced by the theoretical models presented in Chapter Two, a fundamental assumption at the beginning of my research was that the obsidian decline reported in the earlier studies was a real phenomenon. Therefore, the models for time allocation and technological investment were considered useful for explaining the decline in obsidian frequency. However, once my analysis showed there was no decline, my focus shifted to examining and seeking to

explain how and/or why the previous researchers came to the conclusions they did. Consequently, the theoretical models were no longer relevant to the explaining the particular question I was interested in because there was no longer a need to seek an explanation for the decline.

While the results of my research show that the bow and arrow did not fundamentally change the lithic procurement strategies of the aboriginal inhabitants of Edwards AFB, both the time allocation and technological investment models may help when exploring other research topics involving obsidian use on the installation. One such future research topic is an examination of the diachronic change in the lithic material used to manufacture both formal and informal tools at Edwards AFB. This effort would require an examination of the raw materials used to manufacture all of the tools recovered on Edwards AFB to see if such a change is evident, which was a task clearly outside the scope of this thesis.

## CHAPTER SIX

### CONCLUSION

The goal of my thesis was to investigate a pattern of obsidian use in the western Mojave Desert that was proposed by researchers working at Edwards AFB near the end of the last millennium. In their studies, the researchers concluded that prehistoric obsidian use declined sharply after 1500 B.P. This coincides with the transition from the Gypsum to the Saratoga Springs cultural periods. Significantly, this timing also roughly corresponds to when the bow and arrow is believed to have arrived in this region of the Mojave Desert.

The results of my research demonstrate that past perceptions of the intensity of aboriginal obsidian use at Edwards AFB were detrimentally affected by factors of sampling bias and data organization. The sampling bias is likely a byproduct of the reality that many of the past archaeological studies were commissioned to look specifically at sites within a management region rather than across the entire installation. While the effects of sampling bias are something that most people are familiar with, the effect that data organization can have is less well known. Matthew Johnson contends, “theory is *the order we put facts in*” (2011:2, emphasis in original). The implication of this statement is that the ordering of facts – the way data are organized – influences their interpretation. With regard to the earlier studies that inspired my research, the manner in which their data were organized clearly influenced their interpretations.

In contrast to the earlier studies, my research focused on organizing the data into arbitrary, but equal intervals that allowed for meaningful comparisons of the data. In doing so, my research showed that rather than declining, the amount of obsidian entering the region remained at a relatively stable level from 1500 B.P. until European contact. To be sure, minor fluctuations occurred, but any declines observed are nothing like the near total absence reported in the earlier studies.

My research also identified several intriguing patterns in the distribution of obsidian at Edwards AFB that serve as useful springboards for additional research. The first is that significant fluctuations were observed when the late Holocene quantities of obsidian present in the individual management regions were examined. Specifically, for Management Regions 3 and 5 there is a significant difference in the pattern of obsidian frequency before and after 1500 B.P. Whether these shifts in obsidian quantities were the result changing human behavior due to bow and arrow technology or the result of some other aspect of human behavior is something that warrants further exploration. The fact remains that there is no detectable change in the overall amount of obsidian entering the archaeological record at Edwards AFB subsequent to the arrival of the bow and arrow at about 1500 B.P.

The second is that while the overall amount of obsidian entering the archaeological record remained fairly constant, the number of sites where obsidian was being discarded began to shrink after about 5000 B.P. If obsidian

can truly be considered a proxy for habitation intensity, then this pattern suggests that prehistoric people began occupying fewer locations across Edwards AFB even as they continued using the same amount of obsidian. During the late Holocene it appears that aboriginal land use shifted from one that manifests in the archaeological record as small quantities of obsidian distributed in a large number of sites across a wide area, to one where larger quantities of obsidian are found in a smaller number of sites in a more limited area. Additional research is required to gain a better understanding, but possible explanations for this social transformation include changes in the environment, population levels, mobility patterns, or lithic reduction strategies.

These avenues for future research cannot be understated. Despite more than 40 years' worth of investigations, the archaeology of Edwards AFB is not widely known. In journal articles published about the southwestern Great Basin or the western Mojave Desert, the Edwards AFB is notably absent from the research efforts. This is undoubtedly due to the regulatory nature of the bulk of the work that has occurred on the installation; where the goal was to satisfy some aspect of historic preservation law as opposed to provide meaningful contributions to the archaeological literature. Therefore, it is hoped that this aspect of my research can serve to "pull back the curtain" on an archaeologically interesting area that has been shrouded in mystery for too long.

APPENDIX A  
BIBLIOGRAPHY OF REPORTS CONTAINING  
OBSIDIAN HYDRATION DATA



| <b>Date Published</b> | <b>Authors</b>   | <b>Title</b>  |
|-----------------------|--|---|
| 1988                  | Sutton   | Obsidian Analyses in the Mojave Desert, California: Results, Cautions, and Comments   |
| 1988                  | Rosenthal, Breece, Padon, and Cerreto  | Test Level Investigations at CA-LAN-1295, Edwards Air Force Base, California  |
| 1988                  | Hector, Gross, Bull, Wade, Manley, Haynall, and Cheever                                    | Cultural Resource Investigation for the Farm Drop Zone, Edwards Air Force Base, California  |
| 1989                  | Wade and Hector  | Archaeological Testing and National Register Evaluation of Site LAN-1316, Edwards Air Force Base, California  |
| 1990                  | Wessel, Charlton, Crawford, Howard, Kilanowski, Kummer, McIntyre, Perry, Smock, and Wessel | CA-KER-1830 Test and Evaluation: Technical Report   |
| 1991                  | York and Hull  | Archaeological Investigations at CA-KER-2816 and CA-KER-2817, Edwards Air Force Base, California  |
| 1993                  | Macko  | National Register Eligibility Determinations for Historic Resources Along the Proposed AT&T Lightguide System, Victorville to Bakersfield, California                                     |
| 1994                  | Byrd, Palette, and Serr  | Prehistoric Settlement along the Eastern Margin of Rogers Dry Lake, Western Mojave Desert, California   |
| 1995                  | Swope, Clement, and Pfingst  | Phase I Report Cultural Resources Survey for Remedial Investigation/Feasibility Study South Base Operable Unit No. 2, Edwards Air Force Base  |
| 1995                  | Boyer, Underwood, Alexander, and Earle   | Phase II Cultural Resource Evaluation of the Rich Road Area, Edwards AFB, Kern County California  |
| 1995                  | Campbell, Boyer, Johannesmeyer, Ronning, way, and Wessel                                   | Phase II Cultural Resource Evaluation for the Emplacement of an Underground Natural Gas Transmission Pipeline to Boron from the Phillips Laboratory, Edwards AFB, Kern County, California |
| 1996                  | Campbell   | Phase II Cultural Resource Evaluation for the Abandoned Prime Base Emergency Engineering Force (PRIME BEEF) Facility, Edwards AFB, Kern County, California                                |
| 1996                  | Alcock and Torres  | Phase II Cultural Resource Evaluation of Three Branch Memorial Park Sites: California-Kern (CA-KER) -673/H, CA-KER-1822H, and CA-KER-2309/H, Edwards AFB, Kern County, California         |
| 1996                  | Byrd (editor)  | Camping in the Dunes: Archaeological and Geomorphological Investigations of Late Holocene Settlements West of Rogers Dry Lake   |

| <b>Date Published</b> | <b>Authors</b>   | <b>Title</b>   |
|-----------------------|--|--|
| 1996                  | Bupp, Komprolides, Chandler, Doyle, and Meyer  | Cultural Resources Investigations at Phillips Laboratory, Edwards Air Force Base, California, Installation Restoration Program (IRP) Site Inspection Activities  |
| 1996                  | Silsbee  | Phase II Cultural Resource Evaluation of Site CA-KER-2083, Precision Impact Rang Area (PIRA) West Range, Kern County, Edwards AFB, California  |
| 1997                  | York, Wahoff, and Corbett  | Cultural Resource Investigations at Area P Housing Complex and Adjacent Sites, Edwards Air Force Base, California  |
| 1997                  | Taşkiran, Graham, Doyle, Titus, and Komprolides  | The Evaluation of Site CA-LAN-863, South Rogers Lake Area, Edwards Air Force Base, California  |
| 1997                  | Titus, Chandler, Cotterman, Doyle, Guerrero, Knell, Komprolides, Retamal, and Taşkiran | The Evaluation of Five Archaeological Sites Along 140th Street, Edwards Air Force Base, California   |
| 1998                  | Eckhardt   | Phase II Archaeological Test Evaluation of Six Cultural Resource Sites at Edwards AFB, Kern County, California   |
| 1998                  | Bupp, Chandler, Cotterman, Doyle, Guerrero, Hallett, and Smith                         | The Legacy of Buckhorn Springs: Phase I and II Cultural Resources Investigations, Edwards AFB, Kern County, California   |
| 1999                  | Computer Sciences Corporation  | ETSS Support   |
| 1999                  | Pritchard Parker, Wells, Puckett, and Cooper   | Phase II Cultural Resource Evaluation of Five Archaeological Sites in the Rogers Lake North Management Area, Edwards AFB, Kern County, California  |
| 1999                  | Hughes and Origer  | Geochemical Research Laboratory Letter Report 99-82  |
| 2000                  | Giambastiani and Basgall   | Phase II Cultural Resource Evaluation for Sites CA-KER-4773/H and CA-KER-2016 in the Bissell Basin, Edwards Air Force Base, California   |
| 2000                  | Parker   | Phase II Cultural Resource Evaluation for 19 Sites, Edwards AFB, Kern County, California   |
| 2001                  | Walsh  | Cultural Resource Testing and Phase II Evaluation of the Proposed Jackrabbit Hill Archaeological District, Area 5A, West Range, Precision Impact Range Area (PIRA) at Edwards Air Force Base, California |
| 2001                  | Walsh, Clewlow, and Van Wyke   | Cultural Resource Testing and Phase II Evaluation of Seven Archaeological Sites Along the Edwards Air Force Base Research Laboratory (AFRL) Waterline, Kern County, California                           |
| 2001                  | Campbell   | Phase II Evaluation of the Ettinger Cave Area, Management Region 5, Edwards AFB, Kern  |

| <b>Date Published</b> | <b>Authors</b>   | <b>Title</b>   |
|-----------------------|--|--|
|                       |  | County, California   |
| 2002                  | Chatters, Davy, Fogerty, and Flemming                        | Cultural Resource Testing and Evaluation for 30 Sites in Management Region 5, Edwards Air Force Base, Kern, San Bernardino, and Los Angeles Counties, California                                   |
| 2002                  | Walsh and Wells  | Phase II Cultural Resource Evaluation for Five Sites, Management Region 5, Edwards Air Force Base, California  |
| 2002                  | Deis, Gross, and Ludwig                                      | Phase II Cultural Resource Evaluation for Archaeological Sites in Management Region 5 Edwards AFB, Kern, Los Angeles, and San Bernardino Counties, California                                      |
| 2002                  | Gross, Deis, and Ludwig                                      | Phase II Cultural Resource Evaluation for Archaeological Sites in Target PB-6 Area Edwards AFB, San Bernardino County, California  |
| 2002                  | Walsh and Green  | Phase II Cultural Resource Evaluation for Thirty-Two Sites, Management Regions 3 and 5, South Central Region, Edwards AFB, California  |
| 2002                  | Walsh, Green, Crosby, Johnson, and Clewlow                   | Phase II Cultural Resource Evaluation for Twenty-Seven Archaeological Sites in Cultural Resource Management Regions 3 and 4, Edwards Air Force Base, Kern County, California                       |
| 2002                  | Parker   | Phase II Cultural Resources Evaluation for 20 Sites at Edwards AFB, Kern, Los Angeles, and San Bernardino Counties, California   |
| 2004                  | Basgall and Overly   | Prehistoric Archaeology of the Rosamond Lake Basin: Phase II Cultural Resource Evaluations at 41 Sites in Management Region 2, Edwards Air Force Base, California                                  |
| 2004                  | Budinger, Nicoloff, Campbell, and Spinney                    | Classification of Projectile Points from Edwards Air Force Base and the Western Mojave Desert, California and a Guide to Projectile Points of Edwards Air Force Base and the Western Mojave Desert |
| 2005                  | Chatters and Fogerty   | Archaeological Evaluation for 15 Prehistoric Sites Along the Southern Base Boundary, Edwards AFB, Los Angeles County, California   |
| 2005                  | Horne and McDougall  | A Phase II Evaluation of 25 Prehistoric Archaeological Sites Located in Management Region 3, Edwards Air Force Base, California  |
| 2007                  | Fogerty and Farrell  | Archaeological Evaluation of Selected Sites Along the Northeast Boundary Region, Edwards AFB, Kern and San Bernardino Counties, California   |
| 2007                  | Giambastiani, Ghabhláin, Hale, Catacora, Iversen, and Becker | Phase II Cultural Resource Evaluations of 21 Sites Along the West and Northwestern Boundaries, Edwards AFB, Kern and Los Angeles Counties, California  |

| <b>Date Published</b> | <b>Authors</b>   | <b>Title</b>  |
|-----------------------|--|---|
| 2009                  | Hale, Giambastiani, Iversen, and Richards  | Phase II Cultural Resource Evaluations at 51 Archaeological Sites in Management Regions 1A, 1B, 2B, 2C, and 3E, Bissell Hills and Paiute Ponds, Edwards Air Force Base, Kern and Los Angeles Counties, California |
| 2010                  | Hale, Giambastiani, Daniels, and Dalope  | Phase II Cultural Resources Evaluations at 85 Archaeological Sites in Management Areas 2b, 2c, 3F, 3H, 3I, and 4B, Edwards Air Force Base, Kern and Los Angeles Counties, California                              |
| 2010                  | Chandler, Mason, Cotterman, Bholat, Hale, Aguirre, Howard, Knypstra, Budinger, and Puckett | Prehistoric Themes Study for Cultural Resources Management Region 2 at Edwards Air Force Base, California   |
| 2011                  | Giambastiani, Moore, and Giambastiani  | Phase II Cultural Resource Evaluations at 31 Archaeological Sites in Management Areas 3I and 4B, Edwards Air Force Base, Kern County, California  |
| 2014                  | Giambastiani, Hale, Cole, and Moore  | Evaluations, Archaeological Sites (Mesquite Processing), Range: Edwards Air Force Base, California  |
| 2016                  | Pritchard Parker and Lopez   | A Phase II Archaeological Evaluation of 12 Prehistoric Sites in Management Region 2, Edwards Air Force Base, Los Angeles County, California   |

APPENDIX B  
OBSIDIAN DATABASE

| Trinomial     | Cat No.   | Artifact | Unit (Depth) | Raw<br>Microns | Raw<br>Years BP | Adjusted<br>Microns | Adjusted<br>Years BP | Time<br>Period | Source | Sub-<br>source | Site<br>Type | MR | MA |
|---------------|-----------|----------|--------------|----------------|-----------------|---------------------|----------------------|----------------|--------|----------------|--------------|----|----|
| CA-KER-1161   | 716       | Flake    | Surface      | 11.3           | 8,772           | 11.9                | 9,823                | LPL            | UNK    | NS             | TC           | 2  | A  |
| CA-KER-1161   | 5396      | Flake    | Surface      | 10.3           | 7,075           | 10.8                | 7,923                | LMO            | CO     | WS             | TC           | 2  | A  |
| CA-KER-1161   | 5397      | RTF      | UNK          | 9.7            | 6,156           | 10.2                | 6,893                | PTO            | CO     | WS             | TC           | 2  | A  |
| CA-KER-1161   | 5397      | RTF      | UNK          | 14.4           | 15,394          | 15.1                | 17,239               | LPL            | CO     | WS             | TC           | 2  | A  |
| CA-KER-1161   | 5400      | UTF      | UNK          | 10.8           | 7,898           | 11.3                | 8,844                | LMO            | CO     | WS             | TC           | 2  | A  |
| CA-KER-1162   | 68-68-1   | Flake    | UNK          | 8.9            | 5,041           | 9.3                 | 5,646                | PTO            | CO     | WS             | TC           | 3  | G  |
| CA-KER-1162   | 68-68-1   | Flake    | UNK          | 6.2            | 2,179           | 6.5                 | 2,440                | GYP            | CO     | WS             | TC           | 3  | G  |
| CA-KER-1162   | 45-45-1   | UTF      | UNK          | 5.6            | 1,721           | 5.9                 | 1,927                | GYP            | CO     | WS             | TC           | 3  | G  |
| CA-KER-1162   | 230-230-1 | PF       | UNK          | 6.0            | 2,020           | 6.3                 | 2,262                | GYP            | CO     | WS             | TC           | 3  | G  |
| CA-KER-1174   | 718       | Point    | Surface      | 10.3           | 7,075           | 10.8                | 7,923                | LMO            | CO     | WCP            | TC           | 3  | H  |
| CA-KER-1174   | 720       | UTF      | Surface      | 10.3           | 7,075           | 10.8                | 7,923                | LMO            | CO     | WCP            | TC           | 3  | H  |
| CA-KER-1174   | 721       | Flake    | Surface      | 10.4           | 7,236           | 10.9                | 8,103                | LMO            | CO     | WCP            | TC           | 3  | H  |
| CA-KER-1176   | 3-3-1     | Flake    | UNK          | 0.0            | 0               | 0.0                 | 0                    | --             | CO     | WS             | TC           | 3  | H  |
| CA-KER-1176   | 1-1-1     | Flake    | UNK          | 0.0            | 0               | 0.0                 | 0                    | --             | CO     | WS             | TC           | 3  | H  |
| CA-KER-1180/H | 722       | Flake    | Surface      | 0.0            | 0               | 0.0                 | 0                    | --             | UNK    | NS             | TC           | 3  | G  |
| CA-KER-1180/H | 723       | Flake    | Surface      | 0.0            | 0               | 0.0                 | 0                    | --             | UNK    | NS             | TC           | 3  | G  |
| CA-KER-1182   | 724       | Flake    | Surface      | 6.2            | 2,179           | 6.5                 | 2,440                | GYP            | CO     | WCP            | TC           | 3  | I  |
| CA-KER-1183   | 725       | Flake    | Surface      | 11.1           | 8,416           | 11.7                | 9,425                | LPL            | CO     | WCP            | TC           | 3  | I  |
| CA-KER-1183   | 726       | Flake    | Surface      | 9.4            | 5,723           | 9.9                 | 6,409                | PTO            | CO     | WCP            | TC           | 3  | I  |
| CA-KER-1183   | 1         | BFF      | Surface      | 0.0            | 0               | 0.0                 | 0                    | --             | CO     | WS             | TC           | 3  | I  |
| CA-KER-1183   | 2         | Flake    | Surface      | 13.0           | 12,143          | 13.7                | 13,598               | LPL            | CO     | WS             | TC           | 3  | I  |
| CA-KER-1183   | 3         | Flake    | Surface      | 13.8           | 13,947          | 14.5                | 15,619               | LPL            | CO     | WS             | TC           | 3  | I  |
| CA-KER-1183   | 4         | Flake    | Surface      | 0.0            | 0               | 0.0                 | 0                    | --             | CO     | WS             | TC           | 3  | I  |
| CA-KER-1184   | 727       | Flake    | Surface      | 6.5            | 2,432           | 6.8                 | 2,723                | GYP            | CO     | WCP            | TC           | 5  | A  |
| CA-KER-1187   | 728       | Biface   | Surface      | 0.0            | 0               | 0.0                 | 0                    | --             | UNK    | NS             | TC           | 5  | F  |
| CA-KER-11884  | 4820      | Flake    | Surface      | 8.8            | 4,911           | 9.2                 | 5,499                | PTO            | CO     | WS             | TC           | 2  | A  |
| CA-KER-11884  | 4819      | Flake    | Surface      | 6.8            | 2,700           | 7.1                 | 3,024                | PTO            | CO     | WS             | TC           | 2  | A  |
| CA-KER-1189   | 947       | Flake    | Surface      | 12.3           | 10,679          | 12.9                | 11,959               | LPL            | CO     | WS             | TC           | 3  | F  |
| CA-KER-1189   | 947       | Flake    | Surface      | 10.2           | 6,917           | 10.7                | 7,746                | LMO            | CO     | WS             | TC           | 3  | F  |
| CA-KER-1189   | 948       | Flake    | Surface      | 5.2            | 1,449           | 5.5                 | 1,623                | GYP            | CO     | WCP            | TC           | 3  | F  |
| CA-KER-1189   | 950       | Flake    | Surface      | 12.3           | 10,679          | 12.9                | 11,959               | LPL            | CO     | WCP            | TC           | 3  | F  |
| CA-KER-1189   | 160       | Flake    | TU 3 (0-10)  | 7.1            | 2,985           | 7.5                 | 3,342                | PTO            | CO     | CO             | TC           | 3  | F  |
| CA-KER-1189   | 183       | Flake    | TU 3 (60-70) | 10.3           | 7,075           | 10.8                | 7,923                | LMO            | CO     | CO             | TC           | 3  | F  |
| CA-KER-1189   | 186       | Flake    | TU 4 (0-10)  | 4.4            | 983             | 4.6                 | 1,101                | SSP            | CO     | CO             | TC           | 3  | F  |

| Trinomial     | Cat No. | Artifact | Unit (Depth) | Raw Microns | Raw Years BP | Adjusted Microns | Adjusted Years BP | Time Period | Source | Sub-source | Site Type | MR | MA |
|---------------|---------|----------|--------------|-------------|--------------|------------------|-------------------|-------------|--------|------------|-----------|----|----|
| CA-KER-1189   | 190     | Flake    | TU 4 (10-20) | 3.7         | 658          | 3.9              | 737               | SSP         | CO     | CO         | TC        | 3  | F  |
| CA-KER-1189   | 202     | Flake    | TU 5 (10-20) | 8.5         | 4,531        | 8.9              | 5,074             | PTO         | CO     | CO         | TC        | 3  | F  |
| CA-KER-1189   | 202     | Flake    | TU 5 (10-20) | 7.5         | 3,389        | 7.9              | 3,795             | PTO         | CO     | CO         | TC        | 3  | F  |
| CA-KER-1189   | 207     | Flake    | TU 5 (20-30) | 0.0         | 0            | 0.0              | 0                 | --          | CO     | CO         | TC        | 3  | F  |
| CA-KER-1189   | 227     | Flake    | TU 5 (10-20) | 8.6         | 4,656        | 9.0              | 5,214             | PTO         | CO     | CO         | TC        | 3  | F  |
| CA-KER-1208   | 1173    | Scraper  | Surface      | 6.2         | 2,179        | 6.5              | 2,440             | GYP         | CO     | CO         | TC        | 3  | F  |
| CA-KER-1439   | 280     | BTF      | TU 1 (S)     | 7.1         | 2,985        | 7.5              | 3,342             | PTO         | UNK    | NS         | TC        | 3  | B  |
| CA-KER-1439   | 280     | BTF      | TU 1 (S)     | 5.6         | 1,721        | 5.9              | 1,927             | GYP         | UNK    | NS         | TC        | 3  | B  |
| CA-KER-1439   | 281     | BTF      | TU 2 (S)     | 9.8         | 6,304        | 10.3             | 7,059             | PTO         | UNK    | NS         | TC        | 3  | B  |
| CA-KER-1439   | 281     | BTF      | TU 2 (S)     | 8.4         | 4,408        | 8.8              | 4,937             | PTO         | UNK    | NS         | TC        | 3  | B  |
| CA-KER-1439   | 4650    | PF       | Surface      | 2.1         | 177          | 2.2              | 198               | SHO         | UNK    | NS         | TC        | 3  | B  |
| CA-KER-1702/H | 269     | Flake    | TU 4 (30-40) | 6.3         | 2,262        | 6.6              | 2,533             | GYP         | CO     | WCP        | TC        | 5  | D  |
| CA-KER-1753   | 349-191 | Flake    | Surface      | 7.9         | 3,823        | 8.3              | 4,282             | PTO         | UNK    | NS         | TC        | 3  | J  |
| CA-KER-1763   | 12      | DSN      | Surface      | 1.7         | 108          | 1.8              | 121               | SHO         | CO     | WS         | TC        | 3  | J  |
| CA-KER-1763   | 115     | BFF      | Surface      | 6.2         | 2,179        | 6.5              | 2,440             | GYP         | CO     | WCP        | TC        | 3  | J  |
| CA-KER-1764   | 3690    | Dart     | Surface      | 0.0         | 0            | 0.0              | 0                 | --          | UNK    | UNK        | TC        | 3  | J  |
| CA-KER-1810/H | 45      | LSD      | Surface      | 2.9         | 374          | 3.0              | 419               | SHO         | CO     | WS         | TC        | 3  | B  |
| CA-KER-1810/H | 47      | CWT      | Surface      | 3.0         | 404          | 3.2              | 453               | SHO         | CO     | WS         | TC        | 3  | B  |
| CA-KER-1813   | 19      | Flake    | Surface      | 9.2         | 5,444        | 9.7              | 6,097             | PTO         | CO     | CO         | TC        | 3  | B  |
| CA-KER-1813   | 13      | Flake    | Surface      | 10.4        | 7,236        | 10.9             | 8,103             | LMO         | CO     | CO         | TC        | 3  | B  |
| CA-KER-1813   | 17      | Flake    | Surface      | 11.9        | 9,891        | 12.5             | 11,076            | LPL         | CO     | CO         | TC        | 3  | B  |
| CA-KER-1830   | 2       | SLP      | Surface      | 8.4         | 4,408        | 8.8              | 4,937             | PTO         | UNK    | UNK        | TC        | 3  | I  |
| CA-KER-1830   | 15      | FT       | Surface      | 8.4         | 4,408        | 8.8              | 4,937             | PTO         | CO     | WS         | TC        | 3  | I  |
| CA-KER-1830   | 16      | Flake    | Surface      | 13.2        | 12,580       | 13.9             | 14,088            | LPL         | CO     | SL         | TC        | 3  | I  |
| CA-KER-1830   | 17      | Flake    | Surface      | 9.7         | 6,156        | 10.2             | 6,893             | PTO         | CO     | WS         | TC        | 3  | I  |
| CA-KER-1830   | 15      | Flake    | Surface      | 13.1        | 12,360       | 13.8             | 13,842            | LPL         | CO     | WS         | TC        | 3  | I  |
| CA-KER-1830   | 71      | Flake    | Surface      | 8.4         | 4,408        | 8.8              | 4,937             | PTO         | CO     | WS         | TC        | 3  | I  |
| CA-KER-1830   | 144     | FT       | Surface      | 11.0        | 8,241        | 11.6             | 9,229             | LPL         | CO     | WS         | TC        | 3  | I  |
| CA-KER-1830   | 156     | Flake    | Surface      | 8.6         | 4,656        | 9.0              | 5,214             | PTO         | CO     | WS         | TC        | 3  | I  |
| CA-KER-1830   | 171     | Flake    | Surface      | 10.9        | 8,068        | 11.4             | 9,035             | LMO         | CO     | WS         | TC        | 3  | I  |
| CA-KER-1830   | 172     | Flake    | Surface      | 10.0        | 6,606        | 10.5             | 7,398             | LMO         | CO     | WS         | TC        | 3  | I  |
| CA-KER-1830   | 180     | Flake    | Surface      | 19.5        | 31,106       | 20.5             | 34,834            | LPL         | CO     | WS         | TC        | 3  | I  |
| CA-KER-1830   | 180     | Flake    | Surface      | 11.3        | 8,772        | 11.9             | 9,823             | LPL         | CO     | WS         | TC        | 3  | I  |
| CA-KER-1830   | 197     | Flake    | Surface      | 9.1         | 5,308        | 9.6              | 5,944             | PTO         | CO     | WS         | TC        | 3  | I  |

| Trinomial   | Cat No. | Artifact | Unit (Depth) | Raw<br>Microns | Raw<br>Years BP | Adjusted<br>Microns | Adjusted<br>Years BP | Time<br>Period | Source | Sub-<br>source | Site<br>Type | MR | MA |
|-------------|---------|----------|--------------|----------------|-----------------|---------------------|----------------------|----------------|--------|----------------|--------------|----|----|
| CA-KER-1830 | 205     | Flake    | Surface      | 12.4           | 10,882          | 13.0                | 12,186               | LPL            | CO     | WS             | TC           | 3  | I  |
| CA-KER-1830 | 208     | Flake    | Surface      | 12.1           | 10,281          | 12.7                | 11,513               | LPL            | CO     | JR             | TC           | 3  | I  |
| CA-KER-1830 | 209     | FT       | Surface      | 9.6            | 6,009           | 10.1                | 6,730                | PTO            | CO     | WS             | TC           | 3  | I  |
| CA-KER-1830 | 227     | Flake    | Surface      | 8.9            | 5,041           | 9.3                 | 5,646                | PTO            | CO     | WS             | TC           | 3  | I  |
| CA-KER-1830 | 228     | Flake    | Surface      | 8.6            | 4,656           | 9.0                 | 5,214                | PTO            | CO     | WS             | TC           | 3  | I  |
| CA-KER-1830 | 241     | FT       | Surface      | 8.4            | 4,408           | 8.8                 | 4,937                | PTO            | CO     | WS             | TC           | 3  | I  |
| CA-KER-1830 | 268     | Flake    | Surface      | 8.6            | 4,656           | 9.0                 | 5,214                | PTO            | CO     | WS             | TC           | 3  | I  |
| CA-KER-1830 | 289     | BFF      | Surface      | 8.4            | 4,408           | 8.8                 | 4,937                | PTO            | CO     | WS             | TC           | 3  | I  |
| CA-KER-1830 | 309     | FT       | Surface      | 11.0           | 8,241           | 11.6                | 9,229                | LPL            | CO     | WS             | TC           | 3  | I  |
| CA-KER-1830 | 309     | FT       | Surface      | 4.5            | 1,036           | 4.7                 | 1,160                | SSP            | CO     | WS             | TC           | 3  | I  |
| CA-KER-1830 | 341     | BFF      | Surface      | 10.7           | 7,729           | 11.2                | 8,655                | LMO            | CO     | WS             | TC           | 3  | I  |
| CA-KER-1830 | 394     | Flake    | Surface      | 0.0            | 0               | 0.0                 | 0                    | --             | CO     | SL             | TC           | 3  | I  |
| CA-KER-1830 | 398     | Flake    | Surface      | 0.0            | 0               | 0.0                 | 0                    | --             | CO     | SL             | TC           | 3  | I  |
| CA-KER-1830 | 399     | Flake    | Surface      | 8.6            | 4,656           | 9.0                 | 5,214                | PTO            | CO     | WS             | TC           | 3  | I  |
| CA-KER-1830 | 626     | FT       | Surface      | 9.0            | 5,174           | 9.5                 | 5,794                | PTO            | CO     | WS             | TC           | 3  | I  |
| CA-KER-1830 | 626     | FT       | Surface      | 7.9            | 3,823           | 8.3                 | 4,282                | PTO            | CO     | WS             | TC           | 3  | I  |
| CA-KER-1830 | 634     | FT       | Surface      | 8.8            | 4,911           | 9.2                 | 5,499                | PTO            | CO     | CO             | TC           | 3  | I  |
| CA-KER-1830 | 658     | Flake    | Surface      | 9.0            | 5,174           | 9.5                 | 5,794                | PTO            | CO     | CO             | TC           | 3  | I  |
| CA-KER-1830 | 687     | BFF      | Surface      | 0.0            | 0               | 0.0                 | 0                    | --             | CO     | WS             | TC           | 3  | I  |
| CA-KER-1830 | 733     | FT       | Surface      | 9.8            | 6,304           | 10.3                | 7,059                | PTO            | CO     | WS             | TC           | 3  | I  |
| CA-KER-1830 | 745     | Flake    | TU 2 (10-20) | 8.3            | 4,288           | 8.7                 | 4,802                | PTO            | CO     | WS             | TC           | 3  | I  |
| CA-KER-1830 | 868     | Flake    | TU 9 (0-10)  | 9.7            | 6,156           | 10.2                | 6,893                | PTO            | CO     | WS             | TC           | 3  | I  |
| CA-KER-1830 | 901     | Flake    | TU 9 (20-30) | 9.7            | 6,156           | 10.2                | 6,893                | PTO            | CO     | CO             | TC           | 3  | I  |
| CA-KER-1830 | 910     | Flake    | Surface      | 11.0           | 8,241           | 11.6                | 9,229                | LPL            | CO     | WS             | TC           | 3  | I  |
| CA-KER-1830 | 933     | FT       | Surface      | 9.1            | 5,308           | 9.6                 | 5,944                | PTO            | CO     | WS             | TC           | 3  | I  |
| CA-KER-1830 | 935     | Flake    | Surface      | 7.8            | 3,712           | 8.2                 | 4,157                | PTO            | CO     | WS             | TC           | 3  | I  |
| CA-KER-1830 | 936     | Flake    | Surface      | 8.6            | 4,656           | 9.0                 | 5,214                | PTO            | CO     | CO             | TC           | 3  | I  |
| CA-KER-1830 | 942     | Flake    | Surface      | 16.3           | 20,523          | 17.1                | 22,982               | LPL            | CO     | WS             | TC           | 3  | I  |
| CA-KER-1830 | 942     | Flake    | Surface      | 8.7            | 4,782           | 9.1                 | 5,356                | PTO            | CO     | WS             | TC           | 3  | I  |
| CA-KER-1830 | 950     | Flake    | Surface      | 8.8            | 4,911           | 9.2                 | 5,499                | PTO            | CO     | CO             | TC           | 3  | I  |
| CA-KER-1830 | 951     | Flake    | Surface      | 8.8            | 4,911           | 9.2                 | 5,499                | PTO            | CO     | WS             | TC           | 3  | I  |
| CA-KER-1830 | 968     | Flake    | Surface      | 9.9            | 6,454           | 10.4                | 7,228                | PTO            | CO     | WS             | TC           | 3  | I  |
| CA-KER-1830 | 980     | Flake    | Surface      | 17.1           | 22,936          | 18.0                | 25,685               | LPL            | CO     | SL             | TC           | 3  | I  |
| CA-KER-1830 | 982     | Flake    | Surface      | 14.7           | 16,149          | 15.4                | 18,084               | LPL            | CO     | SL             | TC           | 3  | I  |



| Trinomial     | Cat No.   | Artifact | Unit (Depth)  | Raw Microns | Raw Years BP | Adjusted Microns | Adjusted Years BP | Time Period | Source | Sub-source | Site Type | MR | MA |
|---------------|-----------|----------|---------------|-------------|--------------|------------------|-------------------|-------------|--------|------------|-----------|----|----|
| CA-KER-1830   | 986       | Flake    | Surface       | 0.0         | 0            | 0.0              | 0                 | --          | CO     | WS         | TC        | 3  | I  |
| CA-KER-1830   | 988       | Flake    | Surface       | 9.9         | 6,454        | 10.4             | 7,228             | PTO         | CO     | CO         | TC        | 3  | I  |
| CA-KER-1830   | 989       | Flake    | Surface       | 9.8         | 6,304        | 10.3             | 7,059             | PTO         | CO     | CO         | TC        | 3  | I  |
| CA-KER-1830   | 990       | Flake    | Surface       | 0.0         | 0            | 0.0              | 0                 | --          | CO     | WCP        | TC        | 3  | I  |
| CA-KER-1830   | 991       | Flake    | Surface       | 8.9         | 5,041        | 9.3              | 5,646             | PTO         | CO     | WS         | TC        | 3  | I  |
| CA-KER-1830   | 993       | Flake    | Surface       | 7.5         | 3,389        | 7.9              | 3,795             | PTO         | CO     | CO         | TC        | 3  | I  |
| CA-KER-1830   | 994       | Flake    | Surface       | 9.3         | 5,583        | 9.8              | 6,252             | PTO         | CO     | WS         | TC        | 3  | I  |
| CA-KER-1839   | 368-205   | Flake    | Surface       | 6.1         | 2,099        | 6.4              | 2,350             | GYP         | UNK    | NS         | TC        | 3  | I  |
| CA-KER-1839   | 368-206   | PF       | Surface       | 8.1         | 4,052        | 8.5              | 4,537             | PTO         | UNK    | NS         | TC        | 3  | I  |
| CA-KER-1878   | 7308      | HBT      | Surface       | 0.0         | 0            | 0.0              | 0                 | --          | CO     | WS         | TC        | 3  | I  |
| CA-KER-1878   | 13-13-1   | UTF      | UNK           | 6.4         | 2,346        | 6.7              | 2,627             | GYP         | CO     | WS         | TC        | 3  | I  |
| CA-KER-1880   | 382-94    | Flake    | Surface       | 9.1         | 5,308        | 9.6              | 5,944             | PTO         | CO     | WS         | RS        | 5  | A  |
| CA-KER-1880   | 7031      | BFF      | Surface       | 7.2         | 3,083        | 7.6              | 3,452             | PTO         | CO     | SL         | RS        | 5  | A  |
| CA-KER-1883/H | 386-1-6   | Flake    | Surface       | 21.3        | 38,177       | 22.4             | 42,753            | LPL         | CO     | CO         | TC        | 2  | D  |
| CA-KER-1883/H | 386-1-7   | Flake    | Surface       | 9.6         | 6,009        | 10.1             | 6,730             | PTO         | CO     | WS         | TC        | 2  | D  |
| CA-KER-1883/H | 386-10-34 | Flake    | STU (20-30)   | 9.1         | 5,308        | 9.6              | 5,944             | PTO         | CO     | CO         | TC        | 2  | D  |
| CA-KER-1884   | 387-1-2   | Flake    | Surface       | 10.5        | 7,398        | 11.0             | 8,285             | LMO         | CO     | CO         | TC        | 2  | D  |
| CA-KER-1889   | 4660      | CWL      | Surface       | 6.3         | 2,262        | 6.6              | 2,533             | GYP         | CO     | WS         | TC        | 3  | F  |
| CA-KER-1922/H | 173A      | Flake    | TU 1A (0-5)   | 6.3         | 2,262        | 6.6              | 2,533             | GYP         | UNK    | NS         | BC        | 3  | F  |
| CA-KER-1922/H | 173B      | Flake    | TU 1A (0-5)   | 6.6         | 2,519        | 6.9              | 2,821             | GYP         | UNK    | NS         | BC        | 3  | F  |
| CA-KER-1922/H | 183       | Flake    | TU 2A (10-20) | 6.6         | 2,519        | 6.9              | 2,821             | GYP         | UNK    | NS         | BC        | 3  | F  |
| CA-KER-1922/H | 184       | Flake    | TU 2A (20-30) | 5.9         | 1,942        | 6.2              | 2,175             | GYP         | UNK    | NS         | BC        | 3  | F  |
| CA-KER-1922/H | 172       | Flake    | Surface       | 8.6         | 4,656        | 9.0              | 5,214             | PTO         | CO     | WCP        | BC        | 3  | F  |
| CA-KER-1922/H | 242A      | Flake    | 1AAA (0-5)    | 0.0         | 0            | 0.0              | 0                 | --          | UNK    | NS         | BC        | 3  | F  |
| CA-KER-1922/H | 242B      | Flake    | 1AAA (0-5)    | 7.7         | 3,603        | 8.1              | 4,034             | PTO         | UNK    | NS         | BC        | 3  | F  |
| CA-KER-1922/H | 242C      | Flake    | 1AAA (0-5)    | 5.7         | 1,793        | 6.0              | 2,008             | GYP         | UNK    | NS         | BC        | 3  | F  |
| CA-KER-1922/H | 242D      | Flake    | 1AAA (0-5)    | 6.7         | 2,609        | 7.0              | 2,922             | GYP         | UNK    | NS         | BC        | 3  | F  |
| CA-KER-1922/H | 242E      | Flake    | 1AAA (0-5)    | 5.9         | 1,942        | 6.2              | 2,175             | GYP         | UNK    | NS         | BC        | 3  | F  |
| CA-KER-1922/H | 249       | PF       | 1AAA (0-5)    | 6.1         | 2,099        | 6.4              | 2,350             | GYP         | UNK    | NS         | BC        | 3  | F  |
| CA-KER-1922/H | 274B      | Flake    | 3AAA (0-5)    | 6.5         | 2,432        | 6.8              | 2,723             | GYP         | UNK    | NS         | BC        | 3  | F  |
| CA-KER-1922/H | 279       | CWT      | 4AAA (0-10)   | 2.9         | 374          | 3.0              | 419               | SHO         | CO     | WCP        | BC        | 3  | F  |
| CA-KER-1922/H | 288A      | Flake    | 5AAA (0-10)   | 10.0        | 6,606        | 10.5             | 7,398             | LMO         | UNK    | NS         | BC        | 3  | F  |
| CA-KER-1922/H | 294       | Flake    | 5AAA (10-20)  | 5.8         | 1,867        | 6.1              | 2,091             | GYP         | CD     | LM         | BC        | 3  | F  |
| CA-KER-1922/H | 192C      | Flake    | 6AAA (0-5)    | 9.7         | 6,156        | 10.2             | 6,893             | PTO         | UNK    | NS         | BC        | 3  | F  |

| Trinomial     | Cat No. | Artifact | Unit (Depth)   | Raw Microns | Raw Years BP | Adjusted Microns | Adjusted Years BP | Time Period | Source | Sub-source | Site Type | MR | MA |
|---------------|---------|----------|----------------|-------------|--------------|------------------|-------------------|-------------|--------|------------|-----------|----|----|
| CA-KER-1922/H | 192D    | Flake    | 6AAA (0-5)     | 8.4         | 4,408        | 8.8              | 4,937             | PTO         | UNK    | NS         | BC        | 3  | F  |
| CA-KER-1922/H | 192E    | Flake    | 6AAA (0-5)     | 4.8         | 1,203        | 5.0              | 1,348             | GYP         | UNK    | NS         | BC        | 3  | F  |
| CA-KER-1922/H | 192G    | Flake    | 6AAA (0-5)     | 6.1         | 2,099        | 6.4              | 2,350             | GYP         | UNK    | NS         | BC        | 3  | F  |
| CA-KER-1922/H | 192H    | Flake    | 6AAA (0-5)     | 4.6         | 1,090        | 4.8              | 1,221             | SSP         | UNK    | NS         | BC        | 3  | F  |
| CA-KER-1922/H | 192I    | Flake    | 6AAA (0-5)     | 6.1         | 2,099        | 6.4              | 2,350             | GYP         | UNK    | NS         | BC        | 3  | F  |
| CA-KER-1922/H | 192J    | Flake    | 6AAA (0-5)     | 6.2         | 2,179        | 6.5              | 2,440             | GYP         | UNK    | NS         | BC        | 3  | F  |
| CA-KER-1922/H | 192K    | Flake    | 6AAA (0-5)     | 0.0         | 0            | 0.0              | 0                 | --          | UNK    | NS         | BC        | 3  | F  |
| CA-KER-1922/H | 192L    | Flake    | 6AAA (0-5)     | 4.1         | 835          | 4.3              | 935               | SSP         | UNK    | NS         | BC        | 3  | F  |
| CA-KER-1922/H | 192M    | Flake    | 6AAA (0-5)     | 0.0         | 0            | 0.0              | 0                 | --          | UNK    | NS         | BC        | 3  | F  |
| CA-KER-1922/H | 192N    | Flake    | 6AAA (0-5)     | 4.9         | 1,262        | 5.1              | 1,414             | GYP         | UNK    | NS         | BC        | 3  | F  |
| CA-KER-1922/H | 192O    | Flake    | 6AAA (0-5)     | 4.5         | 1,036        | 4.7              | 1,160             | SSP         | UNK    | NS         | BC        | 3  | F  |
| CA-KER-1922/H | 192P    | Flake    | 6AAA (0-5)     | 8.2         | 4,169        | 8.6              | 4,668             | PTO         | UNK    | NS         | BC        | 3  | F  |
| CA-KER-1922/H | 192Q    | Flake    | 6AAA (0-5)     | 9.0         | 5,174        | 9.5              | 5,794             | PTO         | UNK    | NS         | BC        | 3  | F  |
| CA-KER-1922/H | 192R    | Flake    | 6AAA (0-5)     | 6.1         | 2,099        | 6.4              | 2,350             | GYP         | UNK    | NS         | BC        | 3  | F  |
| CA-KER-1922/H | 192S    | Flake    | 6AAA (0-5)     | 8.2         | 4,169        | 8.6              | 4,668             | PTO         | UNK    | NS         | BC        | 3  | F  |
| CA-KER-1922/H | 204A    | Flake    | 7AAA (0-10)    | 7.3         | 3,183        | 7.7              | 3,565             | PTO         | UNK    | NS         | BC        | 3  | F  |
| CA-KER-1922/H | 204B    | Flake    | 7AAA (0-10)    | 7.7         | 3,603        | 8.1              | 4,034             | PTO         | UNK    | NS         | BC        | 3  | F  |
| CA-KER-1922/H | 210     | Flake    | 7AAA           | 12.3        | 10,679       | 12.9             | 11,959            | LPL         | UNK    | NS         | BC        | 3  | F  |
| CA-KER-1922/H | 227A    | Flake    | 8AAA (0-10)    | 7.9         | 3,823        | 8.3              | 4,282             | PTO         | UNK    | NS         | BC        | 3  | F  |
| CA-KER-1922/H | 227B    | Flake    | 8AAA (0-10)    | 6.9         | 2,793        | 7.2              | 3,128             | PTO         | UNK    | NS         | BC        | 3  | F  |
| CA-KER-1922/H | 238A    | Flake    | 8AAA (30-40)   | 4.6         | 1,090        | 4.8              | 1,221             | SSP         | UNK    | NS         | BC        | 3  | F  |
| CA-KER-1922/H | 238B    | Flake    | 8AAA (30-40)   | 7.8         | 3,712        | 8.2              | 4,157             | PTO         | UNK    | NS         | BC        | 3  | F  |
| CA-KER-1922/H | 244     | Flake    | 8AAA (40-50)   | 7.7         | 3,603        | 8.1              | 4,034             | PTO         | UNK    | NS         | BC        | 3  | F  |
| CA-KER-1922/H | 263     | Flake    | 8AAA (130-140) | 6.8         | 2,700        | 7.1              | 3,024             | PTO         | UNK    | NS         | BC        | 3  | F  |
| CA-KER-1922/H | 267     | Flake    | Surface        | 5.4         | 1,582        | 5.7              | 1,771             | GYP         | CO     | WCP        | BC        | 3  | F  |
| CA-KER-1922/H | 276     | Flake    | Surface        | 9.8         | 6,304        | 10.3             | 7,059             | PTO         | CO     | WS         | BC        | 3  | F  |
| CA-KER-1922/H | 291     | Flake    | Surface        | 6.6         | 2,519        | 6.9              | 2,821             | GYP         | CO     | WCP        | BC        | 3  | F  |
| CA-KER-1922/H | 313     | Flake    | 1B (10-20)     | 1.1         | 39           | 1.2              | 44                | SHO         | UNK    | NS         | BC        | 3  | F  |
| CA-KER-1922/H | 323     | Flake    | 1B (60-70)     | 9.6         | 6,009        | 10.1             | 6,730             | PTO         | UNK    | NS         | BC        | 3  | F  |
| CA-KER-1922/H | 332     | Flake    | 3B (0-50)      | 7.7         | 3,603        | 8.1              | 4,034             | PTO         | CO     | WCP        | BC        | 3  | F  |
| CA-KER-1922/H | 336     | Flake    | 4B (0-10)      | 2.0         | 158          | 2.1              | 177               | SHO         | UNK    | NS         | BC        | 3  | F  |
| CA-KER-1922/H | 342     | Flake    | Surface        | 6.4         | 2,346        | 6.7              | 2,627             | GYP         | CO     | WCP        | BC        | 3  | F  |
| CA-KER-1922/H | 841     | Flake    | 31KKK (0-10)   | 8.2         | 4,169        | 8.6              | 4,668             | PTO         | BM     | BM         | BC        | 3  | F  |
| CA-KER-1922/H | 864     | Flake    | 31KKK (40-50)  | 6.6         | 2,519        | 6.9              | 2,821             | GYP         | UNK    | NS         | BC        | 3  | F  |

| Trinomial     | Cat No.    | Artifact | Unit (Depth)   | Raw Microns | Raw Years BP | Adjusted Microns | Adjusted Years BP | Time Period | Source | Sub-source | Site Type | MR | MA |
|---------------|------------|----------|----------------|-------------|--------------|------------------|-------------------|-------------|--------|------------|-----------|----|----|
| CA-KER-1922/H | 650A       | Flake    | 12T (20-30)    | 7.1         | 2,985        | 7.5              | 3,342             | PTO         | UNK    | NS         | BC        | 3  | F  |
| CA-KER-1922/H | 650B       | Flake    | 12T (20-30)    | 6.1         | 2,099        | 6.4              | 2,350             | GYP         | UNK    | NS         | BC        | 3  | F  |
| CA-KER-1922/H | 661        | Flake    | 12T (30-40)    | 4.7         | 1,146        | 4.9              | 1,283             | GYP         | UNK    | NS         | BC        | 3  | F  |
| CA-KER-1922/H | 683        | Flake    | 12T (60-70)    | 0.0         | 0            | 0.0              | 0                 | --          | UNK    | NS         | BC        | 3  | F  |
| CA-KER-1922/H | 712        | Flake    | 12T (100-110)  | 5.2         | 1,449        | 5.5              | 1,623             | GYP         | UNK    | NS         | BC        | 3  | F  |
| CA-KER-1922/H | 395        | Flake    | 5T (30-60)     | 8.9         | 5,041        | 9.3              | 5,646             | PTO         | UNK    | NS         | BC        | 3  | F  |
| CA-KER-1922/H | 467        | Flake    | 13V (0-30)     | 6.9         | 2,793        | 7.2              | 3,128             | PTO         | UNK    | NS         | BC        | 3  | F  |
| CA-KER-1922/H | 543        | Flake    | 17V (0-10)     | 6.6         | 2,519        | 6.9              | 2,821             | GYP         | UNK    | NS         | BC        | 3  | F  |
| CA-KER-1922/H | 1016       | Flake    | Surface        | 7.5         | 3,389        | 7.9              | 3,795             | PTO         | CO     | WCP        | BC        | 3  | F  |
| CA-KER-1922/H | 1017       | Flake    | Surface        | 8.8         | 4,911        | 9.2              | 5,499             | PTO         | FS     | FS         | BC        | 3  | F  |
| CA-KER-1922/H | 920        | Flake    | Surface        | 8.3         | 4,288        | 8.7              | 4,802             | PTO         | CO     | WCP        | BC        | 3  | F  |
| CA-KER-1922/H | 969A       | Flake    | 41 (0-10)      | 8.0         | 3,937        | 8.4              | 4,408             | PTO         | UNK    | NS         | BC        | 3  | F  |
| CA-KER-1922/H | 969B       | Flake    | 41 (0-10)      | 7.0         | 2,888        | 7.4              | 3,234             | PTO         | UNK    | NS         | BC        | 3  | F  |
| CA-KER-1922/H | 969C       | Flake    | 41 (0-10)      | 5.5         | 1,650        | 5.8              | 1,848             | GYP         | UNK    | NS         | BC        | 3  | F  |
| CA-KER-1922/H | 4788       | AB       | Surface        | 2.0         | 158          | 2.1              | 177               | SHO         | CO     | WS         | BC        | 3  | F  |
| CA-KER-1922/H | 423-1023   | DSN      | Surface        | 3.1         | 436          | 3.3              | 489               | SHO         | CO     | WS         | BC        | 3  | F  |
| CA-KER-1922/H | 2018       | DSN      | Surface        | 2.5         | 265          | 2.6              | 297               | SHO         | CO     | WS         | BC        | 3  | F  |
| CA-KER-1922/H | 1018       | DSN      | Surface        | 2.9         | 374          | 3.0              | 419               | SHO         | CO     | JR         | BC        | 3  | F  |
| CA-KER-2007   | 559-1      | Flake    | Surface        | 9.0         | 5,174        | 9.5              | 5,794             | PTO         | CO     | WS         | TC        | 3  | F  |
| CA-KER-2007   | 559-12     | Flake    | STP A (0-10)   | 4.6         | 1,090        | 4.8              | 1,221             | SSP         | CO     | WS         | TC        | 3  | F  |
| CA-KER-2009/H | 1078       | Pinto    | Surface        | 8.5         | 4,531        | 8.9              | 5,074             | PTO         | CO     | WS         | TC        | 1  | A  |
| CA-KER-2016   | 1080       | ECN      | Surface        | 5.2         | 1,449        | 5.5              | 1,623             | GYP         | CO     | WS         | TC        | 1  | A  |
| CA-KER-2016   | 7702       | RSP      | Surface        | 4.2         | 883          | 4.4              | 989               | SSP         | CO     | WS         | TC        | 1  | A  |
| CA-KER-2016   | 568-1-519  | Flake    | Surface        | 0.0         | 0            | 0.0              | 0                 | --          | CO     | WS         | TC        | 1  | A  |
| CA-KER-2016   | 568-1-640  | Flake    | Surface        | 8.8         | 4,911        | 9.2              | 5,499             | PTO         | CO     | WS         | TC        | 1  | A  |
| CA-KER-2016   | 568-1-695a | Flake    | SRU Cell E (S) | 1.4         | 69           | 1.5              | 77                | SHO         | CO     | WS         | TC        | 1  | A  |
| CA-KER-2016   | 561-1-695b | Flake    | SRU Cell E (S) | 8.9         | 5,041        | 9.3              | 5,646             | PTO         | CO     | WS         | TC        | 1  | A  |
| CA-KER-2016   | 561-1-2    | Flake    | Surface        | 0.0         | 0            | 0.0              | 0                 | --          | CO     | WS         | TC        | 1  | A  |
| CA-KER-2016   | 568-1-3    | Flake    | Surface        | 8.8         | 4,911        | 9.2              | 5,499             | PTO         | CO     | WS         | TC        | 1  | A  |
| CA-KER-2016   | 568-1-5    | Flake    | Surface        | 8.9         | 5,041        | 9.3              | 5,646             | PTO         | CO     | WS         | TC        | 1  | A  |
| CA-KER-2016   | 568-1-6    | Point    | Surface        | 8.8         | 4,911        | 9.2              | 5,499             | PTO         | CO     | WS         | TC        | 1  | A  |
| CA-KER-2016   | 568-1-7a   | Flake    | Surface        | 9.0         | 5,174        | 9.5              | 5,794             | PTO         | CO     | WS         | TC        | 1  | A  |
| CA-KER-2016   | 568-1-7b   | Flake    | Surface        | 8.8         | 4,911        | 9.2              | 5,499             | PTO         | CO     | WS         | TC        | 1  | A  |
| CA-KER-2016   | 568-1-9    | Flake    | Surface        | 9.0         | 5,174        | 9.5              | 5,794             | PTO         | CO     | WS         | TC        | 1  | A  |

| Trinomial     | Cat No.     | Artifact | Unit (Depth)      | Raw Microns | Raw Years BP | Adjusted Microns | Adjusted Years BP | Time Period | Source | Sub-source | Site Type | MR | MA |
|---------------|-------------|----------|-------------------|-------------|--------------|------------------|-------------------|-------------|--------|------------|-----------|----|----|
| CA-KER-2016   | 568-1-21    | Flake    | Surface           | 3.5         | 578          | 3.7              | 648               | SSP         | CO     | WS         | TC        | 1  | A  |
| CA-KER-2016   | 568-1-22    | Flake    | Surface           | 8.8         | 4,911        | 9.2              | 5,499             | PTO         | CO     | CO         | TC        | 1  | A  |
| CA-KER-2016   | 568-1-24    | Flake    | Surface           | 4.4         | 983          | 4.6              | 1,101             | SSP         | CO     | WS         | TC        | 1  | A  |
| CA-KER-2016   | 568-1-25    | Flake    | Surface           | 4.5         | 1,036        | 4.7              | 1,160             | SSP         | CO     | WS         | TC        | 1  | A  |
| CA-KER-2016   | 568-1-26    | Point    | Surface           | 4.2         | 883          | 4.4              | 989               | SSP         | CO     | WS         | TC        | 1  | A  |
| CA-KER-2016   | 568-1-28    | Flake    | Surface           | 8.3         | 4,288        | 8.7              | 4,802             | PTO         | CO     | WS         | TC        | 1  | A  |
| CA-KER-2016   | 568-1-29    | Flake    | Surface           | 6.8         | 2,700        | 7.1              | 3,024             | PTO         | CO     | WS         | TC        | 1  | A  |
| CA-KER-2016   | 568-1-30    | Flake    | Surface           | 6.6         | 2,519        | 6.9              | 2,821             | GYP         | CO     | WS         | TC        | 1  | A  |
| CA-KER-2016   | 568-1-31    | Flake    | Surface           | 4.4         | 983          | 4.6              | 1,101             | SSP         | CO     | CO         | TC        | 1  | A  |
| CA-KER-2016   | 568-1-32    | Point    | Surface           | 4.5         | 1,036        | 4.7              | 1,160             | SSP         | CO     | WS         | TC        | 1  | A  |
| CA-KER-2016   | 568-1-243   | Point    | Surface           | 4.4         | 983          | 4.6              | 1,101             | SSP         | CO     | WS         | TC        | 1  | A  |
| CA-KER-2016   | 568-1-316   | Flake    | SRU Cell A (S)    | 4.6         | 1,090        | 4.8              | 1,221             | SSP         | CO     | WS         | TC        | 1  | A  |
| CA-KER-2016   | 568-1-333a  | Flake    | SRU Cell F (S)    | 4.4         | 983          | 4.6              | 1,101             | SSP         | CO     | WS         | TC        | 1  | A  |
| CA-KER-2016   | 568-1-333b  | Flake    | SRU Cell F (S)    | 7.5         | 3,389        | 7.9              | 3,795             | PTO         | CO     | CO         | TC        | 1  | A  |
| CA-KER-2016   | 568-10-360  | Flake    | N1/W4 (10-20)     | 3.2         | 470          | 3.4              | 526               | SHO         | CO     | CO         | TC        | 1  | A  |
| CA-KER-2016   | 568-10-376a | Flake    | N1/W6 (10-20)     | 3.5         | 578          | 3.7              | 648               | SSP         | CO     | WS         | TC        | 1  | A  |
| CA-KER-2016   | 568-10-434  | Point    | S6/W6 (60-70)     | 3.4         | 541          | 3.6              | 606               | SSP         | CO     | WS         | TC        | 1  | A  |
| CA-KER-2016   | 568-10-464  | Point    | S8/W5 (10-20)     | 4.4         | 983          | 4.6              | 1,101             | SSP         | CO     | CO         | TC        | 1  | A  |
| CA-KER-2016   | 568-10-481  | Flake    | S8/W5 (50-60)     | 3.4         | 541          | 3.6              | 606               | SSP         | CO     | CO         | TC        | 1  | A  |
| CA-KER-2016   | 568-1-8     | Flake    | Surface           | 8.0         | 3,937        | 8.4              | 4,408             | PTO         | CO     | CO         | TC        | 1  | A  |
| CA-KER-2016   | 568-1-22    | Flake    | Surface           | 7.3         | 3,183        | 7.7              | 3,565             | PTO         | CO     | WS         | TC        | 1  | A  |
| CA-KER-2016   | 568-1-27    | Flake    | Surface           | 7.5         | 3,389        | 7.9              | 3,795             | PTO         | CO     | WS         | TC        | 1  | A  |
| CA-KER-2016   | 568-1-37    | Point    | Surface           | 6.6         | 2,519        | 6.9              | 2,821             | GYP         | CO     | WS         | TC        | 1  | A  |
| CA-KER-2016   | 568-10-198  | Flake    | N38/W49 (10-20)   | 7.5         | 3,389        | 7.9              | 3,795             | PTO         | CO     | WS         | TC        | 1  | A  |
| CA-KER-2016   | 568-10-211  | Flake    | N40/W49 (10-20)   | 7.9         | 3,823        | 8.3              | 4,282             | PTO         | CO     | WS         | TC        | 1  | A  |
| CA-KER-2016   | 568-10-233  | Flake    | S15.5/E47 (20-30) | 5.7         | 1,793        | 6.0              | 2,008             | GYP         | CO     | CO         | TC        | 1  | A  |
| CA-KER-2025   | 1599        | DSN      | Surface           | 4.0         | 788          | 4.2              | 883               | SSP         | CO     | WS         | TC        | 3  | I  |
| CA-KER-2027   | 1190        | LMO      | Surface           | 9.3         | 5,583        | 9.8              | 6,252             | PTO         | UNK    | UNK        | TC        | 3  | I  |
| CA-KER-2038   | 101         | Dart     | TU 16 (20-30)     | 6.0         | 2,020        | 6.3              | 2,262             | GYP         | CO     | SL         | TC        | 3  | I  |
| CA-KER-2038   | 132         | Pinto    | Surface           | 8.6         | 4,656        | 9.0              | 5,214             | PTO         | CO     | WS         | TC        | 3  | I  |
| CA-KER-2038   | 133         | Dart     | Surface           | 0.0         | 0            | 0.0              | 0                 | --          | CO     | WS         | TC        | 3  | I  |
| CA-KER-2038   | 7269        | Elko     | Surface           | 5.8         | 1,867        | 6.1              | 2,091             | GYP         | CO     | WS         | TC        | 3  | I  |
| CA-KER-2038/H | 7282        | RSP      | Surface           | 4.3         | 932          | 4.5              | 1,044             | SSP         | CO     | WS         | TC        | 3  | I  |
| CA-KER-2053   | 174         | BTF      | TU 6 (20-30)      | 9.3         | 5,583        | 9.8              | 6,252             | PTO         | CO     | WS         | TC        | 4  | B  |

| Trinomial   | Cat No.  | Artifact | Unit (Depth) | Raw Microns | Raw Years BP | Adjusted Microns | Adjusted Years BP | Time Period | Source | Sub-source | Site Type | MR | MA |
|-------------|----------|----------|--------------|-------------|--------------|------------------|-------------------|-------------|--------|------------|-----------|----|----|
| CA-KER-2053 | 106      | BTF      | TU 3 (S)     | 9.2         | 5,444        | 9.7              | 6,097             | PTO         | CO     | WS         | TC        | 4  | B  |
| CA-KER-2053 | 99       | BTF      | TU 3 (S)     | 0.0         | 0            | 0.0              | 0                 | --          | CO     | WCP        | TC        | 4  | B  |
| CA-KER-2059 | 1        | Flake    | Surface      | 9.8         | 6,304        | 10.3             | 7,059             | PTO         | CO     | SL         | TC        | 3  | I  |
| CA-KER-2059 | 2        | Flake    | Surface      | 0.0         | 0            | 0.0              | 0                 | --          | CO     | SL         | TC        | 3  | I  |
| CA-KER-2059 | 3        | Flake    | Surface      | 0.0         | 0            | 0.0              | 0                 | --          | CO     | SL         | TC        | 3  | I  |
| CA-KER-2059 | 4        | Flake    | Surface      | 0.0         | 0            | 0.0              | 0                 | --          | CO     | SL         | TC        | 3  | I  |
| CA-KER-2059 | 5        | Flake    | Surface      | 0.0         | 0            | 0.0              | 0                 | --          | CO     | SL         | TC        | 3  | I  |
| CA-KER-2059 | 6        | Flake    | Surface      | 7.4         | 3,285        | 7.8              | 3,679             | PTO         | CO     | SL         | TC        | 3  | I  |
| CA-KER-2059 | 7        | Flake    | Surface      | 10.2        | 6,917        | 10.7             | 7,746             | LMO         | CO     | SL         | TC        | 3  | I  |
| CA-KER-2059 | 8        | Flake    | Surface      | 9.0         | 5,174        | 9.5              | 5,794             | PTO         | CO     | SL         | TC        | 3  | I  |
| CA-KER-2059 | 9        | Flake    | Surface      | 8.5         | 4,531        | 8.9              | 5,074             | PTO         | CO     | SL         | TC        | 3  | I  |
| CA-KER-2059 | 9        | Flake    | Surface      | 1.5         | 81           | 1.6              | 91                | SHO         | CO     | SL         | TC        | 3  | I  |
| CA-KER-2059 | 10       | Flake    | Surface      | 8.0         | 3,937        | 8.4              | 4,408             | PTO         | CO     | SL         | TC        | 3  | I  |
| CA-KER-2059 | 11       | Flake    | Surface      | 8.4         | 4,408        | 8.8              | 4,937             | PTO         | CO     | SL         | TC        | 3  | I  |
| CA-KER-2059 | 12       | Flake    | Surface      | 12.2        | 10,479       | 12.8             | 11,735            | LPL         | CO     | SL         | TC        | 3  | I  |
| CA-KER-2059 | 13       | Flake    | Surface      | 8.4         | 4,408        | 8.8              | 4,937             | PTO         | CO     | SL         | TC        | 3  | I  |
| CA-KER-2059 | 14       | Flake    | Surface      | 11.5        | 9,137        | 12.1             | 10,232            | LPL         | CO     | SL         | TC        | 3  | I  |
| CA-KER-2059 | 15       | Flake    | Surface      | 8.9         | 5,041        | 9.3              | 5,646             | PTO         | CO     | SL         | TC        | 3  | I  |
| CA-KER-2059 | 16       | Flake    | Surface      | 0.0         | 0            | 0.0              | 0                 | --          | CO     | SL         | TC        | 3  | I  |
| CA-KER-2059 | 17       | Flake    | Surface      | 0.0         | 0            | 0.0              | 0                 | --          | CO     | SL         | TC        | 3  | I  |
| CA-KER-2059 | 18       | Flake    | Surface      | 0.0         | 0            | 0.0              | 0                 | --          | CO     | SL         | TC        | 3  | I  |
| CA-KER-2059 | 19       | Flake    | Surface      | 11.1        | 8,416        | 11.7             | 9,425             | LPL         | CO     | SL         | TC        | 3  | I  |
| CA-KER-2059 | 20       | Flake    | Surface      | 0.0         | 0            | 0.0              | 0                 | --          | CO     | SL         | TC        | 3  | I  |
| CA-KER-2059 | 21       | Flake    | Surface      | 0.0         | 0            | 0.0              | 0                 | --          | CO     | SL         | TC        | 3  | I  |
| CA-KER-2059 | 22       | Flake    | Surface      | 7.2         | 3,083        | 7.6              | 3,452             | PTO         | CO     | WS         | TC        | 3  | I  |
| CA-KER-2059 | 23       | Flake    | Surface      | 0.0         | 0            | 0.0              | 0                 | --          | CO     | SL         | TC        | 3  | I  |
| CA-KER-2059 | 24       | Flake    | Surface      | 11.4        | 8,953        | 12.0             | 10,026            | LPL         | CO     | SL         | TC        | 3  | I  |
| CA-KER-2059 | 25       | Flake    | Surface      | 9.5         | 5,865        | 10.0             | 6,568             | PTO         | CO     | SL         | TC        | 3  | I  |
| CA-KER-2091 | 4912     | PF       | Surface      | 6.5         | 2,432        | 6.8              | 2,723             | GYP         | CO     | WS         | TC        | 3  | J  |
| CA-KER-2124 | 2124-111 | BFF      | Surface      | 4.1         | 835          | 4.3              | 935               | SSP         | CO     | WS         | TC        | 3  | B  |
| CA-KER-2131 | 99       | BTF      | TU 2 (30-40) | 8.8         | 4,911        | 9.2              | 5,499             | PTO         | CO     | CO         | TC        | 3  | F  |
| CA-KER-2131 | 594      | Shatter  | TU 7 (S)     | 8.6         | 4,656        | 9.0              | 5,214             | PTO         | CO     | CO         | TC        | 3  | F  |
| CA-KER-2154 | 6836     | UTF      | UNK          | 8.3         | 4,288        | 8.7              | 4,802             | PTO         | CO     | WS         | HE        | 3  | F  |
| CA-KER-2200 | 6770     | Flake    | Surface      | 5.8         | 1,867        | 6.1              | 2,091             | GYP         | CO     | WS         | RS        | 5  | A  |



| Trinomial     | Cat No.  | Artifact | Unit (Depth)   | Raw Microns | Raw Years BP | Adjusted Microns | Adjusted Years BP | Time Period | Source | Sub-source | Site Type | MR | MA |
|---------------|----------|----------|----------------|-------------|--------------|------------------|-------------------|-------------|--------|------------|-----------|----|----|
| CA-KER-2200   | 6771     | Flake    | Surface        | 10.5        | 7,398        | 11.0             | 8,285             | LMO         | CO     | WCP        | RS        | 5  | A  |
| CA-KER-2200   | 6771     | Flake    | Surface        | 7.9         | 3,823        | 8.3              | 4,282             | PTO         | CO     | WCP        | RS        | 5  | A  |
| CA-KER-2200   | 6772     | Flake    | Surface        | 8.8         | 4,911        | 9.2              | 5,499             | PTO         | CO     | WS         | RS        | 5  | A  |
| CA-KER-2234   | 11-11-1  | Flake    | UNK            | 4.6         | 1,090        | 4.8              | 1,221             | SSP         | CO     | WS         | TC        | 3  | I  |
| CA-KER-2234   | 27-26-2  | UTF      | UNK            | 4.7         | 1,146        | 4.9              | 1,283             | GYP         | CO     | WS         | TC        | 3  | I  |
| CA-KER-2234   | 24-24-1  | UTF      | UNK            | 9.5         | 5,865        | 10.0             | 6,568             | PTO         | CO     | WS         | TC        | 3  | I  |
| CA-KER-2234   | 5-5-1    | UTF      | UNK            | 6.4         | 2,346        | 6.7              | 2,627             | GYP         | CO     | WS         | TC        | 3  | I  |
| CA-KER-2234   | 9-9-1    | RTF      | UNK            | 8.9         | 5,041        | 9.3              | 5,646             | PTO         | CO     | WS         | TC        | 3  | I  |
| CA-KER-2308/H | 2776-1   | Flake    | Surface        | 14.6        | 15,895       | 15.3             | 17,800            | LPL         | CO     | WCP        | LD        | 5  | F  |
| CA-KER-2308/H | 2776-2   | Flake    | Surface        | 6.0         | 2,020        | 6.3              | 2,262             | GYP         | CO     | WCP        | LD        | 5  | F  |
| CA-KER-2308/H | 2776-15  | Flake    | STP 7 (30-40)  | 12.2        | 10,479       | 12.8             | 11,735            | LPL         | CO     | WCP        | LD        | 5  | F  |
| CA-KER-2308/H | 2776-27a | Flake    | STP 15 (10-20) | 16.2        | 20,232       | 17.0             | 22,657            | LPL         | UNK    | NS         | LD        | 5  | F  |
| CA-KER-2346   | 920-02   | Flake    | Surface        | 7.6         | 3,495        | 8.0              | 3,914             | PTO         | CO     | WCP        | TC        | 3  | C  |
| CA-KER-2347   | 921-51   | Flake    | Surface        | 7.9         | 3,823        | 8.3              | 4,282             | PTO         | CO     | WCP        | TC        | 3  | C  |
| CA-KER-2347   | 921-54   | Flake    | Surface        | 8.2         | 4,169        | 8.6              | 4,668             | PTO         | CO     | WCP        | TC        | 3  | C  |
| CA-KER-2347   | 921-54b  | Flake    | Surface        | 9.6         | 6,009        | 10.1             | 6,730             | PTO         | CO     | WCP        | TC        | 3  | C  |
| CA-KER-2351   | 931-51   | Flake    | Surface        | 11.3        | 8,772        | 11.9             | 9,823             | LPL         | CO     | WS         | TC        | 3  | A  |
| CA-KER-2378   | 168      | Flake    | TU 4 (10-20)   | 9.2         | 5,444        | 9.7              | 6,097             | PTO         | CO     | CO         | TC        | 3  | F  |
| CA-KER-2482/H | 53       | Flake    | TU 1 (50-60)   | 7.1         | 2,985        | 7.5              | 3,342             | PTO         | CO     | CO         | TC        | 3  | F  |
| CA-KER-2482/H | 74       | Flake    | TU 1 (100-110) | 8.3         | 4,288        | 8.7              | 4,802             | PTO         | CO     | CO         | TC        | 3  | F  |
| CA-KER-2482/H | 79       | Flake    | TU 1 (110-120) | 8.5         | 4,531        | 8.9              | 5,074             | PTO         | CO     | CO         | TC        | 3  | F  |
| CA-KER-2482/H | 82       | Flake    | TU 2 (0-10)    | 11.9        | 9,891        | 12.5             | 11,076            | LPL         | CO     | CO         | TC        | 3  | F  |
| CA-KER-2482/H | 86       | Flake    | TU 2 (10-20)   | 9.3         | 5,583        | 9.8              | 6,252             | PTO         | CO     | CO         | TC        | 3  | F  |
| CA-KER-2482/H | 113      | Flake    | TU 2 (90-100)  | 0.0         | 0            | 0.0              | 0                 | --          | CO     | CO         | TC        | 3  | F  |
| CA-KER-2482/H | 115      | Flake    | TU 2 (100-110) | 9.2         | 5,444        | 9.7              | 6,097             | PTO         | CO     | CO         | TC        | 3  | F  |
| CA-KER-2482/H | 121      | Flake    | TU 2 (100-110) | 10.9        | 8,068        | 11.4             | 9,035             | LMO         | CO     | CO         | TC        | 3  | F  |
| CA-KER-2482/H | 132      | Flake    | TU 2 (120-130) | 8.8         | 4,911        | 9.2              | 5,499             | PTO         | CO     | CO         | TC        | 3  | F  |
| CA-KER-2532   | 1065-69  | Flake    | Surface        | 9.1         | 5,308        | 9.6              | 5,944             | PTO         | CO     | WCP        | TC        | 3  | J  |
| CA-KER-2533   | 4592     | RSP      | Surface        | 4.2         | 883          | 4.4              | 989               | SSP         | CO     | WS         | HE        | 2  | A  |
| CA-KER-2558/H | 81       | Flake    | Surface        | 14.3        | 15,148       | 15.0             | 16,963            | LPL         | CO     | WS         | TC        | 2  | B  |
| CA-KER-2558/H | 82       | Flake    | Surface        | 13.3        | 12,803       | 14.0             | 14,337            | LPL         | CO     | WS         | TC        | 2  | B  |
| CA-KER-2558/H | 83       | Flake    | Surface        | 10.7        | 7,729        | 11.2             | 8,655             | LMO         | CO     | CO         | TC        | 2  | B  |
| CA-KER-2558/H | 84       | Flake    | Surface        | 0.0         | 0            | 0.0              | 0                 | --          | CO     | WS         | TC        | 2  | B  |
| CA-KER-2558/H | 85       | Flake    | Surface        | 13.1        | 12,360       | 13.8             | 13,842            | LPL         | MO     | MO         | TC        | 2  | B  |

| Trinomial     | Cat No.     | Artifact | Unit (Depth)   | Raw Microns | Raw Years BP | Adjusted Microns | Adjusted Years BP | Time Period | Source | Sub-source | Site Type | MR | MA |
|---------------|-------------|----------|----------------|-------------|--------------|------------------|-------------------|-------------|--------|------------|-----------|----|----|
| CA-KER-2558/H | 86          | Flake    | Surface        | 5.2         | 1,449        | 5.5              | 1,623             | GYP         | MO     | MO         | TC        | 2  | B  |
| CA-KER-2558/H | 87          | Flake    | Surface        | 5.3         | 1,515        | 5.6              | 1,696             | GYP         | CO     | WCP        | TC        | 2  | B  |
| CA-KER-2558/H | 88          | Flake    | Surface        | 0.0         | 0            | 0.0              | 0                 | --          | CO     | WCP        | TC        | 2  | B  |
| CA-KER-2558/H | 89          | Flake    | TU (70-80)     | 11.8        | 9,699        | 12.4             | 10,861            | LPL         | CO     | WS         | TC        | 2  | B  |
| CA-KER-2558/H | 91          | Flake    | TU (60-70)     | 11.8        | 9,699        | 12.4             | 10,861            | LPL         | UNK    | UNK        | TC        | 2  | B  |
| CA-KER-2558/H | 92          | Flake    | TU (0-10)      | 11.8        | 9,699        | 12.4             | 10,861            | LPL         | CO     | CO         | TC        | 2  | B  |
| CA-KER-2562   | 1121-7      | Flake    | Surface        | 7.6         | 3,495        | 8.0              | 3,914             | PTO         | CO     | WCP        | TC        | 3  | D  |
| CA-KER-2562   | 1121-15     | Flake    | Surface        | 6.7         | 2,609        | 7.0              | 2,922             | GYP         | CO     | WCP        | TC        | 3  | D  |
| CA-KER-2710   | 641-3       | Flake    | Surface        | 6.5         | 2,432        | 6.8              | 2,723             | GYP         | UNK    | NS         | TC        | 5  | A  |
| CA-KER-2711   | 1138-Temp6a | Flake    | TU 2 (S)       | 7.4         | 3,285        | 7.8              | 3,679             | PTO         | UNK    | NS         | TC        | 5  | A  |
| CA-KER-2711   | 1138-Temp6b | Flake    | TU 2 (S)       | 7.4         | 3,285        | 7.8              | 3,679             | PTO         | UNK    | NS         | TC        | 5  | A  |
| CA-KER-2711   | 1138-Temp6c | Flake    | TU 2 (S)       | 7.9         | 3,823        | 8.3              | 4,282             | PTO         | UNK    | NS         | TC        | 5  | A  |
| CA-KER-2711   | 1138-Temp6d | Flake    | TU 2 (S)       | 12.1        | 10,281       | 12.7             | 11,513            | LPL         | UNK    | NS         | TC        | 5  | A  |
| CA-KER-2711   | 1138-Temp7a | Flake    | TU 2 (0-10)    | 8.6         | 4,656        | 9.0              | 5,214             | PTO         | UNK    | NS         | TC        | 5  | A  |
| CA-KER-2711   | 1138-Temp7b | Flake    | TU 2 (0-10)    | 8.6         | 4,656        | 9.0              | 5,214             | PTO         | UNK    | NS         | TC        | 5  | A  |
| CA-KER-2711   | 1138-Temp7c | Flake    | TU 2 (0-10)    | 7.7         | 3,603        | 8.1              | 4,034             | PTO         | UNK    | NS         | TC        | 5  | A  |
| CA-KER-2711   | 1138-Temp8  | Flake    | 3 (0-10)       | 8.6         | 4,656        | 9.0              | 5,214             | PTO         | UNK    | NS         | TC        | 5  | A  |
| CA-KER-2711   | 1138-Temp9  | Flake    | 3 (0-10)       | 8.6         | 4,656        | 9.0              | 5,214             | PTO         | UNK    | NS         | TC        | 5  | A  |
| CA-KER-2711   | 1138-Temp10 | Flake    | 4 (40-50)      | 0.0         | 0            | 0.0              | 0                 | --          | UNK    | NS         | TC        | 5  | A  |
| CA-KER-2816   | 27          | Flake    | STP 9 (20-40)  | 9.5         | 5,865        | 10.0             | 6,568             | PTO         | CO     | CO         | TC        | 3  | F  |
| CA-KER-2816   | 52          | Flake    | STP 14 (20-40) | 7.1         | 2,985        | 7.5              | 3,342             | PTO         | CO     | CO         | TC        | 3  | F  |
| CA-KER-2816   | 100         | Flake    | STP 24 (20-40) | 6.5         | 2,432        | 6.8              | 2,723             | GYP         | CO     | CO         | TC        | 3  | F  |
| CA-KER-2816   | 178         | Flake    | TU 1C (10-20)  | 8.7         | 4,782        | 9.1              | 5,356             | PTO         | CO     | CO         | TC        | 3  | F  |
| CA-KER-2816   | 321         | Flake    | TU 20 (30-40)  | 9.5         | 5,865        | 10.0             | 6,568             | PTO         | CO     | CO         | TC        | 3  | F  |
| CA-KER-2816   | 408         | Flake    | TU 3A (10-20)  | 5.8         | 1,867        | 6.1              | 2,091             | GYP         | CO     | CO         | TC        | 3  | F  |
| CA-KER-2816   | 571         | Flake    | TU 7 (40-50)   | 6.3         | 2,262        | 6.6              | 2,533             | GYP         | CO     | CO         | TC        | 3  | F  |
| CA-KER-2816   | 566         | Flake    | TU 7 (20-30)   | 6.8         | 2,700        | 7.1              | 3,024             | PTO         | CO     | CO         | TC        | 3  | F  |
| CA-KER-2816   | 570         | Flake    | TU 7 (30-40)   | 7.0         | 2,888        | 7.4              | 3,234             | PTO         | CO     | CO         | TC        | 3  | F  |
| CA-KER-2816   | 621         | Flake    | TU 8 (60-70)   | 6.8         | 2,700        | 7.1              | 3,024             | PTO         | CO     | CO         | TC        | 3  | F  |
| CA-KER-2816   | 645         | PF       | TS-66 (S)      | 6.4         | 2,346        | 6.7              | 2,627             | GYP         | CO     | CO         | TC        | 3  | F  |
| CA-KER-2816   | 662         | CWB      | TS-95 (S)      | 2.8         | 345          | 2.9              | 386               | SHO         | CO     | CO         | TC        | 3  | F  |
| CA-KER-2816   | 671         | Biface   | TS-111 (S)     | 18.5        | 27,530       | 19.4             | 30,829            | LPL         | CO     | CO         | TC        | 3  | F  |
| CA-KER-2817   | 312         | Dart     | SCU-7H (S)     | 9.3         | 5,583        | 9.8              | 6,252             | PTO         | CO     | CO         | TC        | 3  | F  |
| CA-KER-2817   | 698         | Dart     | TS-90 (S)      | 5.1         | 1,385        | 5.4              | 1,551             | GYP         | CO     | CO         | TC        | 3  | F  |

| Trinomial   | Cat No. | Artifact | Unit (Depth)  | Raw<br>Microns | Raw<br>Years BP | Adjusted<br>Microns | Adjusted<br>Years BP | Time<br>Period | Source | Sub-<br>source | Site<br>Type | MR | MA |
|-------------|---------|----------|---------------|----------------|-----------------|---------------------|----------------------|----------------|--------|----------------|--------------|----|----|
| CA-KER-2817 | 702     | Biface   | TS-97 (S)     | 0.0            | 0               | 0.0                 | 0                    | --             | CO     | CO             | TC           | 3  | F  |
| CA-KER-2817 | 713     | CWU      | TS-108 (S)    | 3.4            | 541             | 3.6                 | 606                  | SSP            | CO     | CO             | TC           | 3  | F  |
| CA-KER-2817 | 687     | CWU      | TS-126 (S)    | 2.5            | 265             | 2.6                 | 297                  | SHO            | CO     | CO             | TC           | 3  | F  |
| CA-KER-2817 | 719     | CWU      | TS-118 (S)    | 9.7            | 6,156           | 10.2                | 6,893                | PTO            | CO     | CO             | TC           | 3  | F  |
| CA-KER-2817 | 719     | CWU      | TS-118 (S)    | 2.2            | 197             | 2.3                 | 221                  | SHO            | CO     | CO             | TC           | 3  | F  |
| CA-KER-2817 | 746     | Biface   | TS-178 (S)    | 5.9            | 1,942           | 6.2                 | 2,175                | GYP            | CO     | CO             | TC           | 3  | F  |
| CA-KER-2817 | 747     | RSP      | TS-179 (S)    | 4.4            | 983             | 4.6                 | 1,101                | SSP            | CO     | CO             | TC           | 3  | F  |
| CA-KER-2817 | 832     | Flake    | STU-9 (20-30) | 5.1            | 1,385           | 5.4                 | 1,551                | GYP            | CO     | CO             | TC           | 3  | F  |
| CA-KER-2817 | 1140    | DSN      | U-4G (10-20)  | 2.5            | 265             | 2.6                 | 297                  | SHO            | CO     | CO             | TC           | 3  | F  |
| CA-KER-2817 | 1286    | Flake    | U-6E (0-10)   | 10.3           | 7,075           | 10.8                | 7,923                | LMO            | CO     | CO             | TC           | 3  | F  |
| CA-KER-2817 | 1290    | RSP      | U-6E (10-20)  | 3.9            | 743             | 4.1                 | 833                  | SSP            | CO     | CO             | TC           | 3  | F  |
| CA-KER-2817 | 1340A   | Flake    | U-7P (0-10)   | 8.2            | 4,169           | 8.6                 | 4,668                | PTO            | CO     | CO             | TC           | 3  | F  |
| CA-KER-2817 | 1340B   | Flake    | U-7P (0-10)   | 8.2            | 4,169           | 8.6                 | 4,668                | PTO            | CO     | CO             | TC           | 3  | F  |
| CA-KER-2817 | 1340C   | Flake    | U-7P (0-10)   | 8.3            | 4,288           | 8.7                 | 4,802                | PTO            | CO     | CO             | TC           | 3  | F  |
| CA-KER-2817 | 1345A   | Flake    | U-7P (10-20)  | 7.7            | 3,603           | 8.1                 | 4,034                | PTO            | CO     | CO             | TC           | 3  | F  |
| CA-KER-2817 | 1345B   | Flake    | U-7P (10-20)  | 7.4            | 3,285           | 7.8                 | 3,679                | PTO            | CO     | CO             | TC           | 3  | F  |
| CA-KER-2817 | 1345C   | Flake    | U-7P (10-20)  | 6.7            | 2,609           | 7.0                 | 2,922                | GYP            | CO     | CO             | TC           | 3  | F  |
| CA-KER-2817 | 1353A   | Flake    | U-7P (20-30)  | 7.1            | 2,985           | 7.5                 | 3,342                | PTO            | CO     | CO             | TC           | 3  | F  |
| CA-KER-2817 | 1353B   | Flake    | U-7P (20-30)  | 7.6            | 3,495           | 8.0                 | 3,914                | PTO            | CO     | CO             | TC           | 3  | F  |
| CA-KER-2817 | 1353C   | Flake    | U-7P (20-30)  | 7.2            | 3,083           | 7.6                 | 3,452                | PTO            | CO     | CO             | TC           | 3  | F  |
| CA-KER-2817 | 1353D   | Flake    | U-7P (20-30)  | 7.1            | 2,985           | 7.5                 | 3,342                | PTO            | CO     | CO             | TC           | 3  | F  |
| CA-KER-2817 | 1353E   | Flake    | U-7P (20-30)  | 8.0            | 3,937           | 8.4                 | 4,408                | PTO            | CO     | CO             | TC           | 3  | F  |
| CA-KER-2817 | 1355A   | Flake    | U-7P (30-40)  | 7.6            | 3,495           | 8.0                 | 3,914                | PTO            | CO     | CO             | TC           | 3  | F  |
| CA-KER-2817 | 1355B   | Flake    | U-7P (30-40)  | 7.1            | 2,985           | 7.5                 | 3,342                | PTO            | CO     | CO             | TC           | 3  | F  |
| CA-KER-2817 | 1355C   | Flake    | U-7P (30-40)  | 7.3            | 3,183           | 7.7                 | 3,565                | PTO            | CO     | CO             | TC           | 3  | F  |
| CA-KER-2817 | 1355D   | Flake    | U-7P (30-40)  | 7.4            | 3,285           | 7.8                 | 3,679                | PTO            | CO     | CO             | TC           | 3  | F  |
| CA-KER-2817 | 1355E   | Flake    | U-7P (30-40)  | 7.4            | 3,285           | 7.8                 | 3,679                | PTO            | CO     | CO             | TC           | 3  | F  |
| CA-KER-2817 | 1355F   | Flake    | U-7P (30-40)  | 7.5            | 3,389           | 7.9                 | 3,795                | PTO            | CO     | CO             | TC           | 3  | F  |
| CA-KER-2817 | 1359    | Flake    | U-7P (40-50)  | 7.7            | 3,603           | 8.1                 | 4,034                | PTO            | CO     | CO             | TC           | 3  | F  |
| CA-KER-2817 | 1364    | CWT      | SCU-8 (S)     | 1.9            | 140             | 2.0                 | 157                  | SHO            | CO     | CO             | TC           | 3  | F  |
| CA-KER-2817 | 1367    | CWT      | U-8 (0-10)    | 2.1            | 177             | 2.2                 | 198                  | SHO            | CO     | CO             | TC           | 3  | F  |
| CA-KER-2817 | 1374    | CWT      | U-8 (10-20)   | 1.8            | 124             | 1.9                 | 138                  | SHO            | CO     | CO             | TC           | 3  | F  |
| CA-KER-2817 | 1426    | Flake    | U-13 (20-30)  | 7.4            | 3,285           | 7.8                 | 3,679                | PTO            | CO     | CO             | TC           | 3  | F  |
| CA-KER-2817 | 1438    | Flake    | U-14 (20-30)  | 6.8            | 2,700           | 7.1                 | 3,024                | PTO            | CO     | CO             | TC           | 3  | F  |



| Trinomial     | Cat No.      | Artifact | Unit (Depth)            | Raw Microns | Raw Years BP | Adjusted Microns | Adjusted Years BP | Time Period | Source | Sub-source | Site Type | MR | MA |
|---------------|--------------|----------|-------------------------|-------------|--------------|------------------|-------------------|-------------|--------|------------|-----------|----|----|
| CA-KER-2817   | 4743         | RSP      | Surface                 | 5.1         | 1,385        | 5.4              | 1,551             | GYP         | CO     | WS         | TC        | 3  | F  |
| CA-KER-2975/H | 1178-1-6     | BFF      | Surface                 | 5.5         | 1,650        | 5.8              | 1,848             | GYP         | CO     | WS         | HE        | 2  | A  |
| CA-KER-3158   | 1223-4       | Flake    | Surface                 | 7.3         | 3,183        | 7.7              | 3,565             | PTO         | CO     | WS         | QUA       | 3  | J  |
| CA-KER-3158   | 1223-4       | Flake    | Surface                 | 4.7         | 1,146        | 4.9              | 1,283             | GYP         | CO     | WS         | QUA       | 3  | J  |
| CA-KER-3273/H | 1225-1-252   | Flake    | Surface                 | 14.4        | 15,394       | 15.1             | 17,239            | LPL         | CO     | CO         | TC        | 2  | B  |
| CA-KER-3273/H | 1225-1-257   | Flake    | Surface                 | 10.3        | 7,075        | 10.8             | 7,923             | LMO         | CO     | WS         | TC        | 2  | B  |
| CA-KER-3273/H | 1225-1-265   | Biface   | Surface                 | 6.5         | 2,432        | 6.8              | 2,723             | GYP         | CO     | CO         | TC        | 2  | B  |
| CA-KER-3273/H | 1225-1-281   | Pinto    | Surface                 | 6.0         | 2,020        | 6.3              | 2,262             | GYP         | CO     | WS         | TC        | 2  | B  |
| CA-KER-3273/H | 1225-1-286   | Flake    | Surface                 | 5.8         | 1,867        | 6.1              | 2,091             | GYP         | CO     | WS         | TC        | 2  | B  |
| CA-KER-3273/H | 1225-1-287   | Biface   | Surface                 | 5.1         | 1,385        | 5.4              | 1,551             | GYP         | CO     | CO         | TC        | 2  | B  |
| CA-KER-3273/H | 1225-1-289   | Flake    | Surface                 | 5.4         | 1,582        | 5.7              | 1,771             | GYP         | CO     | CO         | TC        | 2  | B  |
| CA-KER-3273/H | 1225-1-295   | Flake    | Surface                 | 7.1         | 2,985        | 7.5              | 3,342             | PTO         | CO     | CO         | TC        | 2  | B  |
| CA-KER-3273/H | 1225-1-305   | Flake    | Surface                 | 8.0         | 3,937        | 8.4              | 4,408             | PTO         | CO     | CO         | TC        | 2  | B  |
| CA-KER-3273/H | 1225-1-312   | Biface   | Surface                 | 10.4        | 7,236        | 10.9             | 8,103             | LMO         | CO     | WS         | TC        | 2  | B  |
| CA-KER-3273/H | 1225-1-313   | Flake    | Surface                 | 10.2        | 6,917        | 10.7             | 7,746             | LMO         | CO     | WS         | TC        | 2  | B  |
| CA-KER-3273/H | 1225-1-314   | Flake    | Surface                 | 9.7         | 6,156        | 10.2             | 6,893             | PTO         | CO     | CO         | TC        | 2  | B  |
| CA-KER-3273/H | 1225-1-317   | Flake    | Surface                 | 9.3         | 5,583        | 9.8              | 6,252             | PTO         | CO     | CO         | TC        | 2  | B  |
| CA-KER-3273/H | 1225-1-317   | Flake    | Surface                 | 6.9         | 2,793        | 7.2              | 3,128             | PTO         | CO     | CO         | TC        | 2  | B  |
| CA-KER-3273/H | 1225-1-318   | Flake    | Surface                 | 11.5        | 9,137        | 12.1             | 10,232            | LPL         | CO     | CO         | TC        | 2  | B  |
| CA-KER-3273/H | 1225-1-319   | BFF      | Surface                 | 9.1         | 5,308        | 9.6              | 5,944             | PTO         | CO     | CO         | TC        | 2  | B  |
| CA-KER-3273/H | 1225-10-362  | Flake    | N64/W221 STU (30-40)    | 5.3         | 1,515        | 5.6              | 1,696             | GYP         | CO     | CO         | TC        | 2  | B  |
| CA-KER-3273/H | 1225-10-365  | Flake    | N64/W221 STU (40-50)    | 7.5         | 3,389        | 7.9              | 3,795             | GYP         | CO     | CO         | TC        | 2  | B  |
| CA-KER-3273/H | 1225-10-378  | Flake    | N64/W221 STU (80-90)    | 10.5        | 7,398        | 11.0             | 8,285             | LMO         | CO     | CO         | TC        | 2  | B  |
| CA-KER-3273/H | 1225-10-383  | Flake    | N64/W221 STU (90-100)   | 11.4        | 8,953        | 12.0             | 10,026            | LPL         | CO     | CO         | TC        | 2  | B  |
| CA-KER-3273/H | 1225-10-388  | Flake    | N64/W221 STU (100-110)  | 12.9        | 11,927       | 13.5             | 13,356            | LPL         | CO     | CO         | TC        | 2  | B  |
| CA-KER-3273/H | 1225-10-391  | Flake    | N64/W221 STU (110-120)  | 11.4        | 8,953        | 12.0             | 10,026            | LPL         | CO     | CO         | TC        | 2  | B  |
| CA-KER-3273/H | 1225-10-405  | Flake    | N63/W81 STU (20-30)     | 5.1         | 1,385        | 5.4              | 1,551             | GYP         | CO     | CO         | TC        | 2  | B  |
| CA-KER-3273/H | 1225-10-410  | Flake    | N63/W81 STU (30-40)     | 5.0         | 1,323        | 5.3              | 1,482             | GYP         | CO     | CO         | TC        | 2  | B  |
| CA-KER-3273/H | 1225-10-422  | Flake    | N63/W81 STU (50-60)     | 8.9         | 5,041        | 9.3              | 5,646             | PTO         | CO     | CO         | TC        | 2  | B  |
| CA-KER-3273/H | 1225-10-427  | Flake    | N63/W81 STU (60-70)     | 8.3         | 4,288        | 8.7              | 4,802             | PTO         | CO     | CO         | TC        | 2  | B  |
| CA-KER-3273/H | 1225-10-431  | Flake    | N63/W81 STU (70-80)     | 6.7         | 2,609        | 7.0              | 2,922             | GYP         | CO     | CO         | TC        | 2  | B  |
| CA-KER-3273/H | 1225-10-422A | Flake    | N63/W81 STU (90-100)    | 5.7         | 1,793        | 6.0              | 2,008             | GYP         | CO     | CO         | TC        | 2  | B  |
| CA-KER-3273/H | 1225-10-422B | Flake    | N63/W81 STU (90-100)    | 0.0         | 0            | 0.0              | 0                 | --          | CO     | CO         | TC        | 2  | B  |
| CA-KER-3273/H | 1225-10-457  | Flake    | S174/W291.5 STU (30-40) | 9.0         | 5,174        | 9.5              | 5,794             | PTO         | CO     | CO         | TC        | 2  | B  |

| Trinomial     | Cat No. | Artifact | Unit (Depth) | Raw Microns | Raw Years BP | Adjusted Microns | Adjusted Years BP | Time Period | Source | Sub-source | Site Type | MR | MA |
|---------------|---------|----------|--------------|-------------|--------------|------------------|-------------------|-------------|--------|------------|-----------|----|----|
| CA-KER-3273/H | 4823    | Flake    | Surface      | 4.8         | 1,203        | 5.0              | 1,348             | GYP         | CO     | WS         | TC        | 2  | B  |
| CA-KER-3361   | 4       | BTF      | Surface      | 0.0         | 0            | 0.0              | 0                 | --          | CO     | WS         | TC        | 4  | B  |
| CA-KER-3361   | 6       | BTF      | Surface      | 8.5         | 4,531        | 8.9              | 5,074             | PTO         | CO     | WS         | TC        | 4  | B  |
| CA-KER-3361   | 9       | BTF      | Surface      | 9.3         | 5,583        | 9.8              | 6,252             | PTO         | CO     | WS         | TC        | 4  | B  |
| CA-KER-3361   | 10      | BTF      | Surface      | 12.0        | 10,085       | 12.6             | 11,293            | LPL         | CO     | WCP        | TC        | 4  | B  |
| CA-KER-3361   | 11      | Flake    | Surface      | 10.7        | 7,729        | 11.2             | 8,655             | LMO         | CO     | S2F        | TC        | 4  | B  |
| CA-KER-3361   | 12      | Shatter  | Surface      | 10.1        | 6,761        | 10.6             | 7,571             | LMO         | CO     | S2F        | TC        | 4  | B  |
| CA-KER-3361   | 13      | BTF      | Surface      | 9.9         | 6,454        | 10.4             | 7,228             | PTO         | CO     | WS         | TC        | 4  | B  |
| CA-KER-3361   | 16      | BTF      | Surface      | 10.2        | 6,917        | 10.7             | 7,746             | LMO         | CO     | WS         | TC        | 4  | B  |
| CA-KER-3361   | 43      | Point    | Surface      | 10.0        | 6,606        | 10.5             | 7,398             | LMO         | CO     | WS         | TC        | 4  | B  |
| CA-KER-3361   | 68      | Shatter  | Surface      | 0.0         | 0            | 0.0              | 0                 | --          | CO     | WS         | TC        | 4  | B  |
| CA-KER-3361   | 102     | BTF      | Surface      | 9.5         | 5,865        | 10.0             | 6,568             | PTO         | CO     | WS         | TC        | 4  | B  |
| CA-KER-3361   | 106     | BTF      | Surface      | 10.3        | 7,075        | 10.8             | 7,923             | LMO         | CO     | WS         | TC        | 4  | B  |
| CA-KER-3361   | 108     | BTF      | Surface      | 10.6        | 7,563        | 11.1             | 8,469             | LMO         | CO     | WS         | TC        | 4  | B  |
| CA-KER-3361   | 109     | BFF      | Surface      | 9.8         | 6,304        | 10.3             | 7,059             | PTO         | CO     | WS         | TC        | 4  | B  |
| CA-KER-3361   | 112     | BTF      | Surface      | 9.4         | 5,723        | 9.9              | 6,409             | PTO         | CO     | WS         | TC        | 4  | B  |
| CA-KER-3361   | 115     | BTF      | Surface      | 9.8         | 6,304        | 10.3             | 7,059             | PTO         | CO     | WS         | TC        | 4  | B  |
| CA-KER-3361   | 117     | Flake    | Surface      | 8.6         | 4,656        | 9.0              | 5,214             | PTO         | CO     | WS         | TC        | 4  | B  |
| CA-KER-3361   | 125     | BTF      | Surface      | 11.0        | 8,241        | 11.6             | 9,229             | LPL         | CO     | WS         | TC        | 4  | B  |
| CA-KER-3361   | 126     | BTF      | Surface      | 11.1        | 8,416        | 11.7             | 9,425             | LPL         | CO     | WS         | TC        | 4  | B  |
| CA-KER-3361   | 138     | BTF      | Surface      | 10.7        | 7,729        | 11.2             | 8,655             | LMO         | CO     | WS         | TC        | 4  | B  |
| CA-KER-3361   | 139     | Flake    | Surface      | 9.5         | 5,865        | 10.0             | 6,568             | PTO         | CO     | WS         | TC        | 4  | B  |
| CA-KER-3361   | 140     | Shatter  | Surface      | 10.3        | 7,075        | 10.8             | 7,923             | LMO         | CO     | WS         | TC        | 4  | B  |
| CA-KER-3361   | 141     | Shatter  | Surface      | 9.3         | 5,583        | 9.8              | 6,252             | PTO         | CO     | WS         | TC        | 4  | B  |
| CA-KER-3361   | 142     | BTF      | Surface      | 9.0         | 5,174        | 9.5              | 5,794             | PTO         | CO     | WS         | TC        | 4  | B  |
| CA-KER-3361   | 151     | BTF      | Surface      | 10.9        | 8,068        | 11.4             | 9,035             | LMO         | CO     | S2F        | TC        | 4  | B  |
| CA-KER-3361   | 153     | BTF      | Surface      | 8.7         | 4,782        | 9.1              | 5,356             | PTO         | CO     | WS         | TC        | 4  | B  |
| CA-KER-3361   | 232     | Flake    | TU 2 (10-20) | 9.4         | 5,723        | 9.9              | 6,409             | PTO         | CO     | WS         | TC        | 4  | B  |
| CA-KER-3361   | 254     | BTF      | TU 2 (50-60) | 6.1         | 2,099        | 6.4              | 2,350             | GYP         | CO     | JR         | TC        | 4  | B  |
| CA-KER-3361   | 255     | Flake    | TU 2 (50-60) | 14.0        | 14,420       | 14.7             | 16,149            | LPL         | CO     | SL         | TC        | 4  | B  |
| CA-KER-3361   | 291     | BTF      | TU 6 (10-20) | 9.9         | 6,454        | 10.4             | 7,228             | PTO         | CO     | WS         | TC        | 4  | B  |
| CA-KER-3377   | 106     | Flake    | 1 (10-20)    | 4.8         | 1,203        | 5.0              | 1,348             | GYP         | CO     | CO         | TC        | 3  | H  |
| CA-KER-3377   | 108     | Flake    | 1 (30-40)    | 3.7         | 658          | 3.9              | 737               | SSP         | CO     | CO         | TC        | 3  | H  |
| CA-KER-3377   | 116     | Flake    | 3 (50-60)    | 4.8         | 1,203        | 5.0              | 1,348             | GYP         | CO     | CO         | TC        | 3  | H  |

| Trinomial     | Cat No. | Artifact | Unit (Depth) | Raw Microns | Raw Years BP | Adjusted Microns | Adjusted Years BP | Time Period | Source | Sub-source | Site Type | MR | MA |
|---------------|---------|----------|--------------|-------------|--------------|------------------|-------------------|-------------|--------|------------|-----------|----|----|
| CA-KER-3434   | 1256-1  | Flake    | Surface      | 0.0         | 0            | 0.0              | 0                 | --          | UNK    | UNK        | LD        | 4  | B  |
| CA-KER-3556   | 1306-18 | Flake    | Surface      | 9.7         | 6,156        | 10.2             | 6,893             | PTO         | CO     | WS         | LD        | 3  | I  |
| CA-KER-3556   | 1306-25 | Flake    | TU 6 (10-20) | 11.7        | 9,509        | 12.3             | 10,649            | LPL         | CO     | JR         | LD        | 3  | I  |
| CA-KER-3875/H | 102     | UNK      | Surface      | 9.5         | 5,865        | 10.0             | 6,568             | PTO         | CO     | JR         | TC        | 3  | I  |
| CA-KER-3875/H | 23      | UNK      | Surface      | 0.0         | 0            | 0.0              | 0                 | --          | CO     | WS         | TC        | 3  | I  |
| CA-KER-3875/H | 8a      | Flake    | 4 (0-10)     | 3.2         | 470          | 3.4              | 526               | SHO         | CO     | CO         | TC        | 3  | I  |
| CA-KER-3875/H | 8b      | Flake    | 4 (0-10)     | 2.9         | 374          | 3.0              | 419               | SHO         | CO     | CO         | TC        | 3  | I  |
| CA-KER-3875/H | 8c      | Flake    | 4 (0-10)     | 2.7         | 317          | 2.8              | 355               | SHO         | CO     | CO         | TC        | 3  | I  |
| CA-KER-3875/H | 8d      | Flake    | 4 (0-10)     | 2.9         | 374          | 3.0              | 419               | SHO         | CO     | CO         | TC        | 3  | I  |
| CA-KER-3875/H | 8e      | Flake    | 4 (0-10)     | 0.0         | 0            | 0.0              | 0                 | --          | CO     | CO         | TC        | 3  | I  |
| CA-KER-3875/H | 8f      | Flake    | 4 (0-10)     | 0.0         | 0            | 0.0              | 0                 | --          | CO     | CO         | TC        | 3  | I  |
| CA-KER-3875/H | 8g      | Flake    | 4 (0-10)     | 0.0         | 0            | 0.0              | 0                 | --          | CO     | CO         | TC        | 3  | I  |
| CA-KER-3875/H | 19      | Flake    | 4 (10-20)    | 0.0         | 0            | 0.0              | 0                 | --          | CO     | CO         | TC        | 3  | I  |
| CA-KER-3875/H | 22      | Flake    | 4 (20-30)    | 0.0         | 0            | 0.0              | 0                 | --          | CO     | CO         | TC        | 3  | I  |
| CA-KER-3875/H | 26a     | Flake    | 4 (30-40)    | 2.7         | 317          | 2.8              | 355               | SHO         | CO     | CO         | TC        | 3  | I  |
| CA-KER-3875/H | 26b     | Flake    | 4 (30-40)    | 2.7         | 317          | 2.8              | 355               | SHO         | CO     | CO         | TC        | 3  | I  |
| CA-KER-3875/H | 52      | Flake    | 5 (0-10)     | 2.9         | 374          | 3.0              | 419               | SHO         | CO     | CO         | TC        | 3  | I  |
| CA-KER-3875/H | 79      | Flake    | 5 (30-40)    | 2.6         | 290          | 2.7              | 325               | SHO         | CO     | CO         | TC        | 3  | I  |
| CA-KER-3876/H | 2       | Flake    | Surface      | 8.5         | 4,531        | 8.9              | 5,074             | PTO         | CO     | CO         | TC        | 3  | I  |
| CA-KER-3876/H | 115     | Flake    | 9 (20-30)    | 0.0         | 0            | 0.0              | 0                 | --          | CO     | CO         | TC        | 3  | I  |
| CA-KER-3876/H | 116     | Flake    | 9 (20-30)    | 2.0         | 158          | 2.1              | 177               | SHO         | CO     | CO         | TC        | 3  | I  |
| CA-KER-3876/H | 117     | Flake    | 9 (20-30)    | 0.0         | 0            | 0.0              | 0                 | --          | CO     | CO         | TC        | 3  | I  |
| CA-KER-3876/H | 143     | Flake    | 9 (50-60)    | 2.1         | 177          | 2.2              | 198               | SHO         | CO     | CO         | TC        | 3  | I  |
| CA-KER-3876/H | 176     | Flake    | 10 (30-40)   | 8.7         | 4,782        | 9.1              | 5,356             | PTO         | CO     | CO         | TC        | 3  | I  |
| CA-KER-3876/H | 318     | Flake    | Surface      | 5.8         | 1,867        | 6.1              | 2,091             | GYP         | CO     | CO         | TC        | 3  | I  |
| CA-KER-3877/H | 70      | Flake    | Surface      | 9.0         | 5,174        | 9.5              | 5,794             | PTO         | CO     | CO         | TC        | 3  | I  |
| CA-KER-3878/H | 133     | Flake    | 9 (30-40)    | 9.2         | 5,444        | 9.7              | 6,097             | PTO         | CO     | CO         | TC        | 3  | I  |
| CA-KER-3983   | 27      | Flake    | Surface      | 8.4         | 4,408        | 8.8              | 4,937             | PTO         | CO     | WS         | TC        | 5  | F  |
| CA-KER-3983   | 28      | Flake    | TU (0-20)    | 17.3        | 23,563       | 18.2             | 26,387            | LPL         | CO     | CO         | TC        | 5  | F  |
| CA-KER-3983   | 28      | Flake    | TU (0-20)    | 5.4         | 1,582        | 5.7              | 1,771             | GYP         | CO     | CO         | TC        | 5  | F  |
| CA-KER-3983   | 29      | Flake    | Surface      | 8.9         | 5,041        | 9.3              | 5,646             | PTO         | CO     | SL         | TC        | 5  | F  |
| CA-KER-3983   | 30      | Flake    | TU (0-20)    | 8.6         | 4,656        | 9.0              | 5,214             | PTO         | CO     | SL         | TC        | 5  | F  |
| CA-KER-3983   | 31      | Flake    | Surface      | 9.5         | 5,865        | 10.0             | 6,568             | PTO         | CO     | SL         | TC        | 5  | F  |
| CA-KER-3983   | 32      | Flake    | Surface      | 11.7        | 9,509        | 12.3             | 10,649            | LPL         | CO     | SL         | TC        | 5  | F  |

| Trinomial     | Cat No.  | Artifact | Unit (Depth) | Raw<br>Microns | Raw<br>Years BP | Adjusted<br>Microns | Adjusted<br>Years BP | Time<br>Period | Source | Sub-<br>source | Site<br>Type | MR | MA |
|---------------|----------|----------|--------------|----------------|-----------------|---------------------|----------------------|----------------|--------|----------------|--------------|----|----|
| CA-KER-3983   | 33       | UTF      | Surface      | 10.6           | 7,563           | 11.1                | 8,469                | LMO            | CO     | SL             | TC           | 5  | F  |
| CA-KER-3983   | 34       | Flake    | Surface      | 7.3            | 3,183           | 7.7                 | 3,565                | PTO            | CO     | SL             | TC           | 5  | F  |
| CA-KER-3983   | 35       | Flake    | Surface      | 8.0            | 3,937           | 8.4                 | 4,408                | PTO            | CO     | WS             | TC           | 5  | F  |
| CA-KER-3983   | 36       | PF       | Surface      | 6.3            | 2,262           | 6.6                 | 2,533                | GYP            | CO     | WS             | TC           | 5  | F  |
| CA-KER-4081   | 1544-42  | Flake    | Surface      | 6.6            | 2,519           | 6.9                 | 2,821                | GYP            | CO     | WS             | TC           | 5  | A  |
| CA-KER-4081   | 1544-57  | Flake    | Surface      | 8.8            | 4,911           | 9.2                 | 5,499                | PTO            | CO     | WS             | TC           | 5  | A  |
| CA-KER-4081   | 1544-58  | Flake    | Surface      | 10.7           | 7,729           | 11.2                | 8,655                | LMO            | CO     | WS             | TC           | 5  | A  |
| CA-KER-4129   | 1534-10  | Flake    | Surface      | 9.0            | 5,174           | 9.5                 | 5,794                | PTO            | CO     | WCP            | TC           | 3  | B  |
| CA-KER-4129   | 1534-23  | Flake    | Surface      | 8.4            | 4,408           | 8.8                 | 4,937                | PTO            | CO     | WCP            | TC           | 3  | B  |
| CA-KER-4129   | 1534-32  | Flake    | Surface      | 8.4            | 4,408           | 8.8                 | 4,937                | PTO            | CO     | WCP            | TC           | 3  | B  |
| CA-KER-4153/H | 5342     | HBT      | Surface      | 5.7            | 1,793           | 6.0                 | 2,008                | GYP            | CO     | WS             | TC           | 3  | F  |
| CA-KER-4153/H | 5344     | DSN      | Surface      | 1.9            | 140             | 2.0                 | 157                  | SHO            | CO     | WS             | TC           | 3  | F  |
| CA-KER-4200   | 5154     | Pinto    | Surface      | 8.5            | 4,531           | 8.9                 | 5,074                | PTO            | CO     | WS             | LD           | 3  | F  |
| CA-KER-4231   | 5460     | ECN      | Surface      | 11.1           | 8,416           | 11.7                | 9,425                | LPL            | CO     | CO             | LD           | 5  | A  |
| CA-KER-4233   | 1105-1   | UTF      | Surface      | 13.5           | 13,254          | 14.2                | 14,842               | LPL            | CO     | WCP            | LD           | 5  | A  |
| CA-KER-4277   | 37       | BTF      | TU (0-20)    | 6.2            | 2,179           | 6.5                 | 2,440                | GYP            | CO     | WS             | TC           | 5  | A  |
| CA-KER-4347/H | 26       | BTF      | Surface      | 7.5            | 3,389           | 7.9                 | 3,795                | PTO            | CO     | WS             | LD           | 5  | A  |
| CA-KER-4368   | 1817-25  | Flake    | STP 11 (S)   | 7.8            | 3,712           | 8.2                 | 4,157                | PTO            | CO     | CO             | TC           | 3  | I  |
| CA-KER-4400   | 1920-96  | RSP      | Surface      | 4.1            | 835             | 4.3                 | 935                  | SSP            | CO     | WS             | TC           | 1  | B  |
| CA-KER-4400   | 1920-174 | RSP      | Surface      | 4.0            | 788             | 4.2                 | 883                  | SSP            | CO     | WS             | TC           | 1  | B  |
| CA-KER-4552   | 1870-16  | Flake    | 1 (20-30)    | 6.6            | 2,519           | 6.9                 | 2,821                | GYP            | CO     | WCP            | LD           | 5  | A  |
| CA-KER-4555   | 1875-4   | Flake    | 3 (S)        | 7.1            | 2,985           | 7.5                 | 3,342                | PTO            | CO     | WCP            | LD           | 5  | A  |
| CA-KER-4564   | 1900-1   | Flake    | Surface      | 5.9            | 1,942           | 6.2                 | 2,175                | GYP            | CO     | WCP            | LD           | 5  | A  |
| CA-KER-4565   | 1948-2   | Flake    | 1 (S)        | 7.0            | 2,888           | 7.4                 | 3,234                | PTO            | CO     | WCP            | TC           | 5  | A  |
| CA-KER-4567   | 1950-1   | Flake    | Surface      | 8.7            | 4,782           | 9.1                 | 5,356                | PTO            | CO     | WCP            | TC           | 5  | A  |
| CA-KER-4569   | 1882-2   | Flake    | Surface      | 8.2            | 4,169           | 8.6                 | 4,668                | PTO            | CO     | WCP            | LD           | 5  | A  |
| CA-KER-4571   | 11       | BTF      | STP 7 (S)    | 7.4            | 3,285           | 7.8                 | 3,679                | PTO            | CO     | WCP            | TC           | 5  | A  |
| CA-KER-4600   | 6090     | Preform  | Surface      | 8.2            | 4,169           | 8.6                 | 4,668                | PTO            | CO     | SL             | BC           | 5  | A  |
| CA-KER-4600   | 1991-2   | Flake    | Surface      | 11.1           | 8,416           | 11.7                | 9,425                | LPL            | CO     | WCP            | BC           | 5  | A  |
| CA-KER-4600   | 1991-3   | Flake    | Surface      | 6.1            | 2,099           | 6.4                 | 2,350                | GYP            | CO     | WCP            | BC           | 5  | A  |
| CA-KER-4600   | 1991-5   | Flake    | Surface      | 4.9            | 1,262           | 5.1                 | 1,414                | GYP            | CO     | WCP            | BC           | 5  | A  |
| CA-KER-4600   | 1991-7   | Flake    | Surface      | 7.5            | 3,389           | 7.9                 | 3,795                | PTO            | CO     | WCP            | BC           | 5  | A  |
| CA-KER-4600   | 1991-8   | Flake    | Surface      | 0.0            | 0               | 0.0                 | 0                    | --             | UNK    | NS             | BC           | 5  | A  |
| CA-KER-4600   | 1991-9   | Flake    | Surface      | 7.4            | 3,285           | 7.8                 | 3,679                | PTO            | CO     | WCP            | BC           | 5  | A  |

| Trinomial   | Cat No.   | Artifact | Unit (Depth) | Raw Microns | Raw Years BP | Adjusted Microns | Adjusted Years BP | Time Period | Source | Sub-source | Site Type | MR | MA |
|-------------|-----------|----------|--------------|-------------|--------------|------------------|-------------------|-------------|--------|------------|-----------|----|----|
| CA-KER-4600 | 1991-11   | Flake    | Surface      | 7.1         | 2,985        | 7.5              | 3,342             | PTO         | CO     | WCP        | BC        | 5  | A  |
| CA-KER-4600 | 1991-12   | Flake    | Surface      | 7.2         | 3,083        | 7.6              | 3,452             | PTO         | CO     | WCP        | BC        | 5  | A  |
| CA-KER-4600 | 1991-14   | Flake    | Surface      | 9.0         | 5,174        | 9.5              | 5,794             | PTO         | CO     | WCP        | BC        | 5  | A  |
| CA-KER-4600 | 1991-15   | Flake    | Surface      | 0.0         | 0            | 0.0              | 0                 | --          | UNK    | NS         | BC        | 5  | A  |
| CA-KER-4600 | 1991-16   | Flake    | Surface      | 6.6         | 2,519        | 6.9              | 2,821             | GYP         | CO     | WCP        | BC        | 5  | A  |
| CA-KER-4600 | 1991-22   | Flake    | 1 (10-20)    | 7.8         | 3,712        | 8.2              | 4,157             | PTO         | CO     | WCP        | BC        | 5  | A  |
| CA-KER-4600 | 1991-222  | Flake    | 2 (20-30)    | 7.6         | 3,495        | 8.0              | 3,914             | PTO         | CO     | WCP        | BC        | 5  | A  |
| CA-KER-4600 | 1991-224  | Flake    | 2 (30-40)    | 7.6         | 3,495        | 8.0              | 3,914             | PTO         | CO     | WCP        | BC        | 5  | A  |
| CA-KER-4600 | 1991-228A | Flake    | 2 (40-50)    | 7.9         | 3,823        | 8.3              | 4,282             | PTO         | UNK    | NS         | BC        | 5  | A  |
| CA-KER-4600 | 1991-228B | Flake    | 2 (40-50)    | 5.2         | 1,449        | 5.5              | 1,623             | GYP         | UNK    | NS         | BC        | 5  | A  |
| CA-KER-4600 | 7083      | Dart     | Surface      | 11.3        | 8,772        | 11.9             | 9,823             | LPL         | UNK    | UNK        | BC        | 5  | A  |
| CA-KER-4651 | 7159      | HBT      | Surface      | 8.1         | 4,052        | 8.5              | 4,537             | PTO         | CO     | WS         | LD        | 5  | A  |
| CA-KER-4653 | 1993-22   | Flake    | 1 (S)        | 7.9         | 3,823        | 8.3              | 4,282             | PTO         | CO     | WCP        | TC        | 5  | A  |
| CA-KER-4653 | 1993-38   | Flake    | 3 (40-50)    | 0.0         | 0            | 0.0              | 0                 | --          | UNK    | NS         | TC        | 5  | A  |
| CA-KER-4653 | 1993-53   | Flake    | 3 (80-90)    | 6.4         | 2,346        | 6.7              | 2,627             | GYP         | UNK    | NS         | TC        | 5  | A  |
| CA-KER-4656 | 1996-3    | Flake    | Surface      | 0.0         | 0            | 0.0              | 0                 | --          | UNK    | NS         | TC        | 5  | A  |
| CA-KER-4656 | 1996-26   | Flake    | 2 (S)        | 5.7         | 1,793        | 6.0              | 2,008             | GYP         | CO     | WCP        | TC        | 5  | A  |
| CA-KER-4677 | 7161      | RSP      | Surface      | 4.8         | 1,203        | 5.0              | 1,348             | GYP         | CO     | WS         | TC        | 3  | I  |
| CA-KER-4685 | 2019-169  | Flake    | Surface      | 0.0         | 0            | 0.0              | 0                 | --          | UNK    | NS         | TC        | 3  | I  |
| CA-KER-4696 | 5         | Biface   | Surface      | 13.3        | 12,803       | 14.0             | 14,337            | LPL         | CO     | WS         | TC        | 3  | I  |
| CA-KER-4719 | 6         | Flake    | Surface      | 8.2         | 4,169        | 8.6              | 4,668             | PTO         | CO     | WS         | TC        | 3  | I  |
| CA-KER-4719 | 7         | BFF      | Surface      | 0.0         | 0            | 0.0              | 0                 | --          | CO     | WS         | TC        | 3  | I  |
| CA-KER-4723 | 1-1-1     | BFF      | UNK          | 0.0         | 0            | 0.0              | 0                 | --          | SM     | SM         | LD        | 3  | I  |
| CA-KER-4723 | 5-5-1     | Flake    | UNK          | 9.3         | 5,583        | 9.8              | 6,252             | PTO         | CO     | WS         | LD        | 3  | I  |
| CA-KER-4723 | 2-2-1     | Flake    | UNK          | 0.0         | 0            | 0.0              | 0                 | --          | CO     | WS         | LD        | 3  | I  |
| CA-KER-4723 | 6-6-1     | Flake    | UNK          | 9.1         | 5,308        | 9.6              | 5,944             | PTO         | CO     | WS         | LD        | 3  | I  |
| CA-KER-4723 | 1-1-1     | Flake    | UNK          | 8.6         | 4,656        | 9.0              | 5,214             | PTO         | CO     | WS         | LD        | 3  | I  |
| CA-KER-4754 | 2159-5    | Flake    | Surface      | 3.6         | 617          | 3.8              | 691               | SSP         | CO     | CO         | TC        | 3  | I  |
| CA-KER-4754 | 2159-6    | Flake    | Surface      | 12.3        | 10,679       | 12.9             | 11,959            | LPL         | CO     | CO         | TC        | 3  | I  |
| CA-KER-4754 | 2159-10   | Flake    | Surface      | 5.7         | 1,793        | 6.0              | 2,008             | GYP         | CO     | CO         | TC        | 3  | I  |
| CA-KER-4754 | 2159-11   | Flake    | Surface      | 5.7         | 1,793        | 6.0              | 2,008             | GYP         | CO     | CO         | TC        | 3  | I  |
| CA-KER-4754 | 2159-12   | Flake    | Surface      | 6.1         | 2,099        | 6.4              | 2,350             | GYP         | CO     | CO         | TC        | 3  | I  |
| CA-KER-4754 | 2159-13   | Flake    | Surface      | 5.8         | 1,867        | 6.1              | 2,091             | GYP         | CO     | CO         | TC        | 3  | I  |
| CA-KER-4754 | 2159-14   | Flake    | Surface      | 6.4         | 2,346        | 6.7              | 2,627             | GYP         | CO     | CO         | TC        | 3  | I  |



| Trinomial     | Cat No.      | Artifact | Unit (Depth)        | Raw<br>Microns | Raw<br>Years BP | Adjusted<br>Microns | Adjusted<br>Years BP | Time<br>Period | Source | Sub-<br>source | Site<br>Type | MR | MA |
|---------------|--------------|----------|---------------------|----------------|-----------------|---------------------|----------------------|----------------|--------|----------------|--------------|----|----|
| CA-KER-4754   | 2159-15      | Flake    | Surface             | 5.8            | 1,867           | 6.1                 | 2,091                | GYP            | CO     | CO             | TC           | 3  | I  |
| CA-KER-4754   | 2159-16      | Flake    | Surface             | 5.7            | 1,793           | 6.0                 | 2,008                | GYP            | CO     | CO             | TC           | 3  | I  |
| CA-KER-4754   | 2159-17      | Flake    | Surface             | 6.2            | 2,179           | 6.5                 | 2,440                | GYP            | CO     | CO             | TC           | 3  | I  |
| CA-KER-4754   | 2159-19      | Flake    | STP 4 (S)           | 5.2            | 1,449           | 5.5                 | 1,623                | GYP            | CO     | CO             | TC           | 3  | I  |
| CA-KER-4773/H | 1340-1-8     | Point    | Surface             | 5.7            | 1,793           | 6.0                 | 2,008                | GYP            | CO     | WS             | TC           | 1  | A  |
| CA-KER-4773/H | 1340-1-12    | Flake    | Surface             | 5.7            | 1,793           | 6.0                 | 2,008                | GYP            | CO     | CO             | TC           | 1  | A  |
| CA-KER-4773/H | 1340-1-33    | Flake    | Surface             | 7.2            | 3,083           | 7.6                 | 3,452                | PTO            | CO     | WS             | TC           | 1  | A  |
| CA-KER-4773/H | 1340-1-34    | Flake    | Surface             | 7.5            | 3,389           | 7.9                 | 3,795                | PTO            | CO     | WS             | TC           | 1  | A  |
| CA-KER-4773/H | 1340-1-37    | Flake    | Surface             | 9.3            | 5,583           | 9.8                 | 6,252                | PTO            | CO     | WS             | TC           | 1  | A  |
| CA-KER-4773/H | 1340-1-174   | Flake    | S15/E0 Cell F (S)   | 7.3            | 3,183           | 7.7                 | 3,565                | PTO            | CO     | CO             | TC           | 1  | A  |
| CA-KER-4773/H | 1340-10-252a | Flake    | N5/W15 (0-10)       | 5.9            | 1,942           | 6.2                 | 2,175                | GYP            | CO     | CO             | TC           | 1  | A  |
| CA-KER-4773/H | 1340-10-267  | Point    | N5/W35 (0-10)       | 0.0            | 0               | 0.0                 | 0                    | --             | CO     | WS             | TC           | 1  | A  |
| CA-KER-4773/H | 1340-1-277a  | Flake    | N5/W35 (0-10)       | 6.6            | 2,519           | 6.9                 | 2,821                | GYP            | CO     | CO             | TC           | 1  | A  |
| CA-KER-4773/H | 1340-1-341   | Flake    | S4/E1 (0-10)        | 6.3            | 2,262           | 6.6                 | 2,533                | GYP            | CO     | WS             | TC           | 1  | A  |
| CA-KER-486    | 10738        | BFF      | Surface             | 6.3            | 2,262           | 6.6                 | 2,533                | GYP            | CO     | JR             | LD           | 2  | B  |
| CA-KER-490    | 106          | Flake    | 1 (0-10)            | 10.0           | 6,606           | 10.5                | 7,398                | LMO            | CO     | CO             | TC           | 3  | F  |
| CA-KER-490    | 106          | Flake    | 1 (0-10)            | 7.5            | 3,389           | 7.9                 | 3,795                | PTO            | CO     | CO             | TC           | 3  | F  |
| CA-KER-490    | 155          | Flake    | 4 (10-25)           | 7.7            | 3,603           | 8.1                 | 4,034                | PTO            | CO     | CO             | TC           | 3  | F  |
| CA-KER-490    | 167          | Flake    | 4 (35-47)           | 8.8            | 4,911           | 9.2                 | 5,499                | PTO            | CO     | CO             | TC           | 3  | F  |
| CA-KER-490    | 198          | Flake    | 6 (0-10)            | 10.2           | 6,917           | 10.7                | 7,746                | LMO            | CO     | CO             | TC           | 3  | F  |
| CA-KER-490    | 203          | Flake    | 6 (10-20)           | 8.0            | 3,937           | 8.4                 | 4,408                | PTO            | CO     | CO             | TC           | 3  | F  |
| CA-KER-490    | 211          | Flake    | 6 (20-40)           | 7.2            | 3,083           | 7.6                 | 3,452                | PTO            | CO     | CO             | TC           | 3  | F  |
| CA-KER-490    | 215          | Flake    | 6 (40-50)           | 8.8            | 4,911           | 9.2                 | 5,499                | PTO            | CO     | CO             | TC           | 3  | F  |
| CA-KER-490    | 224          | Flake    | 6 (60-70)           | 6.1            | 2,099           | 6.4                 | 2,350                | GYP            | CO     | CO             | TC           | 3  | F  |
| CA-KER-490    | 226          | Flake    | 6 (60-70)           | 13.4           | 13,027          | 14.1                | 14,588               | LPL            | CO     | CO             | TC           | 3  | F  |
| CA-KER-4926   | 7696         | RSP      | Surface             | 4.2            | 883             | 4.4                 | 989                  | SSP            | CO     | WS             | TC           | 1  | B  |
| CA-KER-4929   | 2402-98      | Flake    | Surface             | 8.9            | 5,041           | 9.3                 | 5,646                | PTO            | CO     | JR             | TC           | 1  | A  |
| CA-KER-4929   | 2402-98      | Flake    | Surface             | 10.0           | 6,606           | 10.5                | 7,398                | LMO            | CO     | JR             | TC           | 1  | A  |
| CA-KER-4929   | 2402-119     | Flake    | Surface             | 11.8           | 9,699           | 12.4                | 10,861               | LPL            | CO     | SL             | TC           | 1  | A  |
| CA-KER-4929   | 2402-5       | Flake    | Surface             | 5.0            | 1,323           | 5.3                 | 1,482                | GYP            | CO     | WS             | TC           | 1  | A  |
| CA-KER-4929   | 2402-49      | Flake    | Surface             | 6.5            | 2,432           | 6.8                 | 2,723                | GYP            | CO     | WS             | TC           | 1  | A  |
| CA-KER-4953   | 2299-10-1    | Flake    | N0.8/W30 STU (0-10) | 9.4            | 5,723           | 9.9                 | 6,409                | PTO            | CO     | CO             | HE           | 2  | A  |
| CA-KER-4953   | 2299-10-1    | Flake    | N0.8/W30 STU (0-10) | 6.9            | 2,793           | 7.2                 | 3,128                | PTO            | CO     | CO             | HE           | 2  | A  |
| CA-KER-4956   | 2302-1-6     | BFF      | Surface             | 4.4            | 983             | 4.6                 | 1,101                | SSP            | CO     | CO             | HE           | 2  | A  |

| Trinomial    | Cat No.    | Artifact | Unit (Depth)            | Raw Microns | Raw Years BP | Adjusted Microns | Adjusted Years BP | Time Period | Sub-source | Site Type | MR | MA  |
|--------------|------------|----------|-------------------------|-------------|--------------|------------------|-------------------|-------------|------------|-----------|----|-----|
| CA-KER-4956  | 2302-1-7   | Flake    | Surface                 | 15.6        | 18,536       | 16.4             | 20,757            | LPL         | CO         | WS        | HE | 2 A |
| CA-KER-4956  | 2302-1-7   | Flake    | Surface                 | 4.8         | 1,203        | 5.0              | 1,348             | GYP         | CO         | WS        | HE | 2 A |
| CA-KER-4956  | 2302-10-14 | Flake    | S11.9/W32.6 STU (20-30) | 9.8         | 6,304        | 10.3             | 7,059             | PTO         | CO         | CO        | HE | 2 A |
| CA-KER-4956  | 2302-10-15 | Flake    | S11.9/W32.6 TU (0-10)   | 5.1         | 1,385        | 5.4              | 1,551             | GYP         | CO         | CO        | HE | 2 A |
| CA-KER-4956  | 2302-10-21 | Flake    | S11.9/W32.6 TU (40-48)  | 5.1         | 1,385        | 5.4              | 1,551             | GYP         | CO         | CO        | HE | 2 A |
| CA-KER-4978  | 1473       | Flake    | Surface                 | 3.9         | 743          | 4.1              | 833               | SSP         | CO         | CO        | TC | 2 D |
| CA-KER-4995  | 2283-1-11  | Flake    | Surface                 | 0.0         | 0            | 0.0              | 0                 | --          | CO         | CO        | TC | 2 D |
| CA-KER-4995  | 2283-1-19  | Flake    | Surface                 | 8.1         | 4,052        | 8.5              | 4,537             | PTO         | CO         | CO        | TC | 2 D |
| CA-KER-4995  | 2283-1-23  | Flake    | Surface                 | 11.0        | 8,241        | 11.6             | 9,229             | LPL         | CO         | CO        | TC | 2 D |
| CA-KER-4995  | 2283-1-28  | Flake    | Surface                 | 7.8         | 3,712        | 8.2              | 4,157             | PTO         | CO         | CO        | TC | 2 D |
| CA-KER-4995  | 2283-1-29  | Flake    | Surface                 | 0.0         | 0            | 0.0              | 0                 | --          | CO         | WS        | TC | 2 D |
| CA-KER-4997  | 2285-1-1   | Flake    | Surface                 | 0.0         | 0            | 0.0              | 0                 | --          | CO         | CO        | LD | 2 D |
| CA-KER-4997  | 2285-1-3   | Flake    | Surface                 | 0.0         | 0            | 0.0              | 0                 | --          | CO         | CO        | LD | 2 D |
| CA-KER-4997  | 2285-1-4   | Flake    | Surface                 | 2.3         | 218          | 2.4              | 245               | SHQ         | CO         | CO        | LD | 2 D |
| CA-KER-500   | 190        | Flake    | 3 (0-10)                | 10.7        | 7,729        | 11.2             | 8,655             | LMO         | CO         | CO        | TC | 3 F |
| CA-KER-500   | 203        | Flake    | 3 (40-50)               | 9.7         | 6,156        | 10.2             | 6,893             | PTO         | CO         | CO        | TC | 3 F |
| CA-KER-500   | 203        | Flake    | 3 (40-50)               | 7.3         | 3,183        | 7.7              | 3,565             | PTO         | CO         | CO        | TC | 3 F |
| CA-KER-500   | 213        | Flake    | 3 (70-80)               | 9.0         | 5,174        | 9.5              | 5,794             | PTO         | CO         | CO        | TC | 3 F |
| CA-KER-501   | 11         | Flake    | 1 (3-10)                | 7.9         | 3,823        | 8.3              | 4,282             | PTO         | CO         | CO        | TC | 3 F |
| CA-KER-501   | 11         | Flake    | 1 (3-10)                | 6.3         | 2,262        | 6.6              | 2,533             | GYP         | CO         | CO        | TC | 3 F |
| CA-KER-501   | 120        | Flake    | 1 (20-30)               | 8.0         | 3,937        | 8.4              | 4,408             | PTO         | CO         | CO        | TC | 3 F |
| CA-KER-501   | 124        | Flake    | 1 (30-40)               | 8.9         | 5,041        | 9.3              | 5,646             | PTO         | CO         | CO        | TC | 3 F |
| CA-KER-501   | 134        | Flake    | 1 (50-60)               | 7.3         | 3,183        | 7.7              | 3,565             | PTO         | CO         | CO        | TC | 3 F |
| CA-KER-501   | 184        | Flake    | TU 2 (60-70)            | 7.8         | 3,712        | 8.2              | 4,157             | PTO         | CO         | CO        | TC | 3 F |
| CA-KER-501   | 171        | Flake    | 2 (40-50)               | 7.8         | 3,712        | 8.2              | 4,157             | PTO         | CO         | CO        | TC | 3 F |
| CA-KER-501   | 227        | Flake    | 3 (70-80)               | 6.9         | 2,793        | 7.2              | 3,128             | PTO         | CO         | CO        | TC | 3 F |
| CA-KER-503   | 236-55     | Flake    | SS 1 (0-5)              | 0.0         | 0            | 0.0              | 0                 | --          | CO         | WCP       | LD | 2 B |
| CA-KER-503   | 236-66     | Flake    | SS1 (0-5)               | 12.0        | 10,085       | 12.6             | 11,293            | LPL         | CO         | WS        | LD | 2 B |
| CA-KER-503   | 236-40     | Flake    | TU 2 (40-50)            | 11.2        | 8,593        | 11.8             | 9,623             | LPL         | CO         | LM        | LD | 2 B |
| CA-KER-505/H | 1075       | Flake    | Surface                 | 13.1        | 12,360       | 13.8             | 13,842            | LPL         | CO         | CO        | TC | 2 B |
| CA-KER-505/H | 1074       | Flake    | Surface                 | 12.5        | 11,086       | 13.1             | 12,415            | LPL         | CO         | CO        | TC | 2 B |
| CA-KER-505/H | 1074       | Flake    | Surface                 | 7.7         | 3,603        | 8.1              | 4,034             | PTO         | CO         | CO        | TC | 2 B |
| CA-KER-505/H | 1077       | Flake    | Surface                 | 15.7        | 18,813       | 16.5             | 21,067            | LPL         | CO         | CO        | TC | 2 B |
| CA-KER-5143  | 7874       | Pinto    | Surface                 | 10.8        | 7,898        | 11.3             | 8,844             | LMO         | CO         | WS        | TC | 3 A |

| Trinomial    | Cat No.  | Artifact | Unit (Depth)  | Raw Microns | Raw Years BP | Adjusted Microns | Adjusted Years BP | Time Period | Source | Sub-source | Site Type | MR | MA |
|--------------|----------|----------|---------------|-------------|--------------|------------------|-------------------|-------------|--------|------------|-----------|----|----|
| CA-KER-5143  | 2503-8   | Flake    | Surface       | 10.5        | 7,398        | 11.0             | 8,285             | LMO         | CO     | WS         | TC        | 3  | A  |
| CA-KER-5143  | 2503-9   | Flake    | Surface       | 9.8         | 6,304        | 10.3             | 7,059             | PTO         | CO     | WS         | TC        | 3  | A  |
| CA-KER-5143  | 2503-10  | Flake    | Surface       | 11.9        | 9,891        | 12.5             | 11,076            | LPL         | CO     | WS         | TC        | 3  | A  |
| CA-KER-5143  | 2503-11  | Flake    | Surface       | 11.3        | 8,772        | 11.9             | 9,823             | LPL         | CO     | WS         | TC        | 3  | A  |
| CA-KER-5143  | 2503-12  | Flake    | Surface       | 9.8         | 6,304        | 10.3             | 7,059             | PTO         | CO     | WS         | TC        | 3  | A  |
| CA-KER-5143  | 2503-12  | Flake    | Surface       | 7.4         | 3,285        | 7.8              | 3,679             | PTO         | CO     | WS         | TC        | 3  | A  |
| CA-KER-5143  | 2503-13  | Flake    | Surface       | 10.5        | 7,398        | 11.0             | 8,285             | LMO         | CO     | WS         | TC        | 3  | A  |
| CA-KER-5143  | 2503-15  | Flake    | Surface       | 10.8        | 7,898        | 11.3             | 8,844             | LMO         | CO     | CO         | TC        | 3  | A  |
| CA-KER-5143  | 2503-16  | Flake    | Surface       | 9.8         | 6,304        | 10.3             | 7,059             | PTO         | CO     | WS         | TC        | 3  | A  |
| CA-KER-5143  | 2503-17  | Flake    | Surface       | 18.6        | 27,876       | 19.5             | 31,217            | LPL         | CO     | CO         | TC        | 3  | A  |
| CA-KER-5143  | 2503-18  | Flake    | Surface       | 9.7         | 6,156        | 10.2             | 6,893             | PTO         | CO     | WS         | TC        | 3  | A  |
| CA-KER-5143  | 2503-26  | Flake    | Surface       | 11.1        | 8,416        | 11.7             | 9,425             | LPL         | CO     | CO         | TC        | 3  | A  |
| CA-KER-5143  | 2503-28  | Flake    | Surface       | 10.8        | 7,898        | 11.3             | 8,844             | LMO         | CO     | WS         | TC        | 3  | A  |
| CA-KER-5143  | 2503-30  | Flake    | Surface       | 9.8         | 6,304        | 10.3             | 7,059             | PTO         | CO     | WS         | TC        | 3  | A  |
| CA-KER-5143  | 2503-33a | Flake    | Surface       | 9.6         | 6,009        | 10.1             | 6,730             | PTO         | CO     | WS         | TC        | 3  | A  |
| CA-KER-5143  | 2503-33b | Flake    | Surface       | 0.0         | 0            | 0.0              | 0                 | --          | CO     | WS         | TC        | 3  | A  |
| CA-KER-5143  | 2503-76  | Flake    | STP 15 (0-50) | 0.0         | 0            | 0.0              | 0                 | --          | CO     | WS         | TC        | 3  | A  |
| CA-KER-5148  | 1768-3   | Flake    | Surface       | 7.5         | 3,389        | 7.9              | 3,795             | PTO         | CO     | CO         | TC        | 4  | B  |
| CA-KER-5148  | 1768-3   | Flake    | Surface       | 5.6         | 1,721        | 5.9              | 1,927             | GYP         | CO     | CO         | TC        | 4  | B  |
| CA-KER-5148  | 1768-6   | Flake    | Surface       | 7.6         | 3,495        | 8.0              | 3,914             | PTO         | CO     | CO         | TC        | 4  | B  |
| CA-KER-5148  | 1768-9   | Flake    | Surface       | 7.4         | 3,285        | 7.8              | 3,679             | PTO         | CO     | CO         | TC        | 4  | B  |
| CA-KER-5148  | 1768-23  | Flake    | 1 (0-10)      | 7.3         | 3,183        | 7.7              | 3,565             | PTO         | CO     | CO         | TC        | 4  | B  |
| CA-KER-5148  | 1768-36  | Flake    | Surface       | 7.1         | 2,985        | 7.5              | 3,342             | PTO         | CO     | CO         | TC        | 4  | B  |
| CA-KER-525/H | 240-41   | Flake    | Surface       | 8.4         | 4,408        | 8.8              | 4,937             | PTO         | CO     | WCP        | BC        | 5  | A  |
| CA-KER-525/H | 240-64   | PF       | TU 21 (S)     | 6.9         | 2,793        | 7.2              | 3,128             | PTO         | CO     | WS         | BC        | 5  | A  |
| CA-KER-525/H | 240-113  | Flake    | TU 26 (S)     | 6.7         | 2,609        | 7.0              | 2,922             | GYP         | CO     | WCP        | BC        | 5  | A  |
| CA-KER-525/H | 240-262  | Flake    | TU 39 (0-10)  | 6.9         | 2,793        | 7.2              | 3,128             | PTO         | CO     | WCP        | BC        | 5  | A  |
| CA-KER-525/H | 240-320  | Flake    | TU 42 (0-10)  | 8.0         | 3,937        | 8.4              | 4,408             | PTO         | CO     | WCP        | BC        | 5  | A  |
| CA-KER-525/H | 340-329  | Flake    | TU 43 (S)     | 8.7         | 4,782        | 9.1              | 5,356             | PTO         | CO     | WCP        | BC        | 5  | A  |
| CA-KER-525/H | 340-329  | Flake    | TU 43 (S)     | 6.1         | 2,099        | 6.4              | 2,350             | GYP         | CO     | WCP        | BC        | 5  | A  |
| CA-KER-525/H | 240-6476 | CWT      | Surface       | 4.6         | 1,090        | 4.8              | 1,221             | SSP         | CO     | WS         | BC        | 5  | A  |
| CA-KER-5257  | 2618-2   | Flake    | Surface       | 10.3        | 7,075        | 10.8             | 7,923             | LMO         | CO     | WS         | LD        | 3  | A  |
| CA-KER-5257  | 2618-4   | Flake    | Surface       | 9.0         | 5,174        | 9.5              | 5,794             | PTO         | CO     | WS         | LD        | 3  | A  |
| CA-KER-5257  | 2618-5   | Flake    | Surface       | 9.8         | 6,304        | 10.3             | 7,059             | PTO         | CO     | WS         | LD        | 3  | A  |



| Trinomial   | Cat No.  | Artifact | Unit (Depth) | Raw<br>Microns | Raw<br>Years BP | Adjusted<br>Microns | Adjusted<br>Years BP | Time<br>period | Source | Sub-<br>source | Site<br>Type | MR | MA |
|-------------|----------|----------|--------------|----------------|-----------------|---------------------|----------------------|----------------|--------|----------------|--------------|----|----|
| CA-KER-5257 | 2618-6   | Flake    | Surface      | 13.0           | 12,143          | 13.7                | 13,598               | LPL            | CO     | JR             | LD           | 3  | A  |
| CA-KER-5258 | 2619-1   | Flake    | Surface      | 9.2            | 5,444           | 9.7                 | 6,097                | PTO            | CO     | WS             | LD           | 3  | A  |
| CA-KER-526  | 241      | Flake    | 2 (90-100)   | 9.6            | 6,009           | 10.1                | 6,730                | PTO            | CO     | CO             | TC           | 3  | G  |
| CA-KER-526  | 435      | Flake    | 9 (40-50)    | 8.7            | 4,782           | 9.1                 | 5,356                | PTO            | CO     | CO             | TC           | 3  | G  |
| CA-KER-526  | 377      | Flake    | 7 (40-50)    | 13.3           | 12,803          | 14.0                | 14,337               | LPL            | CO     | CO             | TC           | 3  | G  |
| CA-KER-526  | 543      | Flake    | 10 (0-10)    | 7.5            | 3,389           | 7.9                 | 3,795                | PTO            | CO     | CO             | TC           | 3  | G  |
| CA-KER-526  | 547      | Flake    | 10 (10-20)   | 7.5            | 3,389           | 7.9                 | 3,795                | PTO            | CO     | CO             | TC           | 3  | G  |
| CA-KER-526  | 642      | Flake    | 17 (0-10)    | 7.6            | 3,495           | 8.0                 | 3,914                | PTO            | CO     | CO             | TC           | 3  | G  |
| CA-KER-5292 | 8        | Flake    | Surface      | 7.9            | 3,823           | 8.3                 | 4,282                | PTO            | CO     | WS             | TC           | 3  | I  |
| CA-KER-5306 | 2555-31  | Flake    | 2 (S)        | 6.8            | 2,700           | 7.1                 | 3,024                | PTO            | CO     | WS             | BC           | 3  | G  |
| CA-KER-5306 | 2555-31  | Flake    | 2 (S)        | 3.3            | 505             | 3.5                 | 565                  | SHO            | CO     | WS             | BC           | 3  | G  |
| CA-KER-5306 | 6727     | ECN      | Surface      | 3.9            | 743             | 4.1                 | 833                  | SSP            | CO     | WS             | BC           | 3  | G  |
| CA-KER-5306 | 6730     | Drill    | Surface      | 3.1            | 436             | 3.3                 | 489                  | SHO            | CO     | WS             | BC           | 3  | G  |
| CA-KER-5306 | 7989     | CWT      | Surface      | 3.0            | 404             | 3.2                 | 453                  | SHO            | CO     | WS             | BC           | 3  | G  |
| CA-KER-533  | 246-5    | Flake    | Surface      | 7.0            | 2,888           | 7.4                 | 3,234                | PTO            | CO     | SL             | TC           | 3  | G  |
| CA-KER-534  | 5455     | RSP      | Surface      | 3.8            | 700             | 4.0                 | 784                  | SSP            | CO     | WS             | TC           | 3  | H  |
| CA-KER-5341 | 2720-1   | Flake    | Surface      | 9.0            | 5,174           | 9.5                 | 5,794                | PTO            | CO     | SL             | LD           | 3  | A  |
| CA-KER-5341 | 2720-27  | Flake    | Surface      | 9.0            | 5,174           | 9.5                 | 5,794                | PTO            | UNK    | UNK            | LD           | 3  | A  |
| CA-KER-549  | 7222     | Pinto    | Surface      | 4.9            | 1,262           | 5.1                 | 1,414                | GYP            | CO     | JR             | TC           | 5  | A  |
| CA-KER-549  | 8-8-1    | Flake    | UNK          | 6.4            | 2,346           | 6.7                 | 2,627                | GYP            | CO     | WS             | TC           | 3  | I  |
| CA-KER-549  | 2-2-1    | Flake    | UNK          | 4.4            | 983             | 4.6                 | 1,101                | SSP            | CO     | JR             | TC           | 3  | I  |
| CA-KER-5517 | 2785-1   | Flake    | Surface      | 0.0            | 0               | 0.0                 | 0                    | --             | UNK    | NS             | LD           | 5  | A  |
| CA-KER-5578 | 2777-6   | Flake    | Surface      | 9.3            | 5,583           | 9.8                 | 6,252                | PTO            | CO     | WCP            | TC           | 5  | F  |
| CA-KER-5578 | 2777-7   | Flake    | Surface      | 8.5            | 4,531           | 8.9                 | 5,074                | PTO            | CO     | WCP            | TC           | 5  | F  |
| CA-KER-5578 | 2777-8   | Flake    | 1 (0-10)     | 10.5           | 7,398           | 11.0                | 8,285                | LMO            | CO     | WCP            | TC           | 5  | F  |
| CA-KER-5578 | 2777-12  | Flake    | 4 (0-10)     | 8.0            | 3,937           | 8.4                 | 4,408                | PTO            | CO     | WCP            | TC           | 5  | F  |
| CA-KER-5578 | 2777-14  | Flake    | 5 (0-10)     | 9.6            | 6,009           | 10.1                | 6,730                | PTO            | CO     | WCP            | TC           | 5  | F  |
| CA-KER-5578 | 2777-17a | Flake    | 7 (S)        | 8.7            | 4,782           | 9.1                 | 5,356                | PTO            | CO     | WCP            | TC           | 5  | F  |
| CA-KER-5578 | 2777-17b | Flake    | 7 (S)        | 8.4            | 4,408           | 8.8                 | 4,937                | PTO            | CO     | WCP            | TC           | 5  | F  |
| CA-KER-5578 | 2777-23  | Flake    | ST 21 (0-10) | 6.4            | 2,346           | 6.7                 | 2,627                | GYP            | CO     | WCP            | TC           | 5  | F  |
| CA-KER-5626 | 2232     | Flake    | Surface      | 15.6           | 18,536          | 16.4                | 20,757               | LPL            | CO     | SL             | TC           | 5  | A  |
| CA-KER-5627 | 6773     | Shatter  | Surface      | 7.9            | 3,823           | 8.3                 | 4,282                | PTO            | CO     | WS             | TC           | 4  | B  |
| CA-KER-5627 | 6774     | Shatter  | Surface      | 8.4            | 4,408           | 8.8                 | 4,937                | PTO            | CO     | WS             | TC           | 4  | B  |
| CA-KER-5661 | 10742    | RSP      | Surface      | 5.0            | 1,323           | 5.3                 | 1,482                | GYP            | CO     | WS             | TC           | 2  | B  |

| Trinomial    | Cat No.  | Artifact | Unit (Depth) | Raw<br>Microns | Raw<br>Years BP | Adjusted<br>Microns | Adjusted<br>Years BP | Time<br>Period | Source | Sub-<br>source | Site<br>Type | MR | MA |
|--------------|----------|----------|--------------|----------------|-----------------|---------------------|----------------------|----------------|--------|----------------|--------------|----|----|
| CA-KER-5716  | 55       | Flake    | Surface      | 7.7            | 3,603           | 8.1                 | 4,034                | PTO            | CO     | WS             | TC           | 5  | F  |
| CA-KER-5716  | 56       | Flake    | Surface      | 2.9            | 374             | 3.0                 | 419                  | SHO            | CO     | WS             | TC           | 5  | F  |
| CA-KER-5717  | 57       | Flake    | Surface      | 7.5            | 3,389           | 7.9                 | 3,795                | PTO            | CO     | WS             | TC           | 5  | F  |
| CA-KER-5717  | 58       | Flake    | Surface      | 0.0            | 0               | 0.0                 | 0                    | --             | CO     | WS             | TC           | 5  | F  |
| CA-KER-5717  | 59       | Flake    | Surface      | 6.6            | 2,519           | 6.9                 | 2,821                | GYP            | CO     | WS             | TC           | 5  | F  |
| CA-KER-5717  | 60       | Flake    | Surface      | 6.6            | 2,519           | 6.9                 | 2,821                | GYP            | CO     | CO             | TC           | 5  | F  |
| CA-KER-5717  | 61       | Flake    | Surface      | 7.1            | 2,985           | 7.5                 | 3,342                | PTO            | CO     | SL             | TC           | 5  | F  |
| CA-KER-5717  | 62       | Flake    | Surface      | 7.1            | 2,985           | 7.5                 | 3,342                | PTO            | CO     | WS             | TC           | 5  | F  |
| CA-KER-5717  | 63       | Flake    | Surface      | 7.3            | 3,183           | 7.7                 | 3,565                | PTO            | CO     | WS             | TC           | 5  | F  |
| CA-KER-5717  | 64       | Flake    | Surface      | 8.0            | 3,937           | 8.4                 | 4,408                | PTO            | CO     | WS             | TC           | 5  | F  |
| CA-KER-5717  | 65       | Flake    | Surface      | 10.9           | 8,068           | 11.4                | 9,035                | LMO            | CO     | WS             | TC           | 5  | F  |
| CA-KER-5717  | 66       | Flake    | Surface      | 6.3            | 2,262           | 6.6                 | 2,533                | GYP            | CO     | WS             | TC           | 5  | F  |
| CA-KER-5717  | 67       | Biface   | Surface      | 8.6            | 4,656           | 9.0                 | 5,214                | PTO            | CO     | WS             | TC           | 5  | F  |
| CA-KER-5717  | 68       | Biface   | Surface      | 9.0            | 5,174           | 9.5                 | 5,794                | PTO            | CO     | WS             | TC           | 5  | F  |
| CA-KER-5717  | 69       | DSN      | Surface      | 3.5            | 578             | 3.7                 | 648                  | SSP            | CO     | WS             | TC           | 5  | F  |
| CA-KER-5717  | 70       | Flake    | Surface      | 7.5            | 3,389           | 7.9                 | 3,795                | PTO            | CO     | CO             | TC           | 5  | F  |
| CA-KER-5717  | 71       | Flake    | Surface      | 0.0            | 0               | 0.0                 | 0                    | --             | CO     | WS             | TC           | 5  | F  |
| CA-KER-5717  | 72       | Flake    | Surface      | 9.1            | 5,308           | 9.6                 | 5,944                | PTO            | CO     | WS             | TC           | 5  | F  |
| CA-KER-5717  | 73       | Flake    | Surface      | 8.0            | 3,937           | 8.4                 | 4,408                | PTO            | CO     | SL             | TC           | 5  | F  |
| CA-KER-5756  | 75       | Biface   | Surface      | 7.2            | 3,083           | 7.6                 | 3,452                | PTO            | CO     | WS             | HE           | 5  | F  |
| CA-KER-5756  | 76       | Flake    | STP 6 (0-20) | 7.2            | 3,083           | 7.6                 | 3,452                | PTO            | CO     | WS             | HE           | 5  | F  |
| CA-KER-5802  | 6954     | Pinto    | Surface      | 11.4           | 8,953           | 12.0                | 10,026               | LPL            | CO     | WS             | TC           | 1  | A  |
| CA-KER-5815  | 6952     | Dart     | Surface      | 7.0            | 2,888           | 7.4                 | 3,234                | PTO            | CO     | WS             | LD           | 1  | A  |
| CA-KER-5933  | 3283-18  | Biface   | 4 (S)        | 8.7            | 4,782           | 9.1                 | 5,356                | PTO            | CO     | WCP            | TC           | 5  | A  |
| CA-KER-5933  | 3283-34  | Flake    | 6 (S)        | 0.0            | 0               | 0.0                 | 0                    | --             | UNK    | NS             | TC           | 5  | A  |
| CA-KER-6029  | 2442-1-2 | UTF      | Surface      | 6.0            | 2,020           | 6.3                 | 2,262                | GYP            | CO     | WS             | HE           | 2  | A  |
| CA-KER-6046  | 3122-3   | Flake    | Surface      | 0.0            | 0               | 0.0                 | 0                    | --             | UNK    | NS             | TC           | 5  | F  |
| CA-KER-6046  | 3122-4   | BFF      | Surface      | 4.6            | 1,090           | 4.8                 | 1,221                | SSP            | CO     | WCP            | TC           | 5  | F  |
| CA-KER-6046  | 3122-6   | PF       | Surface      | 4.6            | 1,090           | 4.8                 | 1,221                | SSP            | CO     | WCP            | TC           | 5  | F  |
| CA-KER-673/H | 276-336  | Shatter  | U 10 [50-60] | 15.8           | 19,092          | 16.6                | 21,380               | LPL            | CO     | CO             | TC           | 3  | F  |
| CA-KER-6790  | 6864     | PF       | Surface      | 7.5            | 3,389           | 7.9                 | 3,795                | PTO            | CO     | SL             | TC           | 5  | A  |
| CA-KER-6790  | 3        | PF       | Surface      | 9.2            | 5,444           | 9.7                 | 6,097                | PTO            | CO     | WCP            | TC           | 5  | A  |
| CA-KER-6797  | 94       | Flake    | Surface      | 6.2            | 2,179           | 6.5                 | 2,440                | GYP            | CO     | WS             | LD           | 1  | A  |
| CA-KER-6797  | 95       | Flake    | Surface      | 10.2           | 6,917           | 10.7                | 7,746                | LMO            | CO     | WS             | LD           | 1  | A  |

| Trinomial    | Cat No.  | Artifact | Unit (Depth) | Raw Microns | Raw Years BP | Adjusted Microns | Adjusted Years BP | Time Period | Source | Sub-source | Site Type | MR | MA |
|--------------|----------|----------|--------------|-------------|--------------|------------------|-------------------|-------------|--------|------------|-----------|----|----|
| CA-KER-6797  | 96       | Flake    | Surface      | 9.2         | 5,444        | 9.7              | 6,097             | PTO         | CO     | WS         | LD        | 1  | A  |
| CA-KER-6797  | 97       | Flake    | Surface      | 9.7         | 6,156        | 10.2             | 6,893             | PTO         | CO     | WS         | LD        | 1  | A  |
| CA-KER-6797  | 98       | Flake    | Surface      | 9.2         | 5,444        | 9.7              | 6,097             | PTO         | CO     | WS         | LD        | 1  | A  |
| CA-KER-6801  | 5        | Flake    | Surface      | 7.9         | 3,823        | 8.3              | 4,282             | PTO         | CO     | CO         | TC        | 1  | A  |
| CA-KER-6804  | 6        | Flake    | Surface      | 8.5         | 4,531        | 8.9              | 5,074             | PTO         | CO     | WS         | LD        | 1  | A  |
| CA-KER-6804  | 6        | Flake    | Surface      | 0.0         | 0            | 0.0              | 0                 | --          | CO     | WS         | LD        | 1  | A  |
| CA-KER-6812  | 73       | Flake    | Surface      | 7.8         | 3,712        | 8.2              | 4,157             | PTO         | CO     | WS         | TC        | 1  | A  |
| CA-KER-6812  | 74       | Flake    | Surface      | 7.9         | 3,823        | 8.3              | 4,282             | PTO         | CO     | WS         | TC        | 1  | A  |
| CA-KER-6812  | 75       | Flake    | Surface      | 0.0         | 0            | 0.0              | 0                 | --          | CO     | WS         | TC        | 1  | A  |
| CA-KER-6812  | 76       | RTF      | Surface      | 6.3         | 2,262        | 6.6              | 2,533             | GYP         | CO     | WS         | TC        | 1  | A  |
| CA-KER-6812  | 77       | Flake    | Surface      | 0.0         | 0            | 0.0              | 0                 | --          | CO     | WS         | TC        | 1  | A  |
| CA-KER-6812  | 78       | Flake    | Surface      | 0.0         | 0            | 0.0              | 0                 | --          | CO     | WS         | TC        | 1  | A  |
| CA-KER-6812  | 79       | Flake    | Surface      | 0.0         | 0            | 0.0              | 0                 | --          | CO     | WS         | TC        | 1  | A  |
| CA-KER-6812  | 80       | Flake    | Surface      | 10.7        | 7,729        | 11.2             | 8,655             | LMO         | CO     | WS         | TC        | 1  | A  |
| CA-KER-6817  | 93       | Biface   | Surface      | 0.0         | 0            | 0.0              | 0                 | --          | CO     | WS         | QUA       | 2  | A  |
| CA-KER-698/H | 10691    | Flake    | STP 12 (S)   | 0.0         | 0            | 0.0              | 0                 | --          | CO     | WS         | TC        | 3  | A  |
| CA-KER-7578  | 4188-172 | Flake    | Surface      | 6.8         | 2,700        | 7.1              | 3,024             | PTO         | CO     | WS         | TC        | 1  | A  |
| CA-KER-7578  | 4188-95  | Flake    | Surface      | 8.1         | 4,052        | 8.5              | 4,537             | PTO         | CO     | WS         | TC        | 1  | A  |
| CA-KER-7578  | 4188-182 | Flake    | ST 6 (0-10)  | 7.7         | 3,603        | 8.1              | 4,034             | PTO         | CO     | WS         | TC        | 1  | A  |
| CA-KER-863/H | 1383     | CWL      | Surface      | 0.0         | 0            | 0.0              | 0                 | --          | CO     | WS         | BC        | 5  | D  |
| CA-KER-863/H | 1796     | Point    | Surface      | 9.0         | 5,174        | 9.5              | 5,794             | PTO         | CO     | WS         | BC        | 5  | D  |
| CA-KER-XXXX  | 3        | Arrow    | Surface      | 3.3         | 505          | 3.5              | 565               | SHO         | CO     | WS         | TC        | 3  | E  |
| CA-KER-XXXX  | 4        | Arrow    | Surface      | 3.8         | 700          | 4.0              | 784               | SSP         | CO     | WS         | TC        | 3  | E  |
| CA-KER-XXXX  | 12       | Arrow    | Surface      | 5.0         | 1,323        | 5.3              | 1,482             | GYP         | CO     | WS         | TC        | 3  | E  |
| CA-KER-XXXX  | 16       | Arrow    | Surface      | 3.8         | 700          | 4.0              | 784               | SSP         | CO     | WS         | TC        | 3  | E  |
| CA-KER-XXXX  | 6        | Flake    | Surface      | 4.4         | 983          | 4.6              | 1,101             | SSP         | CO     | WS         | TC        | 3  | E  |
| CA-KER-XXXX  | 27       | Arrow    | Surface      | 4.6         | 1,090        | 4.8              | 1,221             | SSP         | CO     | WS         | TC        | 3  | E  |
| CA-KER-XXXX  | 28       | Flake    | Surface      | 5.5         | 1,650        | 5.8              | 1,848             | GYP         | CO     | WS         | TC        | 3  | E  |
| CA-KER-XXXX  | 14       | Flake    | Surface      | 4.5         | 1,036        | 4.7              | 1,160             | SSP         | CO     | WS         | TC        | 3  | E  |
| CA-KER-XXXX  | 25       | Flake    | Surface      | 4.5         | 1,036        | 4.7              | 1,160             | SSP         | CO     | WS         | TC        | 3  | E  |
| CA-KER-XXXX  | 7        | Flake    | Surface      | 4.0         | 788          | 4.2              | 883               | SSP         | CO     | WS         | TC        | 1  | B  |
| CA-KER-XXXX  | 1        | ECN      | Surface      | 8.1         | 4,052        | 8.5              | 4,537             | PTO         | CO     | WS         | TC        | 1  | B  |
| CA-KER-XXXX  | 14       | Flake    | Surface      | 11.6        | 9,322        | 12.2             | 10,439            | LPL         | CO     | WS         | LD        | 2  | C  |
| CA-KER-XXXX  | 34       | Flake    | Surface      | 18.4        | 27,186       | 19.3             | 30,444            | LPL         | CO     | SL         | LD        | 2  | C  |

| Trinomial     | Cat No.   | Artifact | Unit (Depth)      | Raw<br>Microns | Raw<br>Years BP | Adjusted<br>Microns | Adjusted<br>Years BP | Time<br>Period | Source | Sub-<br>source | Site<br>Type | MR | MA |
|---------------|-----------|----------|-------------------|----------------|-----------------|---------------------|----------------------|----------------|--------|----------------|--------------|----|----|
| CA-KER-XXXX   | 160       | Flake    | Surface           | 10.2           | 6,917           | 10.7                | 7,746                | LMO            | CO     | WS             | LD           | 2  | C  |
| CA-KER-XXXX   | 66        | Flake    | Surface           | 11.2           | 8,593           | 11.8                | 9,623                | LPL            | CO     | SL             | LD           | 2  | C  |
| CA-KER-XXXX   | 5         | Flake    | Surface           | 0.0            | 0               | 0.0                 | 0                    | --             | CO     | WS             | LD           | 1  | B  |
| CA-KER-XXXX   | 96        | Flake    | Surface           | 0.0            | 0               | 0.0                 | 0                    | --             | CO     | WS             | LD           | 1  | B  |
| CA-KER-XXXX   | 4418-113  | BFF      | Surface           | 2.2            | 197             | 2.3                 | 221                  | SHO            | CO     | WS             | TC           | 3  | F  |
| CA-KER-XXXX   | 4320-341  | RTF      | Surface           | 9.2            | 5,444           | 9.7                 | 6,097                | PTO            | CO     | WS             | TC           | 3  | I  |
| CA-KER-XXXX   | 4311-347  | Flake    | Surface           | 12.8           | 11,714          | 13.4                | 13,117               | LPL            | CO     | SL             | LD           | 3  | I  |
| CA-KER-XXXX   | 4292-342  | flake    | STP (0-20)        | 11.8           | 9,699           | 12.4                | 10,861               | LPL            | CO     | SL             | LD           | 3  | I  |
| CA-KER-XXXX   | 4292-346  | RTF      | Surface           | 11.1           | 8,416           | 11.7                | 9,425                | LPL            | CO     | SL             | LD           | 3  | I  |
| CA-KER-XXXX   | 4337-20   | Flake    | Surface           | 6.6            | 2,519           | 6.9                 | 2,821                | GYP            | CO     | WS             | TC           | 5  | F  |
| CA-KER-XXXX   | 4394-349  | UTF      | Surface           | 7.9            | 3,823           | 8.3                 | 4,282                | PTO            | CO     | WS             | LD           | 3  | F  |
| CA-KER-XXXX   | 9         | Flake    | STU-2 (0-20)      | 0.0            | 0               | 0.0                 | 0                    | --             | CO     | WS             | LD           | 3  | I  |
| CA-KER-XXXX   | 10        | Flake    | STU-3 (20-40)     | 11.0           | 8,241           | 11.6                | 9,229                | LPL            | CO     | WS             | LD           | 3  | I  |
| CA-LAN-1067/H | 717       | Flake    | Surface           | 10.6           | 7,563           | 11.1                | 8,469                | LMO            | CO     | WCP            | LD           | 2  | C  |
| CA-LAN-1067/H | 2955.1069 | Flake    | Surface           | 0.0            | 0               | 0.0                 | 0                    | --             | CO     | WS             | LD           | 2  | C  |
| CA-LAN-1067/H | 2955.1121 | Flake    | Surface           | 7.6            | 3,495           | 8.0                 | 3,914                | PTO            | CO     | WS             | LD           | 2  | C  |
| CA-LAN-1067/H | 2955.1139 | Flake    | Surface           | 0.0            | 0               | 0.0                 | 0                    | --             | CO     | WS             | LD           | 2  | C  |
| CA-LAN-1103   | 218       | BTF      | Surface           | 7.0            | 2,888           | 7.4                 | 3,234                | PTO            | CO     | WS             | TC           | 3  | F  |
| CA-LAN-1103   | 218       | BTF      | Surface           | 4.9            | 1,262           | 5.1                 | 1,414                | GYP            | CO     | WS             | TC           | 3  | F  |
| CA-LAN-1103   | 219       | Biface   | Surface           | 8.3            | 4,288           | 8.7                 | 4,802                | PTO            | CO     | WS             | TC           | 3  | F  |
| CA-LAN-1103   | 219       | Biface   | Surface           | 8.0            | 3,937           | 8.4                 | 4,408                | PTO            | CO     | WS             | TC           | 3  | F  |
| CA-LAN-1103   | 220       | Scraper  | Surface           | 1.6            | 94              | 1.7                 | 105                  | SHO            | CO     | WS             | TC           | 3  | F  |
| CA-LAN-1103   | 242       | BTF      | SRU 1, Cell C (S) | 14.3           | 15,148          | 15.0                | 16,963               | LPL            | CO     | WS             | TC           | 3  | F  |
| CA-LAN-1103   | 242       | BTF      | SRU 1, Cell C (S) | 12.0           | 10,085          | 12.6                | 11,293               | LPL            | CO     | WS             | TC           | 3  | F  |
| CA-LAN-1103   | 402       | BTF      | SRU 3, Cell D (S) | 9.7            | 6,156           | 10.2                | 6,893                | PTO            | CO     | WS             | TC           | 3  | F  |
| CA-LAN-1103   | 443       | BTF      | SRU 3, Cell G (S) | 7.4            | 3,285           | 7.8                 | 3,679                | PTO            | CO     | WS             | TC           | 3  | F  |
| CA-LAN-1103   | 511       | BTF      | SRU 4, Cell C (S) | 7.4            | 3,285           | 7.8                 | 3,679                | PTO            | CO     | WS             | TC           | 3  | F  |
| CA-LAN-1103   | 511       | BTF      | SRU 4, Cell C (S) | 6.0            | 2,020           | 6.3                 | 2,262                | GYP            | CO     | WS             | TC           | 3  | F  |
| CA-LAN-1103   | 794a      | Flake    | TU 3 (0-10)       | 8.0            | 3,937           | 8.4                 | 4,408                | PTO            | CO     | WS             | TC           | 3  | F  |
| CA-LAN-1103   | 794a      | Flake    | TU 3 (0-10)       | 7.0            | 2,888           | 7.4                 | 3,234                | PTO            | CO     | WS             | TC           | 3  | F  |
| CA-LAN-1103   | 794b      | Shatter  | TU 3 (0-10)       | 4.3            | 932             | 4.5                 | 1,044                | SSP            | CO     | WS             | TC           | 3  | F  |
| CA-LAN-1103   | 815       | BTF      | TU 3 (30-40)      | 7.0            | 2,888           | 7.4                 | 3,234                | PTO            | CO     | WS             | TC           | 3  | F  |
| CA-LAN-1103   | 822a      | BTF      | TU 3 (40-50)      | 7.1            | 2,985           | 7.5                 | 3,342                | PTO            | CO     | SL             | TC           | 3  | F  |
| CA-LAN-1103   | 822b      | BTF      | TU 3 (40-50)      | 7.0            | 2,888           | 7.4                 | 3,234                | PTO            | CO     | WS             | TC           | 3  | F  |

| Trinomial     | Cat No. | Artifact | Unit (Depth)  | Raw<br>Microns | Raw<br>Years BP | Adjusted<br>Microns | Adjusted<br>Years BP | Time<br>period | Source | Sub-<br>source | Site<br>Type | MR | MA |
|---------------|---------|----------|---------------|----------------|-----------------|---------------------|----------------------|----------------|--------|----------------|--------------|----|----|
| CA-LAN-1103   | 992a    | BTF      | TU 8 (0-10)   | 7.0            | 2,888           | 7.4                 | 3,234                | PTO            | CO     | WS             | TC           | 3  | F  |
| CA-LAN-1103   | 992b    | Flake    | TU 8 (0-10)   | 9.0            | 5,174           | 9.5                 | 5,794                | PTO            | CO     | WS             | TC           | 3  | F  |
| CA-LAN-1103   | 992c    | Flake    | TU 8 (0-10)   | 8.1            | 4,052           | 8.5                 | 4,537                | PTO            | CO     | WS             | TC           | 3  | F  |
| CA-LAN-1103   | 992c    | Flake    | TU 8 (0-10)   | 7.0            | 2,888           | 7.4                 | 3,234                | PTO            | CO     | WS             | TC           | 3  | F  |
| CA-LAN-1103   | 1014    | BTF      | TU 8 (40-50)  | 4.2            | 883             | 4.4                 | 989                  | SSP            | CO     | WS             | TC           | 3  | F  |
| CA-LAN-1148   | 1120    | Biface   | Surface       | 8.2            | 4,169           | 8.6                 | 4,668                | PTO            | CO     | WS             | TC           | 3  | F  |
| CA-LAN-1148   | 1189    | BTF      | STP 1 (20-45) | 8.0            | 3,937           | 8.4                 | 4,408                | PTO            | CO     | WS             | TC           | 3  | F  |
| CA-LAN-1158   | 602     | Shatter  | Surface       | 9.2            | 5,444           | 9.7                 | 6,097                | PTO            | CO     | CO             | TC           | 3  | F  |
| CA-LAN-1161   | 2-2-1   | Biface   | UNK           | 7.5            | 3,389           | 7.9                 | 3,795                | PTO            | CO     | WS             | TC           | 3  | G  |
| CA-LAN-1162   | 56      | Pinto    | Surface       | 4.1            | 835             | 4.3                 | 935                  | SSP            | CO     | WS             | TC           | 3  | G  |
| CA-LAN-1185   | 71      | CWL      | Surface       | 4.2            | 883             | 4.4                 | 989                  | SSP            | CO     | WS             | TC           | 5  | D  |
| CA-LAN-1185   | 393-93  | Flake    | SC 4 (S)      | 3.9            | 743             | 4.1                 | 833                  | SSP            | CO     | WCP            | TC           | 5  | D  |
| CA-LAN-1185   | 393-123 | Flake    | 1 (S)         | 6.2            | 2,179           | 6.5                 | 2,440                | GYP            | CO     | WCP            | TC           | 5  | D  |
| CA-LAN-1185   | 393-124 | Flake    | 2 (S)         | 4.4            | 983             | 4.6                 | 1,101                | SSP            | CO     | WCP            | TC           | 5  | D  |
| CA-LAN-1185   | 393-126 | Flake    | 4 (S)         | 6.3            | 2,262           | 6.6                 | 2,533                | GYP            | CO     | WS             | TC           | 5  | D  |
| CA-LAN-1185   | 393-129 | Flake    | 7 (S)         | 0.0            | 0               | 0.0                 | 0                    | --             | UNK    | NS             | TC           | 5  | D  |
| CA-LAN-1185   | 393-130 | Flake    | 8 (S)         | 7.7            | 3,603           | 8.1                 | 4,034                | PTO            | CO     | WCP            | TC           | 5  | D  |
| CA-LAN-1189/H | 83      | HBT      | Surface       | 6.4            | 2,346           | 6.7                 | 2,627                | GYP            | CO     | WS             | TC           | 5  | D  |
| CA-LAN-1189/H | 38      | Drill    | Surface       | 7.2            | 3,083           | 7.6                 | 3,452                | PTO            | UNK    | NS             | TC           | 5  | D  |
| CA-LAN-1189/H | 194     | Flake    | TU 2 (20-30)  | 5.5            | 1,650           | 5.8                 | 1,848                | GYP            | UNK    | NS             | TC           | 5  | D  |
| CA-LAN-1189/H | 202     | Flake    | TU 2 (40-50)  | 4.4            | 983             | 4.6                 | 1,101                | SSP            | UNK    | NS             | TC           | 5  | D  |
| CA-LAN-1189/H | 261     | Flake    | TU 4 (10-20)  | 4.5            | 1,036           | 4.7                 | 1,160                | SSP            | UNK    | NS             | TC           | 5  | D  |
| CA-LAN-1189/H | 289     | Flake    | TU 4 (40-50)  | 4.6            | 1,090           | 4.8                 | 1,221                | SSP            | UNK    | NS             | TC           | 5  | D  |
| CA-LAN-1189/H | 308     | Flake    | TU 5 (30-56)  | 4.5            | 1,036           | 4.7                 | 1,160                | SSP            | UNK    | NS             | TC           | 5  | D  |
| CA-LAN-1189/H | 400-42  | HBT      | Surface       | 9.1            | 5,308           | 9.6                 | 5,944                | PTO            | CO     | WS             | TC           | 5  | D  |
| CA-LAN-1189/H | 400-22  | Dart     | 121 (0-5)     | 7.2            | 3,083           | 7.6                 | 3,452                | PTO            | CO     | LM             | TC           | 5  | D  |
| CA-LAN-1189/H | 400-46  | PF       | Surface       | 6.0            | 2,020           | 6.3                 | 2,262                | GYP            | CO     | WS             | TC           | 5  | D  |
| CA-LAN-1190/H | 401-81  | Flake    | 8 (S)         | 5.7            | 1,793           | 6.0                 | 2,008                | GYP            | CO     | WCP            | TC           | 3  | G  |
| CA-LAN-1190/H | 401-85  | PF       | PP 4 (S)      | 6.0            | 2,020           | 6.3                 | 2,262                | GYP            | CO     | WCP            | TC           | 3  | G  |
| CA-LAN-1190/H | 401-86  | PF       | PP 5 (S)      | 11.4           | 8,953           | 12.0                | 10,026               | LPL            | CO     | WS             | TC           | 3  | G  |
| CA-LAN-1193   | 77      | Flake    | Surface       | 7.2            | 3,083           | 7.6                 | 3,452                | PTO            | CO     | WS             | LD           | 5  | D  |
| CA-LAN-1207   | 288-3   | PF       | PP 3 (S)      | 3.6            | 617             | 3.8                 | 691                  | SSP            | CO     | WCP            | TC           | 3  | G  |
| CA-LAN-1207   | 288-5   | Flake    | OBS 1 (S)     | 5.2            | 1,449           | 5.5                 | 1,623                | GYP            | CO     | WCP            | TC           | 3  | G  |
| CA-LAN-1207   | 288-6   | Flake    | OBS A (S)     | 7.0            | 2,888           | 7.4                 | 3,234                | PTO            | CO     | WCP            | TC           | 3  | G  |



| Trinomial     | Cat No.   | Artifact | Unit (Depth) | Raw<br>Microns | Raw<br>Years BP | Adjusted<br>Microns | Adjusted<br>Years BP | Time<br>Period | Source | Sub-<br>source | Site<br>Type | MR | MA |
|---------------|-----------|----------|--------------|----------------|-----------------|---------------------|----------------------|----------------|--------|----------------|--------------|----|----|
| CA-LAN-1207   | 288-7     | Flake    | OBS B (S)    | 0.0            | 0               | 0.0                 | 0                    | --             | CO     | WCP            | TC           | 3  | G  |
| CA-LAN-1207   | 288-8     | Flake    | OBS C (S)    | 8.7            | 4,782           | 9.1                 | 5,356                | PTO            | CO     | WCP            | TC           | 3  | G  |
| CA-LAN-1207   | 288-27    | Flake    | A 19 (S)     | 7.8            | 3,712           | 8.2                 | 4,157                | PTO            | CO     | WCP            | TC           | 3  | G  |
| CA-LAN-1227   | 527-1     | DSN      | Surface      | 2.7            | 317             | 2.8                 | 355                  | SHO            | CO     | WPS            | TC           | 3  | G  |
| CA-LAN-1227   | 527-5     | Flake    | Surface      | 5.8            | 1,867           | 6.1                 | 2,091                | GYP            | CO     | WS             | TC           | 3  | G  |
| CA-LAN-1243/H | 1425      | BTF      | Surface      | 7.0            | 2,888           | 7.4                 | 3,234                | PTO            | CO     | JR             | BC           | 3  | F  |
| CA-LAN-1243/H | 1425      | BTF      | Surface      | 7.0            | 2,888           | 7.4                 | 3,234                | PTO            | CO     | JR             | BC           | 3  | F  |
| CA-LAN-1243/H | 1428      | BTF      | Surface      | 7.9            | 3,823           | 8.3                 | 4,282                | PTO            | CO     | WS             | BC           | 3  | F  |
| CA-LAN-1243/H | 1543      | BTF      | TU 3 (10-20) | 6.9            | 2,793           | 7.2                 | 3,128                | PTO            | CO     | WCP            | BC           | 3  | F  |
| CA-LAN-1243/H | 1547      | BTF      | TU 3 (20-30) | 5.9            | 1,942           | 6.2                 | 2,175                | GYP            | CO     | WCP            | BC           | 3  | F  |
| CA-LAN-1243/H | 1566a     | BTF      | TU 3 (50-60) | 6.0            | 2,020           | 6.3                 | 2,262                | GYP            | CO     | WS             | BC           | 3  | F  |
| CA-LAN-1243/H | 1566b     | BTF      | TU 3 (50-60) | 6.0            | 2,020           | 6.3                 | 2,262                | GYP            | CO     | WS             | BC           | 3  | F  |
| CA-LAN-1243/H | 1571      | BTF      | TU 3 (60-70) | 6.6            | 2,519           | 6.9                 | 2,821                | GYP            | CO     | WS             | BC           | 3  | F  |
| CA-LAN-1283   | 630-136   | Flake    | Surface      | 3.9            | 743             | 4.1                 | 833                  | SSP            | CO     | WS             | TC           | 3  | F  |
| CA-LAN-1283   | 630-144   | Flake    | Surface      | 7.4            | 3,285           | 7.8                 | 3,679                | PTO            | CO     | WS             | TC           | 3  | F  |
| CA-LAN-1283   | 630-146   | Flake    | Surface      | 5.9            | 1,942           | 6.2                 | 2,175                | GYP            | CO     | WS             | TC           | 3  | F  |
| CA-LAN-1283   | 630-154   | Dart     | Surface      | 6.1            | 2,099           | 6.4                 | 2,350                | GYP            | CO     | WS             | TC           | 3  | F  |
| CA-LAN-1283   | 630-160   | Arrow    | Surface      | 6.0            | 2,020           | 6.3                 | 2,262                | GYP            | CO     | JR             | TC           | 3  | F  |
| CA-LAN-1283   | 630-164   | Flake    | Surface      | 5.8            | 1,867           | 6.1                 | 2,091                | GYP            | CO     | WS             | TC           | 3  | F  |
| CA-LAN-1283   | 630-171   | Flake    | 21 (0-10)    | 6.9            | 2,793           | 7.2                 | 3,128                | PTO            | CO     | WS             | TC           | 3  | F  |
| CA-LAN-1283   | 630-175   | Flake    | 20 (S)       | 5.8            | 1,867           | 6.1                 | 2,091                | GYP            | CO     | WS             | TC           | 3  | F  |
| CA-LAN-1283   | 630-177   | Flake    | 20 (S)       | 6.6            | 2,519           | 6.9                 | 2,821                | GYP            | CO     | WS             | TC           | 3  | F  |
| CA-LAN-1283   | 630-180   | Flake    | 20 (S)       | 7.5            | 3,389           | 7.9                 | 3,795                | PTO            | CO     | WS             | TC           | 3  | F  |
| CA-LAN-1283   | 1819      | Flake    | Surface      | 6.1            | 2,099           | 6.4                 | 2,350                | GYP            | CO     | WS             | TC           | 3  | F  |
| CA-LAN-1286/H | 1         | Flake    | Surface      | 9.3            | 5,583           | 9.8                 | 6,252                | PTO            | CD     | SR             | TC           | 3  | G  |
| CA-LAN-1286/H | 2         | BFF      | Surface      | 5.1            | 1,385           | 5.4                 | 1,551                | GYP            | CO     | SL             | TC           | 3  | G  |
| CA-LAN-1286/H | 3         | Flake    | Surface      | 5.3            | 1,515           | 5.6                 | 1,696                | GYP            | CO     | CO             | TC           | 3  | G  |
| CA-LAN-1289/H | 4738      | ESN      | Surface      | 8.2            | 4,169           | 8.6                 | 4,668                | PTO            | CO     | WS             | TC           | 2  | D  |
| CA-LAN-1289/H | 4738      | ESN      | Surface      | 4.7            | 1,146           | 4.9                 | 1,283                | GYP            | CO     | WS             | TC           | 2  | D  |
| CA-LAN-1289/H | 2956-1-7  | Flake    | Surface      | 5.6            | 1,721           | 5.9                 | 1,927                | GYP            | CO     | CO             | TC           | 2  | D  |
| CA-LAN-1289/H | 2956-1-9  | Flake    | Surface      | 5.8            | 1,867           | 6.1                 | 2,091                | GYP            | CO     | CO             | TC           | 2  | D  |
| CA-LAN-1289/H | 2956-1-9  | Flake    | Surface      | 4.1            | 835             | 4.3                 | 935                  | SSP            | CO     | CO             | TC           | 2  | D  |
| CA-LAN-1289/H | 2956-1-35 | Flake    | Surface      | 8.4            | 4,408           | 8.8                 | 4,937                | PTO            | CO     | WS             | TC           | 2  | D  |
| CA-LAN-1289/H | 2956-1-46 | Flake    | Surface      | 9.9            | 6,454           | 10.4                | 7,228                | PTO            | CO     | CO             | TC           | 2  | D  |

| Trinomial     | Cat No.     | Artifact | Unit (Depth)        | Raw Microns | Raw Years BP | Adjusted Microns | Adjusted Years BP | Time Period | Source | Sub-source | Site Type | MR | MA |
|---------------|-------------|----------|---------------------|-------------|--------------|------------------|-------------------|-------------|--------|------------|-----------|----|----|
| CA-LAN-1289/H | 2956-1-65   | Flake    | S153/E25 Cell F (S) | 0.0         | 0            | 0.0              | 0                 | --          | CO     | WS         | TC        | 2  | D  |
| CA-LAN-1289/H | 2956-1-113  | Flake    | S55/W23 Cell E (S)  | 8.0         | 3,937        | 8.4              | 4,408             | PTO         | CO     | CO         | TC        | 2  | D  |
| CA-LAN-1289/H | 2956-1-121  | Flake    | S55/W23 Cell G (S)  | 8.4         | 4,408        | 8.8              | 4,937             | PTO         | CO     | CO         | TC        | 2  | D  |
| CA-LAN-1289/H | 2956-1-201  | Flake    | S21/E44 Cell A (S)  | 5.8         | 1,867        | 6.1              | 2,091             | GYP         | CO     | CO         | TC        | 2  | D  |
| CA-LAN-1289/H | 2956-1-209  | Flake    | S21/E44 Cell B (S)  | 6.3         | 2,262        | 6.6              | 2,533             | GYP         | CO     | WS         | TC        | 2  | D  |
| CA-LAN-1289/H | 2956-10-232 | Flake    | S2/E47 STU (0-10)   | 5.2         | 1,449        | 5.5              | 1,623             | GYP         | CO     | CO         | TC        | 2  | D  |
| CA-LAN-1289/H | 2956-10-252 | Flake    | S2/E47 STU (90-100) | 4.3         | 932          | 4.5              | 1,044             | SSP         | CO     | CO         | TC        | 2  | D  |
| CA-LAN-1295   | 472         | Flake    | U1 (10-20)          | 8.9         | 5,041        | 9.3              | 5,646             | PTO         | CO     | CO         | TC        | 3  | G  |
| CA-LAN-1296/H | 2149        | CWT      | Surface             | 9.8         | 6,304        | 10.3             | 7,059             | PTO         | CO     | WS         | BC        | 3  | F  |
| CA-LAN-1296/H | 2149        | CWT      | Surface             | 3.3         | 505          | 3.5              | 565               | SHO         | CO     | WS         | BC        | 3  | F  |
| CA-LAN-1296/H | 2205        | BFF      | Surface             | 0.0         | 0            | 0.0              | 0                 | --          | CO     | WS         | BC        | 3  | F  |
| CA-LAN-1296/H | 037b        | Flake    | U4 (0-10)           | 3.9         | 743          | 4.1              | 833               | SSP         | CO     | CO         | BC        | 3  | F  |
| CA-LAN-1296/H | 430         | UNK      | Surface             | 7.6         | 3,495        | 8.0              | 3,914             | PTO         | CO     | CO         | BC        | 3  | F  |
| CA-LAN-1296/H | 261         | Shatter  | U29 (0-10)          | 5.2         | 1,449        | 5.5              | 1,623             | GYP         | CO     | CO         | BC        | 3  | F  |
| CA-LAN-1296/H | 050b        | Flake    | U7 (0-10)           | 2.6         | 290          | 2.7              | 325               | SHO         | CO     | CO         | BC        | 3  | F  |
| CA-LAN-1296/H | 050a        | BTF      | U7 (S)              | 3.2         | 470          | 3.4              | 526               | SHO         | CO     | CO         | BC        | 3  | F  |
| CA-LAN-1296/H | 076         | Shatter  | U8 (S)              | 5.9         | 1,942        | 6.2              | 2,175             | GYP         | CO     | CO         | BC        | 3  | F  |
| CA-LAN-1296/H | 606         | Shatter  | U8 (S)              | 10.5        | 7,398        | 11.0             | 8,285             | LMO         | CO     | CO         | BC        | 3  | F  |
| CA-LAN-1296/H | 510         | Flake    | U9 (0-10)           | 3.4         | 541          | 3.6              | 606               | SSP         | CO     | CO         | BC        | 3  | F  |
| CA-LAN-1296/H | 537c        | Flake    | U10 (10-20)         | 2.8         | 345          | 2.9              | 386               | SHO         | CO     | CO         | BC        | 3  | F  |
| CA-LAN-1296/H | 537a        | Flake    | U10 (10-20)         | 3.0         | 404          | 3.2              | 453               | SHO         | CO     | CO         | BC        | 3  | F  |
| CA-LAN-1296/H | 537b        | Flake    | U10 (10-20)         | 3.4         | 541          | 3.6              | 606               | SSP         | CO     | CO         | BC        | 3  | F  |
| CA-LAN-1296/H | 612         | BFF      | U10 (S)             | 1.9         | 140          | 2.0              | 157               | SHO         | CO     | CO         | BC        | 3  | F  |
| CA-LAN-1296/H | 615         | Flake    | U10 (S)             | 4.8         | 1,203        | 5.0              | 1,348             | GYP         | CO     | CO         | BC        | 3  | F  |
| CA-LAN-1296/H | 611         | BFF      | U10 (S)             | 5.2         | 1,449        | 5.5              | 1,623             | GYP         | CO     | CO         | BC        | 3  | F  |
| CA-LAN-1296/H | 608         | BFF      | U10 (S)             | 5.6         | 1,721        | 5.9              | 1,927             | GYP         | CO     | CO         | BC        | 3  | F  |
| CA-LAN-1296/H | 616         | BFF      | U10 (S)             | 5.6         | 1,721        | 5.9              | 1,927             | GYP         | CO     | CO         | BC        | 3  | F  |
| CA-LAN-1296/H | 618         | BFF      | U10 (S)             | 7.3         | 3,183        | 7.7              | 3,565             | PTO         | CD     | CD         | BC        | 3  | F  |
| CA-LAN-1296/H | 619         | Biface   | U11 (S)             | 2.5         | 265          | 2.6              | 297               | SHO         | CO     | CO         | BC        | 3  | F  |
| CA-LAN-1296/H | 082         | Shatter  | U11 (S)             | 3.5         | 578          | 3.7              | 648               | SSP         | CO     | CO         | BC        | 3  | F  |
| CA-LAN-1296/H | 080         | BFF      | U11 (S)             | 5.0         | 1,323        | 5.3              | 1,482             | GYP         | CO     | CO         | BC        | 3  | F  |
| CA-LAN-1296/H | 117         | Flake    | U12 (S)             | 4.7         | 1,146        | 4.9              | 1,283             | GYP         | CO     | CO         | BC        | 3  | F  |
| CA-LAN-1296/H | 158         | FT       | U13 (S)             | 3.6         | 617          | 3.8              | 691               | SSP         | CO     | CO         | BC        | 3  | F  |
| CA-LAN-1296/H | 172         | Shatter  | U14 (0-10)          | 5.2         | 1,449        | 5.5              | 1,623             | GYP         | CO     | CO         | BC        | 3  | F  |

| Trinomial     | Cat No.      | Artifact | Unit (Depth)   | Raw Microns | Raw Years BP | Adjusted Microns | Adjusted Years BP | Time Period | Source | Sub-source | Site Type | MR | MA |
|---------------|--------------|----------|----------------|-------------|--------------|------------------|-------------------|-------------|--------|------------|-----------|----|----|
| CA-LAN-1296/H | 170b         | Flake    | U14 (S)        | 3.5         | 578          | 3.7              | 648               | SSP         | CO     | CO         | BC        | 3  | F  |
| CA-LAN-1296/H | 170a         | Flake    | U14 (S)        | 5.4         | 1,582        | 5.7              | 1,771             | GYP         | CO     | CO         | BC        | 3  | F  |
| CA-LAN-1296/H | 182          | Flake    | U15 (S)        | 2.4         | 241          | 2.5              | 270               | SHO         | CO     | CO         | BC        | 3  | F  |
| CA-LAN-1296/H | 202          | Shatter  | U18 (0-10)     | 5.1         | 1,385        | 5.4              | 1,551             | GYP         | CO     | CO         | BC        | 3  | F  |
| CA-LAN-1296/H | 198a         | BTF      | U18 (S)        | 2.8         | 345          | 2.9              | 386               | SHO         | CO     | CO         | BC        | 3  | F  |
| CA-LAN-1296/H | 198b         | Flake    | U18 (S)        | 3.7         | 658          | 3.9              | 737               | SSP         | CO     | CO         | BC        | 3  | F  |
| CA-LAN-1296/H | 623          | BFF      | U18 (S)        | 3.7         | 658          | 3.9              | 737               | SSP         | QU     | QU         | BC        | 3  | F  |
| CA-LAN-1296/H | 624          | Shatter  | U18 (S)        | 4.5         | 1,036        | 4.7              | 1,160             | SSP         | CO     | CO         | BC        | 3  | F  |
| CA-LAN-1296/H | 598          | BFF      | U34 (S)        | 3.0         | 404          | 3.2              | 453               | SHO         | CO     | CO         | BC        | 3  | F  |
| CA-LAN-1296/H | 309          | BFF      | U34 (S)        | 4.8         | 1,203        | 5.0              | 1,348             | GYP         | CO     | CO         | BC        | 3  | F  |
| CA-LAN-1296/H | 627          | UNK      | U45 (S)        | 5.9         | 1,942        | 6.2              | 2,175             | GYP         | CO     | CO         | BC        | 3  | F  |
| CA-LAN-1296/H | 431          | PF       | Surface        | 4.5         | 1,036        | 4.7              | 1,160             | SSP         | CO     | CO         | BC        | 3  | F  |
| CA-LAN-1296/H | 604          | BTF      | U69 (S)        | 6.9         | 2,793        | 7.2              | 3,128             | PTO         | CO     | CO         | BC        | 3  | F  |
| CA-LAN-1307   | 616-1        | RSP      | Surface        | 3.6         | 617          | 3.8              | 691               | SSP         | CO     | WS         | TC        | 3  | G  |
| CA-LAN-1310/H | 744-150      | Flake    | 11 (0-10)      | 4.8         | 1,203        | 5.0              | 1,348             | GYP         | CO     | WS         | TC        | 3  | F  |
| CA-LAN-1310/H | 744-197      | BFF      | Surface        | 6.7         | 2,609        | 7.0              | 2,922             | GYP         | CO     | WS         | TC        | 3  | F  |
| CA-LAN-1310/H | 744-220      | CWT      | Surface        | 3.8         | 700          | 4.0              | 784               | SSP         | CO     | WS         | TC        | 3  | F  |
| CA-LAN-1310/H | 744-295      | Flake    | 14 (40-50)     | 6.7         | 2,609        | 7.0              | 2,922             | GYP         | CO     | WS         | TC        | 3  | F  |
| CA-LAN-1316   | 1316-195-147 | Point    | Surface        | 0.0         | 0            | 0.0              | 0                 | --          | CO     | WCP        | TC        | 2  | C  |
| CA-LAN-1316   | 195-7        | BTF      | Surface        | 13.2        | 12,580       | 13.9             | 14,088            | LPL         | CO     | SL         | TC        | 2  | C  |
| CA-LAN-1316   | 195-42L      | Flake    | Surface        | 8.8         | 4,911        | 9.2              | 5,499             | PTO         | CO     | CO         | TC        | 2  | C  |
| CA-LAN-1316   | 195-80L      | Flake    | Surface        | 14.2        | 14,903       | 14.9             | 16,689            | LPL         | CO     | SL         | TC        | 2  | C  |
| CA-LAN-1316   | 195-111      | BTF      | Surface        | 9.2         | 5,444        | 9.7              | 6,097             | PTO         | CO     | SL         | TC        | 2  | C  |
| CA-LAN-1317   | 6            | Flake    | Surface        | 6.8         | 2,700        | 7.1              | 3,024             | PTO         | CO     | WS         | TC        | 2  | D  |
| CA-LAN-1317   | 7            | Biface   | Surface        | 8.6         | 4,656        | 9.0              | 5,214             | PTO         | UNK    | UNK        | TC        | 2  | D  |
| CA-LAN-1317   | 8            | Flake    | STU 19 (20-40) | 7.8         | 3,712        | 8.2              | 4,157             | PTO         | CO     | CO         | TC        | 2  | D  |
| CA-LAN-1317   | 9            | Flake    | STU 28 (0-20)  | 11.1        | 8,416        | 11.7             | 9,425             | LPL         | CO     | CO         | TC        | 2  | D  |
| CA-LAN-1317/H | 860-1-57     | Flake    | Surface        | 12.1        | 10,281       | 12.7             | 11,513            | LPL         | CO     | CO         | TC        | 2  | D  |
| CA-LAN-1317/H | 860-1-58     | Flake    | Surface        | 12.5        | 11,086       | 13.1             | 12,415            | LPL         | CO     | CO         | TC        | 2  | D  |
| CA-LAN-1317/H | 860-1-58     | Flake    | Surface        | 10.2        | 6,917        | 10.7             | 7,746             | LMO         | CO     | CO         | TC        | 2  | D  |
| CA-LAN-1317/H | 860-1-77     | Flake    | Surface        | 9.5         | 5,865        | 10.0             | 6,568             | PTO         | CO     | CO         | TC        | 2  | D  |
| CA-LAN-1317/H | 860-1-82     | Flake    | Surface        | 12.0        | 10,085       | 12.6             | 11,293            | LPL         | CO     | CO         | TC        | 2  | D  |
| CA-LAN-1317/H | 860-1-83     | Flake    | Surface        | 10.5        | 7,398        | 11.0             | 8,285             | LMO         | CO     | CO         | TC        | 2  | D  |
| CA-LAN-1317/H | 860-1-84     | Flake    | Surface        | 11.5        | 9,137        | 12.1             | 10,232            | LPL         | CO     | CO         | TC        | 2  | D  |



| Trinomial     | Cat No.   | Artifact | Unit (Depth)             | Raw<br>Microns | Raw<br>Years BP | Adjusted<br>Microns | Adjusted<br>Years BP | Time<br>period | Source | Sub-<br>source | Site<br>Type | MR | MA |
|---------------|-----------|----------|--------------------------|----------------|-----------------|---------------------|----------------------|----------------|--------|----------------|--------------|----|----|
| CA-LAN-1317/H | 860-1-85  | Flake    | Surface                  | 14.0           | 14,420          | 14.7                | 16,149               | LPL            | CO     | CO             | TC           | 2  | D  |
| CA-LAN-1317/H | 860-1-85  | Flake    | Surface                  | 12.5           | 11,086          | 13.1                | 12,415               | LPL            | CO     | CO             | TC           | 2  | D  |
| CA-LAN-1317/H | 860-1-86  | Flake    | Surface                  | 22.1           | 41,586          | 23.2                | 46,571               | LPL            | CO     | CO             | TC           | 2  | D  |
| CA-LAN-1317/H | 860-1-86  | Flake    | Surface                  | 19.3           | 30,371          | 20.3                | 34,011               | LPL            | CO     | CO             | TC           | 2  | D  |
| CA-LAN-1317/H | 860-1-88  | Flake    | Surface                  | 11.0           | 8,241           | 11.6                | 9,229                | LPL            | CO     | CO             | TC           | 2  | D  |
| CA-LAN-1317/H | 860-1-90  | Flake    | Surface                  | 12.5           | 11,086          | 13.1                | 12,415               | LPL            | CO     | CO             | TC           | 2  | D  |
| CA-LAN-1317/H | 860-1-90  | Flake    | Surface                  | 7.7            | 3,603           | 8.1                 | 4,034                | PTO            | CO     | CO             | TC           | 2  | D  |
| CA-LAN-1317/H | 860-1-91  | Flake    | Surface                  | 13.1           | 12,360          | 13.8                | 13,842               | LPL            | CO     | CO             | TC           | 2  | D  |
| CA-LAN-1317/H | 860-1-91  | Flake    | Surface                  | 7.0            | 2,888           | 7.4                 | 3,234                | PTO            | CO     | CO             | TC           | 2  | D  |
| CA-LAN-1317/H | 860-1-131 | Flake    | S197.5/E242.5 Cell A (S) | 13.9           | 14,183          | 14.6                | 15,882               | LPL            | CO     | WS             | TC           | 2  | D  |
| CA-LAN-1317/H | 860-1-146 | Flake    | S292/E206 Cell D (S)     | 11.6           | 9,322           | 12.2                | 10,439               | LPL            | CO     | CO             | TC           | 2  | D  |
| CA-LAN-1317/H | 1085      | Flake    | Surface                  | 0.0            | 0               | 0.0                 | 0                    | --             | CO     | CO             | TC           | 2  | D  |
| CA-LAN-1318/H | 7542      | RSP      | Surface                  | 12.8           | 11,714          | 13.4                | 13,117               | LPL            | CO     | SL             | TC           | 2  | D  |
| CA-LAN-1318/H | 7542      | RSP      | Surface                  | 9.9            | 6,454           | 10.4                | 7,228                | PTO            | CO     | SL             | TC           | 2  | D  |
| CA-LAN-1318/H | 4         | Flake    | Surface                  | 11.0           | 8,241           | 11.6                | 9,229                | LPL            | CO     | WS             | TC           | 2  | D  |
| CA-LAN-1318/H | 5         | Flake    | Surface                  | 6.7            | 2,609           | 7.0                 | 2,922                | GYP            | CD     | SR             | TC           | 2  | D  |
| CA-LAN-1318/H | 5         | Flake    | Surface                  | 4.4            | 983             | 4.6                 | 1,101                | SSP            | CD     | SR             | TC           | 2  | D  |
| CA-LAN-1318/H | 1414      | Flake    | Surface                  | 10.8           | 7,898           | 11.3                | 8,844                | LMO            | CO     | CO             | TC           | 2  | D  |
| CA-LAN-1329   | 870-1912  | Elko     | Surface                  | 6.1            | 2,099           | 6.4                 | 2,350                | GYP            | CO     | WS             | TC           | 3  | G  |
| CA-LAN-1329   | 43-28-2   | RSP      | UNK                      | 5.3            | 1,515           | 5.6                 | 1,696                | GYP            | CO     | WS             | TC           | 3  | G  |
| CA-LAN-1329   | 75-25-3a  | Flake    | UNK                      | 0.0            | 0               | 0.0                 | 0                    | --             | CO     | WS             | TC           | 3  | G  |
| CA-LAN-1329   | 75-25-3b  | Flake    | UNK                      | 0.0            | 0               | 0.0                 | 0                    | --             | CO     | WS             | TC           | 3  | G  |
| CA-LAN-1329   | 7-7-1     | Flake    | UNK                      | 0.0            | 0               | 0.0                 | 0                    | --             | CO     | WS             | TC           | 3  | G  |
| CA-LAN-1409   | 888-1-5   | BFF      | Surface                  | 7.0            | 2,888           | 7.4                 | 3,234                | PTO            | CO     | WS             | TC           | 2  | D  |
| CA-LAN-1409   | 888-1-46  | Flake    | Surface                  | 5.8            | 1,867           | 6.1                 | 2,091                | GYP            | CO     | WS             | TC           | 2  | D  |
| CA-LAN-1409   | 888-1-61  | Flake    | Surface                  | 0.0            | 0               | 0.0                 | 0                    | --             | CO     | CO             | TC           | 2  | D  |
| CA-LAN-1465/H | 4024      | Flake    | Surface                  | 9.6            | 6,009           | 10.1                | 6,730                | PTO            | CO     | WS             | ISO          | 2  | C  |
| CA-LAN-1585   | 1040-12   | Flake    | OBS 1 (S)                | 9.3            | 5,583           | 9.8                 | 6,252                | PTO            | CO     | WCP            | TC           | 3  | G  |
| CA-LAN-1585   | 1040-13   | Flake    | OBS 1 (S)                | 9.5            | 5,865           | 10.0                | 6,568                | PTO            | CO     | WCP            | TC           | 3  | G  |
| CA-LAN-1585   | 1040-13   | Flake    | OBS 1 (S)                | 3.4            | 541             | 3.6                 | 606                  | SSP            | CO     | WCP            | TC           | 3  | G  |
| CA-LAN-1585   | 1040-14   | Flake    | OBS 3 (S)                | 8.1            | 4,052           | 8.5                 | 4,537                | PTO            | CO     | WCP            | TC           | 3  | G  |
| CA-LAN-1585   | 1040-15   | Scraper  | Uniface 1 (S)            | 5.8            | 1,867           | 6.1                 | 2,091                | GYP            | CO     | WCP            | TC           | 3  | G  |
| CA-LAN-1585   | 1040-15   | Scraper  | Uniface 1 (S)            | 3.7            | 658             | 3.9                 | 737                  | SSP            | CO     | WCP            | TC           | 3  | G  |
| CA-LAN-1585   | 1040-51   | BFF      | Biface 7 (S)             | 7.5            | 3,389           | 7.9                 | 3,795                | PTO            | CO     | WS             | TC           | 3  | G  |

| Trinomial     | Cat No.      | Artifact | Unit (Depth)        | Raw Microns | Raw Years BP | Adjusted Microns | Adjusted Years BP | Time Period | Source | Sub-source | Site Type | MR | MA |
|---------------|--------------|----------|---------------------|-------------|--------------|------------------|-------------------|-------------|--------|------------|-----------|----|----|
| CA-LAN-1705/H | 99           | Flake    | Surface             | 7.9         | 3,823        | 8.3              | 4,282             | PTO         | CO     | WS         | LD        | 2  | C  |
| CA-LAN-1798   | 5892         | CWT      | Surface             | 3.7         | 658          | 3.9              | 737               | SSP         | CO     | WS         | TC        | 5  | D  |
| CA-LAN-1805   | 1047-1       | Flake    | OBS 1 (S)           | 7.8         | 3,712        | 8.2              | 4,157             | PTO         | CO     | WCP        | TC        | 3  | G  |
| CA-LAN-1805   | 1147-2       | Flake    | OBS 2 (S)           | 9.1         | 5,308        | 9.6              | 5,944             | PTO         | CO     | WCP        | TC        | 3  | G  |
| CA-LAN-1805   | 1147-4       | Flake    | OBS 4 (S)           | 6.5         | 2,432        | 6.8              | 2,723             | GYP         | CO     | WCP        | TC        | 3  | G  |
| CA-LAN-1805   | 1147-28      | Flake    | SU 2 (S)            | 3.3         | 505          | 3.5              | 565               | SHO         | BM     | BM         | TC        | 3  | G  |
| CA-LAN-1805   | 1147-51      | Flake    | STP 1 (0-10)        | 6.9         | 2,793        | 7.2              | 3,128             | PTO         | CO     | WCP        | TC        | 3  | G  |
| CA-LAN-2254   | 220-3        | Flake    | Surface             | 4.0         | 788          | 4.2              | 883               | SSP         | CO     | WS         | TC        | 3  | G  |
| CA-LAN-2271   | 1694-1-2     | Flake    | Surface             | 5.7         | 1,793        | 6.0              | 2,008             | GYP         | CO     | WS         | TC        | 2  | C  |
| CA-LAN-2271   | 1694-1-3     | Flake    | Surface             | 11.4        | 8,953        | 12.0             | 10,026            | LPL         | CO     | WS         | TC        | 2  | C  |
| CA-LAN-2271   | 1694-1-3     | Flake    | Surface             | 11.1        | 8,416        | 11.7             | 9,425             | LPL         | CO     | WS         | TC        | 2  | C  |
| CA-LAN-2271   | 1694-1-4     | Flake    | Surface             | 13.0        | 12,143       | 13.7             | 13,598            | LPL         | CO     | CO         | TC        | 2  | C  |
| CA-LAN-2271   | 1694-1-5     | Flake    | Surface             | 0.0         | 0            | 0.0              | 0                 | --          | CO     | WS         | TC        | 2  | C  |
| CA-LAN-2286   | 1710-1-1     | Flake    | Surface             | 0.0         | 0            | 0.0              | 0                 | --          | CO     | CO         | LD        | 2  | C  |
| CA-LAN-2286   | 1710-1-2     | Flake    | Surface             | 11.2        | 8,593        | 11.8             | 9,623             | LPL         | CO     | CO         | LD        | 2  | C  |
| CA-LAN-2286   | 1710-1-2     | Flake    | Surface             | 4.9         | 1,262        | 5.1              | 1,414             | GYP         | CO     | CO         | LD        | 2  | C  |
| CA-LAN-2286   | 1710-1-3     | Flake    | Surface             | 4.8         | 1,203        | 5.0              | 1,348             | GYP         | CO     | CO         | LD        | 2  | C  |
| CA-LAN-2286   | 1710-1-4     | Flake    | Surface             | 0.0         | 0            | 0.0              | 0                 | --          | CO     | CO         | LD        | 2  | C  |
| CA-LAN-2286   | 1710-10-18   | Flake    | N48.5/E6 STU (0-10) | 0.0         | 0            | 0.0              | 0                 | --          | CO     | CO         | LD        | 2  | C  |
| CA-LAN-2302   | 10           | Flake    | Surface             | 2.3         | 218          | 2.4              | 245               | SHO         | CO     | CO         | TC        | 2  | C  |
| CA-LAN-2303   | 1721-1-3     | Flake    | Surface             | 0.0         | 0            | 0.0              | 0                 | --          | CO     | CO         | TC        | 2  | C  |
| CA-LAN-2303   | 1721-10-74   | Flake    | N2/W5 STU (40-50)   | 14.0        | 14,420       | 14.7             | 16,149            | LPL         | CO     | CO         | TC        | 2  | C  |
| CA-LAN-2303   | 1721-10-105  | Flake    | N2/W4.5 TU (40-50)  | 5.4         | 1,582        | 5.7              | 1,771             | GYP         | CO     | CO         | TC        | 2  | C  |
| CA-LAN-2303   | 1721-10-115  | Flake    | N2/W4.5 TU (50-60)  | 10.5        | 7,398        | 11.0             | 8,285             | LMO         | CO     | CO         | TC        | 2  | C  |
| CA-LAN-2303   | 1721-10-127A | Flake    | N2/W4.5 TU (70-80)  | 10.6        | 7,563        | 11.1             | 8,469             | LMO         | CO     | CO         | TC        | 2  | C  |
| CA-LAN-2303   | 1721-10-127A | Flake    | N2/W4.5 TU (70-80)  | 9.6         | 6,009        | 10.1             | 6,730             | PTO         | CO     | CO         | TC        | 2  | C  |
| CA-LAN-2303   | 1721-10-127B | Flake    | N2/W4.5 TU (70-80)  | 9.6         | 6,009        | 10.1             | 6,730             | PTO         | CO     | CO         | TC        | 2  | C  |
| CA-LAN-2303   | 1721-10-127C | Flake    | N2/W4.5 TU (70-80)  | 9.9         | 6,454        | 10.4             | 7,228             | PTO         | CO     | CO         | TC        | 2  | C  |
| CA-LAN-2303   | 1721-10-127C | Flake    | N2/W4.5 TU (70-80)  | 8.3         | 4,288        | 8.7              | 4,802             | PTO         | CO     | CO         | TC        | 2  | C  |
| CA-LAN-2397   | 2021-27b     | Flake    | ST 2 (S)            | 4.6         | 1,090        | 4.8              | 1,221             | SSP         | CO     | WS         | TC        | 3  | G  |
| CA-LAN-2397   | 2021-2       | Flake    | Surface             | 7.5         | 3,389        | 7.9              | 3,795             | PTO         | CO     | WS         | TC        | 3  | G  |
| CA-LAN-2397   | 2021-13      | Flake    | Surface             | 9.2         | 5,444        | 9.7              | 6,097             | PTO         | CO     | WS         | TC        | 3  | G  |
| CA-LAN-2397   | 2021-22      | Flake    | Surface             | 9.6         | 6,009        | 10.1             | 6,730             | PTO         | CO     | WS         | TC        | 3  | G  |
| CA-LAN-2397   | 2021-27a     | Flake    | ST 2 (S)            | 9.8         | 6,304        | 10.3             | 7,059             | PTO         | CO     | WS         | TC        | 3  | G  |

| Trinomial   | Cat No.      | Artifact | Unit (Depth)          | Raw<br>Microns | Raw<br>Years BP | Adjusted<br>Microns | Adjusted<br>Years BP | Time<br>Period | Source | Sub-<br>source | Site<br>Type | MR | MA |
|-------------|--------------|----------|-----------------------|----------------|-----------------|---------------------|----------------------|----------------|--------|----------------|--------------|----|----|
| CA-LAN-2399 | 8045         | AB       | Surface               | 9.8            | 6,304           | 10.3                | 7,059                | PTO            | CO     | WS             | TC           | 3  | G  |
| CA-LAN-2399 | 8045         | AB       | Surface               | 7.5            | 3,389           | 7.9                 | 3,795                | PTO            | CO     | WS             | TC           | 3  | G  |
| CA-LAN-2421 | 2131-1-21    | Flake    | S8/E15 Cell A (S)     | 0.0            | 0               | 0.0                 | 0                    | --             | CO     | CO             | LD           | 2  | C  |
| CA-LAN-2422 | 2132-1-6     | Flake    | Surface               | 0.0            | 0               | 0.0                 | 0                    | --             | CO     | CO             | TC           | 2  | C  |
| CA-LAN-2422 | 2132-1-7     | Flake    | Surface               | 0.0            | 0               | 0.0                 | 0                    | --             | CO     | CO             | TC           | 2  | C  |
| CA-LAN-2422 | 2132-1-8     | Flake    | NO/E0 (S)             | 0.0            | 0               | 0.0                 | 0                    | --             | CO     | CO             | TC           | 2  | C  |
| CA-LAN-2422 | 2132-1-91    | Flake    | NO/E10 (S)            | 0.0            | 0               | 0.0                 | 0                    | --             | CO     | CO             | TC           | 2  | C  |
| CA-LAN-2423 | 2133-1-1     | Flake    | NO/E0 Cell A (S)      | 0.0            | 0               | 0.0                 | 0                    | --             | CO     | CO             | LD           | 2  | C  |
| CA-LAN-2423 | 2133-1-2     | Flake    | NO/E0 Cell A (S)      | 0.0            | 0               | 0.0                 | 0                    | --             | CO     | CO             | LD           | 2  | C  |
| CA-LAN-2423 | 2133-1-4     | Flake    | NO/E0 Cell B (S)      | 2.2            | 197             | 2.3                 | 221                  | SHO            | CO     | CO             | LD           | 2  | C  |
| CA-LAN-2423 | 2133-1-7     | Flake    | NO/E0 Cell B (S)      | 0.0            | 0               | 0.0                 | 0                    | --             | CO     | CO             | LD           | 2  | C  |
| CA-LAN-2423 | 2133-1-12A   | Flake    | NO/E0 Cell E (S)      | 0.0            | 0               | 0.0                 | 0                    | --             | CO     | CO             | LD           | 2  | C  |
| CA-LAN-2432 | 2145-10-55   | Flake    | N18/E10 TU (40-50)    | 9.7            | 6,156           | 10.2                | 6,893                | PTO            | CO     | CO             | LD           | 2  | C  |
| CA-LAN-2440 | 7498         | Pinto    | Surface               | 8.0            | 3,937           | 8.4                 | 4,408                | PTO            | UNK    | UNK            | TC           | 2  | C  |
| CA-LAN-2493 | 7543         | Arrow    | Surface               | 8.2            | 4,169           | 8.6                 | 4,668                | PTO            | CO     | WS             | LD           | 2  | D  |
| CA-LAN-2503 | 2171-1-3     | Flake    | Surface               | 8.4            | 4,408           | 8.8                 | 4,937                | PTO            | CO     | CO             | TC           | 2  | D  |
| CA-LAN-2503 | 2171-1-4     | Flake    | Surface               | 7.2            | 3,083           | 7.6                 | 3,452                | PTO            | CO     | CO             | TC           | 2  | D  |
| CA-LAN-2503 | 2171-1-21    | Flake    | Surface               | 9.0            | 5,174           | 9.5                 | 5,794                | PTO            | CO     | CO             | TC           | 2  | D  |
| CA-LAN-2503 | 2171-10-70   | Flake    | S7/E14.5 STU (10-20)  | 8.0            | 3,937           | 8.4                 | 4,408                | PTO            | CO     | CO             | TC           | 2  | D  |
| CA-LAN-2503 | 2171-10-72A  | Flake    | S7/E14.5 STU (20-30)  | 7.4            | 3,285           | 7.8                 | 3,679                | PTO            | CO     | CO             | TC           | 2  | D  |
| CA-LAN-2503 | 2171-10-72B  | Flake    | S7/E14.5 STU (20-30)  | 7.4            | 3,285           | 7.8                 | 3,679                | PTO            | CO     | CO             | TC           | 2  | D  |
| CA-LAN-2503 | 2171-10-99   | Flake    | N5.5/E186 STU (10-20) | 0.0            | 0               | 0.0                 | 0                    | --             | CO     | CO             | TC           | 2  | D  |
| CA-LAN-2511 | 2267-10-112B | Flake    | NO/W24 TU (30-40)     | 10.0           | 6,606           | 10.5                | 7,398                | LMO            | CO     | CO             | TC           | 2  | D  |
| CA-LAN-2511 | 2267-10-112C | Flake    | NO/W24 TU (30-40)     | 10.3           | 7,075           | 10.8                | 7,923                | LMO            | CO     | WS             | TC           | 2  | D  |
| CA-LAN-2511 | 2267-10-116  | Flake    | NO/W24 TU (50-60)     | 9.9            | 6,454           | 10.4                | 7,228                | PTO            | CO     | CO             | TC           | 2  | D  |
| CA-LAN-2511 | 2267-10-123  | Flake    | NO/W24 TU (70-80)     | 11.0           | 8,241           | 11.6                | 9,229                | LPL            | CO     | WS             | TC           | 2  | D  |
| CA-LAN-2511 | 2267-10-135  | Flake    | S2/W21.5 TU (20-30)   | 11.0           | 8,241           | 11.6                | 9,229                | LPL            | CO     | CO             | TC           | 2  | D  |
| CA-LAN-2511 | 2267-10-138A | Flake    | S2/W21.5 TU (30-40)   | 12.3           | 10,679          | 12.9                | 11,959               | LPL            | CO     | CO             | TC           | 2  | D  |
| CA-LAN-2511 | 2267-10-138A | Flake    | S2/W21.5 TU (30-40)   | 11.1           | 8,416           | 11.7                | 9,425                | LPL            | CO     | CO             | TC           | 2  | D  |
| CA-LAN-2511 | 2267-10-138B | Flake    | S2/W21.5 TU (30-40)   | 11.4           | 8,953           | 12.0                | 10,026               | LPL            | CO     | CO             | TC           | 2  | D  |
| CA-LAN-2511 | 2267-10-138B | Flake    | S2/W21.5 TU (30-40)   | 8.8            | 4,911           | 9.2                 | 5,499                | PTO            | CO     | CO             | TC           | 2  | D  |
| CA-LAN-2511 | 2267-10-140A | Flake    | S2/W21.5 TU (40-50)   | 11.1           | 8,416           | 11.7                | 9,425                | LPL            | CO     | CO             | TC           | 2  | D  |
| CA-LAN-2511 | 2267-10-140B | Flake    | S2/W21.5 TU (40-50)   | 12.0           | 10,085          | 12.6                | 11,293               | LPL            | CO     | CO             | TC           | 2  | D  |
| CA-LAN-2511 | 2267-10-140C | Flake    | S2/W21.5 TU (40-50)   | 10.0           | 6,606           | 10.5                | 7,398                | LMO            | CO     | CO             | TC           | 2  | D  |

| Trinomial   | Cat No.      | Artifact | Unit (Depth)        | Raw<br>Microns | Raw<br>Years BP | Adjusted<br>Microns | Adjusted<br>Years BP | Time<br>Period | Source | Sub-<br>source | Site<br>Type | MR | MA |
|-------------|--------------|----------|---------------------|----------------|-----------------|---------------------|----------------------|----------------|--------|----------------|--------------|----|----|
| CA-LAN-2511 | 2267-10-143A | Flake    | S2/W21.5 TU (50-60) | 12.3           | 10,679          | 12.9                | 11,959               | LPL            | CO     | CO             | TC           | 2  | D  |
| CA-LAN-2511 | 2267-10-143A | Flake    | S2/W21.5 TU (50-60) | 10.0           | 6,606           | 10.5                | 7,398                | LMO            | CO     | CO             | TC           | 2  | D  |
| CA-LAN-2511 | 2267-10-143B | Flake    | S2/W21.5 TU (50-60) | 12.1           | 10,281          | 12.7                | 11,513               | LPL            | CO     | CO             | TC           | 2  | D  |
| CA-LAN-2511 | 2267-10-158  | Flake    | S8/W28 TU (30-40)   | 9.0            | 5,174           | 9.5                 | 5,794                | PTO            | CO     | CO             | TC           | 2  | D  |
| CA-LAN-2511 | 2267-10-165  | Flake    | S8/W28 TU (60-70)   | 13.4           | 13,027          | 14.1                | 14,588               | LPL            | CO     | CO             | TC           | 2  | D  |
| CA-LAN-2511 | 2267-10-168A | Flake    | S8/W28 TU (70-80)   | 13.6           | 13,483          | 14.3                | 15,098               | LPL            | CO     | CO             | TC           | 2  | D  |
| CA-LAN-2511 | 2267-10-168B | Flake    | S8/W28 TU (70-80)   | 12.3           | 10,679          | 12.9                | 11,959               | LPL            | CO     | CO             | TC           | 2  | D  |
| CA-LAN-2634 | 2374         | Shatter  | Surface             | 0.0            | 0               | 0.0                 | 0                    | --             | CO     | WS             | TC           | 3  | F  |
| CA-LAN-2661 | 2775-31      | Flake    | 2 (20-30)           | 3.4            | 541             | 3.6                 | 606                  | SSP            | CO     | WS             | LD           | 3  | F  |
| CA-LAN-3394 | 23           | BFT      | Surface             | 0.0            | 0               | 0.0                 | 0                    | --             | CO     | WS             | TC           | 2  | C  |
| CA-LAN-3406 | 11           | BFT      | Surface             | 7.6            | 3,495           | 8.0                 | 3,914                | PTO            | CO     | SL             | TC           | 3  | F  |
| CA-LAN-3406 | 12           | BFF      | Surface             | 5.1            | 1,385           | 5.4                 | 1,551                | GYP            | CO     | WS             | TC           | 3  | F  |
| CA-LAN-3406 | 13           | BFF      | Surface             | 2.8            | 345             | 2.9                 | 386                  | SHO            | CO     | WS             | TC           | 3  | F  |
| CA-LAN-3406 | 14           | Flake    | Surface             | 6.8            | 2,700           | 7.1                 | 3,024                | PTO            | CO     | WS             | TC           | 3  | F  |
| CA-LAN-3406 | 15           | Flake    | Surface             | 3.3            | 505             | 3.5                 | 565                  | SHO            | CO     | CO             | TC           | 3  | F  |
| CA-LAN-3406 | 16           | Flake    | Surface             | 7.0            | 2,888           | 7.4                 | 3,234                | PTO            | CO     | CO             | TC           | 3  | F  |
| CA-LAN-3406 | 17           | Flake    | Surface             | 5.7            | 1,793           | 6.0                 | 2,008                | GYP            | CO     | WS             | TC           | 3  | F  |
| CA-LAN-3406 | 18           | Flake    | Surface             | 5.9            | 1,942           | 6.2                 | 2,175                | GYP            | CO     | WS             | TC           | 3  | F  |
| CA-LAN-3406 | 19           | Flake    | Surface             | 3.7            | 658             | 3.9                 | 737                  | SSP            | CO     | WS             | TC           | 3  | F  |
| CA-LAN-3406 | 20           | Flake    | Surface             | 6.4            | 2,346           | 6.7                 | 2,627                | GYP            | CO     | CO             | TC           | 3  | F  |
| CA-LAN-3406 | 21           | Flake    | STU 48 (0-20)       | 6.2            | 2,179           | 6.5                 | 2,440                | GYP            | CO     | CO             | TC           | 3  | F  |
| CA-LAN-3410 | 22           | Flake    | Surface             | 11.3           | 8,772           | 11.9                | 9,823                | LPL            | CO     | CO             | TC           | 2  | C  |
| CA-LAN-3472 | 7            | Flake    | Surface             | 8.0            | 3,937           | 8.4                 | 4,408                | PTO            | CO     | WS             | LD           | 2  | C  |
| CA-LAN-3472 | 8            | Flake    | Surface             | 12.9           | 11,927          | 13.5                | 13,356               | LPL            | CO     | WS             | LD           | 2  | C  |
| CA-LAN-3472 | 9            | Flake    | Surface             | 0.0            | 0               | 0.0                 | 0                    | --             | CO     | WS             | LD           | 2  | C  |
| CA-LAN-3472 | 10           | Flake    | Surface             | 12.7           | 11,502          | 13.3                | 12,881               | LPL            | CO     | CO             | LD           | 2  | C  |
| CA-LAN-3472 | 11           | Flake    | Surface             | 12.1           | 10,281          | 12.7                | 11,513               | LPL            | CO     | WS             | LD           | 2  | C  |
| CA-LAN-3472 | 12           | Flake    | Surface             | 2.1            | 177             | 2.2                 | 198                  | SHO            | CO     | CO             | LD           | 2  | C  |
| CA-LAN-3472 | 13           | Flake    | Surface             | 12.7           | 11,502          | 13.3                | 12,881               | LPL            | CO     | CO             | LD           | 2  | C  |
| CA-LAN-3472 | 13           | Flake    | Surface             | 7.7            | 3,603           | 8.1                 | 4,034                | PTO            | CO     | CO             | LD           | 2  | C  |
| CA-LAN-3472 | 14           | Flake    | Surface             | 17.4           | 23,880          | 18.3                | 26,742               | LPL            | CO     | SL             | LD           | 2  | C  |
| CA-LAN-3472 | 15           | Flake    | Surface             | 0.0            | 0               | 0.0                 | 0                    | --             | CO     | WCP            | LD           | 2  | C  |
| CA-LAN-3472 | 16           | Flake    | Surface             | 6.2            | 2,179           | 6.5                 | 2,440                | GYP            | CO     | WS             | LD           | 2  | C  |
| CA-LAN-3472 | 17           | Flake    | Surface             | 1.5            | 81              | 1.6                 | 91                   | SHO            | CO     | WS             | LD           | 2  | C  |



| Trinomial   | Cat No. | Artifact | Unit (Depth) | Raw<br>Microns | Raw<br>Years BP | Adjusted<br>Microns | Adjusted<br>Years BP | Time<br>Period | Source | Sub-<br>source | Site<br>Type | MR | MA |
|-------------|---------|----------|--------------|----------------|-----------------|---------------------|----------------------|----------------|--------|----------------|--------------|----|----|
| CA-LAN-3472 | 18      | Flake    | Surface      | 12.9           | 11,927          | 13.5                | 13,356               | LPL            | CO     | JR             | LD           | 2  | C  |
| CA-LAN-3472 | 19      | Flake    | Surface      | 10.9           | 8,068           | 11.4                | 9,035                | LMO            | CO     | JR             | LD           | 2  | C  |
| CA-LAN-3472 | 20      | Flake    | Surface      | 12.5           | 11,086          | 13.1                | 12,415               | LPL            | CO     | WS             | LD           | 2  | C  |
| CA-LAN-3472 | 21      | Flake    | Surface      | 0.0            | 0               | 0.0                 | 0                    | --             | CO     | CO             | LD           | 2  | C  |
| CA-LAN-3472 | 22      | Flake    | Surface      | 3.6            | 617             | 3.8                 | 691                  | SSP            | CO     | WS             | LD           | 2  | C  |
| CA-LAN-3472 | 23      | Flake    | Surface      | 3.6            | 617             | 3.8                 | 691                  | SSP            | CO     | CO             | LD           | 2  | C  |
| CA-LAN-3472 | 24      | Flake    | Surface      | 11.1           | 8,416           | 11.7                | 9,425                | LPL            | CO     | CO             | LD           | 2  | C  |
| CA-LAN-3472 | 25      | Flake    | Surface      | 0.0            | 0               | 0.0                 | 0                    | --             | CO     | WS             | LD           | 2  | C  |
| CA-LAN-3472 | 26      | Flake    | Surface      | 0.0            | 0               | 0.0                 | 0                    | --             | CO     | CO             | LD           | 2  | C  |
| CA-LAN-3472 | 27      | Flake    | Surface      | 0.0            | 0               | 0.0                 | 0                    | --             | CO     | WS             | LD           | 2  | C  |
| CA-LAN-3472 | 28      | Flake    | Surface      | 10.9           | 8,068           | 11.4                | 9,035                | LMO            | CO     | WS             | LD           | 2  | C  |
| CA-LAN-3472 | 29      | Flake    | Surface      | 0.0            | 0               | 0.0                 | 0                    | --             | CO     | WS             | LD           | 2  | C  |
| CA-LAN-3472 | 30      | Flake    | Surface      | 2.3            | 218             | 2.4                 | 245                  | SHO            | CO     | CO             | LD           | 2  | C  |
| CA-LAN-3472 | 31      | Flake    | Surface      | 0.0            | 0               | 0.0                 | 0                    | --             | CO     | CO             | LD           | 2  | C  |
| CA-LAN-3472 | 32      | Flake    | Surface      | 0.0            | 0               | 0.0                 | 0                    | --             | CO     | CO             | LD           | 2  | C  |
| CA-LAN-3472 | 33      | Flake    | Surface      | 6.1            | 2,099           | 6.4                 | 2,350                | GYP            | CO     | WS             | LD           | 2  | C  |
| CA-LAN-3472 | 34      | Flake    | Surface      | 0.0            | 0               | 0.0                 | 0                    | --             | CO     | WCP            | LD           | 2  | C  |
| CA-LAN-3472 | 35      | Flake    | Surface      | 4.8            | 1,203           | 5.0                 | 1,348                | GYP            | CO     | WS             | LD           | 2  | C  |
| CA-LAN-3472 | 37      | Flake    | Surface      | 0.0            | 0               | 0.0                 | 0                    | --             | CO     | WS             | LD           | 2  | C  |
| CA-LAN-3472 | 38      | Flake    | Surface      | 0.0            | 0               | 0.0                 | 0                    | --             | CO     | CO             | LD           | 2  | C  |
| CA-LAN-3472 | 39      | Flake    | Surface      | 9.7            | 6,156           | 10.2                | 6,893                | PTO            | CO     | CO             | LD           | 2  | C  |
| CA-LAN-3472 | 40      | Flake    | Surface      | 5.4            | 1,582           | 5.7                 | 1,771                | GYP            | CO     | CO             | LD           | 2  | C  |
| CA-LAN-3472 | 41      | Flake    | Surface      | 9.4            | 5,723           | 9.9                 | 6,409                | PTO            | CO     | WS             | LD           | 2  | C  |
| CA-LAN-3472 | 42      | Flake    | Surface      | 0.0            | 0               | 0.0                 | 0                    | --             | UNK    | UNK            | LD           | 2  | C  |
| CA-LAN-3472 | 43      | Flake    | Surface      | 0.0            | 0               | 0.0                 | 0                    | --             | CO     | WS             | LD           | 2  | C  |
| CA-LAN-3472 | 44      | Flake    | Surface      | 12.5           | 11,086          | 13.1                | 12,415               | LPL            | CO     | WS             | LD           | 2  | C  |
| CA-LAN-3472 | 45      | Flake    | Surface      | 11.5           | 9,137           | 12.1                | 10,232               | LPL            | CO     | CO             | LD           | 2  | C  |
| CA-LAN-3472 | 46      | Flake    | Surface      | 0.0            | 0               | 0.0                 | 0                    | --             | CO     | SL             | LD           | 2  | C  |
| CA-LAN-3472 | 47      | Flake    | Surface      | 0.0            | 0               | 0.0                 | 0                    | --             | CO     | CO             | LD           | 2  | C  |
| CA-LAN-3472 | 48      | Flake    | Surface      | 8.0            | 3,937           | 8.4                 | 4,408                | PTO            | CO     | WCP            | LD           | 2  | C  |
| CA-LAN-3472 | 49      | Flake    | Surface      | 0.0            | 0               | 0.0                 | 0                    | --             | CO     | CO             | LD           | 2  | C  |
| CA-LAN-3472 | 50      | Flake    | Surface      | 0.0            | 0               | 0.0                 | 0                    | --             | CO     | WS             | LD           | 2  | C  |
| CA-LAN-3472 | 51      | Flake    | Surface      | 0.0            | 0               | 0.0                 | 0                    | --             | CO     | CO             | LD           | 2  | C  |
| CA-LAN-3472 | 52      | Flake    | Surface      | 0.0            | 0               | 0.0                 | 0                    | --             | CO     | WS             | LD           | 2  | C  |

| Trinomial   | Cat No. | Artifact | Unit (Depth)  | Raw Microns | Raw Years BP | Adjusted Microns | Adjusted Years BP | Time Period | Source | Sub-source | Site Type | MR | MA |
|-------------|---------|----------|---------------|-------------|--------------|------------------|-------------------|-------------|--------|------------|-----------|----|----|
| CA-LAN-3472 | 53      | Flake    | Surface       | 0.0         | 0            | 0.0              | 0                 | --          | CO     | CO         | LD        | 2  | C  |
| CA-LAN-3472 | 54      | Flake    | Surface       | 0.0         | 0            | 0.0              | 0                 | --          | CO     | CO         | LD        | 2  | C  |
| CA-LAN-3472 | 55      | Flake    | Surface       | 3.5         | 578          | 3.7              | 648               | SSP         | CO     | WS         | LD        | 2  | C  |
| CA-LAN-3472 | 56      | Flake    | Surface       | 12.1        | 10,281       | 12.7             | 11,513            | LPL         | CO     | WS         | LD        | 2  | C  |
| CA-LAN-3472 | 57      | Flake    | Surface       | 2.4         | 241          | 2.5              | 270               | SHO         | CO     | WS         | LD        | 2  | C  |
| CA-LAN-3472 | 58      | Flake    | Surface       | 12.9        | 11,927       | 13.5             | 13,356            | LPL         | CO     | CO         | LD        | 2  | C  |
| CA-LAN-3472 | 59      | Flake    | Surface       | 0.0         | 0            | 0.0              | 0                 | --          | CO     | WS         | LD        | 2  | C  |
| CA-LAN-3472 | 60      | Flake    | Surface       | 12.9        | 11,927       | 13.5             | 13,356            | LPL         | CO     | WS         | LD        | 2  | C  |
| CA-LAN-3472 | 61      | Flake    | Surface       | 8.9         | 5,041        | 9.3              | 5,646             | PTO         | CO     | WS         | LD        | 2  | C  |
| CA-LAN-3472 | 62      | Flake    | Surface       | 11.8        | 9,699        | 12.4             | 10,861            | LPL         | CO     | WS         | LD        | 2  | C  |
| CA-LAN-3472 | 63      | Flake    | Surface       | 0.0         | 0            | 0.0              | 0                 | --          | CO     | WS         | LD        | 2  | C  |
| CA-LAN-3472 | 64      | Flake    | Surface       | 0.0         | 0            | 0.0              | 0                 | --          | CO     | WS         | LD        | 2  | C  |
| CA-LAN-3472 | 65      | Flake    | Surface       | 0.0         | 0            | 0.0              | 0                 | --          | CO     | WS         | LD        | 2  | C  |
| CA-LAN-3472 | 66      | Flake    | Surface       | 10.8        | 7,898        | 11.3             | 8,844             | LMO         | CO     | WS         | LD        | 2  | C  |
| CA-LAN-3472 | 67      | Flake    | Surface       | 0.0         | 0            | 0.0              | 0                 | --          | CO     | WCP        | LD        | 2  | C  |
| CA-LAN-3472 | 68      | Flake    | Surface       | 0.0         | 0            | 0.0              | 0                 | --          | CO     | WCP        | LD        | 2  | C  |
| CA-LAN-3472 | 69      | Flake    | Surface       | 14.4        | 15,394       | 15.1             | 17,239            | LPL         | CO     | WCP        | LD        | 2  | C  |
| CA-LAN-3472 | 70      | Flake    | Surface       | 0.0         | 0            | 0.0              | 0                 | --          | CO     | WS         | LD        | 2  | C  |
| CA-LAN-3472 | 71      | Flake    | Surface       | 0.0         | 0            | 0.0              | 0                 | --          | CO     | WS         | LD        | 2  | C  |
| CA-LAN-3472 | 72      | Flake    | Surface       | 0.0         | 0            | 0.0              | 0                 | --          | UNK    | UNK        | LD        | 2  | C  |
| CA-LAN-4053 | 2046    | Shatter  | Surface       | 9.9         | 6,454        | 10.4             | 7,228             | PTO         | CO     | WS         | TC        | 3  | F  |
| CA-LAN-4055 | 2114    | Biface   | Surface       | 8.0         | 3,937        | 8.4              | 4,408             | PTO         | CO     | WS         | LD        | 3  | F  |
| CA-LAN-4055 | 2119    | BTF      | Surface       | 9.0         | 5,174        | 9.5              | 5,794             | PTO         | CO     | WS         | LD        | 3  | F  |
| CA-LAN-4055 | 2120    | BTF      | Surface       | 10.0        | 6,606        | 10.5             | 7,398             | LMO         | CO     | WS         | LD        | 3  | F  |
| CA-LAN-4055 | 2121    | Shatter  | Surface       | 9.0         | 5,174        | 9.5              | 5,794             | PTO         | CO     | WS         | LD        | 3  | F  |
| CA-LAN-4055 | 2236    | BTF      | STP 3 (40-60) | 7.0         | 2,888        | 7.4              | 3,234             | PTO         | CO     | WS         | LD        | 3  | F  |
| CA-LAN-4055 | 2242    | BTF      | STP 4 (0-20)  | 8.8         | 4,911        | 9.2              | 5,499             | PTO         | CO     | WS         | LD        | 3  | F  |
| CA-LAN-4055 | 2260    | BTF      | STP 6 (20-40) | 7.8         | 3,712        | 8.2              | 4,157             | PTO         | CO     | WS         | LD        | 3  | F  |
| CA-LAN-4055 | 2260    | BTF      | STP 6 (20-40) | 6.9         | 2,793        | 7.2              | 3,128             | PTO         | CO     | WS         | LD        | 3  | F  |
| CA-LAN-4055 | 2263    | BTF      | STP 6 (40-60) | 8.0         | 3,937        | 8.4              | 4,408             | PTO         | CO     | WS         | LD        | 3  | F  |
| CA-LAN-4055 | 2263    | BTF      | STP 6 (40-60) | 7.0         | 2,888        | 7.4              | 3,234             | PTO         | CO     | WS         | LD        | 3  | F  |
| CA-LAN-715  | 180.1   | Flake    | Surface       | 2.5         | 265          | 2.6              | 297               | SHO         | CO     | WS         | TC        | 2  | C  |
| CA-LAN-715  | 180.222 | Flake    | TU-B (20-30)  | 0.0         | 0            | 0.0              | 0                 | --          | CO     | WS         | TC        | 2  | C  |
| CA-LAN-715  | 180.235 | Shatter  | TU-B (60-70)  | 5.1         | 1,385        | 5.4              | 1,551             | GYP         | CO     | WS         | TC        | 2  | C  |

| Trinomial    | Cat No.  | Artifact | Unit (Depth)   | Raw<br>Microns | Raw<br>Years BP | Adjusted<br>Microns | Adjusted<br>Years BP | Time<br>Period | Source | Sub-<br>source | Site<br>Type | MR | MA |
|--------------|----------|----------|----------------|----------------|-----------------|---------------------|----------------------|----------------|--------|----------------|--------------|----|----|
| CA-LAN-715   | 10658    | BFF      | Surface        | 5.9            | 1,942           | 6.2                 | 2,175                | GYP            | CO     | WS             | TC           | 2  | C  |
| CA-LAN-716   | 10818    | Flake    | Surface        | 4.8            | 1,203           | 5.0                 | 1,348                | GYP            | SA     | SV             | TC           | 2  | C  |
| CA-LAN-716   | 10819    | Flake    | Surface        | 6.3            | 2,262           | 6.6                 | 2,533                | GYP            | SA     | SV             | TC           | 2  | C  |
| CA-LAN-769/H | 732      | Flake    | Surface        | 6.8            | 2,700           | 7.1                 | 3,024                | PTO            | CO     | WCP            | TC           | 3  | F  |
| CA-LAN-769/H | 733      | Flake    | Surface        | 9.1            | 5,308           | 9.6                 | 5,944                | PTO            | CO     | WCP            | TC           | 3  | F  |
| CA-LAN-769/H | 734      | Flake    | Surface        | 0.0            | 0               | 0.0                 | 0                    | --             | UNK    | NS             | TC           | 3  | F  |
| CA-LAN-769/H | 735      | Flake    | Surface        | 7.1            | 2,985           | 7.5                 | 3,342                | PTO            | UNK    | NS             | TC           | 3  | F  |
| CA-LAN-769/H | 823      | LSD      | Surface        | 0.0            | 0               | 0.0                 | 0                    | --             | CO     | WS             | TC           | 3  | F  |
| CA-LAN-769/H | 958      | DSN      | Surface        | 5.1            | 1,385           | 5.4                 | 1,551                | GYP            | CO     | WS             | TC           | 3  | F  |
| CA-LAN-828/H | 38       | RSP      | Surface        | 5.7            | 1,793           | 6.0                 | 2,008                | GYP            | CO     | WS             | BC           | 3  | F  |
| CA-LAN-828/H | 1074     | CWT      | Surface        | 3.4            | 541             | 3.6                 | 606                  | SSP            | OB     | OB             | BC           | 3  | F  |
| CA-LAN-863   | 166      | Biface   | Surface        | 8.6            | 4,656           | 9.0                 | 5,214                | PTO            | CO     | WS             | BC           | 5  | D  |
| CA-LAN-863   | 165      | Biface   | Surface        | 2.9            | 374             | 3.0                 | 419                  | SHO            | CO     | WS             | BC           | 5  | D  |
| CA-LAN-863   | 167      | Biface   | Surface        | 8.6            | 4,656           | 9.0                 | 5,214                | PTO            | CO     | WS             | BC           | 5  | D  |
| CA-LAN-863   | 167      | Biface   | Surface        | 6.5            | 2,432           | 6.8                 | 2,723                | GYP            | CO     | WS             | BC           | 5  | D  |
| CA-LAN-863   | 585      | BTF      | 4 (20-30)      | 8.5            | 4,531           | 8.9                 | 5,074                | PTO            | CO     | WS             | BC           | 5  | D  |
| CA-LAN-863   | 214      | Flake    | 1 (20-30)      | 6.4            | 2,346           | 6.7                 | 2,627                | GYP            | CO     | CO             | BC           | 5  | D  |
| CA-LAN-863   | 6        | Flake    | 3 (10-20)      | 11.0           | 8,241           | 11.6                | 9,229                | LPL            | CO     | CO             | BC           | 5  | D  |
| CA-LAN-863   | 201-2022 | Flake    | A22 (S)        | 9.0            | 5,174           | 9.5                 | 5,794                | PTO            | CO     | WS             | BC           | 5  | D  |
| CA-LAN-863   | 201-2009 | Flake    | A9 (S)         | 8.5            | 4,531           | 8.9                 | 5,074                | PTO            | CO     | WCP            | BC           | 5  | D  |
| CA-LAN-863   | 201-2028 | Flake    | A28 (S)        | 8.9            | 5,041           | 9.3                 | 5,646                | PTO            | CO     | WCP            | BC           | 5  | D  |
| CA-LAN-863   | 201-2044 | Flake    | A44 (S)        | 8.9            | 5,041           | 9.3                 | 5,646                | PTO            | CO     | WCP            | BC           | 5  | D  |
| CA-LAN-863   | 201-2050 | Flake    | A50 (S)        | 9.1            | 5,308           | 9.6                 | 5,944                | PTO            | CO     | WCP            | BC           | 5  | D  |
| CA-LAN-863   | 201-2512 | Flake    | 12A STP (0-10) | 7.5            | 3,389           | 7.9                 | 3,795                | PTO            | UNK    | NS             | BC           | 5  | D  |
| CA-LAN-863/H | 729      | Flake    | Surface        | 0.0            | 0               | 0.0                 | 0                    | --             | UNK    | NS             | BC           | 5  | D  |
| CA-LAN-863/H | 730      | Flake    | Surface        | 9.7            | 6,156           | 10.2                | 6,893                | PTO            | UNK    | NS             | BC           | 5  | D  |
| CA-LAN-863/H | 731      | Flake    | Surface        | 10.2           | 6,917           | 10.7                | 7,746                | LMO            | CO     | WS             | BC           | 5  | D  |
| CA-LAN-863/H | 91       | ESN      | Surface        | 6.6            | 2,519           | 6.9                 | 2,821                | GYP            | CO     | WS             | BC           | 5  | D  |
| CA-LAN-XXXX  | 4392-160 | Flake    | Surface        | 0.0            | 0               | 0.0                 | 0                    | --             | CO     | WS             | LD           | 3  | F  |
| CA-SBR-4052  | 715      | Scraper  | Surface        | 10.7           | 7,729           | 11.2                | 8,655                | LMO            | CO     | WCP            | LD           | 5  | B  |
| CA-SBR-4052  | 702      | Scraper  | Surface        | 0.0            | 0               | 0.0                 | 0                    | --             | UNK    | NS             | LD           | 5  | B  |
| CA-SBR-5088  | 5769     | ESN      | Surface        | 9.9            | 6,454           | 10.4                | 7,228                | PTO            | CO     | CO             | LD           | 5  | B  |
| CA-SBR-5088  | 5771     | BTF      | Surface        | 7.3            | 3,183           | 7.7                 | 3,565                | PTO            | CO     | CO             | LD           | 5  | B  |
| CA-SBR-5173  | 464      | LSD      | Surface        | 9.7            | 6,156           | 10.2                | 6,893                | PTO            | CO     | WCP            | LD           | 5  | B  |

| Trinomial     | Cat No.  | Artifact | Unit (Depth) | Raw Microns | Raw Years BP | Adjusted Microns | Adjusted Years BP | Time Period | Source | Sub-source | Site Type | MR | MA |
|---------------|----------|----------|--------------|-------------|--------------|------------------|-------------------|-------------|--------|------------|-----------|----|----|
| CA-SBR-5321/H | 1        | Flake    | Surface      | 7.3         | 3,183        | 7.7              | 3,565             | PTO         | CO     | WS         | TC        | 5  | B  |
| CA-SBR-5321/H | 2        | Biface   | Surface      | 5.2         | 1,449        | 5.5              | 1,623             | GYP         | CO     | SL         | TC        | 5  | B  |
| CA-SBR-5789   | 202-2    | Flake    | Surface      | 9.0         | 5,174        | 9.5              | 5,794             | PTO         | CO     | WS         | TC        | 5  | B  |
| CA-SBR-5789   | 202-3    | Flake    | Surface      | 11.2        | 8,593        | 11.8             | 9,623             | LPL         | CO     | WS         | TC        | 5  | B  |
| CA-SBR-5789   | 202-4    | Flake    | Surface      | 8.2         | 4,169        | 8.6              | 4,668             | PTO         | CO     | S2F        | TC        | 5  | B  |
| CA-SBR-5789   | 202-6    | Flake    | Surface      | 10.0        | 6,606        | 10.5             | 7,398             | LMO         | CO     | WS         | TC        | 5  | B  |
| CA-SBR-5789   | 202-7    | Flake    | Surface      | 8.4         | 4,408        | 8.8              | 4,937             | PTO         | CO     | WS         | TC        | 5  | B  |
| CA-SBR-5789   | 202-10   | Flake    | Surface      | 12.5        | 11,086       | 13.1             | 12,415            | LPL         | CO     | WS         | TC        | 5  | B  |
| CA-SBR-5789   | 202-12   | Flake    | Surface      | 8.8         | 4,911        | 9.2              | 5,499             | PTO         | CO     | WS         | TC        | 5  | B  |
| CA-SBR-5789   | 202-73   | Flake    | SSU 9 (0-5)  | 3.5         | 578          | 3.7              | 648               | SSP         | CO     | WS         | TC        | 5  | B  |
| CA-SBR-5789   | 202-151  | Flake    | Surface      | 10.5        | 7,398        | 11.0             | 8,285             | LMO         | CO     | WS         | TC        | 5  | B  |
| CA-SBR-5789   | 202-152A | Flake    | Surface      | 10.7        | 7,729        | 11.2             | 8,655             | LMO         | CO     | WS         | TC        | 5  | B  |
| CA-SBR-5789   | 202-1    | Flake    | Surface      | 0.0         | 0            | 0.0              | 0                 | --          | CO     | CO         | LD        | 5  | B  |
| CA-SBR-5789   | 202-5    | Flake    | Surface      | 0.0         | 0            | 0.0              | 0                 | --          | CO     | WS         | LD        | 5  | B  |
| CA-SBR-5789   | 202-8    | Flake    | Surface      | 0.0         | 0            | 0.0              | 0                 | --          | CO     | WS         | LD        | 5  | B  |
| CA-SBR-5789   | 202-9    | UTF      | Surface      | 0.0         | 0            | 0.0              | 0                 | --          | CO     | JR         | LD        | 5  | B  |
| CA-SBR-5789   | 202-152B | Flake    | Surface      | 0.0         | 0            | 0.0              | 0                 | --          | CO     | WS         | LD        | 5  | B  |
| CA-SBR-5789   | 202-153  | Flake    | Surface      | 0.0         | 0            | 0.0              | 0                 | --          | CO     | WS         | LD        | 5  | B  |
| CA-SBR-6151   | 3        | Flake    | Surface      | 8.9         | 5,041        | 9.3              | 5,646             | PTO         | CO     | WS         | TC        | 5  | B  |
| CA-SBR-6151   | 4        | Flake    | Surface      | 0.0         | 0            | 0.0              | 0                 | --          | CO     | WS         | TC        | 5  | B  |
| CA-SBR-6151   | 5        | Flake    | Surface      | 9.0         | 5,174        | 9.5              | 5,794             | PTO         | CO     | JR         | TC        | 5  | B  |
| CA-SBR-6151   | 6        | Flake    | Surface      | 7.3         | 3,183        | 7.7              | 3,565             | PTO         | CO     | WS         | TC        | 5  | B  |
| CA-SBR-6151   | 7        | Tool     | Surface      | 0.0         | 0            | 0.0              | 0                 | --          | CO     | WS         | TC        | 5  | B  |
| CA-SBR-6151   | 8        | Preform  | Surface      | 8.6         | 4,656        | 9.0              | 5,214             | PTO         | CO     | WS         | TC        | 5  | B  |
| CA-SBR-6151   | 9        | Flake    | Surface      | 7.1         | 2,985        | 7.5              | 3,342             | PTO         | CO     | SL         | TC        | 5  | B  |
| CA-SBR-6151   | 10       | Flake    | TU (S)       | 5.1         | 1,385        | 5.4              | 1,551             | GYP         | CO     | CO         | TC        | 5  | B  |
| CA-SBR-6151   | 11       | Flake    | Surface      | 9.6         | 6,009        | 10.1             | 6,730             | PTO         | CO     | JR         | TC        | 5  | B  |
| CA-SBR-6151   | 12       | Flake    | Surface      | 8.2         | 4,169        | 8.6              | 4,668             | PTO         | CO     | WS         | TC        | 5  | B  |
| CA-SBR-6151   | 13       | Flake    | Surface      | 8.0         | 3,937        | 8.4              | 4,408             | PTO         | CO     | WS         | TC        | 5  | B  |
| CA-SBR-6151   | 14       | Flake    | Surface      | 7.3         | 3,183        | 7.7              | 3,565             | PTO         | CO     | WS         | TC        | 5  | B  |
| CA-SBR-6151   | 15       | Flake    | Surface      | 14.5        | 15,644       | 15.2             | 17,518            | LPL         | CO     | CO         | TC        | 5  | B  |
| CA-SBR-6151   | 16       | Flake    | Surface      | 4.6         | 1,090        | 4.8              | 1,221             | SSP         | CO     | CO         | TC        | 5  | B  |
| CA-SBR-6151   | 17       | Flake    | Surface      | 14.9        | 16,663       | 15.6             | 18,660            | LPL         | CO     | WS         | TC        | 5  | B  |
| CA-SBR-6151   | 17       | Flake    | Surface      | 6.8         | 2,700        | 7.1              | 3,024             | PTO         | CO     | WS         | TC        | 5  | B  |



| Trinomial   | Cat No. | Artifact | Unit (Depth) | Raw<br>Microns | Raw<br>Years BP | Adjusted<br>Microns | Adjusted<br>Years BP | Time<br>Period | Source | Sub-<br>source | Site<br>Type | MR | MA |
|-------------|---------|----------|--------------|----------------|-----------------|---------------------|----------------------|----------------|--------|----------------|--------------|----|----|
| CA-SBR-6151 | 18      | Preform  | Surface      | 9.7            | 6,156           | 10.2                | 6,893                | PTO            | CO     | WS             | TC           | 5  | B  |
| CA-SBR-6151 | 19      | Flake    | Surface      | 7.5            | 3,389           | 7.9                 | 3,795                | PTO            | CO     | WS             | TC           | 5  | B  |
| CA-SBR-6151 | 20      | Flake    | Surface      | 7.5            | 3,389           | 7.9                 | 3,795                | PTO            | CO     | WS             | TC           | 5  | B  |
| CA-SBR-6151 | 21      | Flake    | Surface      | 5.7            | 1,793           | 6.0                 | 2,008                | GYP            | CO     | WS             | TC           | 5  | B  |
| CA-SBR-6151 | 22      | Point    | Surface      | 8.0            | 3,937           | 8.4                 | 4,408                | PTO            | CO     | SL             | TC           | 5  | B  |
| CA-SBR-6151 | 23      | Preform  | Surface      | 7.7            | 3,603           | 8.1                 | 4,034                | PTO            | CO     | WS             | TC           | 5  | B  |
| CA-SBR-6151 | 24      | Biface   | Surface      | 9.0            | 5,174           | 9.5                 | 5,794                | PTO            | CO     | WS             | TC           | 5  | B  |
| CA-SBR-6151 | 25      | Point    | Surface      | 7.3            | 3,183           | 7.7                 | 3,565                | PTO            | CO     | WS             | TC           | 5  | B  |
| CA-SBR-8034 | 39      | Flake    | Surface      | 10.0           | 6,606           | 10.5                | 7,398                | LMO            | CO     | WS             | LD           | 5  | C  |
| CA-SBR-8034 | 40      | Flake    | Surface      | 7.8            | 3,712           | 8.2                 | 4,157                | PTO            | CO     | WS             | LD           | 5  | C  |
| CA-SBR-8034 | 41      | Flake    | Surface      | 8.4            | 4,408           | 8.8                 | 4,937                | PTO            | CO     | WS             | LD           | 5  | C  |
| CA-SBR-8034 | 42      | Flake    | Surface      | 10.1           | 6,761           | 10.6                | 7,571                | LMO            | CO     | WS             | LD           | 5  | C  |
| CA-SBR-8034 | 43      | Flake    | Surface      | 8.0            | 3,937           | 8.4                 | 4,408                | PTO            | CO     | WS             | LD           | 5  | C  |
| CA-SBR-8034 | 44      | Flake    | Surface      | 10.7           | 7,729           | 11.2                | 8,655                | LMO            | CO     | CO             | LD           | 5  | C  |
| CA-SBR-8155 | 5672    | Flake    | Surface      | 12.1           | 10,281          | 12.7                | 11,513               | LPL            | CO     | CO             | TC           | 5  | C  |
| CA-SBR-8155 | 5672    | Flake    | Surface      | 6.6            | 2,519           | 6.9                 | 2,821                | GYP            | CO     | CO             | TC           | 5  | C  |
| CA-SBR-8155 | 5681    | Flake    | Surface      | 9.3            | 5,583           | 9.8                 | 6,252                | PTO            | CO     | CO             | TC           | 5  | C  |
| CA-SBR-8159 | 5686    | Flake    | Surface      | 0.0            | 0               | 0.0                 | 0                    | --             | CO     | CO             | TC           | 5  | C  |
| CA-SBR-8159 | 5689    | Flake    | Surface      | 9.7            | 6,156           | 10.2                | 6,893                | PTO            | CO     | CO             | TC           | 5  | C  |
| CA-SBR-8159 | 5685    | Pinto    | Surface      | 7.5            | 3,389           | 7.9                 | 3,795                | PTO            | CO     | WS             | TC           | 5  | C  |
| CA-SBR-8160 | 5763    | BFF      | Surface      | 10.3           | 7,075           | 10.8                | 7,923                | LMO            | CO     | CO             | TC           | 5  | C  |
| CA-SBR-8160 | 119     | Scraper  | Surface      | 15.3           | 17,719          | 16.1                | 19,843               | LPL            | UNK    | NS             | TC           | 5  | C  |
| CA-SBR-8160 | 119     | Scraper  | Surface      | 7.4            | 3,285           | 7.8                 | 3,679                | PTO            | UNK    | NS             | TC           | 5  | C  |
| CA-SBR-8160 | 158     | Flake    | TU 1 (10-20) | 6.4            | 2,346           | 6.7                 | 2,627                | GYP            | UNK    | CO             | TC           | 5  | C  |
| CA-SBR-8183 | 5750    | Flake    | Surface      | 10.1           | 6,761           | 10.6                | 7,571                | LMO            | CO     | CO             | LD           | 5  | C  |
| CA-SBR-8197 | 28      | BTF      | SSU 1 (0-5)  | 6.4            | 2,346           | 6.7                 | 2,627                | GYP            | CO     | SL             | TC           | 5  | B  |
| CA-SBR-8204 | 6       | Flake    | SSU 1 (0-5)  | 9.0            | 5,174           | 9.5                 | 5,794                | PTO            | CO     | WCP            | TC           | 5  | C  |
| CA-SBR-8204 | 6       | Flake    | SSU 1 (0-5)  | 6.4            | 2,346           | 6.7                 | 2,627                | GYP            | CO     | WCP            | TC           | 5  | C  |
| CA-SBR-8216 | 45      | Scraper  | Surface      | 8.0            | 3,937           | 8.4                 | 4,408                | PTO            | CO     | WS             | LD           | 5  | C  |
| CA-SBR-8219 | 5795    | Core     | Surface      | 14.0           | 14,420          | 14.7                | 16,149               | LPL            | CO     | CO             | LD           | 5  | B  |
| CA-SBR-8222 | 5652    | BTF      | Surface      | 8.5            | 4,531           | 8.9                 | 5,074                | PTO            | CO     | CO             | LD           | 5  | B  |
| CA-SBR-8222 | 38      | Flake    | Surface      | 8.1            | 4,052           | 8.5                 | 4,537                | PTO            | CO     | WS             | LD           | 5  | B  |
| CA-SBR-8304 | 5780    | Biface   | Surface      | 8.2            | 4,169           | 8.6                 | 4,668                | PTO            | CO     | CO             | LD           | 5  | C  |
| CA-SBR-8306 | 5793    | BTF      | Surface      | 9.6            | 6,009           | 10.1                | 6,730                | PTO            | CO     | CO             | TC           | 5  | C  |

| Trinomial   | Cat No.  | Artifact | Unit (Depth)  | Raw<br>Microns | Raw<br>Years BP | Adjusted<br>Microns | Adjusted<br>Years BP | Time<br>Period | Source | Sub-<br>source | Site<br>Type | MR | MA |
|-------------|----------|----------|---------------|----------------|-----------------|---------------------|----------------------|----------------|--------|----------------|--------------|----|----|
| CA-SBR-8852 | 7969     | Dart     | Surface       | 3.9            | 743             | 4.1                 | 833                  | SSP            | CO     | WS             | TC           | 4  | A  |
| CA-SBR-9507 | 46       | Flake    | Surface       | 11.6           | 9,322           | 12.2                | 10,439               | LPL            | CO     | WCP            | TC           | 5  | B  |
| CA-SBR-9507 | 47       | Flake    | Surface       | 8.8            | 4,911           | 9.2                 | 5,499                | PTO            | CO     | WS             | TC           | 5  | B  |
| CA-SBR-9507 | 48       | Flake    | Surface       | 6.3            | 2,262           | 6.6                 | 2,533                | GYP            | CO     | WS             | TC           | 5  | B  |
| CA-SBR-9507 | 49       | Biface   | Surface       | 13.7           | 13,714          | 14.4                | 15,357               | LPL            | CO     | WCP            | TC           | 5  | B  |
| CA-SBR-9507 | 50       | Biface   | Surface       | 8.7            | 4,782           | 9.1                 | 5,356                | PTO            | CO     | WS             | TC           | 5  | B  |
| CA-SBR-9507 | 51       | UTF      | Surface       | 8.7            | 4,782           | 9.1                 | 5,356                | PTO            | CO     | WS             | TC           | 5  | B  |
| CA-SBR-9507 | 52       | Flake    | Surface       | 10.2           | 6,917           | 10.7                | 7,746                | LMO            | CO     | WCP            | TC           | 5  | B  |
| CA-SBR-9507 | 53       | Flake    | Surface       | 10.2           | 6,917           | 10.7                | 7,746                | LMO            | CO     | WS             | TC           | 5  | B  |
| CA-SBR-9507 | 54       | Flake    | Surface       | 8.2            | 4,169           | 8.6                 | 4,668                | PTO            | CO     | SL             | TC           | 5  | B  |
| CA-SBR-9770 | 2707-5   | Flake    | Surface       | 6.8            | 2,700           | 7.1                 | 3,024                | PTO            | CO     | WS             | TC           | 5  | B  |
| CA-SBR-9770 | 2707-6   | Flake    | Surface       | 6.8            | 2,700           | 7.1                 | 3,024                | PTO            | CO     | WS             | TC           | 5  | B  |
| CA-SBR-9770 | 2707-26a | Flake    | TU 11 (0-10)  | 8.7            | 4,782           | 9.1                 | 5,356                | PTO            | CO     | WS             | TC           | 5  | B  |
| CA-SBR-9770 | 2707-26a | Flake    | TU 11 (0-10)  | 6.8            | 2,700           | 7.1                 | 3,024                | PTO            | CO     | WS             | TC           | 5  | B  |
| CA-SBR-9770 | 2707-26b | Flake    | TU 11 (0-10)  | 10.1           | 6,761           | 10.6                | 7,571                | LMO            | CO     | CO             | TC           | 5  | B  |
| CA-SBR-9770 | 2707-67  | Flake    | TU 18 (0-10)  | 10.3           | 7,075           | 10.8                | 7,923                | LMO            | CO     | WS             | TC           | 5  | B  |
| CA-SBR-9770 | 2707-72  | Flake    | STP 23 (0-50) | 6.9            | 2,793           | 7.2                 | 3,128                | PTO            | CO     | WS             | TC           | 5  | B  |
| CA-SBR-9891 | 74       | Biface   | Surface       | 8.9            | 5,041           | 9.3                 | 5,646                | PTO            | CO     | WS             | TC           | 5  | E  |
| ISO         | 327      | Flake    | Surface       | 6.6            | 2,519           | 6.9                 | 2,821                | GYP            | CO     | WCP            | ISO          | 5  | A  |
| ISO         | 397      | Point    | Surface       | 0.0            | 0               | 0.0                 | 0                    | --             | UNK    | NS             | ISO          | 3  | F  |
| ISO         | 418      | Flake    | Surface       | 7.8            | 3,712           | 8.2                 | 4,157                | PTO            | CO     | WCP            | ISO          | 5  | A  |
| ISO         | 827      | Flake    | Surface       | 9.3            | 5,583           | 9.8                 | 6,252                | PTO            | CO     | WCP            | ISO          | 5  | A  |
| ISO         | 828      | Flake    | Surface       | 9.8            | 6,304           | 10.3                | 7,059                | PTO            | UNK    | NS             | ISO          | 5  | A  |
| ISO         | 426      | Flake    | Surface       | 0.0            | 0               | 0.0                 | 0                    | --             | UNK    | NS             | ISO          | 3  | F  |
| ISO         | 832      | Flake    | Surface       | 0.0            | 0               | 0.0                 | 0                    | --             | CO     | WCP            | ISO          | 3  | F  |
| ISO         | 303      | Flake    | Surface       | 9.1            | 5,308           | 9.6                 | 5,944                | PTO            | CO     | WCP            | ISO          | 5  | B  |
| ISO         | 102      | RSP      | Surface       | 4.3            | 932             | 4.5                 | 1,044                | SSP            | CO     | WS             | ISO          | 3  | F  |
| ISO         | 124      | HBT      | Surface       | 4.7            | 1,146           | 4.9                 | 1,283                | GYP            | CO     | WS             | ISO          | 3  | E  |
| ISO         | 2047     | HBT      | Surface       | 5.4            | 1,582           | 5.7                 | 1,771                | GYP            | CO     | WS             | ISO          | 5  | A  |
| ISO         | 4561     | Arrow    | Surface       | 0.0            | 0               | 0.0                 | 0                    | --             | CO     | WS             | ISO          | 2  | C  |
| ISO         | 5745     | EDF      | Surface       | 10.9           | 8,068           | 11.4                | 9,035                | LMO            | CO     | CO             | ISO          | 5  | B  |
| ISO         | 7029     | SLP      | Surface       | 7.8            | 3,712           | 8.2                 | 4,157                | PTO            | CO     | JR             | ISO          | 5  | A  |
| ISO         | 7136     | LMO      | Surface       | 8.5            | 4,531           | 8.9                 | 5,074                | PTO            | CO     | WS             | ISO          | 5  | B  |
| ISO         | 6769     | Flake    | Surface       | 7.4            | 3,285           | 7.8                 | 3,679                | PTO            | CO     | WS             | ISO          | 5  | A  |

| Trinomial | Cat No.   | Artifact | Unit (Depth) | Raw<br>Microns | Raw<br>Years BP | Adjusted<br>Microns | Adjusted<br>Years BP | Time<br>Period | Source | Sub-<br>source | Site<br>Type | MR | MA |
|-----------|-----------|----------|--------------|----------------|-----------------|---------------------|----------------------|----------------|--------|----------------|--------------|----|----|
| ISO       | 6775      | Shatter  | Surface      | 13.5           | 13,254          | 14.2                | 14,842               | LPL            | CO     | WS             | ISO          | 4  | B  |
| ISO       | 7458      | Dart     | Surface      | 7.8            | 3,712           | 8.2                 | 4,157                | PTO            | CO     | WS             | ISO          | 4  | A  |
| ISO       | 8294      | Dart     | Surface      | 0.0            | 0               | 0.0                 | 0                    | --             | CO     | WS             | ISO          | 2  | E  |
| ISO       | 8783      | Flake    | Surface      | 8.4            | 4,408           | 8.8                 | 4,937                | PTO            | CO     | WS             | ISO          | 1  | A  |
| ISO       | 8784      | Flake    | Surface      | 9.3            | 5,583           | 9.8                 | 6,252                | PTO            | CO     | WS             | ISO          | 1  | A  |
| ISO       | 8785      | Flake    | Surface      | 6.9            | 2,793           | 7.2                 | 3,128                | PTO            | CO     | WS             | ISO          | 1  | A  |
| ISO       | 8786      | Flake    | Surface      | 8.9            | 5,041           | 9.3                 | 5,646                | PTO            | CO     | WS             | ISO          | 1  | A  |
| ISO       | 10716     | Flake    | Surface      | 0.0            | 0               | 0.0                 | 0                    | --             | CO     | WS             | ISO          | 2  | B  |
| TBD       | 4461.265  | Flake    | Surface      | 12.7           | 11,502          | 13.3                | 12,881               | LPL            | CO     | WS             | LD           | 2  | C  |
| TBD       | 4461.503  | Flake    | TU A (50-60) | 0.0            | 0               | 0.0                 | 0                    | --             | CO     | WS             | LD           | 2  | C  |
| TBD       | 6332.1739 | Dart     | Surface      | 11.3           | 8,772           | 11.9                | 9,823                | LPL            | CO     | WS             | LD           | 2  | C  |
| TBD       | 6332.1743 | Flake    | Surface      | 13.4           | 13,027          | 14.1                | 14,588               | LPL            | CO     | WS             | LD           | 2  | C  |
| TBD       | 6332.1743 | Flake    | Surface      | 9.2            | 5,444           | 9.7                 | 6,097                | PTO            | CO     | WS             | LD           | 2  | C  |
| TBD       | 10600     | Flake    | Surface      | 4.1            | 835             | 4.3                 | 935                  | SSP            | CO     | WS             | LD           | 2  | C  |
| TBD       | 6341.14   | Flake    | Surface      | 12.4           | 10,882          | 13.0                | 12,186               | LPL            | CO     | WS             | LD           | 2  | C  |
| TBD       | 6341.24   | Flake    | TU A (S)     | 0.0            | 0               | 0.0                 | 0                    | --             | CO     | WS             | LD           | 2  | C  |
| TBD       | 6348.699  | Flake    | Surface      | 0.0            | 0               | 0.0                 | 0                    | --             | UNK    | UNK            | LD           | 2  | C  |
| TBD       | 6348.745  | Flake    | Surface      | 11.7           | 9,509           | 12.3                | 10,649               | LPL            | CO     | WS             | LD           | 2  | C  |
| TBD       | 6348.778  | Flake    | Surface      | 0.0            | 0               | 0.0                 | 0                    | --             | UNK    | UNK            | LD           | 2  | C  |
| TBD       | 6348.817  | Flake    | TU B (10-20) | 4.0            | 788             | 4.2                 | 883                  | SSP            | CO     | WS             | LD           | 2  | C  |
| TBD       | 6348.856  | Flake    | SRU 1 (S)    | 0.0            | 0               | 0.0                 | 0                    | --             | CD     | CD             | LD           | 2  | C  |
| TBD       | 6348.879  | Flake    | SRU 1 (S)    | 0.0            | 0               | 0.0                 | 0                    | --             | UNK    | UNK            | LD           | 2  | C  |
| TBD       | 6348.906  | Flake    | SRU 1 (S)    | 0.0            | 0               | 0.0                 | 0                    | --             | UNK    | UNK            | LD           | 2  | C  |
| TBD       | 10638     | Flake    | Surface      | 0.0            | 0               | 0.0                 | 0                    | --             | UNK    | UNK            | LD           | 2  | C  |
| TBD       | 6354.565  | Flake    | Surface      | 5.7            | 1,793           | 6.0                 | 2,008                | GYP            | CO     | WS             | LD           | 2  | C  |
| TBD       | 6358.1369 | Flake    | Surface      | 2.3            | 218             | 2.4                 | 245                  | SHO            | CO     | WS             | LD           | 2  | C  |
| TBD       | 6358.1370 | Flake    | Surface      | 2.5            | 265             | 2.6                 | 297                  | SHO            | CO     | WS             | LD           | 2  | C  |
| TBD       | 6358.1391 | Flake    | Surface      | 0.0            | 0               | 0.0                 | 0                    | --             | CO     | WS             | LD           | 2  | C  |
| TBD       | 10649     | Flake    | Surface      | 14.3           | 15,148          | 15.0                | 16,963               | LPL            | CO     | WS             | LD           | 2  | C  |
| TBD       | 6359.1312 | Flake    | Surface      | 11.9           | 9,891           | 12.5                | 11,076               | LPL            | CO     | WS             | LD           | 2  | C  |
| TBD       | 6359.1325 | Flake    | Surface      | 0.0            | 0               | 0.0                 | 0                    | --             | CO     | SL             | LD           | 2  | C  |
| TBD       | 6359.1337 | Flake    | Surface      | 0.0            | 0               | 0.0                 | 0                    | --             | CO     | WS             | LD           | 2  | C  |
| TBD       | 10654     | BFF      | Surface      | 15.0           | 16,924          | 15.8                | 18,952               | LPL            | CO     | WCP            | LD           | 2  | C  |
| TBD       | 10721     | BFF      | Surface      | 14.9           | 16,663          | 15.6                | 18,660               | LPL            | CO     | WS             | LD           | 1  | B  |

| Trinomial | Cat No. | Artifact | Unit (Depth) | Raw<br>Microns | Raw<br>Years BP | Adjusted<br>Microns | Adjusted<br>Years BP | Time<br>period | Source | Sub-<br>source | Site<br>Type | MR | MA |
|-----------|---------|----------|--------------|----------------|-----------------|---------------------|----------------------|----------------|--------|----------------|--------------|----|----|
| TBD       | 10727   | LMO      | Surface      | 11.9           | 9,891           | 12.5                | 11,076               | LPL            | CO     | WS             | LD           | 2  | C  |
| TBD       | 10729   | Flake    | STP 13 (S)   | 0.0            | 0               | 0.0                 | 0                    | --             | CO     | WS             | TC           | 2  | C  |
| TBD       | 10735   | BFF      | Surface      | 8.1            | 4,052           | 8.5                 | 4,537                | PTO            | CO     | WS             | TC           | 2  | B  |

**General notes:**

ISO=Isolate  
TBD=To be determined  
UNK=Unknown

**Artifact notes:**

BTF=Blade thinning flake  
CWB=Cottonwood base  
CWL=Cottonwood leafshaped  
CWT=Cottonwood triangular  
CWU=Cottonwood unifacial  
DSN=Desert side notched  
ECN=Elko corner notched  
EDF=Edge damaged flake  
ESN=Elko side notched  
LSD=Leaf shaped dart  
RTF=Retouched flake  
UTF=Utilized flake

**Unit notes:**

S=Surface  
SC=Surface collection  
SCU=Surface collection unit  
SRU=Surface recoordination unit  
SSU=Surface scrape unit  
STP=Shovel test pit  
TS=Transit shot  
TU=Test unit  
U=Unit

**Time period notes:**

GYP=Gypsum  
LMO=Lake Mojave  
LPL=Late Pleistocene  
PTO=Pinto  
SHO=Shoshonean  
SSP=Saratoga Springs

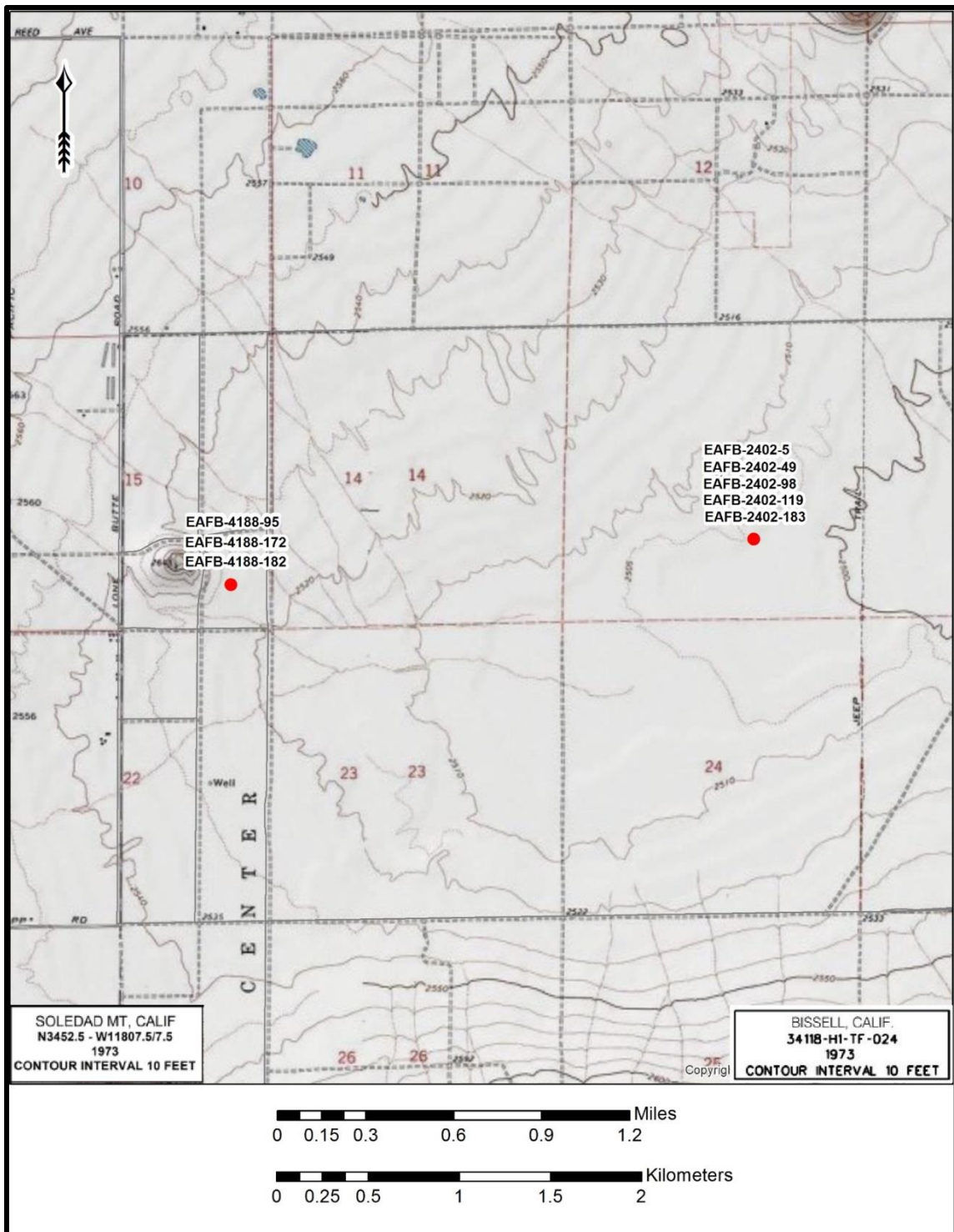
**Source and Subsource notes:**

BM = Bristol Mountain  
CD = Casa Diablo  
CO = Coso  
FS = Fish Spring  
JR = Joshua Ridge  
LM = Lookout Mountain  
MO = Mono  
NS = Not sourced  
OB = Obsidian Butte  
QU = Queen  
S2F = Site 2 Flow  
SA = Saline  
SL = Sugarloaf Mountain  
SM = Shoshone Mountain  
SR = Sawmill Ridge  
SV = Saline Valley  
WCP = West Cactus Peak  
WS = West Sugarloaf

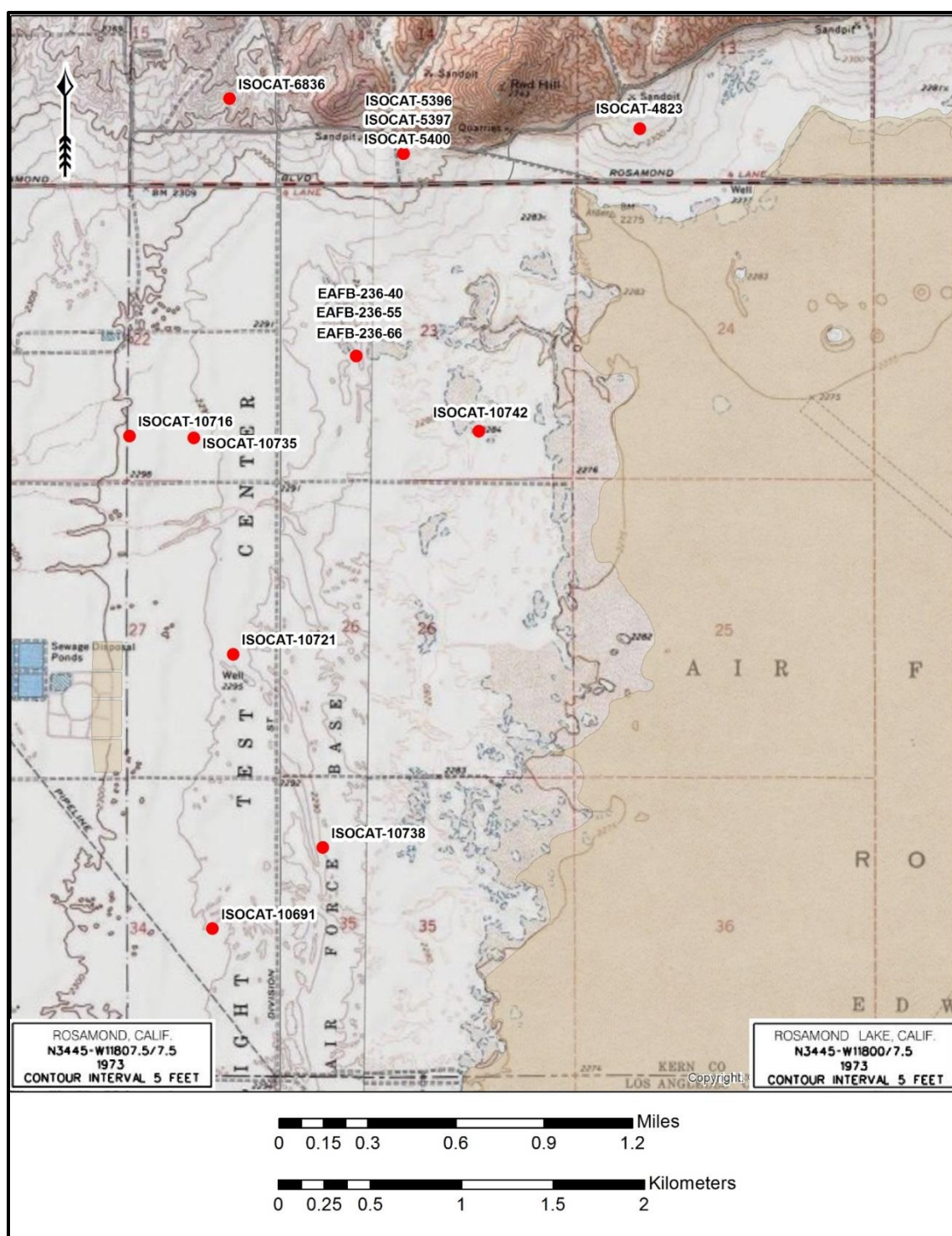
**Site type notes:**

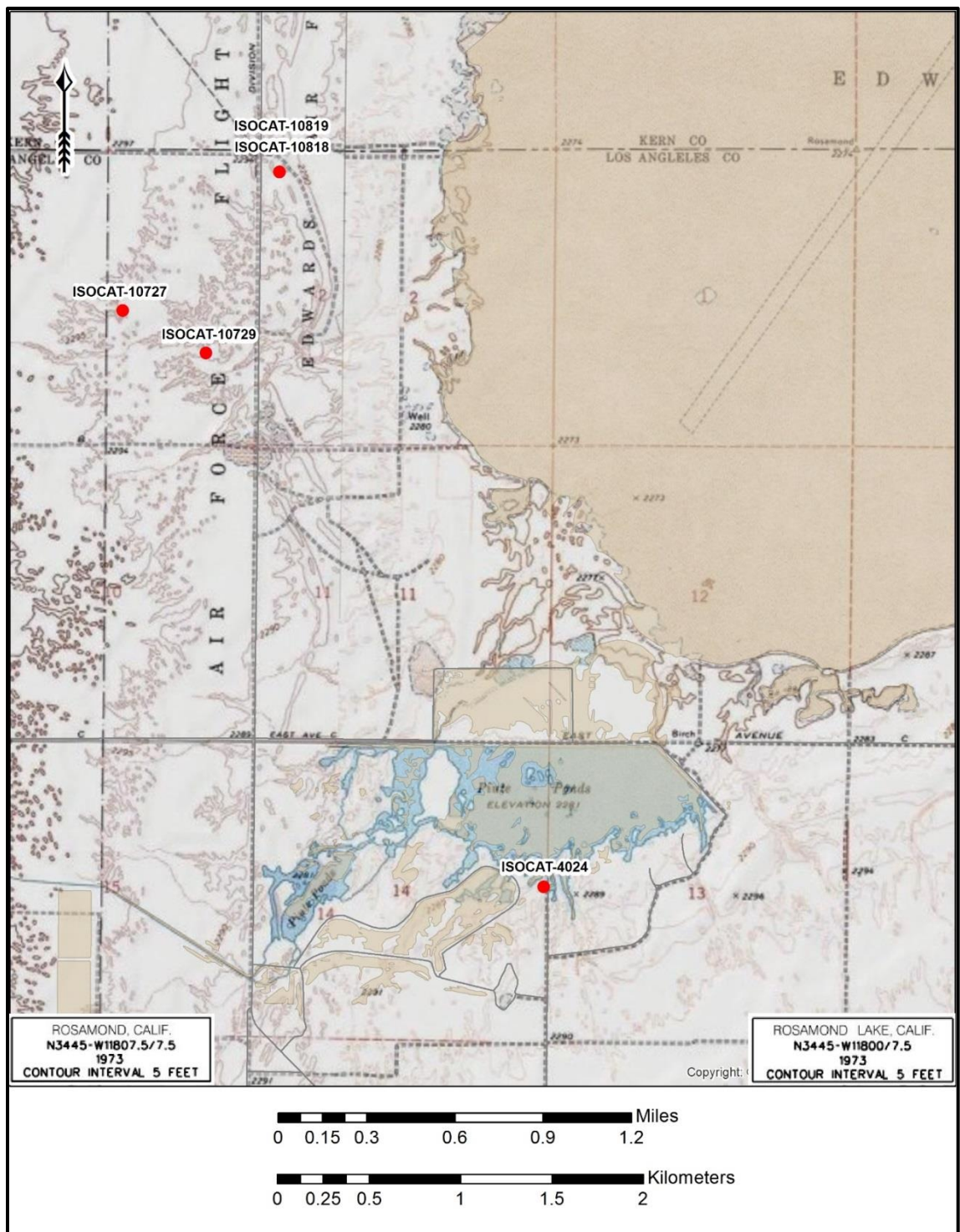
BC = Base camp  
HE = Hearth  
LD = Lithic deposit  
QUA = Quarry  
RS = Rock shelter  
TC = Temporary camp

APPENDIX C  
SUPPLEMENTAL OBSIDIAN LOCATION MAPS

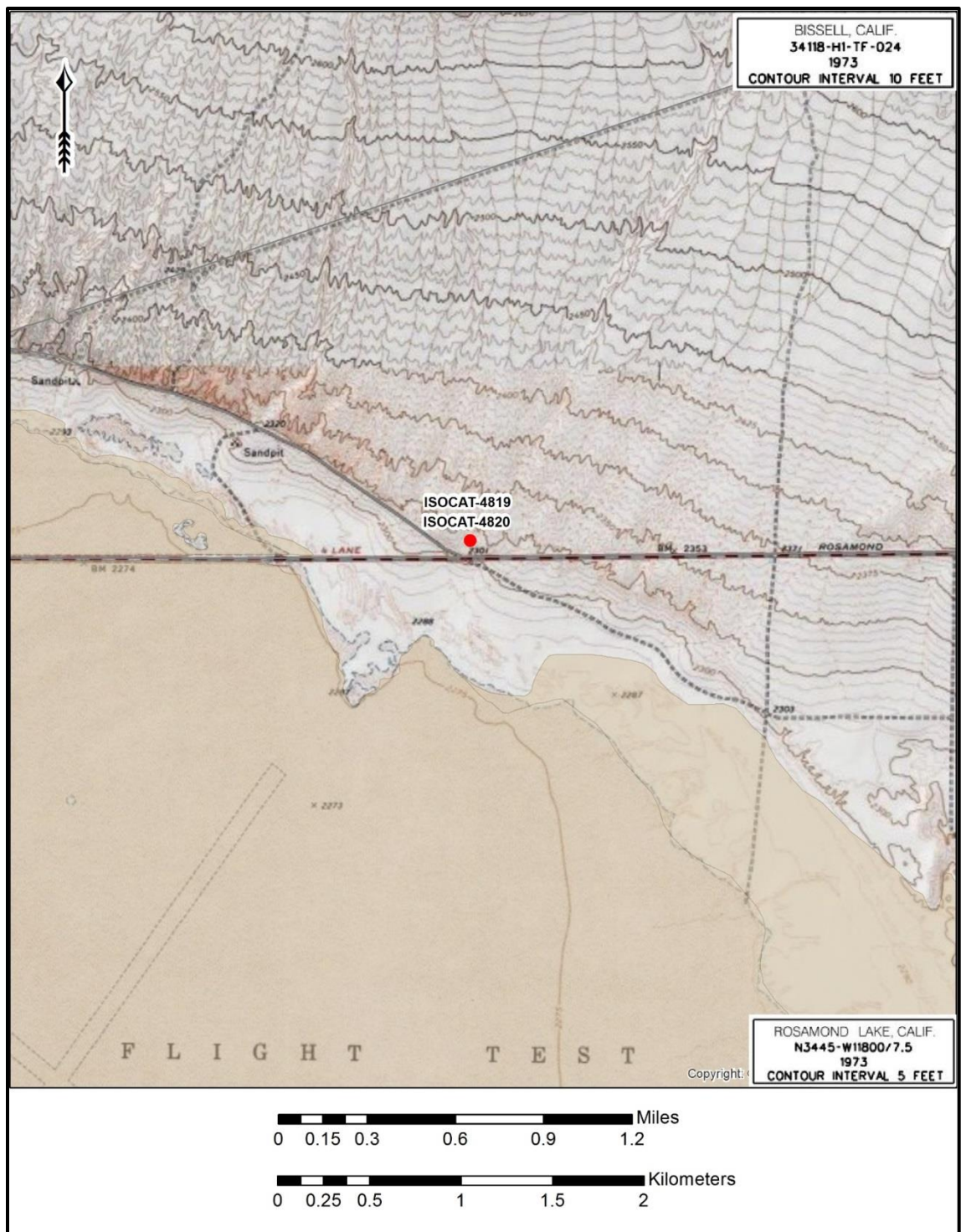






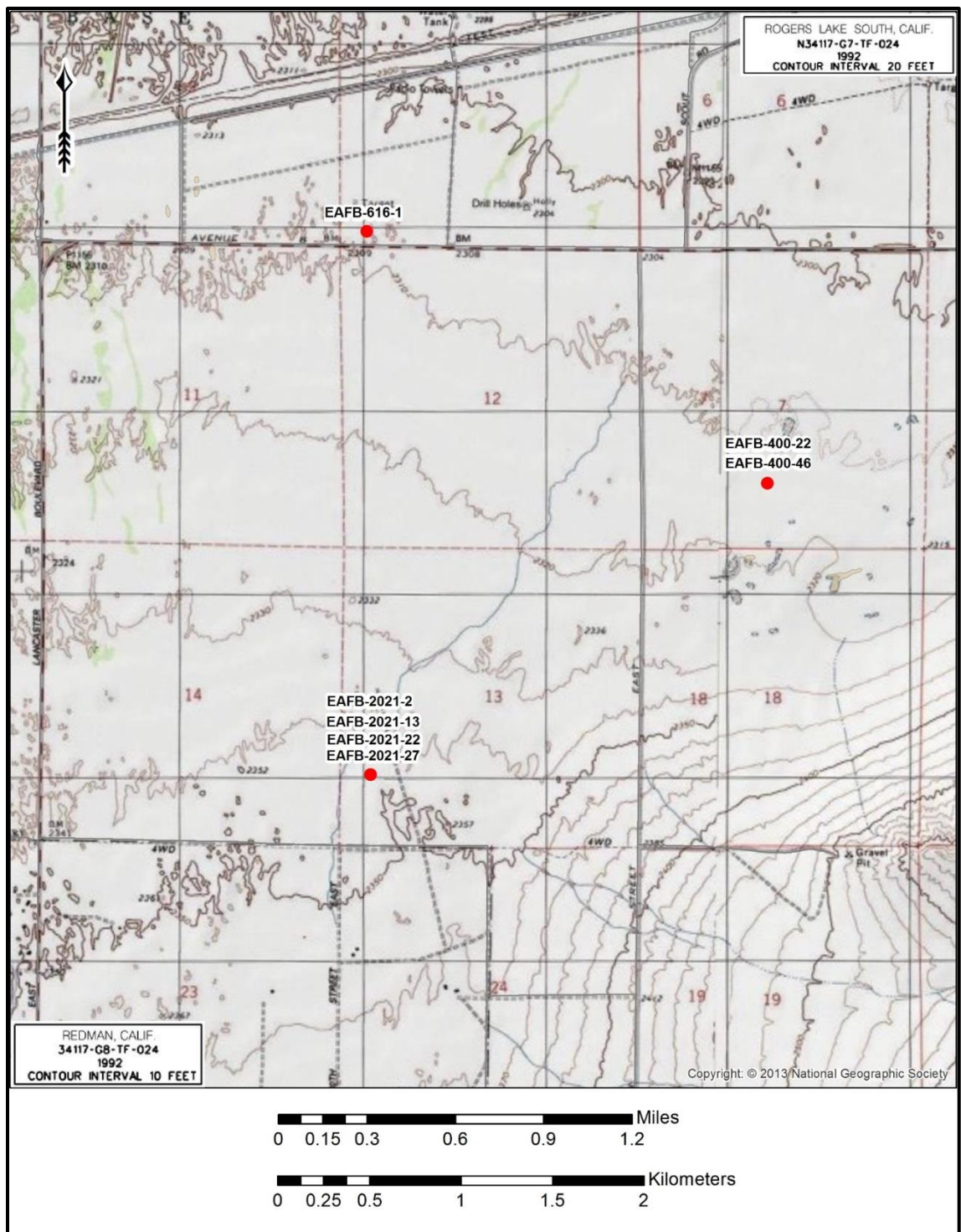














APPENDIX D  
SUPPLEMENTAL OBSIDIAN SOURCING AND  
HYDRATION REPORTS

Geochemical Research Laboratory Letter Report 2016-91

*Energy Dispersive X-ray Fluorescence Analysis of Obsidian Artifacts  
from 22 Archaeological Sites Within Edwards Air Force Base, California*

November 29, 2016

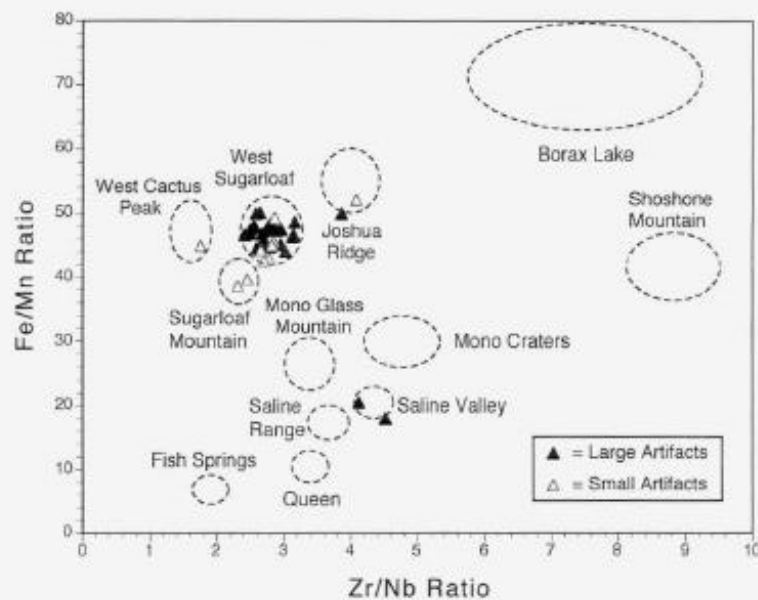
Mr. Richard G. Bark  
Applied Archaeology Program  
CSU San Bernardino  
3026 Neary Court  
Rosamond, CA 93560

Dear Mr. Bark:

This letter contains tables and a figure reporting the results of energy dispersive x-ray fluorescence (edxf) analysis of 40 obsidian artifacts from 22 archaeological sites within Edwards Air Force Base, California. This research was conducted pursuant to Edwards Project # 2016-E. Laboratory equipment and instrumentation, calibration, artifact-to-source (geochemical type) attribution procedures, element-specific measurement resolution, and literature references applicable to analysis of these samples (except as noted) are the same as I reported for artifacts from EAFB 3793 (Hughes 2006) and other sites located within the confines of the base (Hughes 2016).

Figure 1

Fe/Mn vs. Zr/Nb Plots for Obsidian Artifacts from Edwards Air Force Base, California



Dashed lines represent range of variation in regionally significant obsidian source samples. Filled triangles plot the specimens listed in Table 1, open triangles plots artifacts in Table 2. *Note:* values for artifacts 236-40 and 400-22 plot off the chart at this scale.



Twenty-nine of the artifacts you sent were large enough to generate reliable quantitative composition estimates. Edxrf data in Table 1 and Figure 1 indicate that 25 artifacts were made from Coso Volcanic Field obsidians (West Sugarloaf, n= 24; and Joshua Ridge, n= 1 each; cf. Hughes 1988). Two artifacts were made from Lookout Mountain obsidian from the Casa Diablo area (Hughes 1994) and two others were fashioned from Saline Valley volcanic glass.

**Table 2**

Integrated Net Count Rate Data for Small/Thin Obsidian Artifacts from Edwards Air Force Base Sites

| Element Intensities |     |    |     |            |      |      |      | Intensity Ratios |       |      |      |       |      |                    | Obsidian Source |
|---------------------|-----|----|-----|------------|------|------|------|------------------|-------|------|------|-------|------|--------------------|-----------------|
| Cat. no.            | Rb  | Sr | Zr  | Σ Rb,Sr,Zr | Rb%  | Sr%  | Zr%  | Fe/Mn            | Rb/Sr | Zr/Y | Y/Nb | Zr/Nb | Sr/Y | (Chemical Type)    |                 |
| 236-55              | 729 | 5  | 449 | 1183       | .616 | .004 | .380 | 45.0             | 145.8 | 2.2  | .8   | 1.8   | <.1  | West Cactus Peak   |                 |
| 236-66              | 578 | 21 | 506 | 1105       | .523 | .019 | .458 | 42.9             | 27.5  | 3.1  | .9   | 2.8   | .1   | West Sugarloaf     |                 |
| 383-4820            | 592 | 16 | 491 | 1099       | .539 | .015 | .447 | 44.3             | 37.0  | 3.1  | .9   | 2.7   | .1   | West Sugarloaf     |                 |
| 426-5               | 560 | 12 | 409 | 981        | .571 | .012 | .417 | 38.6             | 46.7  | 2.7  | .9   | 2.3   | .1   | Sugarloaf Mountain |                 |
| 559-1               | 611 | 20 | 545 | 1176       | .520 | .017 | .463 | 45.6             | 30.6  | 3.3  | .9   | 2.8   | .1   | West Sugarloaf     |                 |
| 559-12              | 654 | 19 | 541 | 1214       | .539 | .016 | .446 | 45.1             | 34.4  | 3.1  | .8   | 2.8   | .1   | West Sugarloaf     |                 |
| 2021-27b            | 586 | 23 | 516 | 1125       | .521 | .020 | .459 | 42.6             | 25.5  | 3.0  | .9   | 2.7   | .1   | West Sugarloaf     |                 |
| 2402-98             | 506 | 24 | 612 | 1142       | .443 | .021 | .536 | 52.1             | 21.1  | 4.3  | 1.0  | 4.1   | .2   | Joshua Ridge       |                 |
| 2402-119            | 523 | 8  | 414 | 945        | .553 | .009 | .438 | 39.7             | 65.3  | 3.1  | .8   | 2.5   | .1   | Sugarloaf Mountain |                 |
| 2402-183            | 4   | 19 | 4   | 27         | .148 | .704 | .148 | nc               | nc    | nc   | nc   | nc    | 2.5  | Not Obsidian       |                 |
| 4188-172            | 625 | 17 | 563 | 1205       | .519 | .014 | .467 | 49.3             | 36.8  | 3.5  | .8   | 2.9   | .1   | West Sugarloaf     |                 |


Elemental intensities (peak counts/second above background) generated at 40 seconds livetime. nc= not computed.

I typically report trace element measurements in quantitative units (i.e. ppm) and make artifact-to-source attributions on the basis of correspondences in diagnostic trace element concentration values (e.g. those presented in Table 1), but 11 of the specimens you sent were too small and thin to generate x-ray counting statistics adequate for proper conversion from background-corrected intensities to quantitative concentration estimates (i.e., ppm). I analyzed all 11 artifacts to generate integrated net count (intensity) data for the elements Rb, Sr, Y, Zr, Nb, Fe and Mn. After background subtraction, the intensities (counts per second) were converted to percentages. The counting data and derived ratios appear in Table 2, and the plotted values appear in Figure 1. Source assignments were made by comparing the plots for various element intensity ratios for artifacts against the parameters of known source types identified in my extensive in-house reference collection. Further discussion of this laboratory analysis protocol appears in Hughes (2010). The Fe/Mn vs. Zr/Nb plots for the small specimens in Table 2 (see Figure 1) effectively identify all ten obsidian artifacts as matching the profile of Coso Volcanic Field obsidian (West Sugarloaf, n= 6; Sugarloaf Mountain, n =2; West Cactus Peak and Joshua Ridge, n= 1 each). One specimen (2402-183) was made from a non-obsidian parent material.

Combining the results of quantitative composition estimates (n= 29; Table 1) and integrated net peak intensity analysis (n= 11; Table 2) shows that 35 artifacts were made from Coso Volcanic Field obsidians (West Sugarloaf, n= 30; Sugarloaf Mountain and Joshua Ridge, n= 2 each; and West Cactus Peak, n= 1). Two artifacts were made from Lookout Mountain (Casa Diablo area) volcanic glass, and two others were fashioned from obsidian of the Saline Valley chemical type. The remaining artifact was manufactured from a non-obsidian parent material.

I hope this information will help in your analysis and interpretation of the significance of these artifacts. Please contact me at my laboratory (phone: [650] 851-1410; e-mail: rehughes@silcon.com) if I can provide any further assistance or information. As you requested I have forwarded the specimen to Tom Origer for obsidian hydration analysis.

Sincerely,



Richard E. Hughes, Ph.D., RPA  
Director, Geochemical Research Laboratory

#### References

Hughes, Richard E.

- 1988 The Coso Volcanic Field Reexamined: Implications for Obsidian Sourcing and Hydration Dating Research. **Geoarchaeology** 3: 253-265.
- 1994 Intrasource Chemical Variability of Artefact-Quality Obsidians from the Casa Diablo Area, California. **Journal of Archaeological Science** 21: 263-271.
- 2006 Energy Dispersive X-ray Fluorescence Analysis of Three Obsidian Artifacts from Archaeological Site EAFB 3793, Edwards Air Force Base, California. Geochemical Research Laboratory Letter Report 2006-109 submitted to James Johannesmeyer, JT3/CH2M Hill, November 20, 2006.
- 2010 Determining the Geologic Provenance of Tiny Obsidian Flakes in Archaeology Using Nondestructive EDXRF. **American Laboratory** 42 (7): 27-31.
- 2016 Energy Dispersive X-ray Fluorescence Analysis of Obsidian Artifacts from Archaeological Sites Within Edwards Air Force Base, California. Geochemical Research Laboratory Letter Report 2016-40 submitted to Richard Bark, Environmental Assets Program, JT3/CH2M Hill, May 9, 2016.



Table 1

Quantitative Composition Estimates for Obsidian Artifacts from Sites Within Edwards Air Force Base, CA

| Site/Cat.<br>Number   | Trace and Selected Minor Element Concentrations |    |           |          |          |           |          |             |    |    |   | Ratio | Obsidian Source<br>(Chemical Type)     |
|-----------------------|---|----|-----------|----------|----------|-----------|----------|-------------|----|----|---|-------|--|
|                       | Zn  | Ga | Rb        | Sr       | Y        | Zr        | Nb       | Ba          | Ti | Mn | Fe <sub>2</sub> O <sub>3</sub> <sup>T</sup> | Fe/Mn |  |
| EAFB 181,<br>10818    | nm  | nm | 155<br>±4 | 90<br>±4 | 24<br>±3 | 138<br>±4 | 39<br>±3 | 265<br>±26  | nm | nm | nm  | 21    | Saline Valley                          |
| EAFB 181,<br>10819    | nm  | nm | 141<br>±4 | 89<br>±4 | 25<br>±3 | 131<br>±4 | 32<br>±3 | 273<br>±19  | nm | nm | nm  | 18    | Saline Valley                          |
| EAFB 221,<br>10738    | nm  | nm | 210<br>±5 | 12<br>±2 | 50<br>±3 | 160<br>±4 | 46<br>±3 | nm          | nm | nm | nm  | 50    | Joshua Ridge,<br>Coso Volcanic Field   |
| EAFB 236,<br>236-40   | nm  | nm | 138<br>±4 | 93<br>±4 | 20<br>±3 | 181<br>±4 | 13<br>±2 | 1008<br>±21 | nm | nm | nm  | 50    | Lookout Mountain,<br>Casa Diablo area  |
| EAFB 283,<br>10691    | nm  | nm | 268<br>±5 | 6<br>±2  | 60<br>±3 | 137<br>±4 | 55<br>±3 | nm          | nm | nm | nm  | 45    | West Sugarloaf,<br>Coso Volcanic Field |
| EAFB 296,<br>5396     | nm  | nm | 250<br>±5 | 9<br>±2  | 56<br>±3 | 140<br>±4 | 52<br>±3 | nm          | nm | nm | nm  | 44    | West Sugarloaf,<br>Coso Volcanic Field |
| EAFB 296,<br>5397     | nm  | nm | 235<br>±5 | 6<br>±2  | 55<br>±3 | 122<br>±4 | 52<br>±3 | nm          | nm | nm | nm  | 45    | West Sugarloaf,<br>Coso Volcanic Field |
| EAFB 296,<br>5400     | nm  | nm | 261<br>±5 | 6<br>±2  | 60<br>±3 | 139<br>±4 | 56<br>±3 | nm          | nm | nm | 1.22<br>±.02                                | 45    | West Sugarloaf,<br>Coso Volcanic Field |
| EAFB 383,<br>4819     | nm  | nm | 270<br>±5 | 6<br>±2  | 60<br>±3 | 137<br>±4 | 55<br>±3 | 4<br>±17    | nm | nm | nm  | 48    | West Sugarloaf,<br>Coso Volcanic Field |
| EAFB 400,<br>400-22   | nm  | nm | 152<br>±4 | 94<br>±4 | 20<br>3  | 184<br>±4 | 15<br>±2 | 1001<br>±24 | nm | nm | nm  | 46    | Lookout Mountain,<br>Casa Diablo area  |
| EAFB 400,<br>400-46   | nm  | nm | 212<br>±5 | 10<br>±2 | 51<br>±3 | 140<br>±4 | 49<br>±3 | nm          | nm | nm | nm  | 46    | West Sugarloaf,<br>Coso Volcanic Field |
| EAFB 616,<br>516-1    | nm  | nm | 272<br>±5 | 8<br>±2  | 60<br>±3 | 135<br>±4 | 60<br>±3 | nm          | nm | nm | nm  | 48    | West Sugarloaf,<br>Coso Volcanic Field |
| EAFB 713,<br>4024     | nm  | nm | 262<br>±5 | 8<br>±2  | 58<br>±3 | 136<br>±4 | 56<br>±3 | 19<br>±16   | nm | nm | 1.26<br>±.02                                | 45    | West Sugarloaf,<br>Coso Volcanic Field |
| EAFB 857,<br>6836     | nm  | nm | 231<br>±5 | 11<br>±2 | 53<br>±3 | 140<br>±4 | 50<br>±3 | nm          | nm | nm | 1.29<br>±.02                                | 47    | West Sugarloaf,<br>Coso Volcanic Field |
| EAFB 1225,<br>4823    | nm  | nm | 247<br>±5 | 6<br>±2  | 55<br>±3 | 126<br>±4 | 54<br>±3 | nm          | nm | nm | nm  | 48    | West Sugarloaf,<br>Coso Volcanic Field |
| EAFB 2021,<br>2021-2  | nm  | nm | 270<br>±6 | 6<br>±2  | 60<br>±3 | 138<br>±4 | 55<br>±3 | nm          | nm | nm | nm  | 47    | West Sugarloaf,<br>Coso Volcanic Field |
| EAFB 2021,<br>2021-13 | nm  | nm | 268<br>±6 | 11<br>±2 | 60<br>±3 | 134<br>±4 | 56<br>±3 | nm          | nm | nm | nm  | 45    | West Sugarloaf,<br>Coso Volcanic Field |

Values in parts per million (ppm) except total iron (in weight percent) and Fe/Mn ratios; ± = two  $\sigma$  estimate (in ppm) of x-ray counting uncertainty and regression fitting error at 120-240 seconds livetime; nm = not measured.

Table 1

Quantitative Composition Estimates for Obsidian Artifacts from Sites Within Edwards Air Force Base, CA

| Site/Cat.<br>Number                              | Trace and Selected Minor Element Concentrations |    |           |           |          |           |          |            |      |     |   | Ratio | Obsidian Source<br>(Chemical Type)     |
|--|---|----|-----------|-----------|----------|-----------|----------|------------|------|-----|---|-------|--|
|  | Zn  | Ga | Rb        | Sr        | Y        | Zr        | Nb       | Ba         | Ti   | Mn  | Fe <sub>2</sub> O <sub>3</sub> <sup>T</sup> | Fe/Mn |  |
| EAFB 2021,<br>2021-22                            | nm  | nm | 260<br>±5 | 8<br>±2   | 61<br>±3 | 140<br>±4 | 55<br>±3 | nm         | nm   | nm  | nm  | 47    | West Sugarloaf,<br>Coso Volcanic Field |
| EAFB 2021,<br>2021-27a                           | nm  | nm | 261<br>±5 | 6<br>±2   | 60<br>±3 | 134<br>±4 | 55<br>±3 | nm         | nm   | nm  | nm  | 46    | West Sugarloaf,<br>Coso Volcanic Field |
| EAFB 2402,<br>2402-5                             | nm  | nm | 261<br>±5 | 8<br>±2   | 53<br>±3 | 132<br>±4 | 56<br>±3 | nm         | nm   | nm  | 1.21<br>±.02                                | 50    | West Sugarloaf,<br>Coso Volcanic Field |
| EAFB 2402,<br>2402-49                            | nm  | nm | 247<br>±5 | 7<br>±2   | 59<br>±3 | 131<br>±4 | 52<br>±3 | nm         | nm   | nm  | nm  | 48    | West Sugarloaf,<br>Coso Volcanic Field |
| EAFB 2926,<br>10742                              | nm  | nm | 271<br>±5 | 7<br>±2   | 63<br>±3 | 138<br>±4 | 62<br>±3 | nm         | nm   | nm  | nm  | 47    | West Sugarloaf,<br>Coso Volcanic Field |
| EAFB 4188,<br>4188-95                            | nm  | nm | 265<br>±5 | 8<br>±2   | 61<br>±3 | 136<br>±4 | 60<br>±3 | nm         | nm   | nm  | 1.27<br>±.02                                | 50    | West Sugarloaf,<br>Coso Volcanic Field |
| EAFB 4188,<br>4188-182                           | nm  | nm | 256<br>±5 | 8<br>±2   | 55<br>±3 | 133<br>±4 | 56<br>±3 | nm         | nm   | nm  | nm  | 47    | West Sugarloaf,<br>Coso Volcanic Field |
| EAFB 4381,<br>10721                              | nm  | nm | 234<br>±5 | 10<br>±2  | 55<br>±3 | 140<br>±4 | 52<br>±3 | nm         | nm   | nm  | 1.23<br>±.02                                | 49    | West Sugarloaf,<br>Coso Volcanic Field |
| EAFB 4846,<br>10727                              | nm  | nm | 253<br>±5 | 12<br>±2  | 55<br>±3 | 141<br>±4 | 56<br>±3 | nm         | nm   | nm  | nm  | 48    | West Sugarloaf,<br>Coso Volcanic Field |
| EAFB 4848,<br>10729                              | nm  | nm | 263<br>±5 | 9<br>±2   | 60<br>±3 | 137<br>±4 | 60<br>±3 | nm         | nm   | nm  | 1.29<br>±.02                                | 45    | West Sugarloaf,<br>Coso Volcanic Field |
| EAFB 4860,<br>10735                              | nm  | nm | 244<br>±5 | 7<br>±2   | 57<br>±3 | 126<br>±4 | 56<br>±3 | nm         | nm   | nm  | nm  | 48    | West Sugarloaf,<br>Coso Volcanic Field |
| IF,<br>10716                                     | nm  | nm | 270<br>±5 | 8<br>±2   | 53<br>±3 | 131<br>±4 | 50<br>±3 | nm         | nm   | nm  | nm  | 47    | West Sugarloaf,<br>Coso Volcanic Field |
| <i>U.S. Geological Survey Reference Standard</i> |   |    |           |           |          |           |          |            |      |     |   |       |  |
| RGM-1<br>(measured)                              | nm  | nm | 148<br>±4 | 111<br>±3 | 28<br>±3 | 222<br>±4 | 10<br>±3 | 820<br>±21 | nm   | nm  | 1.85<br>±.02                                | 63    | Glass Mtn., CA                         |
| RGM-1<br>(recommended)                           | nm  | nm | 149       | 108       | 25       | 219       | 9        | 807        | 1600 | 279 | 1.86  | nr    | Glass Mtn., CA                         |

Values in parts per million (ppm) except total iron (in weight percent) and Fe/Mn ratios; ± = two  $\sigma$  estimate (in ppm) of x-ray counting uncertainty and regression fitting error at 120-240 seconds livetime; nm = not measured.

## ORIGER'S OBSIDIAN LABORATORY

P.O. BOX 1531  
ROHNERT PARK, CALIFORNIA 94927  
(707) 584-8200, FAX 584-8300  
ORIGER@ORIGER.COM

December 30, 2016

Richard Bark  
California State University, San Bernardino  
3026 Neary Court  
Rosamond, California 93560

Dear Mr. Bark:

I write to report the results of obsidian hydration band analysis of 39 specimens from multiple sites within the Edwards Air Force Base in Kern County, California. This work was completed following source determination by Richard Hughes, Geochemical Research Laboratory, who forwarded the specimens to us on your behalf.

Procedures typically used by our lab for preparation of thin sections and measurement of hydration bands are described here. Specimens are examined to find two or more surfaces that will yield edges that will be perpendicular to the microslides when preparation of each thin section is done. Generally, two parallel cuts are made at an appropriate location along the edge of each specimen with a four-inch diameter circular saw blade mounted on a lapidary trimsaw. The cuts result in the isolation of small samples with a thickness of about one millimeter. The samples are removed from the specimens and mounted with Lakeside Cement onto etched glass micro-slides.

The thickness of the sample was reduced by manual grinding with a slurry of #600 silicon carbide abrasive on plate glass. Grinding was completed in two steps. The first grinding is stopped when the samples thickness is reduced by approximately one-half. This eliminates micro-flake scars created by the saw blade during the cutting process. The slide is then reheated, which liquefies the Lakeside Cement, and the sample is inverted. The newly exposed surfaces are then ground until proper thickness is attained.

Correct thin section thickness is determined by the "touch" technique. A finger is rubbed across the slide, onto the sample, and the difference (sample thickness) is "felt." The second technique used to arrive at proper thin section thickness is the "transparency" test where the micro-slide is held up to a strong source of light and the translucency of each sample is observed. The sample is reduced enough when it readily allows the passage of light. A cover glass is affixed over the sample when grinding is completed. The slide and paperwork are on file at the offices of Origer's Obsidian Laboratory under File No. OOL-1033.

The hydration bands were measured with a strainfree 60-power objective and a Bausch and Lomb 12.5-power filar micrometer eyepiece mounted on a Nikon Labophot-Pol polarizing microscope. Hydration band measurements have a range of  $\pm 0.2$  microns due to normal equipment limitations. Six measurements are taken at several locations along the edge of the thin section, and the mean of the measurements are calculated and listed on the enclosed data pages.

Richard Bark  
December 30, 2016  
Page 2

Four specimens failed to yield hydration band measurements. Two of the four specimens (Lab Nos. 24 and 33) were marked by diffuse hydration (DH), and one (Lab No. 33) had weathered surfaces. One of the four specimens (Lab No. 32) was marked by no visible band (NVB), and it also had weathered surfaces. The last of the four specimens (Lab No. 36) was marked by hydration of variable width (VW) and weathered surfaces. The remaining 35 specimens yielded normal hydration band measurements.

Do not hesitate to contact me with any questions.

Sincerely,



Thomas M. Origer  
Director

December 2016

Submitter: R. Bark - CSU, San Bernardino

| Site          | Lab# | Sample#       | Description            | Unit | Depth   | Remarks           | Measurements                  | Mean | Source |
|---------------|------|---------------|------------------------|------|---------|-------------------|-------------------------------|------|--------|
| CA-KER-1161   | 1    | 5396          | Debitage               |      |         | Weathered         | 10.1 10.2 10.2 10.3 10.5 10.5 | 10.3 |        |
| CA-KER-1161   | 2.1  | 5397          | Debitage               |      |         | Band 1; Weathered | 9.5 9.5 9.6 9.8 9.9 9.9       | 9.7  |        |
| CA-KER-1161   | 2.2  | 5397          | Debitage               |      |         | Band 2; Crack     | 14.3 14.3 14.4 14.4 14.4 14.6 | 14.4 |        |
| CA-KER-1161   | 3    | 5400          | Debitage               |      |         |                   | 10.6 10.7 10.7 10.9 10.9 11.0 | 10.8 |        |
| CA-KER-1881   | 4    | 4819          | Debitage               |      | Surface |                   | 6.7 6.7 6.7 6.7 6.8 7.0       | 6.8  |        |
| CA-KER-1881   | 5    | 4820          | Debitage               |      | Surface | Weathered         | 8.6 8.6 8.7 8.8 8.9 9.1       | 8.8  |        |
| CA-KER-2154   | 6    | 6836          | Debitage               |      |         | Weathered         | 8.0 8.1 8.3 8.4 8.4 8.6       | 8.3  |        |
| CA-KER-3273   | 7    | 4823          | Debitage               |      | Surface |                   | 4.7 4.7 4.7 4.8 4.9 5.0       | 4.8  |        |
| CA-LAN-716/H  | 8    | 10818         | Debitage               |      | Surface |                   | 4.7 4.8 4.8 4.8 4.9 5.0       | 4.8  |        |
| CA-LAN-716/H  | 9    | 10819         | Debitage               |      | Surface |                   | 6.2 6.2 6.3 6.4 6.4 6.4       | 6.3  |        |
| CA-LAN-1189/H | 10   | 400-22        | Biface Frag.           | 121  | 0-5     |                   | 7.0 7.0 7.2 7.3 7.3 7.5       | 7.2  |        |
| CA-LAN-1189/H | 11   | 400-46        | Projectile Point Frag. |      | Surface |                   | 5.8 5.8 6.0 6.0 6.1 6.2       | 6.0  |        |
| CA-LAN-1307   | 12   | 616-01        | Projectile Point       |      | Surface |                   | 3.5 3.6 3.6 3.6 3.6 3.6       | 3.6  |        |
| CA-LAN-1465   | 13   | 4024          | Debitage               |      | Surface | Weathered         | 9.3 9.3 9.5 9.6 9.8 9.8       | 9.6  |        |
| CA-LAN-1465   | 14   | 1 (559-1)     | Debitage               |      | Surface | Weathered         | 8.8 8.9 8.9 9.1 9.2 9.2       | 9.0  |        |
| CA-LAN-1465   | 15   | 2 (2021-2)    | Debitage               |      | Surface | Weathered         | 7.4 7.4 7.4 7.5 7.6 7.8       | 7.5  |        |
| CA-LAN-1465   | 16   | 5 (2402-5)    | Debitage               |      | Surface |                   | 4.8 4.9 5.0 5.0 5.1 5.1       | 5.0  |        |
| CA-LAN-1465   | 17   | 5 (426-5)     | Debitage               |      | Surface |                   | 6.8 6.9 6.9 7.0 7.2 7.2       | 7.0  |        |
| CA-LAN-1465   | 18   | 12 (559-12)   | Debitage               | ST A |         |                   | 4.4 4.5 4.5 4.5 4.7 4.7       | 4.6  |        |
| CA-LAN-1465   | 19   | 13 (2021-13)  | Debitage               |      | Surface | Weathered         | 8.9 9.1 9.1 9.2 9.4 9.5       | 9.2  |        |
| CA-LAN-1465   | 20   | 22 (2021-22)  | Debitage               |      | Surface | Weathered         | 9.4 9.4 9.5 9.6 9.8 9.9       | 9.6  |        |
| CA-LAN-1465   | 21   | 27A (2021-27) | Debitage               | ST 2 |         | Weathered         | 9.6 9.8 9.8 9.8 9.9 10.1      | 9.8  |        |
| CA-LAN-1465   | 22   | 40 (236-40)   | Debitage               | TU 2 |         | Weathered         | 10.9 11.0 11.0 11.2 11.3 11.5 | 11.2 |        |
| CA-LAN-1465   | 23   | 46 (2402-49)  | Debitage               |      | Surface |                   | 6.4 6.4 6.4 6.6 6.7 6.7       | 6.5  |        |

DH = Diffuse Hydration

NVB = No Visible Band

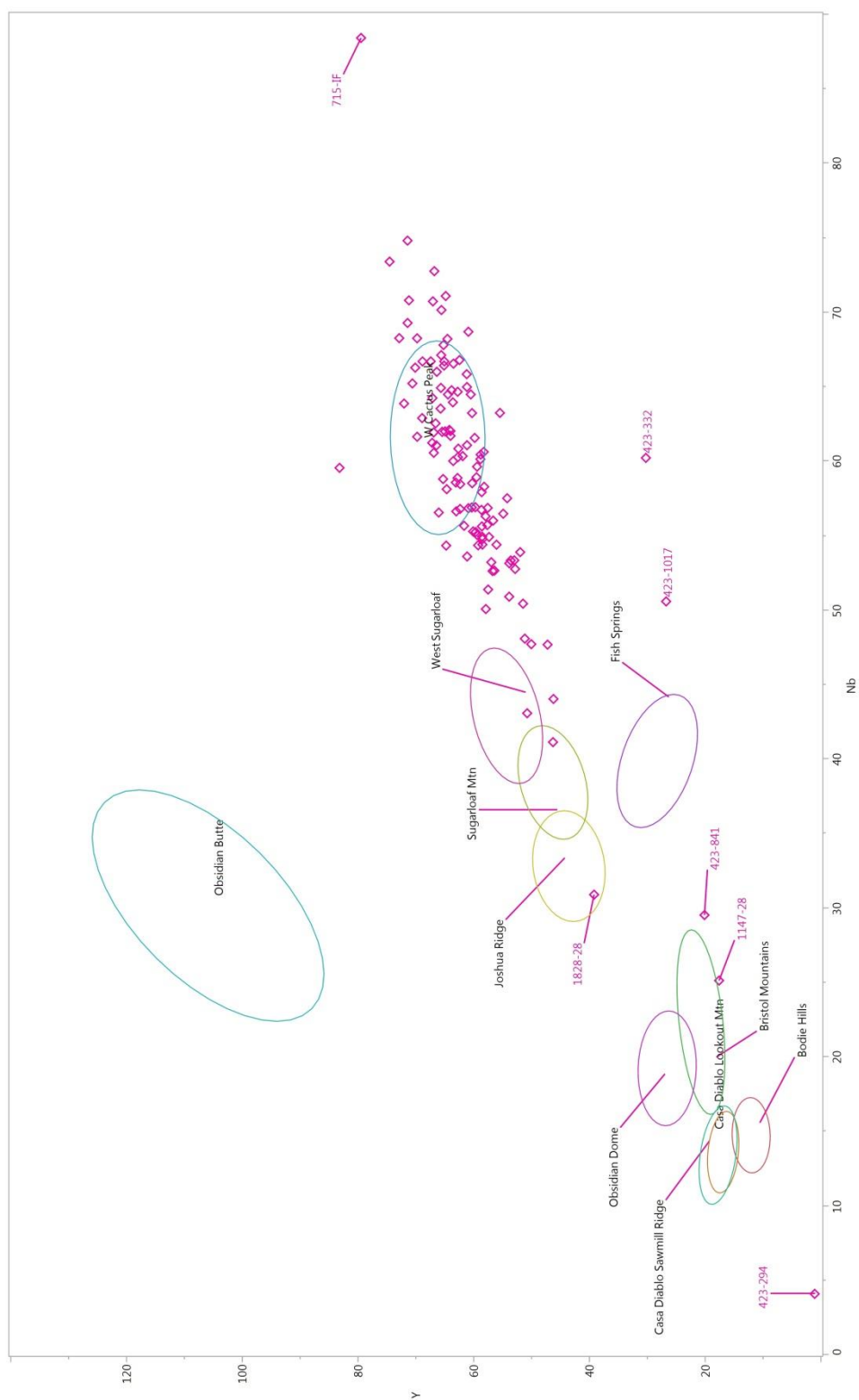
VW = Variable Width

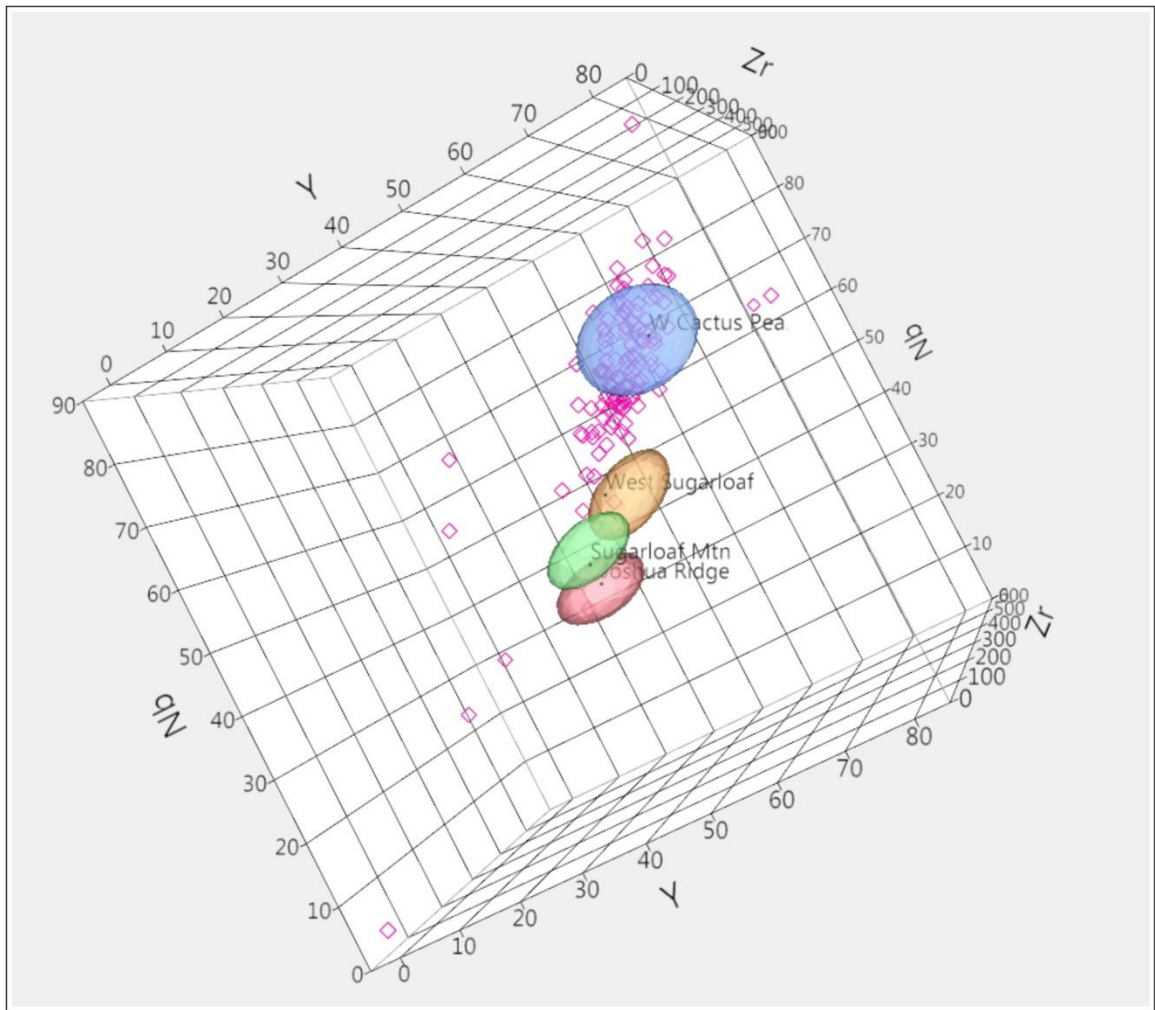
Data Page 1 of 2

| Site                       | Lab# | Sample#        | Description      | Unit   | Depth   | Remarks           | Measurements                  | Mean | Source |
|----------------------------|------|----------------|------------------|--------|---------|-------------------|-------------------------------|------|--------|
| CA-LAN-1465                | 24   | 55 (236-55)    | Debitage         | SS 1   |         |                   |                               | DH   |        |
| CA-LAN-1465                | 25   | 66 (236-66)    | Debitage         | SS 1   |         |                   | 11.7 11.7 11.9 12.0 12.2 12.3 | 12.0 |        |
| CA-LAN-1465                | 26   | 95 (4188-95)   | Debitage         |        | Surface | Weathered         | 7.8 7.9 8.0 8.2 8.2 8.4       | 8.1  |        |
| CA-LAN-1465                | 27.1 | 98 (2402-98)   | Debitage         |        | Surface | Band 1            | 8.8 8.8 8.8 8.9 9.1 9.2       | 8.9  |        |
| CA-LAN-1465                | 27.2 | 98 (2402-98)   | Debitage         |        | Surface | Band 2; Weathered | 9.8 9.9 9.9 10.0 10.1 10.3    | 10.0 |        |
| CA-LAN-1465                | 28   | 119 (2402-119) | Debitage         |        | Surface | Weathered         | 11.6 11.6 11.7 11.8 11.9 12.0 | 11.8 |        |
| CA-LAN-1465                | 29   | 172 (4188-172) | Debitage         |        | Surface |                   | 6.6 6.7 6.7 6.8 7.0 7.0       | 6.8  |        |
| CA-LAN-1465                | 30   | 182 (4188-182) | Debitage         | ST 6   |         |                   | 7.5 7.6 7.6 7.8 7.9 7.9       | 7.7  |        |
| CA-LAN-1465                | 31   | 183 (2402-183) | Debitage         |        | Surface | Not Obsidian      | .                             | .    |        |
| CA-LAN-1465                | 32   | 10691          | Debitage         | STP 12 | Surface | Weathered         |                               | NVB  |        |
| CA-LAN-1465                | 33   | 10716          | Debitage         |        | Surface | Weathered         |                               | DH   |        |
| CA-LAN-1465                | 34   | 10721          | Tool             |        | Surface |                   | 14.6 14.7 14.7 14.9 15.0 15.2 | 14.9 |        |
| CA-LAN-1465                | 35   | 10727          | Projectile Point | STP 13 | Surface | Weathered         | 11.7 11.7 11.8 11.9 12.0 12.2 | 11.9 |        |
| CA-LAN-1465                | 36   | 10729          | Debitage         | STP 13 | Surface | Weathered         |                               | VW   |        |
| CA-LAN-1465                | 37   | 10735          | Debitage         |        | Surface |                   | 8.0 8.0 8.0 8.1 8.2 8.4       | 8.1  |        |
| CA-LAN-1465                | 38   | 10738          | Biface Frag.     |        | Surface |                   | 6.2 6.2 6.3 6.3 6.3 6.4       | 6.3  |        |
| CA-LAN-1465                | 39   | 10742          | Projectile Point | TU 1   | Surface |                   | 4.8 4.8 4.9 5.0 5.1 5.1       | 5.0  |        |
| CA-LAN-1465                | 40   | 27B (2021-27)  | Debitage         | ST 2   |         | Weathered         | 4.4 4.5 4.5 4.7 4.7 4.7       | 4.6  |        |
| Lab Accession No: OOL-1033 |      |                |                  |        |         |                   | Technician: Thomas M. Origer  |      |        |

DH = Diffuse Hydration  
NVB = No Visible Band  
VW = Variable Width

# SOURCE ANALYSIS CONDUCTED BY JIMMY DANIELS







| ID       | Mn      | Fe       | Zn     | Rb     | Sr     | Y     | Zr     | Nb    | Predicted         | Probability | Other Possible Source |
|----------|---------|----------|--------|--------|--------|-------|--------|-------|-------------------|-------------|-----------------------|
| 1000-735 | 1021.58 | 12845.56 | 93.41  | 398.71 | 11.08  | 68.77 | 188.22 | 66.72 | W Cactus Peak     | 1           |                       |
| 1040-12  | 838.38  | 9508.57  | 44.97  | 325.79 | 5.27   | 63.46 | 163.35 | 60.03 | W Cactus Peak     | 1           |                       |
| 1040-13  | 1050.88 | 11648.75 | 60.04  | 362.22 | 7.89   | 64.37 | 168.54 | 64.5  | W Cactus Peak     | 1           |                       |
| 1040-14  | 815.71  | 10090.58 | 57.48  | 324    | 5.39   | 60.26 | 167.15 | 56.91 | W Cactus Peak     | 1           |                       |
| 1040-15  | 778.65  | 9541.18  | 57.33  | 318.59 | 4.65   | 58.58 | 155.04 | 56.75 | W Cactus Peak     | 1           |                       |
| 1040-51  | 568.92  | 8603.29  | 52.72  | 247.2  | 8.14   | 49.97 | 165.2  | 47.73 | West Sugarloaf    | 1           |                       |
| 1065-69  | 513.89  | 9404.85  | 43.12  | 298.54 | 4.05   | 57.27 | 145.07 | 54.93 | W Cactus Peak     | 1           |                       |
| 1105-1   | 1       | 8594.84  | 55.7   | 301.03 | 5.25   | 59.58 | 150.84 | 55.26 | W Cactus Peak     | 1           |                       |
| 1121-15  | 950.39  | 11165.82 | 69.48  | 360.42 | 7.5    | 65.38 | 168.24 | 61.99 | W Cactus Peak     | 1           |                       |
| 1121-7   | 682.51  | 10244.89 | 47.84  | 303.34 | 6.5    | 58.42 | 164.13 | 54.42 | W Cactus Peak     | 1           |                       |
| 1147-1   | 910.17  | 11016.44 | 66.24  | 362.81 | 6.54   | 67.1  | 171.47 | 61.25 | W Cactus Peak     | 1           |                       |
| 1147-2   | 1       | 7967.38  | 48.47  | 279.01 | 3.38   | 58.46 | 148.07 | 54.95 | W Cactus Peak     | 1           |                       |
| 1147-28  | 1       | 7733.5   | 34.7   | 200.6  | 141.37 | 17.52 | 134.26 | 25.14 | Bristol Mountains | 1           |                       |
| 1147-4   | 1350.62 | 17700.98 | 96.17  | 461.2  | 10.59  | 74.46 | 192.21 | 73.42 | W Cactus Peak     | 1           |                       |
| 1147-51  | 675.99  | 10877.5  | 59.19  | 281.37 | 8.59   | 53.79 | 165.27 | 50.92 | W Cactus Peak     | 0.5242      | West Sugarloaf 0.48   |
| 1534-10  | 963.13  | 11524.01 | 74.74  | 342.49 | 9.65   | 63.75 | 178.3  | 64.78 | W Cactus Peak     | 1           |                       |
| 1534-23  | 959.68  | 10080.93 | 46.66  | 342.83 | 9.81   | 61.09 | 168.4  | 65    | W Cactus Peak     | 1           |                       |
| 1534-32  | 1203.23 | 17697.25 | 103.76 | 427.2  | 12.67  | 64.76 | 204.68 | 71.11 | W Cactus Peak     | 1           |                       |
| 1828-28  | 586.2   | 10657.72 | 22.49  | 236.23 | 45.14  | 39.12 | 183.14 | 30.91 | Sugarloaf Mtn     | 0.7674      | West Sugarloaf 0.23   |
| 1831-158 | 972.43  | 10992.29 | 72.05  | 367.79 | 7.05   | 65    | 167.32 | 66.72 | W Cactus Peak     | 1           |                       |
| 1870-16  | 1075.25 | 14265.15 | 75.69  | 359.08 | 8.37   | 66.82 | 171.59 | 60.58 | W Cactus Peak     | 1           |                       |
| 1875-4   | 946.99  | 11322.67 | 57.3   | 363.78 | 5.74   | 67.34 | 170.81 | 66.72 | W Cactus Peak     | 1           |                       |
| 1882-2   | 842.83  | 10682.15 | 62.41  | 321.39 | 8.84   | 57.87 | 172.33 | 56.32 | W Cactus Peak     | 1           |                       |
| 1885-11  | 1       | 9646.51  | 43.38  | 300.03 | 5.01   | 58.41 | 158.78 | 54.79 | W Cactus Peak     | 1           |                       |
| 1900-1   | 1099.31 | 15646.68 | 84.69  | 452.54 | 10.89  | 71.11 | 192.32 | 70.82 | W Cactus Peak     | 1           |                       |
| 1905-6   | 1       | 8443.5   | 45.55  | 292.59 | 4.6    | 56.56 | 148.29 | 56.03 | W Cactus Peak     | 1           |                       |
| 191-732  | 779.58  | 9110.15  | 50.21  | 322.53 | 4.01   | 60.19 | 160.8  | 58.54 | W Cactus Peak     | 1           |                       |
| 191-733  | 999.91  | 11849.42 | 58.02  | 376.43 | 8.91   | 67.05 | 180.92 | 64.26 | W Cactus Peak     | 1           |                       |
| 1948-2   | 1041.49 | 13015.1  | 79.39  | 400.6  | 8.91   | 72.79 | 180.12 | 68.28 | W Cactus Peak     | 1           |                       |
| 1950-1   | 1081.12 | 11179.02 | 58.76  | 312.56 | 4.46   | 59.32 | 143.34 | 55.06 | W Cactus Peak     | 1           |                       |
| 1991-11  | 842.2   | 10997.24 | 53.61  | 353.69 | 8.38   | 69.7  | 173.89 | 68.27 | W Cactus Peak     | 1           |                       |
| 1991-12  | 822.52  | 10233.62 | 48.09  | 300.33 | 10.16  | 60.03 | 177.75 | 55.3  | W Cactus Peak     | 1           |                       |
| 1991-14  | 532     | 9181.47  | 45.46  | 284.48 | 6.67   | 52.76 | 158.11 | 52.78 | W Cactus Peak     | 0.9997      |                       |
| 1991-16  | 964.17  | 11777.93 | 66.76  | 397.49 | 8.35   | 65.54 | 179.2  | 67.14 | W Cactus Peak     | 1           |                       |
| 1991-2   | 669.29  | 9730.13  | 51.3   | 316.27 | 6.86   | 58.12 | 169.95 | 58.3  | W Cactus Peak     | 1           |                       |

| ID       | Mn      | Fe       | Zn     | Rb     | Sr    | Y     | Zr     | Nb    | Predicted      | Probability | Other Possible Source |
|----------|---------|----------|--------|--------|-------|-------|--------|-------|----------------|-------------|-----------------------|
| 1991-22  | 896.26  | 10214.74 | 39.16  | 349.87 | 7.15  | 60.21 | 166.99 | 63.25 | W Cactus Peak  | 1           |                       |
| 1991-222 | 1047.64 | 11635.01 | 55.39  | 363.08 | 8.52  | 68.83 | 176.15 | 62.91 | W Cactus Peak  | 1           |                       |
| 1991-224 | 1095.7  | 12796.38 | 72.54  | 339.33 | 11.5  | 64.87 | 192.13 | 62.02 | W Cactus Peak  | 1           |                       |
| 1991-3   | 866.65  | 9347.27  | 50.74  | 342.92 | 6.64  | 62.26 | 164.42 | 58.48 | W Cactus Peak  | 1           |                       |
| 1991-5   | 972.91  | 10469.66 | 60.63  | 365.82 | 7.2   | 71.96 | 592.47 | 63.89 | W Cactus Peak  | 1           |                       |
| 1991-7   | 1053.98 | 11620    | 60.25  | 318.19 | 9.52  | 64.59 | 178.62 | 58.14 | W Cactus Peak  | 1           |                       |
| 1991-9   | 1147.45 | 15235.41 | 80.34  | 408.43 | 11.86 | 65.5  | 201.48 | 70.17 | W Cactus Peak  | 1           |                       |
| 1993-22  | 778.47  | 10234.64 | 64.41  | 317.76 | 6.65  | 60.84 | 161    | 56.86 | W Cactus Peak  | 1           |                       |
| 1996-26  | 574.38  | 10169.13 | 52.38  | 306.05 | 6.11  | 59.64 | 154.42 | 56.93 | W Cactus Peak  | 1           |                       |
| 201-2009 | 774.94  | 9755.51  | 46.76  | 334.93 | 4.72  | 62.94 | 159.76 | 56.65 | W Cactus Peak  | 1           |                       |
| 201-2022 | 1       | 7436.96  | 42.26  | 271.04 | 4.2   | 57.83 | 145.41 | 50.09 | West Sugarloaf | 0.9998      |                       |
| 201-2028 | 846.98  | 9847.08  | 58.74  | 336.92 | 5.16  | 63.94 | 162.61 | 62.04 | W Cactus Peak  | 1           |                       |
| 201-2044 | 712.69  | 9405.61  | 60.17  | 291.46 | 6.33  | 53.77 | 162.13 | 53.16 | W Cactus Peak  | 1           |                       |
| 201-2050 | 1066.35 | 13422.05 | 56.86  | 415.13 | 8.35  | 71.35 | 216.44 | 69.3  | W Cactus Peak  | 1           |                       |
| 201-731  | 1       | 8386.83  | 47.7   | 224.42 | 9.63  | 46.14 | 163.92 | 44.05 | West Sugarloaf | 0.8879      | Sugarloaf Mtn 0.11    |
| 240-113  | 824.19  | 11396.88 | 61.11  | 372.89 | 6.08  | 62.37 | 167.71 | 66.81 | W Cactus Peak  | 1           |                       |
| 240-262  | 865.14  | 10893.8  | 76.94  | 375.56 | 7.89  | 65.65 | 172.82 | 63.55 | W Cactus Peak  | 1           |                       |
| 240-320  | 1081.86 | 17436.61 | 105.62 | 459.69 | 10.92 | 71.36 | 196.74 | 74.83 | W Cactus Peak  | 1           |                       |
| 240-329  | 1015.28 | 10524.88 | 49.54  | 347.2  | 6.19  | 66.84 | 163.58 | 61.95 | W Cactus Peak  | 1           |                       |
| 240-41   | 1135.33 | 13264.63 | 90.71  | 402.91 | 10.18 | 66.97 | 176.63 | 70.75 | W Cactus Peak  | 1           |                       |
| 240-64   | 591.99  | 7035.4   | 31.54  | 248.08 | 1     | 47.16 | 109.56 | 47.7  | West Sugarloaf | 0.9997      |                       |
| 2776-1   | 1018.7  | 10300.94 | 60.2   | 321.82 | 4.6   | 58.51 | 141.23 | 55.64 | W Cactus Peak  | 1           |                       |
| 2776-15  | 921.27  | 9954.89  | 54.32  | 318.81 | 5.19  | 62.72 | 138.11 | 58.89 | W Cactus Peak  | 1           |                       |
| 2776-2   | 580.14  | 9425.66  | 56.84  | 311.27 | 4.5   | 64.68 | 160.29 | 54.35 | W Cactus Peak  | 1           |                       |
| 2777-12  | 950.08  | 9465.67  | 60.87  | 341.09 | 5.87  | 69.69 | 167.02 | 61.66 | W Cactus Peak  | 1           |                       |
| 2777-12  | 937.38  | 11232.64 | 75.88  | 372.58 | 6.76  | 65.14 | 175.44 | 67.82 | W Cactus Peak  | 1           |                       |
| 2777-14  | 921.41  | 10913.19 | 81.21  | 367.88 | 7.52  | 65.05 | 170.04 | 66.44 | W Cactus Peak  | 1           |                       |
| 2777-17a | 1       | 9563.51  | 60     | 296.98 | 5.45  | 51.89 | 146.18 | 53.91 | W Cactus Peak  | 1           |                       |
| 2777-17b | 817.45  | 9887.49  | 42.12  | 329.94 | 4.38  | 59.34 | 161.42 | 59.65 | W Cactus Peak  | 1           |                       |
| 2777-23  | 851.73  | 9883.39  | 69.08  | 332.92 | 5.68  | 63.93 | 163.32 | 61.72 | W Cactus Peak  | 1           |                       |
| 2777-6   | 1011.42 | 9813.9   | 45.58  | 335.25 | 3.46  | 64.13 | 209.69 | 62.12 | W Cactus Peak  | 1           |                       |
| 2777-7   | 877.27  | 12326.75 | 71.46  | 356.27 | 8.25  | 61.13 | 171.81 | 65.86 | W Cactus Peak  | 1           |                       |
| 2777-8   | 709.32  | 9335.71  | 53.43  | 319.06 | 5.21  | 62.28 | 160.18 | 56.81 | W Cactus Peak  | 1           |                       |
| 288-27   | 816.38  | 9822.52  | 54     | 334.63 | 7.15  | 61.08 | 158.09 | 61.09 | W Cactus Peak  | 1           |                       |
| 288-3    | 968.58  | 11683.15 | 60.03  | 376.54 | 6.85  | 70.52 | 180.01 | 65.24 | W Cactus Peak  | 1           |                       |

| ID       | Mn      | Fe       | Zn     | Rb     | Sr     | Y     | Zr     | Nb    | Predicted               | Probability | Other Possible Source |
|----------|---------|----------|--------|--------|--------|-------|--------|-------|-------------------------|-------------|-----------------------|
| 288-5    | 1       | 9934.63  | 61.26  | 308.93 | 3.87   | 61.06 | 152.48 | 53.62 | W Cactus Peak           | 1           |                       |
| 288-6    | 1094.77 | 16569.02 | 105.82 | 426.3  | 13.16  | 63.42 | 194.94 | 66.57 | W Cactus Peak           | 1           |                       |
| 288-7    | 1       | 8923.38  | 40.34  | 287.66 | 5.58   | 56.35 | 146.34 | 52.67 | W Cactus Peak           | 0.9993      |                       |
| 288-8    | 747.44  | 10872.04 | 60.65  | 354.17 | 6.59   | 63.52 | 175.12 | 63.97 | W Cactus Peak           | 1           |                       |
| 303-IF   | 919.92  | 11448.23 | 62.96  | 371.22 | 8.46   | 66.3  | 177.59 | 66.02 | W Cactus Peak           | 1           |                       |
| 3109-3   | 1       | 8429.52  | 47.63  | 291.37 | 5.32   | 57.43 | 146.12 | 51.4  | W Cactus Peak           | 0.9395      |                       |
| 3122-4   | 523.24  | 11420.92 | 74.17  | 358.27 | 6.14   | 61.83 | 171.03 | 60.36 | W Cactus Peak           | 1           |                       |
| 3122-6   | 1       | 7129.61  | 47.95  | 278.1  | 3.89   | 53.52 | 144.58 | 53.35 | W Cactus Peak           | 0.9995      |                       |
| 327-IF   | 740.79  | 10147.44 | 57.44  | 328.02 | 5.19   | 58.76 | 159.64 | 60.15 | W Cactus Peak           | 1           |                       |
| 3283-18  | 497.61  | 11293.92 | 222.39 | 348.99 | 5.93   | 65.21 | 171.1  | 58.82 | W Cactus Peak           | 1           |                       |
| 333-947  | 640.86  | 9163.99  | 52.73  | 260.32 | 10.29  | 51.4  | 184.1  | 50.45 | West Sugarloaf          | 0.9978      |                       |
| 333-948  | 868.31  | 10989.45 | 54.24  | 282.92 | 11.1   | 56.67 | 193.33 | 52.64 | W Cactus Peak           | 0.9997      |                       |
| 333-950  | 975.55  | 12092.02 | 74.1   | 374.06 | 7.62   | 60.43 | 172.83 | 64.5  | W Cactus Peak           | 1           |                       |
| 393-123  | 1160.24 | 14800.78 | 71.44  | 427.17 | 11.18  | 66.73 | 178.36 | 72.78 | W Cactus Peak           | 1           |                       |
| 393-124  | 646.6   | 7985.05  | 47.49  | 291.68 | 4.06   | 59.16 | 150.61 | 54.37 | W Cactus Peak           | 1           |                       |
| 393-126  | 1       | 11242.29 | 60.8   | 230.08 | 6.93   | 50.68 | 170.38 | 43.09 | West Sugarloaf          | 0.9899      |                       |
| 393-130  | 790.54  | 8037.1   | 31.41  | 290.5  | 1      | 52.91 | 125.92 | 53.36 | W Cactus Peak           | 0.9999      |                       |
| 393-93   | 672.29  | 10209.57 | 52.78  | 318.13 | 7.98   | 59.44 | 176.24 | 58.94 | W Cactus Peak           | 1           |                       |
| 401-81   | 1242.91 | 17386.97 | 94.58  | 342.92 | 14.27  | 57.57 | 206.92 | 55.73 | W Cactus Peak           | 1           |                       |
| 401-85   | 1       | 6672.58  | 41.23  | 276.11 | 4.77   | 56.88 | 148.54 | 53.23 | W Cactus Peak           | 0.9982      |                       |
| 401-86   | 1       | 8229.36  | 41.05  | 222.75 | 5.8    | 46.22 | 181.93 | 41.15 | West Sugarloaf          | 0.716       | Sugarloaf Mtn 0.28    |
| 418-IF   | 1079.74 | 9000.5   | 45.56  | 317.7  | 5.63   | 63.02 | 160.02 | 58.59 | W Cactus Peak           | 1           |                       |
| 423-1016 | 1032.55 | 10430.04 | 63.05  | 370.57 | 5.54   | 60.84 | 170.71 | 68.71 | W Cactus Peak           | 1           |                       |
| 423-1017 | 1552.64 | 7141.87  | 47.1   | 230.57 | 18.7   | 26.67 | 157.15 | 50.6  | Fish Springs            | 1           |                       |
| 423-172  | 728.42  | 9855.22  | 51.15  | 332.98 | 5.2    | 58.19 | 158.96 | 60.64 | W Cactus Peak           | 1           |                       |
| 423-267  | 1117.31 | 12163.04 | 67.96  | 346.27 | 11.82  | 62.58 | 185.23 | 60.86 | W Cactus Peak           | 1           |                       |
| 423-276  | 820.65  | 9349.79  | 44.85  | 266.3  | 5.78   | 51.09 | 117.19 | 48.1  | West Sugarloaf          | 1           |                       |
| 423-279  | 1       | 6733.07  | 31.51  | 280.97 | 4.55   | 55.98 | 146.43 | 54.41 | W Cactus Peak           | 1           |                       |
| 423-291  | 798.64  | 9746.77  | 58.45  | 336.51 | 5.21   | 59.75 | 159.63 | 61.58 | W Cactus Peak           | 1           |                       |
| 423-294  | 687.36  | 194.95   | 1      | 1      | 36.42  | 1     | 2.97   | 4.1   | Casa Diablo Lookout Mtn | 1           |                       |
| 423-332  | 2310.8  | 12728.3  | 116.43 | 304.14 | 29.14  | 30.17 | 186.9  | 60.24 | W Cactus Peak           | 1           |                       |
| 423-342  | 728.72  | 9867.91  | 51.06  | 305.91 | 6.06   | 57.5  | 152.37 | 56.88 | W Cactus Peak           | 1           |                       |
| 423-841  | 1216.95 | 19589.95 | 56.51  | 261.2  | 131.26 | 20.04 | 250.91 | 29.54 | Bristol Mountains       | 1           |                       |
| 423-920  | 732.86  | 9006.31  | 48.2   | 332.02 | 6.89   | 65.59 | 162.84 | 64.94 | W Cactus Peak           | 1           |                       |
| 715-IF   | 979.04  | 9517.34  | 79.3   | 398.52 | 1      | 79.39 | 136.17 | 88.44 | W Cactus Peak           | 1           |                       |

| ID      | Mn      | Fe       | Zn    | Rb     | Sr    | Y     | Zr     | Nb    | Predicted     | Probability | Other Possible Source |
|---------|---------|----------|-------|--------|-------|-------|--------|-------|---------------|-------------|-----------------------|
| 717-IF  | 683.62  | 9323.9   | 61.01 | 307.21 | 6.16  | 61.58 | 156.83 | 55.68 | W Cactus Peak | 1           |                       |
| 718-IF  | 698.68  | 10235.22 | 46.92 | 326    | 5.78  | 58.72 | 156.41 | 60.46 | W Cactus Peak | 1           |                       |
| 720-IF  | 790.32  | 12794.23 | 79.17 | 375.35 | 7.25  | 64.46 | 177.99 | 68.23 | W Cactus Peak | 1           |                       |
| 721-IF  | 865.19  | 10322.62 | 63.2  | 354.41 | 6.39  | 66.51 | 165.47 | 62.56 | W Cactus Peak | 1           |                       |
| 724-IF  | 1       | 8619.45  | 50.33 | 295.77 | 6.36  | 54.82 | 151    | 56.49 | W Cactus Peak | 1           |                       |
| 725-IF  | 752.51  | 9799.09  | 65.54 | 318.57 | 2.64  | 54.14 | 130.73 | 57.53 | W Cactus Peak | 1           |                       |
| 726-IF  | 835.25  | 9883.22  | 63.52 | 325.15 | 4.23  | 62.64 | 162.01 | 60.29 | W Cactus Peak | 1           |                       |
| 727-IF  | 813.77  | 10131.33 | 54.33 | 345.38 | 6.3   | 55.39 | 163.42 | 63.26 | W Cactus Peak | 1           |                       |
| 827-IF  | 720.97  | 8841.58  | 59.2  | 319.92 | 5.06  | 58.54 | 166.26 | 57.94 | W Cactus Peak | 1           |                       |
| 832-IF  | 768.89  | 10589.71 | 63.77 | 326.79 | 4.66  | 65.96 | 166.17 | 56.57 | W Cactus Peak | 1           |                       |
| 920-2   | 760.7   | 10089.13 | 54.38 | 336.23 | 5.43  | 66.37 | 170.01 | 61.08 | W Cactus Peak | 1           |                       |
| 921-51  | 1025.53 | 11527.9  | 55.36 | 370.93 | 8.64  | 62.69 | 170.83 | 64.68 | W Cactus Peak | 1           |                       |
| 921-54  | 893.45  | 12628.82 | 64.88 | 371.29 | 7.19  | 70.03 | 175.58 | 66.3  | W Cactus Peak | 1           |                       |
| 921-54b | 1214.82 | 20808.92 | 99.16 | 332.82 | 25.31 | 83.11 | 247.83 | 59.57 | W Cactus Peak | 1           |                       |

## REFERENCES CITED

- Aitken, M. J.  
1990     *Science-Based Dating in Archaeology*. Longman Archaeological Series. London and New York.
- Anderson, N.  
2016     *Edwards AFB Archaeological Site Protection and Preservation Report, Fiscal Year 2016*. JT3/CH3M, Edwards California. Document on file at the 412 Test Wing Cultural Resources Management Office, Edwards Air Force Base, California.
- Andrefsky, W.  
1994     Raw-Material Availability and the Organization of Technology. *American Antiquity* 59(1):21-34.
- Anovitz, L. M., J. M. Elam, L. R. Piciputi, and D. R. Cole  
1999     The Failure of Obsidian Hydration Dating: Sources, Implications, and New Directions. *Journal of Archaeological Science* 26:735-752.
- Bamforth, D. B.  
1991     Technological Organization and Hunter-Gatherer Land Use: A California Example. *American Antiquity* 56(2):216-234.
- Basgall, M. E.  
1990     *Hydration Dating of Coso Obsidian: Problems and Prospects*. Paper presented at the 24<sup>th</sup> annual meeting of the Society for California Archaeology, Foster City.
- Basgall, M., and M. Giambastiani  
2000     *An Archaeological Evaluation of 13 Locations in the Deadman Lake Basin, Marine Corps Air Ground Combat Center, Twentynine Palms, California*. Report submitted to U.S. Army Corps of Engineers, Fort Worth, Texas.



Basgall, M. E., and S. A. Overly

- 2004 *Prehistoric Archaeology of the Rosamond Lake Basin: Phase II Cultural Resource Evaluations at 41 Sites in Management Region 2, Edwards Air Force Base, California*. Archaeological Research Center, California State University, Sacramento, California. Document on file at the 412 Test Wing Cultural Resources Management Office, Edwards Air Force Base, California.

Bettinger, R. L.

- 1980 Explanatory/Predictive Models of Hunter-Gatherer Adaptation. *Advances in Archaeological Method and Theory* 3, 189-255.
- 1991 *Hunter-Gatherers: Archaeological and Evolutionary Theory*. Plenum Press, New York.
- 2009 *Hunter-Gatherer Foraging: Five Simple Models*. Eliot Werner Publications, New York.
- 2013 Effects of the Bow on Social Organization in Western North America. *Evolutionary Anthropology* 22(3):118-123.
- 2015 *Orderly Anarchy: Sociopolitical Evolution in Aboriginal California*, Vol. 8. University of California Press, Oakland, California.

Bettinger, R.L., and M. A. Baumhoff

- 1982 The Numic Spread: Great Basin Cultures in Competition. *American Antiquity* 47(3):485-503.

Binford, L. R.

- 1980 Willow Smoke and Dogs' Tails: Hunter-Gather Settlement Systems and Archaeological Site Formation. *American Antiquity* 45(1):4-20.

Bleed, P.

- 1986 The Optimal Design of Hunting Weapons: Maintainability or Reliability. *American Antiquity* 51(4):737-747.

Blitz, J. H.

- 1988 Adoption of the Bow in Prehistoric North America. *North American Archaeologist* 9(2):123-145.

Broughton, J. M., and J. F. O'Connell

- 1999 On Evolutionary Ecology, Selectionist Archaeology, and Behavioral Archaeology. *American Antiquity* 64(1):153-165.

Byrd, B. F.

- 1996      *Camping in the Dunes: Archaeological and Geomorphological Investigations of Late Holocene Settlements West of Rogers Dry Lake*. ASM Affiliates, Encinitas California. Document on file at the 412 Test Wing Cultural Resources Management Office, Edwards Air Force Base, California.

Earle, D., B. Boyer, R. Bryson, M. Campbell, J. Johannesmeyer, K. Lark, C. Parker, M. Pittman, L. Ramirez, M. Ronning, and J. Underwood

- 1997      *Cultural Resources Overview and Management Plan for Edwards AFB, California, Volume 1: Overview of Prehistoric Cultural Resources*. Computer Sciences Corporation, Edwards Air Force Base, California. Document on file at the 412 Test Wing Cultural Resources Management Office, Edwards Air Force Base, California.

Eerkens, J. W., A. M. Spurling, and M. A. Gras

- 2007      Measuring Prehistoric Mobility Strategies Based on Obsidian Geochemical and Technological Signatures in the Owens Valley, California. *Journal of Archaeological Science* 35:668-680.

Evans, C., and B. J. Meggers

- 1960      A New Dating Method Using Obsidian: Part II, An Archaeological Evaluation of the Method. *American Antiquity* 25(4):523-537.

Flenniken, J. J., and P. J. Wilke

- 1989      Typology, Technology, and Chronology of the Great Basin Dart Points. *American Anthropologist* 91(1):149-158.

Friedman, I., and W. Long

- 1976      Hydration Rate of Obsidian. *Science* 191:347-352.

Friedman, I., and R. L. Smith

- 1960      A New Dating Method Using Obsidian: Part I, The Development of the Method. *American Antiquity* 25(4):476-493.

Friedman, I., and F. Trembour

- 1983      Obsidian Hydration Dating Update. *American Antiquity* 48(3):544-547.

- Friedman, I., F. W. Trembour, and R. E. Hughes  
1997      Obsidian Hydration Dating. In *Chronometric Dating in Archaeology*, edited by R. E. Taylor and Martin J. Aitken, pp. 297-321. Plenum Press, New York and London.
- Friedman, I., F. W. Trembour, F. L. Smith, and G. I. Smith  
1994      Is Obsidian Hydration Dating Affected by Relative Humidity? *Quaternary Research* 41(2):185-190.
- Giambastiani, M. A., and M. E. Basgall  
2000      *An Archaeological Evaluation of Sites CA-KER-4733/H and CA-KER-2016 in the Bissell Basin, Edwards Air Force Base, California*. Document on file at the 412 Test Wing Cultural Resources Management Office, Edwards Air Force Base, California.
- Giambastiani, M. A., M. Hale, C. R. Cole, and S. J. Moore  
2014      *Evaluations, Archaeological Sites (Mesquite Processing), Range: Edwards Air Force Base, California*. ASM Affiliates, Reno. Document on file at the 412 Test Wing Cultural Resources Management Office, Edwards Air Force Base, California.
- Gilreath, A. J., and W. R. Hildebrandt  
2011      Current Perspectives on the Production and Conveyance of Coso Obsidian. In *Perspectives on Prehistoric Trade and Exchange in California and the Great Basin*, edited by Richard E. Hughes, pp. 171-188. University of Utah Press, Salt Lake City.
- Hale, M., M. Giambastiani, D. Iversen, and M. Richards  
2009      *Phase II Cultural Resource Evaluations at 51 Archaeological Sites in Management Regions 1A, 1B, 2B, 2C, and 3E, Bissell Hills and Paiute Ponds, Edwards Air Force Base, Kern and Los Angeles Counties, California*. ASM Affiliates, Carlsbad California. Document on file at the 412 Test Wing Cultural Resources Management Office, Edwards Air Force Base, California.



- Hale, M., M. Giambastiani, J. Daniels, and M. Dalope  
2010 *Phase II Cultural Resource Evaluations at 85 Archaeological Sites in Management Areas 2B, 2C, 3F, 3H, 3I, and 4B, Edwards Air Force Base, Kern and Los Angeles Counties, California*. ASM Affiliates, Carlsbad California. Document on file at the 412 Test Wing Cultural Resources Management Office, Edwards Air Force Base, California.
- Hames, R.  
1992 Time Allocation. In *Evolutionary Ecology and Human Behavior*, edited by Eric Alden Smith and Bruce Winterhalder, pp. 2013-235. Aldine De Gruyter, New York.
- Hildebrandt, W. R., and J. H. King  
2012 Distinguishing Between Darts and Arrows in the Archaeological Record: Implications for Technological Change in the American West. *American Antiquity* 77(4):789-799.
- Hughes, R. E., and R. Milliken  
2007 Prehistoric Material Conveyance. In *California Prehistory: Colonization, Culture, and Complexity*, edited by Terry L. Jones and Kathryn A. Klar, pp. 259-271. Altamira Press.
- Hull, K. L.  
2001 Reasserting the Utility of Obsidian Hydration Dating: A Temperature-Dependent Empirical Approach to Practical Temporal Resolution with Archaeological Obsidians. *Journal of Archaeological Science* 28:1025-1040.
- Huntington, E.  
1922 *Civilization and Climate*. Yale University Press, New Haven.
- Jack, R. N., and I. S. E. Carmichael  
1969 The Chemical "Fingerprinting" of Acid Volcanic Rocks. *California Division of Mines and Geology Special Report* 100:17-32.
- Johnson, M.  
2010 *Archaeological Theory: An Introduction*. 2nd ed. John Wiley & Sons, 2011.

- Jordan, P., and V. Cummings  
2014 Introduction. In *The Oxford Handbook of the Archaeology and Anthropology of Hunter-Gatherers*. Oxford University Press.
- Kelly, R. L.  
1988 The Three Sides of a Biface. *American Antiquity* 53(4):717-734.  
2007 *The Foraging Spectrum: Diversity in Hunter-Gatherer Lifeways*. Percheron Press, New York.
- King, J.  
2004 Re-Examining Coso Obsidian Hydration Rates. *Proceedings of the Society for California Archaeology* 14:135-142.
- Kroeber, A. L.  
1925 Handbook of the Indians of California. *Bureau of American Ethnography Bulletin* 78. Washington.  
1939 *Cultural and Natural Areas of Native North America*. University of California Press.
- Meggers, B. J.  
1955 Environmental Limitation on the Development of Culture. *American Anthropologist* 56(5):801-824.
- Orme, A. R., and R. Yuretich  
2004 *Lake Thompson, Mojave Desert, California: A Desiccating Later Quaternary Lake System*. Cold Regions Research and Engineering Laboratory, Engineer Research and Development Center, Hanover, New Hampshire.
- Parry, W. J. and R. L. Kelly  
1986 Expedient Core Technology and Sedentism. In *The Organization of Core Technology*, edited by Jay K. Johnson and Carol A. Morrow. Westview Press, Boulder.
- Railey, J. A.  
2010 Reduced Mobility or the Bow and Arrow? Another Look at "Expedient" Technologies and Sedentism. *American Antiquity* 75(2):259-286.
- Ridings, R.  
1996 Where in the World Does Obsidian Hydration Dating Work? *American Antiquity* 61(1):136-148.

Rogers, A. K.

- 2007 Effective Hydration Temperature of Obsidian: A Diffusion Theory Analysis of Time-Dependent Hydration Rates. *Journal of Archaeological Science* 34:656-665.
- 2008 Obsidian Hydration Dating: Accuracy and Resolution Limitations Imposed by Intrinsic Water Variability. *Journal of Archaeological Science* 35:2009-2016.
- 2017 *A New and Simple Laboratory Method for Estimating Hydration Rate of Obsidian*. Paper presented at the 2017 Annual Meeting of the Society for California Archaeology.

Rogers, A. K., and R. M. Yohe

- 2011 An Improved Equation for Coso Obsidian Hydration Dating, Based on Obsidian-Radiocarbon Association. *Society for California Archaeology Proceedings* 25:1-15
- 2014 Obsidian Re-Use at the Rose Spring Site (CA-INY-372), Eastern California: Evidence from Obsidian Hydration Studies. *Journal of California and Great Basin Anthropology* 34(2):273-286.

Rondeau, M. F.

- 2016 *A Fluted Point from Edwards Air Force Base, Los Angeles County, California*. Rondeau Archaeological, Sacramento, CA. Document on file at the 412 Test Wing Cultural Resources Management Office, Edwards Air Force Base, California.

SAS Institute Inc.

- 1999 Canonical Discriminant Analysis. Electronic document, <https://v8doc.sas.com/sashtml/insight/chap40/sect7.htm>, accessed March 5, 2017.

Sawyer, J. O.

- 1994 *Draft Series Descriptions of California Vegetation*. California Native Plant Society, Sacramento, California.

Scharlotta, I.

- 2014 Trade Routes and Contradictory Spheres of Influence: Movement of Rhyolite Through the Hearth of the Western Mojave Desert. *California Archaeology* 6(2):219-246.

Slocum, S.

- 2103 Woman the Gatherer: Male Bias in Anthropology. In *Readings for a History of Anthropological Theory*, edited by Paul A. Erickson and Liam D. Murphy, pp. 307-314. 4<sup>th</sup> ed. University of Toronto Press, Toronto.

- Smith, G. M.  
 2010 Shifting stones and changing homes: using toolstone ratios to consider relative occupation span in the northwestern Great Basin. *Journal of Archaeological Science* 38:461-469.
- Stevens, N. E.  
 2002 *Prehistoric Use of the Alpine Sierra Nevada: Archaeological Investigations at Taboose Pass, Kings Canyon National Park, California*. M.A. thesis, California State University, Sacramento.  
 2005 Changes in Prehistoric Land Use in the Alpine Sierra Nevada: A Regional Exploration Using Temperature-Adjusted Obsidian Hydration Rates. *Journal of California and Great Basin Anthropology* 25(2):41-50.
- Steward, Julian H.  
 1955 *Theory of Culture Change: The Methodology of Multilinear Evolution*. University of Illinois Press, Urbana, Illinois.
- Sutton, M. Q.  
 2017 Chasing Ghosts? Rethinking the Prehistory of the Late Holocene Mojave Desert. *Pacific Coast Archaeological Society Quarterly* 53(1):1-70.
- VanPool, T. L., and R. D. Leonard  
 2011 *Quantitative Analysis in Archaeology*. John Wiley and Sons.
- Vasek, F. C., and M. G. Barbour  
 1977 Mojave Desert Scrub Vegetation, in *Terrestrial Vegetation of California*. John Wiley and Sons.
- Warren, C.  
 1984 The Desert Region. In *California Archaeology*, by M. J. Moratto; pp. 339-430. Academic Press, Orlando, Florida.
- Warren, C., and R. H. Crabtree  
 1987 Prehistory of the Southwestern Area. In *Handbook of North American Indians, Vol. 11: Great Basin*. Edited by Warren L. d'Azevedo, pp. 183-193. Smithsonian Institution Press, Washington, D. C.
- White, L. A.  
 1949 *The Science of Culture: A Study of Man and Civilization*. Farrar, Straus and Company, New York.
- Willey, G. R., and J. A. Sabloff  
 1993 *A History of American Archaeology*. 3rd ed. W. H. Freeman, New York.

Winterhalder, B., and A. E. Smith

1992 Evolutionary Ecology and the Social Sciences. In *Evolutionary Ecology and Human Behavior*, edited by Eric A. Smith and Bruce Winterhalder, pp. 3-23. Aldine De Gruyter, New York.

Yohe, R.

1998 The Introduction of the Bow and Arrow and Lithic Resources Use at Rose Spring (CA-INY-372). *Journal of California and Great Basin Anthropology* 20(1):26-52.